THE UNIVERSITY
of EDINBURGH

Cervical epithelial damage and preterm birth

Ioannis Pavlidis MD MSc DIC

THE UNIVERSITY
of EDINBURGH

Thesis submitted to the University of Edinburgh for the degree of Doctor of Philosophy

September 2018

Acknowledgements

I would like to thank my supervisors Dr Sarah Stock, Professor Jane Norman and Professor Sarah Howie for all their help and support during this PhD. I would also like to thank them for their guidance and support for my next career steps. I am particularly grateful to them for giving me the opportunity to work at the Tommy's Centre for Maternal and Fetal Health.

A big part of this project would not have been possible without the invaluable contribution of Dr Brad Spiller. I would like to thank him for our many Skype meetings and his visit to Edinburgh to share with me his expertise with *Ureaplasma*.

My 2-month visit to Yale University School of Medicine was one of the great experiences of my PhD. For this, I would like to thank Professor Gil Mor who gave me the chance to work at the Reproductive Immunology Unit.

A big thank you goes to all the current and previous members of the Tommy's Centre, with whom I shared an office and a lab for the past 3 years. Special thanks to Dr Heather MacPherson, Dr Sara Rinaldi, Dr Marian Aldhous, Dr Ashley Boyle, Dr Caterina Fazzi and Ms Rose Leask. I would also like to thank our MSc student Dr Gabriella Sammut Demarco, who I supervised for the past 6 months.

Finally, I would like to thank Tommy's for funding my PhD and the University of Edinburgh for providing financial support for my research visit to Yale.

Declarations

The composition of this thesis and the studies undertaken were the unaided work of the author, except where due acknowledgment is made by reference. No part of the work described in this thesis has been previously accepted for is currently being submitted for another degree or qualification.

I acknowledge the assistance of the following people:

Dr Forbes Howie, for performing the mycoplasma testing on cell lines (Chapter 3).

Mrs Paulomi Aldo, for performing the Luminex assays on cell lines (Chapter 3).

Mr Michael Dodds and Mrs Carrie Owen, for setting up the mice time-matings and performing plug checks (Chapters 4 and 5).

Dr Brad Spiller, for providing the NanoLuc-expressing *Ureaplasma parvum* (Chapter 5).

Dr Gabriella Sammut Demarco, for performing some of the qRT-PCR reactions (Chapter 5).

Mr Ronnie Grant, for assistance with graphic design (Chapter 1).

Ioannis Pavlidis

List of presentations

A new model of cervical damage during pregnancy. Oral presentation.
3rd Annual UK Preterm Birth Conference, Leeds, UK. September 2017.

A new model of cervical damage during pregnancy. Oral presentation.
2nd Interdisciplinary Autumn School in Reproductive Sciences and Related Fields, Magdeburg, Germany. October 2017.

A new model of cervical damage during pregnancy and its effects on timing of delivery. Poster presentation.
65th Annual Scientific Meeting of the Society for Reproductive Investigation (SRI), San Diego, California, USA. March 2018.

A novel model of cervical damage-mediated ascending infection. Oral presentation.
3rd European Spontaneous Preterm Birth Congress (ESPBC), Edinburgh, UK. May 2018.

Intrauterine inflammatory response to *Ureaplasma parvum* in a mouse model of cervical damage-mediated ascending infection. Oral presentation.
4th Annual UK Preterm Birth Conference, Bristol, UK. September 2018.

Scientific Abstract

Preterm birth is the leading cause of neonatal mortality and morbidity. The uterine cervix is key in maintaining a healthy pregnancy. Excisional procedures for the treatment of cervical intraepithelial neoplasia (CIN) are associated with preterm birth (PTB), but underlying mechanisms are yet to be described. Intrauterine infection is involved in 40% of PTB and cervical damage is likely to facilitate ascending infection with vaginal bacteria. The aim of this thesis was to establish and characterise an *in vitro* and *in vivo* model of cervical damage to study its interplay with ascending infection. For this, the surfactant N-9 was used as a damage agent.

N-9 was found to reduce the endocervical epithelial cells' viability and compromise their epithelial permeability *in vitro*. When vaginally administered in pregnant C57Bl/6 mice, N-9 disrupted the structural integrity of the cervical epithelium, caused an influx of neutrophils and resulted in increased cell proliferation in the basement membrane of the cervix. Similar where the findings in the vaginal epithelium. However, N-9-induced epithelial damage had no effect on timing of delivery or pup survival.

Following vaginal infection with a luciferase-expressing *Ureaplasma parvum,* mice previously treated with N-9 exhibited higher rates of ascending infection, with increased bioluminescence signal in the upper reproductive tract. They also demonstrated higher bacterial titres in the amniotic fluid and higher bacterial product copy numbers in the reproductive tissues. This resulted in increased preterm birth rates among mice in this group compared to vehicle-treated controls. Infection with *Ureaplasma parvum* was characterised by an inflammatory response in the uterus, the placenta and the fetal membranes with increased expression of the proinflammatory cytokines TNFa, IL-1b, CXCL-1 and CXCL-2. This effect may be mediated by TLR2, the expression of which was also shown to increase accordingly.

Overall, these findings suggest that cervical epithelial damage facilitates ascending infection. This is a potential mechanism explaining the higher PTB incidence among women treated for CIN. The robust model of cervical epithelial damage during pregnancy described in this thesis can be used to study the barrier function of the cervix and its interplay with ascending infection in future studies.

Lay Abstract

Preterm birth is any birth before 37 completed weeks of pregnancy and it occurs in about 10% of pregnancies. It is a very risky situation as babies born early are at increased risk of death and are also likely to face problems with any of their developing organs. The main reason why babies are born early is an infection with bacteria that takes place inside the womb. These bacteria travel there from the vagina, where they normally reside. The cervix is a little tube that stands between the vagina and the womb. When the cervix is damaged, then women are more likely to deliver preterm. Due to obvious ethical restrictions, experiments to find out why this happens cannot be done in women. The aim of this thesis was to mimic the above case in the laboratory setting using human cells and laboratory mice and to study whether damage in the cervix can increase the risk of infection in the womb. A substance called N-9 was used to cause cervical injury.

When N-9 was applied to cells from the cervix in the laboratory, the cells started to die. It also disrupted their ability to filter what goes through them, a crucial feature for protecting against infection. When mice received N-9 in their vagina, the cells that form the lining of the cervix and the vagina, called the epithelium, started to die. In addition, specialised cells called neutrophils that participate in repair processes after injury were recruited on site. Finally, cells of the epithelium that survived started multiplying faster in order to replace the missing parts. These features were indicative of a successful mimicking of cervical damage.

The interplay between cervical damage and infection was studied using N-9 and the most common bacteria in preterm birth, *Ureaplasma parvum*. In mice that had their cervix damaged by N-9, it was more likely for *Ureaplasma parvum* to manage to go from the vagina to the womb. This led to more mice in this group delivering preterm compared to the ones that had an intact cervix. It was also found that the presence of

Ureaplasma parvum causes the immune system of the mice to respond by producing specialised agents that cause inflammation.

Overall, the work in this thesis suggests that damage to the cervix can increase preterm birth by allowing bacteria to pass through the cervix and infect the womb.

Contents

List of Figures

List of Tables

Abbreviations

AB/PAS	Alcian blue/Periodic acid Schiff
ACTH	Adrenocorticotropic hormone
ANOVA	Analysis of variance
AP-1	Activator protein 1
ARDS	Acute Respiratory Distress Syndrome
ART	Assisted reproductive technology
ATP	Adenosine triphosphate
BCP	1-bromo-3-chloropropane
BLI	Bioluminescence imaging
BSA	Bovine serum albumin
BPE	Bovine pituitary extract
CCL-2	C-C motif chemokine ligand 2
CCM	Cell culture medium
CDC	Centres for Disease Control and Prevention
cDNA	Complementary deoxyribonucleic acid
ChIP	Chromatin immunoprecipitation
CI	Confidence intervals

COL 1A1	Collagen 1A1
COX-2	Cyclooxygenase-2
CO$_2$	Carbon dioxide
Ct	Threshold cycle
CXCL-1	C-X-C motif chemokine ligand 1
CXCL-2	C-X-C motif chemokine ligand 2
CXCL-8	C-X-C motif chemokine ligand 8
CXCL-10	C-X-C motif chemokine ligand 10
Cx-43	Connexin-43
DAB	3,3'- diaminobenzidine
DAMP	Damage-associated molecular pattern
DES	Diethylstilbestrol
DMEM	Dulbeco's modified Eagle medium
DMF	Dimethylformamide
DMSO	Dimethylsulfoxide
DNA	Deoxyribonucleic acid
dNTPs	Deoxyribonucleotide triphosphates
EDTA	Ethylenediaminetetraacetic acid
EGF	Epidermal growth factor

ELISA	Enzyme-linked immunosorbent assay
FBS	Fetal bovine serum
F. I.	Fluorescence intensity
FITC	Fluorescein
FOI	Field of interest
G-CSF	Granulocyte-colony stimulating facror
GM-CSF	Granulocyte-macrophage colony-stimulating facror
GROa	Growth related oncogene-a
HA	Hyaluronic acid
HBD-1	Human β-defensin 1
HESC	Human endometrial stromal cells
HEPES	4-(2-hydroxyethyl)-1-piperazineethanesulfonic acid
HIER	Heat-induced epitope retrieval
HIV	Human immunodeficiency virus
HMGB1	High-mobility group box 1
HPA	Hypothalamus-Pituitary-Adrenal
HPV16	Human Papilloma Virus type 16
HRP	Horseradish peroxidase
Hz	Hertz

H$_2$O	Water
H$_2$O$_2$	Hydrogen peroxide
H$_2$SO$_4$	Sulfuric acid
IgA	Immunoglobulin A
IL-1b	Interleukin-1b
IL-6	Interleukin-6
IL-8	Interleukin-8
IL-10	Interleukin-10
IL-18	Interleukin-18
IFNγ	Interferon gamma
IP-10	Interferon gamma-induced protein 10
IRAK1	interleukin-1 receptor-associated kinase 1
IRAK4	interleukin-1 receptor-associated kinase 4
KO	Knockout
LDH	Lactate dehydrogonase
LEEP	Loop electrosurgical excision procedure
LLETZ	Large loop excision of the transformation zone
LMP	Last menstrual period
LTA	Lipoteichoic acid

Ly6G	Lymphocyte antigen 6 complex locus G6D
MBA	Multiple-banded antigen
M-CSF	Macrophage colony-stimulating factor
MCP-1	Monocyte chemoattractant protein 1
MIAC	Microbial invasion of the amniotic cavity
MIP-1a	Macrophage inflammatory protein-1 alpha
MIP-1b	Macrophage inflammatory protein-1 beta
MMPs	Matrix metalloproteinases
mRNA	Messenger ribonucleic acid
MTS	(3-(4,5-dimethylthiazol-2-yl)-5-(3-carboxymethoxyphenyl)-2-(4-sulfophenyl)-2H-tetrazolium
MTT	3-(4,5-dimethylthiazol-2-yl)-2,5-dyphenyltetrazolium
MyD88	Myeloid differentiation response element 88
NaCl	Sodium chloride
NADH	Nicotinamide adenine dinucleotide
NFκB	Nuclear factor kappa B
NGS	Normal goat serum
NLRs	Nod-like receptors
NO	Nitric oxide
N-9	Nonoxynol-9

ON	Overnight
OR	Odds ratio
OTR	Oxytocin receptor
P	Probability
PBS	Phosphate buffered saline
PDE4	Phosphodiesterase 4
PFA	Polymeric formaldehyde
PGDH	Hydroxyprostaglandin dehydrogenase
PGE$_2$	Prostaglandin E$_2$
PGF$_{2a}$	Prostaglandin F$_{2a}$
PGs	Prostaglandins
PPROM	Preterm premature rupture of membranes
PRRs	Pattern Recognition Receptors
PTB	Preterm birth
PTL	Preterm labour
RANTES	Regulated on activation, normal T cell expressed and secreted
RCT	Randomised clinical trial
RIPA	Radioimmunoprecipitation
RNA	Ribonucleic acid

ROI	Region of interest
RR	Relative risk
RT	Room temperature
RU486	Mifepristone
SD	Standard deviation
SEM	Standard error of the mean
SLPI	Secretory Leukocyte Protease Inhibitor
STDs	Sexually transmitted diseases
SuRF	Shared University Research Facilities
TBS	Tris-buffered saline
TGF-β	Transforming growth factor beta
TIMPs	Tissue inhibitors of metalloproteinases
TLRs	Toll-like Receptors
TMB	3, 3', 5, 5'- Tetramethylbenzidine
TNFa	Tumour necrosis factor A
TRAF6	TNF receptor associated factor 6
UK	United Kingdom
UP	*Ureaplasma parvum*
UreC	Urease C

USA	United States of America
USM	Ureaplasma selective medium
WHO	World Health Organisation
WST	2-[4-iodophenyl]-3-[4-nitrophenyl]-5-[2,4-disulfophenyl]-2H-tetrazolium, monosodium salt
WT	Wildtype
β-ME	β-Mercaptoethanol

Chapter 1   Literature review

1.1 Definition

The definition of Preterm birth (PTB) was suggested by the World Health Organisation (WHO) in 1975 and refers to any delivery before 37 completed weeks of pregnancy (1). This is the equivalent of 259 days since the day of the last menstrual period (LMP). No global definition has been adopted for the lower limit, although this is generally set at 20 or 22 weeks of gestation (2). PTB can be further sub-classified into extremely preterm for babies born before 28 weeks, very preterm for babies born between 28 and 32 weeks and moderate or late preterm for those born between 32 and 36 weeks (1).

1.2   Epidemiology

Preterm birth affects 11.1% of all live births worldwide with an prevalence that ranges from 5% to 18% (3). The incidence is between 5-10% in Europe, more than 10% in the United States and approaching 15% or more in Africa and South-East Asia (3). This results in about 15 million babies being delivered prematurely on an annual basis (4). About 80% of those are in Africa and Asia (5).

Preterm birth can be iatrogenic due to medical indications or occur after spontaneous onset of preterm labour (PTL) or preterm premature rupture of membranes (PPROM). Despite this division, a spontaneous PTB increases the risk for a subsequent medically indicated PTB and *vice versa* (6). This indicates that common underlying mechanisms are likely to be shared in both conditions (7).

Medical indications for a preterm delivery account for about 30% of PTBs and include conditions that put either the maternal (such as preeclampsia) or fetal (such as intrauterine growth restriction) health at risk (3). The number of medically indicated PTBs has been shown to have increased in industrialised countries over the past two decades (8). This is partly due to an increase in the use of assisted reproductive

technology (ART) which in itself increases the risk for preterm delivery, even in singleton pregnancies (9).

1.3 Mortality and morbidity

1.3.1 Mortality

Over the past few decades, medical advances have improved mortality rates of babies born preterm. These include the use of assisted ventilation (10), surfactant administration (11) (12), widespread use of antenatal corticosteroids for preterm lung maturation (13) and the treatment of preterm babies in the intensive care unit (14). These advances have been pivotal for the striking improvement in preterm mortality rates, especially in the extremely preterm group (15). However, by 2013 preterm birth and its complications were still the leading cause of death during the neonatal period (16). These account for a total of approximately 1 million neonatal deaths annually (16).

The mortality risk largely increases with smaller gestation age (17). Most studies report their data by birthweight (18) which can be used as an indication of gestational age (19). For example, survival to discharge ranges from less than 20% at 401-500g birthweight to more than 90% at 1401-1500g birthweight (20). The high mortality risk of this very small group has a vast effect on the overall mortality rates. In particular, babies below 1,000g birthweight account for almost half infant deaths in the US annually, despite them representing only 0.8% of the total number of births (21). The same pattern is also found for infants in the extremely preterm group of earlier than 28 weeks gestation (21).

1.3.2 Morbidity

Surviving infants are potentially exposed to a wide spectrum of short-term complications that predispose and may lead to severe long-term outcomes.

Shortly after delivery, preterm neonates are at increased risk of severe respiratory complications such as Acute Respiratory Distress Syndrome (ARDS) and

bronchopulmonary dysplasia. These conditions result in a poorer lung function later on in life (22) with a concurrent tendency for increased hospitalisation and more hospital re-admissions (23).

Ocular complications such as retinopathy or prematurity are also common, especially in the extremely preterm group. This can lead to moderate morbidity such as myopia or hypermetropia (24). Importantly, it can lead to severe complications including retinal detachment (25), severe visual impairment or even blindness (26).

Premature babies are also at increased risk of developing type 2 diabetes (27), renal (28) and cardiovascular disease (28) in their adulthood. These conditions further increase mortality and morbidity risks on their own.

The most dramatic impact is arguably seen in the preterm infant's brain. Preterm neonates are at increased risk of intraventricular haemorrhage (29). Given the brain's immature status at this critical developmental window, this can lead to cerebral palsy (30) and neurosensory disabilities (31). These can evolve into permanent neurological disabilities with life-long morbidity (32). This becomes apparent as they face learning difficulties (33), cognitive deficit (34) and altered social behaviour (35).

1.4 Financial implications

Besides the detrimental effects on life, health and wellbeing of premature infants, PTB-related morbidity also has important financial consequences on healthcare services both in the short and in the long-term. A cohort study from California reported that in the short-term, the cost of post-delivery hospitalisation of a premature baby at 24 weeks has a median value of $216,814 for a median 92-day stay at the hospital (36). At 37 weeks however, the hospitalisation cost is at $591 for a 2-day stay (36). This highlights a remarkable cost reduction of more than 99%.. Similar results regarding hospitalisation length were also reported using a Swedish registry (37). This emphasizes the huge cost of PTB, even for those that manage to survive without any impairment.

Following hospital discharge, re-admissions related to prematurity complications are quite likely. Further costs related to social care and special education are also implicated as direct consequences of prematurity. In the UK, a fair total estimate of the financial burden of PTB to the public sector for 2006 was £2.946 billion which corresponds to $4.567 billion at the time the study was conducted (38). Predictably, the study found that the average cost for each preterm child increased as the gestational length got shorter as part of a direct inverse relationship (38). The respective financial burden for the US in 2005 was $26.2 billion, which is in line with the UK data, the difference being reflective of the population difference as well as the increased incidence (39).

A recent study has estimated that a relative 5% reduction of preterm births in countries with a very high human development index would translate into 58,000 fewer preterm deliveries. This would result in global savings of $3 billion annually (40). Collectively, these data suggest that reducing preterm birth and/or alleviating its effects will have a huge financial benefit on healthcare systems.

1.5 Key structures in the parturition process

Parturition is a well-synchronised series of events that result in profound biological and clinical changes in three key reproductive tissues: the myometrium, the fetal membranes and the cervix. Synchronous activation of the 3 at term marks what has been described as "the common pathway of parturition" (41).

1.5.1 The myometrium

The reproductive tissue where the conceptus attaches, grows and develops during pregnancy is the uterus. The uterus consists of three distinct layers. The outer layer is called the perimetrium and the inner layer is called the endometrium. During gestation, the endometrium undergoes changes under the influence of the pregnancy-related hormones, such as progesterone, to become the decidua (42). The middle muscular layer is called the myometrium (42). The myometrium primarily consists of densely packed smooth muscle fibres (42). In addition is also has dense vasculature with many

blood and lymph vessels as well as connective tissue and immune cells (42). As gestation advances, the uterine smooth muscle cells undergo stretch-induced hypetrophy (43). The hallmark of myometrial transition to a labouring phenotype is initiation of co-ordinated contractions, resulting in the expulsion of the fetus and the placenta (44). This transition is termed "activation" (44).

1.5.2 The fetal membranes

The fetal membranes are comprised of the chorion and the amnion, the two of them being closely adherent (45). The thicker chorion is the exterior layer and mainly consists of a dense cellular population (46). The amnion is the thinner and inner-most layer and is rich in extracellular matrix formed of collagen fibrils (46). They surround the fetus which they manage to retain along with the amniotic fluid (47). Constitutively, they protect the fetus by forming a physical protective barrier (48). At the same time, they critically contribute to fetal nutrition by secreting nutritious substances (48). During parturition, the fetal membranes undergo extensive remodelling that leads to their weakening, rupture and finally separation from the fetus (49).

1.5.3 The cervix

The cervix is a tube-like tissue located between the uterus and the vagina. In the non-pregnant state, it has an average length of 3-4 cm and it mainly consists of collagen-rich extracellular matrix with only a minimal cellular component of fibroblasts, smooth muscle, epithelial and immune cells (50). It consists of two main areas: the ectocervix and the endocervix. The ectocervix is the cervical part protruding into the vagina. Like the vagina, it is lined with a non-keratinised stratified squamous epithelium (51). The endocervix or the endocervical canal is the tube part of the cervix that connects the uterine cavity to the ectocervical opening to the vagina, called the external os. The endocervical epithelium is a single layer of mucus-producing columnar cells (51). During pregnancy, the mucus produced by the endocervical cells forms the cervical plug or operculum (52). This is a physical and functional barrier that contributes to the protection of the fetus (53). For parturition to occur, the cervix undergoes effacement

and dilatation, which are mainly driven by the mechanical forces exerted by the myometrial contractions (54). This allows passage of the fetus through the cervical canal (55).

Activation of one or more of the above-mentioned components of parturition - myometrium, fetal membranes, cervix - can lead to spontaneous onset of the parturition cascade. Untimely activation can lead to preterm birth.
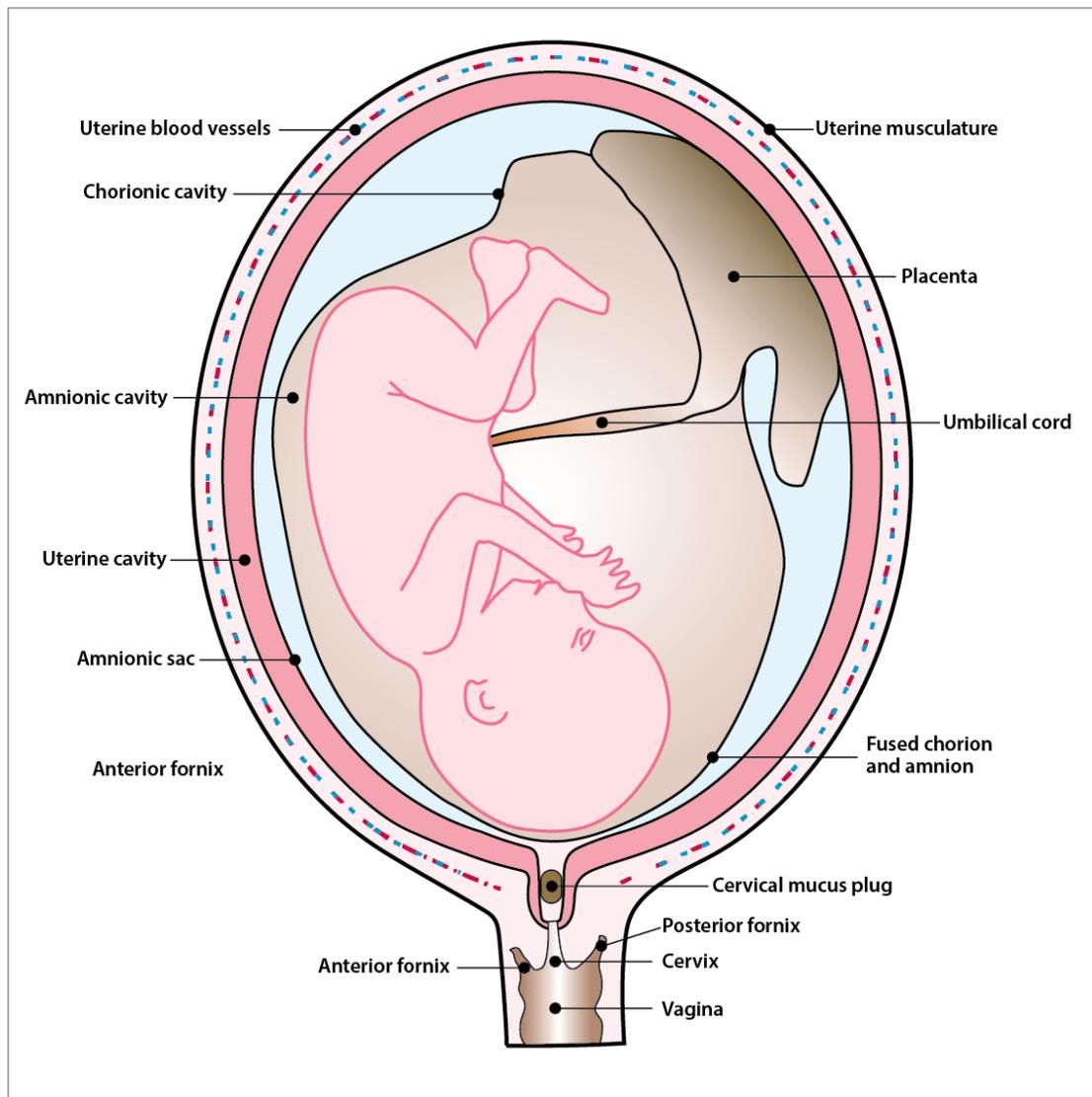
Figure 1.1 Basic anatomy of the reproductive tissues during pregnancy.

1.6 Risk factors

The pathophysiology of preterm birth is still incompletely understood. This is further complicated by the fact that it does not represent a single clinical condition, but rather a syndrome. The notion that preterm birth is a syndrome is strongly supported by its diverse aetiology, with multiple pathologies involved (56).

Several factors have been shown to increase the risk for preterm delivery. Among them, the most consistent is a previous history of preterm birth which results in a 2.5-fold increase in the risk of preterm birth in the current pregnancy, the effect being stronger in extremely preterm deliveries (57). Moreover, recurrent PTB tends to occur around the same time as the previous event (58), with most women delivering within a couple of weeks of their first delivery (59). In addition, a large population-based study from Sweden found that sisters of women that delivered preterm have a 1.8-fold increased odds ratio (OR) of delivering preterm themselves (60). As environmental factors might be the reason for this association (61), another population-based study adjusted for known environmental risk factors only to find an even higher OR of 4.2 in siblings of women that gave birth preterm (62). Collectively, these data highlight the importance of genetic predisposition as a risk factor for preterm birth.

PTB tends to occur more often and earlier in gestation in black women (63). Racial disparities among population sub-groups have long been observed in the USA (64). A study in a low income population consisting of 69% black and 31% white women found that the higher incidence of PTB in black compared to white women was quite consistent even when controlled for other risk factors and cannot be explained based on separate maternal characteristics, such as smoking or alcohol consumption (65). Disparities in socioeconomic status are also involved, as substantial socioeconomic deprivation can increase the risk of very preterm births by a factor of 2 (66).

Another factor implicated with preterm birth is the work environment. Although employment itself does not increase the risk for preterm delivery (67), long hours and physically or mentally demanding jobs are associated with increased risks (67) (68). These conditions increase the levels of maternal stress, which is an independent risk

factor in itself as it almost doubles the risk for preterm delivery (69). Extremes of these psychosocial factors, such as maternal depression have also been associated with PTB (70).

The social factor that has been more firmly associated with preterm delivery is smoking. The association was first suggested in 1957 (71) and has since been confirmed in different cohorts (72) (73). The effect has been shown to be dose-dependent and is more strongly associated with very preterm birth (74).

Despite the fact that the above-mentioned conditions are observed risk factors for preterm delivery, there is no robust mechanistic evidence that fully explains the associations. Conditions that can predispose to preterm birth and for whom some mechanistic insights have been described are discussed right below.

1.7 Causes of preterm birth

1.7.1 Uterine overdistention

An abnormal shape or size of the uterus confers an increased risk for preterm birth. In support of the former, patients having uterine malformations such as a bicornuate or septate uterus are at increased risk for preterm labour and subsequently preterm birth (75). This is also the case for patients with an increase in the size of the gravid uterus because of conditions such as polyhydramnios (76) (77) and multifetal pregnancies (78). This increase in size leads to overdistention of the uterus with a consequent stretching of the myometrium. Mechanistically, a stretching-induced increase in myometrial contractility that can predispose to preterm labour has long been described (79). In addition, myometrial stretching can induce the release of prostaglandins, which are key mediators of the activation of all three components of the parturition pathway (80). Stretching has also been shown to induce the mRNA levels of the contraction associated proteins Connexin-43 (Cx-43) (81) and Oxytocin Receptor (OTR) (82).

However, uterine overdistention also results in the stretching of fetal membranes. Similar to what happens in the myometrium, stretching of amniotic epithelial cells *in*

vitro results in the release of prostaglandin E_2 (PGE_2) and interleukin-8 (IL-8) (83) (84). This indicates that stretching can induce an activation phenotype in the amnion that is compatible with membrane rupture.

1.7.2 Vascularisation disorders

Bleeding and vascularisation disorders have been linked with an increased risk for PTB. Intrauterine bleeding caused by conditions such as placental abruption significantly increase the risk for preterm delivery (85). Potential mechanistic insights have put the coagulation cascade in the centrepiece of the disease pathophysiology (86). In particular, the coagulation factor thrombin has been shown to be able to stimulate contractions of rat myometrial tissue both *in vivo* and *ex vivo* (86). Poor vascularisation can result in abnormal placentation and a consequent placental under-perfusion (87). This unfavourable environment has been associated with PTB (88). A cross-sectional study found that patients delivering early after preterm labour with intact membranes exhibited higher rates of spiral arteries' physiological transformation failure both in the myometrium and the decidua compared to normal term deliveries (88). In further support of the association between vascularization factors imbalance and PTB, it has been reported that a subset of women delivering prematurely demonstrate an anti-angiogenic profile in the maternal plasma that is apparent about 5 weeks prior to spontaneous onset of labour (89). This profile is characterised by both an increase in anti-angiogenic factors as well as an increase in factors that promote vascularisation (89).

1.7.3 Insufficient tolerance to the fetus

Both the fetus and placenta express tissue-specific maternal and paternal antigens. For a successful pregnancy to occur, immune tolerance mechanisms are in place both for the maternal (90) and the fetal side (91). These mechanisms induce the production of tolerogenic maternal and fetal regulatory T cells and safeguard the pregnancy by preventing the gestation equivalents of graft rejection and graft versus host disease respectively. Dysregulation of this tolerogenic state with maternal effector T cell infiltrations and cytokine secretion in the placenta, as in chronic chorioamnionitis, is

often observed especially in late preterm births (92). In addition, increased production of fetal antigens as is the case in antenatal fetal interventions significantly increase the risk for preterm delivery (93) (94). Potential mechanistic insights from mouse models have revealed that this increased production of fetal antigens triggers a breakdown of maternal-fetal tolerance, with a subsequent activation of maternal effector T cells (95).

Even though potential mechanistic insights have been described for the above conditions, further studies are necessary in order for a causal relationship between them and PTB to be established. To date, the only cause of PTB with a well-established causality link and a properly described pathophysiology is an intrauterine infection.

1.7.4 Cervical disorders

Given the importance of the functions of the cervix for a healthy pregnancy, it is no surprise that cervical disorders could account for a number of pregnancy losses and preterm deliveries. Cervical insufficiency is a condition characterized by a painless dilation of the cervix in the absence of myometrial contractions that leads to a recurrent pregnancy loss during in the second trimester. It is reflective of the incompetence of the cervix to retain the uterine content within the uterus.

Cervical insufficiency can be clinically diagnosed depending on specific cervical characteristics. Previous obstetric history of recurrent pregnancy loss after painless cervical dilation in the second trimester is indicative of cervical insufficiency. Clinical presentation with painless cervical dilation in the second trimester is also suggestive of cervical insufficiency. Finally, a short cervix as assessed by transvaginal ultrasound is associated with an increased risk for preterm delivery and can be a predictor of spontaneous PTB, although not necessarily due to cervical insufficiency (96).

Congenital diseases such as a hypoplastic cervix (97) or exposure to diethylstilbestrol *in utero* (DES) (98) could result in cervical insufficiency (99). Genetic factors have also been implicated in the aetiology of cervical insufficiency (100). In particular, specific polymorphisms of the genes collagen 1A1 (COL 1A1) and transforming growth factor beta (TGF-β) are associated with cervical insufficiency (101). Both of

these genes are involved in diseases characterised by dysregulation of the extracellular matrix formation, such as osteoporosis (102) and tumour invasion (103).

The relationship between an inflammatory state and cervical insufficiency is still unclear. A study reported that women with cervical insufficiency had higher levels of the proinflammatory cytokine IL-6 in the amniotic fluid compared to controls (104). From a genetics perspective, a specific polymorphism in the gene of the anti-inflammatory cytokine IL-10 appears to occur more frequently in women with cervical insufficiency compared to healthy controls (105). This could imply that variations in the inflammatory balance during pregnancy might have a role in the pathogenesis of cervical insufficiency.

1.7.5 Infection/inflammation

The first suggestion that infection is implicated in the pathogenesis of preterm birth by being able to cause membrane rupture and preterm labour was reported almost 70 years ago (106). For the next decades the focus was given on extrauterine and often systemic infections that could compromise the maternal health and thus predispose to preterm birth. Examples of such infections include malaria (107) and pyelonephritis (108), pneumonia (109), asymptomatic bacteriuria (110) and more recently periodontal disease (111). However, for the last 30 years the attention has been shifted towards an infection within the intrauterine tissues. This was driven by the finding that bacteria that have invaded the amniotic cavity can induce an inflammatory response in the fetal membranes and the choriodecidual space in patients presenting with preterm labour (112). Overall, infection is considered to account for a minimum of 25-40% of all preterm deliveries, making it the most common cause of preterm birth (113). Percentages vary significantly with gestational age. In particular, infection is implicated in about 10% of late preterm births. By contrast, the rate exceeds 80% in the extremely preterm population (114) (115). The fact that these are the infants facing the greatest risks of neonatal morbidity and mortality showcases the importance of infection as a cause of preterm birth.

The fact that both intrauterine and extrauterine infections have been associated with PTB constitutes one line of support for the suggested causal relationship. Further evidence comes from the fact that preterm birth can be induced by administering live bacteria or bacterial products in different mouse models such as mice (116), rabbits (117) and rhesus macaques (118). This effect can be reversed by the use of antibiotics, as has been shown from both animal (119) and human studies (120). In humans however it has been shown that the only cases that are likely to benefit from antibiotic administration are those with evidence of clinical infection, this being consistent with the causation argument (121). In addition, the presence of cytokines such as IL-6 (122) and matrix degrading enzymes such as MMP-8 (123) in the amniotic fluid significantly increase the risk for PTB. These products are indicative of an inflammatory process secondary to an infectious trigger that is usually subclinical in nature (124).

Mechanism of action

1.7.5.1.1 Toll-like receptors

Once the microorganisms invade the reproductive tissues, they first encounter the innate immune system. To sense the infection, the immune system uses specialised soluble, transmembrane or intracellular proteins that are expressed in immune and epithelial cells and are termed Pattern Recognition Receptors (PRRs). These receptors can recognise molecular structures that are unique to microbes and shared between them. Following ligation of such a structure to its receptor triggers the downstream activation of a non-specific immune response that helps clear the infection. Among the different families of PRRs, the most well-studied in the female reproductive tract that has an active role in the pathophysiology of PTB is the family of Toll-like receptors (TLRs).

To date, ten different TLRs (TLR1-10) have been described in humans and thirteen in mice (TLR1-13) (125). TLR1, 2, 4, and 6 are expressed on the cellular membrane and they can recognize bacterial structures to mount an inflammatory response. By contrast, TLR3, 7, 8 and 9 are intracellular receptors expressed on specialized compartments that are mostly involved in antiviral immunity. The biological function

of TLR10 is not very well defined.In the human reproductive tissues TLR1, TLR2, TLR3, TLR4, TLR5 and TLR6 are expressed both in the lower and the upper reproductive tract. In particular, the vagina and the cervix express TLR1, 2, 3, 5 and 6 (126). The upper reproductive tract is dominated by the expression of TLR2 and TLR4, although TLR1, 3, 5 and 6 are also expressed in the endometrium and the fallopian tubes (127). During pregnancy, the decidua has been shown to express all TLRs throughout the course of gestation (128). TLR2 and TLR4 are also expressed in the pregnant myometrium (129) and the fetal membranes (130) and the expression of both is significantly increased during labour, indicating a role in the parturition process. Important downstream molecules involved in the TLR pathway such as the Myeloid differentiation primary response element 88 (MyD88) protein and CD14 are also expressed in the reproductive tissues (127) (128).

Overall, this body of literature suggests that the reproductive tissues during pregnancy are able to sense a microbial infection to mount an inflammatory response though the TLR family of PRRs, similar to what happens in other tissues. Crucial to this suggestion has been the finding that blocking the activity of TLR4 either by TLR4-specific monoclonal antibodies (131) or by using a receptor antagonist (132) can stop preterm birth induced by live bacteria or bacterial products. Similarly, mice that express a mutant TLR4 receptor are resistant to PTB induced by the same substances (133). This has led to the theory that TLR4 signalling could be targeted as a potential a therapeutic strategy for PTB (134).

Recently, it was reported that in the presence of chorioamnionitis, the most common infection preceding preterm birth, there is an increased upregulation of TLR-1 and TLR-2 in the amnion, the chorion and the decidua (135). In addition, another study found that that TLR-1 is also upregulated in pregnancies complicated by chorioamnionitis that eventually deliver prematurely (136).

Upon ligation of specific microbial or viral molecular structures called PAMPs (Pathogen-associated molecular patterns), TLRs undergo conformational changes that lead to the recruitment of specialised adaptor molecules. These molecules drive the

signalling pathways downstream of TLRs. Four such adaptor molecules have been discovered to date: MyD88 (137), TIR- associated protein (TIRAP) (138), TIR-domain-containing adaptor protein-inducing IFN-β (TRIF) (139) and TRIF-related adaptor molecule (TRAM) (140). Ligation of different PAMPs stimulates different TLRs leading to recruitment and activation of different adaptor molecules. Downstream signalling via MyD88 leads to the transcription of genes encoding proinflammatory cytokines whereas signalling through TRIF leads to the transcription of genes encoding interferons.

Most TLRs signal through the adaptor molecule MyD88. This signal, via recruitment and activation of the intermediate molecules interleukin-1 receptor-associated kinase 1 (IRAK1) (141) and IRAK4 (142) and then TNF receptor associated factor 6 (TRAF6) (143) leads to phosphorylation and nuclear translocation of the transcription factor nuclear factor kappa B (NFκB). In addition, these pathway leads to the phosphorylation of MAP kinase kinase 6 (MKK6) which then subsequently phosphorylates further MAP kinases (144). The endopoint of the cascade is the production of inflammatory mediators such as cytokines and chemokines (145).

1.7.5.1.2 Cytokines and chemokines

Cytokines and chemokines have been central to the pathophysiology of preterm birth. The first cytokine to be associated with the mechanisms of infection-induced preterm birth was Interleukin 1 (IL-1). The study found that women in preterm labour with intra-amniotic infection had increased IL-1 activity in the amniotic fluid that correlated with an increase in prostaglandins E2 and F2a (146). The amnion itself can produce prostaglandins in response to IL-1 treatment in a dose-dependent manner (147). Another reproductive tissue capable of secreting IL-1 is the decidua (148). In addition, IL-1 family and IL-1b in particular has been shown to have the capacity to stimulate myometrial contractions during pregnancy in a non-human primate model using rhesus monkeys. Furthermore, it increased the production of other proinflammatory cytokines and prostaglandins in the amniotic fluid on the rhesus monkeys (149). In mice, a subcutaneous injection of IL-1 was used to establish the first mouse model of preterm

birth as all mice that were injected delivered prematurely (150). In further support of the role of IL-1 in this model, abrogating IL-1 activity by using an IL-1 receptor antagonist managed to stop preterm delivery in these mice (151).

Production and release of IL-1b is done through a distinctively characteristic intracellular pathway (152). Initially, following gene transcription mediated by NFκB, an inactive precursor of IL-1b is produced, termed pro-IL-1b (153). This is then proteolytically cleaved by a protease called caspase-1 to acquire its active form, IL-1b (154). The activation of caspase-1 is mediated by a protein complex called the inflammasome. The different components that form the inflammasome complex are: a sensor molecule, an adaptor molecule called ASC and caspase-1 (155). A wide range of sensor molecules has been described to date (156). Most of them contain a NOD-like receptor sensor, most notably, in the case of bacterial infections, NLRP3 (157). ASC then mediates the assembly of several pro-caspase 1 molecules, the self-cleavage of which leads to the formation of the active caspase-1 which then connects to NLRP3 (155).

The number of cytokines with a role in preterm birth expands beyond the IL-1 family. Interleukin-6 (IL-6) was the next cytokine to be associated with infection-induced preterm birth. It was found that women presenting with preterm labour that have an intra-amniotic infection exhibit significantly higher levels of IL-6 in the amniotic fluid (158). Higher IL-6 levels were also observed in women in preterm labour failing to respond to tocolytic therapy (158). IL-6 can also be used for detecting women at term with microbial invasion of the amniotic cavity (MIAC) as it demonstrates significantly increased levels in the amniotic fluid (159) (160).

Similar were the findings for the proinflammatory chemokine Interleukin-8 (IL-8). The levels of IL-8 were found to be higher in the amniotic fluid of women in preterm labour with PPROM and positive amniotic fluid cultures (161) (162).

Such is the case also for Tumor necrosis factor A (TNFα). Its levels were measurable in the amniotic fluid of women in preterm labour and with intra-amniotic infection as opposed to women without infection who had no detectable TNFα levels even in the

presence of preterm labour (163). Also bacterial products can stimulate reproductive tissues, such as the decidua to produce TNFα (164) (165).

Other studies examined a series of proinflammatory cytokines rather individual ones. Similar to previously described studies, the levels of both IL-6 and IL-8, as well as the inflammatory cytokine Granulocyte-colony stimulating factor (G-CSF) were found to be increased in the amniotic fluid of women with intrauterine infection, more so for those in preterm labour (166). Another study reported that increased levels of IL-1a, IL-1b, IL-6, IL-8 and TNFα in the amniotic fluid were associated with histologic chorioamnionitis and the presence of bacteria in the amniotic fluid (167). The same study also found that elevated levels of the above cytokines can predict delivery with 7 days of the measurements as well as delivery before 34 weeks (167). Early onset neonatal infection is a significant cause of neonatal morbidity and mortality. Responsible pathogens can often be acquired *in utero*. Infected newborns have elevated plasma levels of both IL-6 and TNFα (168).

A very important finding supporting the concept that infection-induced preterm birth is mediated by cytokines came from mice. By using animals lacking both the IL-1 and TNF receptor, the group made the observation that these mice had significantly lower preterm birth rates compared to their wildtype counterparts after intrauterine administration of live *Escherichia coli* (169). This means that the IL-1 and TNF signalling pathways are necessary for *E. coli*-induced preterm delivery in mice, highlighting the importance of these cytokines (169). In addition, in mouse models of preterm birth that use bacterial products such as Lipopolysaccharide (LPS) (170) and Lipotechoic acid (LTA) (171) as a stimulus, there is significant upregulation of an array of cytokines and chemokines in the plasma and the amniotic fluid, notably IL-1a, IL-6 and TNFα.

Collectively, these data solidify the essential role of proinflammatory cytokines in infection-mediated preterm birth. Crucial for the pathophysiology of preterm parturition is the ability of these cytokines to regulate the production of the key proteins prostaglandins and matrix metalloproteinases.

1.7.5.1.3 Prostaglandins and Matrix metalloproteinases

Both prostaglandins and matrix metalloproteinases (MMPs) are key to the inflammatory response and have a central role in the parturition process. Prostaglandins are lipid mediators that exert their actions in a paracrine and autocrine fashion. The function of prostaglandins is crucial to parturition as they promote myometrial contractility, membrane rupture, cervical dilatation, placental separation and finally uterine involution (172). MMPs are proteolytic enzymes that participate in extracellular matrix degradation processes. They are particularly involved in the remodelling and rupture of the fetal membranes and the remodelling and ripening of the cervix during parturition (173).

An important aspect in the pathophysiology of infection-mediated preterm birth is the regulation of prostaglandins by proinflammatory cytokines. Both IL-1 and TNF stimulation has been shown to increase the expression of prostaglandins or the main prostaglandin synthesising enzyme Cyclooxygenase-2 (COX-2) both *ex vivo* (174) and *in vitro* (175). Such is the case for other tissues of the upper reproductive tract including the decidua (176), the amnion (177) and the chorion (178). Other cytokines, such as IL-6 (179) and macrophage inflammatory protein-1 alpha (MIP-1a) (180) in the amnion and the decidua and in both membranes respectively.

As further indication of the link between infection, cytokines and prostaglandins, the bacterial product LPS has been shown to signal through the TNFα pathway to stimulate PGE_2 production by human choriodecidual explants (181). In addition, the expression of COX-2 in the amnion depends on the NFκB activation, which is downstream of TLR signalling and can also be increased by IL-1b (182). Instead of promoting the expression of prostaglandin synthesising exzymes, cytokines such as IL-1b and TNFα (183), and bacterial products such as LPS (184) act to enhance prostaglandin activity by decreasing the catabolic activity of the enzyme Hydroxyprostaglandin dehydrogenase (PGDH) (185).

The production of the extracellular matrix-degrading enzymes MMPs in the reproductive tissues can be stimulated both by cytokines and by prostaglandins. In the

upper reproductive tract, TNFα, IL-1b and Macrophage colony-stimulating factor (M-CSF) can increase the secretion of MMP-9 by first trimester trophoblast cells with a subsequent increase in its collagenase activity (186). IL-1a can stimulate chorionic cells to produce MMP-1 *in vitro* (187). *In vivo*, IL-1b can increase the secretion of MMP-9 by the chorion and amnion resulting in increased MMP-9 concentrations in the amniotic fluid (188). Prostaglandins such as PGF_{2a} also increase the expression of MMP-2 and MMP-9 in decidual explants *ex vivo* (189).

Similar is the effect of infectious agents and live bacteria in the production of MMPs. LPS can increase the production of both MMP-2 and MMP-9 by human amniochorionic membranes, an effect that can be ameliorated by the anti-inflammatory cytokine Interleukin-10 (IL-10) (190). In non-human primate model using rhesus monkeys, the researchers found that group B streptococci bacterial infection of the choriodecidual space results in increased MMP-9 expression and activity in the amniotic fluid, an effect almost identical to that of IL-1b (188).

In the lower reproductive tract, the production of MMPs is also stimulated by cytokines. In particular, TNFα has been shown to induce the expression of MMP-1, MMP-2 and MMP-9 by cervical smooth muscle cells *in vitro* (191). There is also a correlation between the expression levels of the chemokine IL-8 and those of MMP-8 and MMP-9 in the lower uterine segment and the cervical stroma that is consistent between different studies (192) (193). The same association between IL-8 and MMP-8 and -9 has also been observed in upper reproductive tissues including the myometrium, the decidua and the fetal membranes (194). Furthermore, on top of promoting the expression and activity of MMPs, cytokines like TNFα have the capacity to suppress the production of the MMP inhibitors called tissue inhibitors of metalloproteinases (TIMPs) (195).

To summarise this section, current evidence describes a well-defined pathophysiology of how intrauterine infection can lead to preterm birth. Upon recognition of the microorganism by TLRs, an inflammatory process orchestrated by NFκB is initiated. This leads to a secretion of cytokines and chemokines by the reproductive tissues

involved, which in turn stimulate the production of prostaglandins and MMPs. The latter can then activate all three components of the parturition process, the onset of which can thus be dictated by the intrauterine infection.
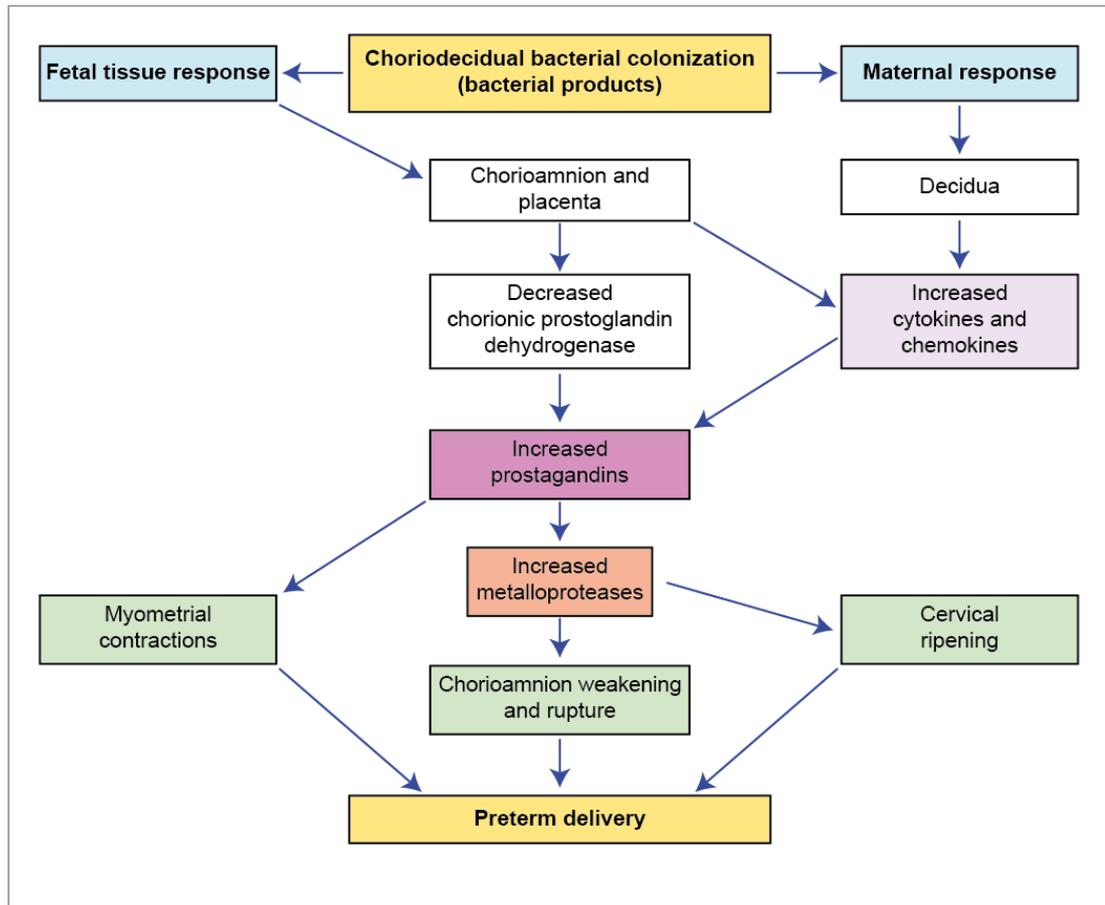
Figure 1.2 Proposed pathway leading from bacterial uterine colonization to preterm delivery. Adapted from (113).

Routes of infection and pathogens

Several hypotheses have been postulated regarding the route leading to an intrauterine infection. Potential routes include the following: i) Ascending infection from the vagina and through the cervix. ii) Haematogenous dissemination through the placenta. iii) Accidental introduction during invasive medical procedures such as amniocentesis

and chorionic villous sampling that could penetrate the reproductive tissues. iv) By retrograde spread from the abdominal cavity and through the fallopian tubes (113).
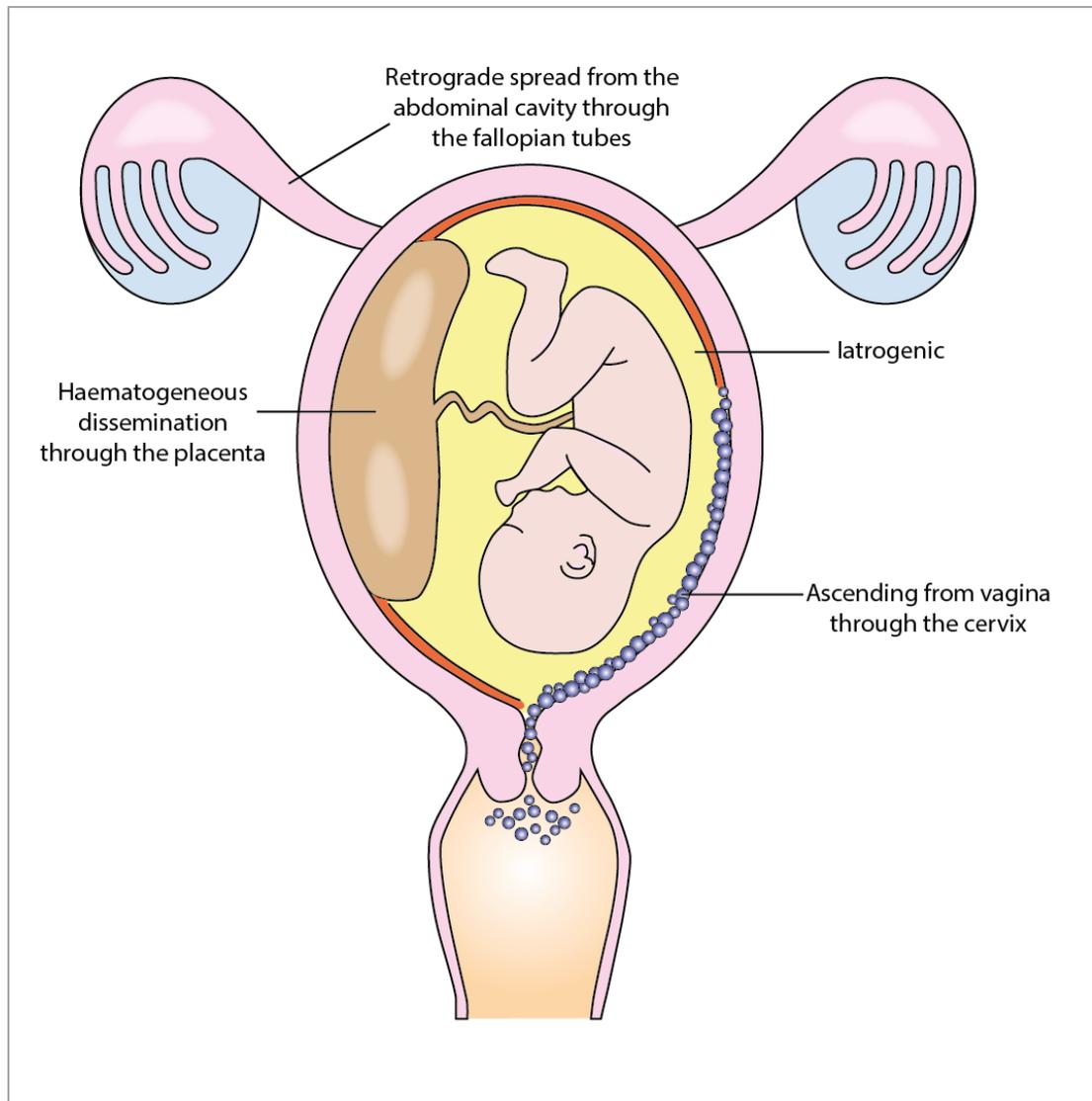
Figure 1.3 Most common routes of intrauterine infection. Adapted from (196).

Among the microorganisms that have been associated with preterm delivery are the following: *Ureaplasma* species (197) (198), *Gardnerella vaginalis* (199) (198), *Mycoplasma hominis* (197) (199), *Bacteroides* species (199) and *Fusobacterium* species (197). What these bacteria have in common is that they are of vaginal origin

and that most of them belong to the genital mycoplasma species. Much rarer is the case for bacteria that are commonly implicated in genital tract infections in non-pregnant women, such as *Chlamydia trachomatis and Trichomonas vaginalis* (160). The presence of non-genital bacteria has been reported but it is quite rare (200). This means that the microorganisms most frequently isolated from the amniotic cavity of women that deliver preterm are of vaginal origin. This suggests the most common route of intrauterine infection is the ascending vaginal infection through the cervix. This concept is supported by a clinical study which found that microbial invasion of the amniotic cavity (MIAC) precedes the invasion of the chorioamniotic membranes in most cases of chorioamnionitis (201). The only route of infection consistent with this finding is the ascending infection through the cervix.

Among the bacteria that have been associated with preterm delivery the most common ones belong to the *Ureaplasma* species (198) (202). They are also the bacteria most commonly isolated from the amniotic fluid of women with chorioamnionitis (203) and of women with chorioamnionits and preterm birth (204).

1.8 The *Ureaplasma* species

The *Ureaplasma spp* were first discovered in 1954 as a potential causative agent of non-gonococcal urethritis in males (205). They do not have a cell wall and thus cannot be stained by the Gram staining. Instead, they are surrounded by a plasma membrane and can therefore acquire a wide range of shapes and structures. This results in significant size variations (100 nm to 1 µm) even between *Ureaplasmas* of the same colony (206). This ranks them among the smallest microorganisms. The colonies themselves can range in size from 5 to 20 µm. An important distinguishing figure of *Ureaplasmas* is the fact that they produce a urease enzyme. This enzyme catalyses the hydrolysis of urea, in a reaction that allows the bacteria to produce virtually all of its energy requirements (207).

There are two species of the human *Ureaplasmas*: *Ureaplasma urealyticum* and *Ureaplasma parvum* (208). Fourteen (14) strains or serovars have been recognised to date. Serovars 1, 3, 6 and 14 belong to *U. parvum* and the rest to *U. urealyticum* (208).

U. parvum is smaller than *U. urealyticum* (209) and they also have differences in their urease genes (210) as well as their main pathogenicity factor, the multiple-banded antigen (MBA) (211) (212).

The potential of *Ureaplasmas* to adhere to mammalian cells has been described. Specifically, they have been shown to adhere to human erythrocytes (213) and epithelial cells (214). In addition, their ability to adhere to and stimulate placental endothelial cells has also been reported (215). However, little is known about the mechanisms utilised by the *Ureplasma* spp to facilitate this. Cell surface receptors terminating in sialic acid have been implicated in these mechanisms, since a marked reduction in bacterial adherence to HeLa cells and erythrocytes was noticed following pre-treatment with neuraminidase (214).

With regards to cellular responses to *Ureaplasma* infection, mechanistic studies have provided insights towards stimulation of different pathways. In placental endothelial cells, *Ureaplasmas* can induce a stress response characterised by reduced expression of heat shock protein 70 (215). This renders host cells more susceptible to apoptosis and is mechanism commonly utilised by different bacteria (216) (217). They can also cause a significant significantly increase the levels of intracellular calcium and iron, in line with a stress response (215). Furthermore, *in vitro* studies have demonstrated the potential of *Ureaplasma* spp to induce apoptosis in human type II lung epithelial cells and macrophages (218). Both *U. parvum* and *U. urealyticum* can also deploy immune evasion mechanisms by downregulating the gene expression of antimicrobial peptides such as DEFB1, DEFA5, DEFA6 and CAMP in human THP-1 cells (219).

The major virulence peptide of *Ureaplasma* spp is called Multiple-Banded Antigen (MBA) (220). This is a factor that can only be found in this species (221) and constitutes a potent cytokine inducer (222). It is thought to exert its actions by stimulating the toll-like receptors -1, -2, -6 and -9 (223) (224) (225). In addition, specific *U. parvum* (Serovar 3) and *U. urealyticum* (Serovars 4, 8) serovars express the enzymes Phospholipase A1, A2 and C (226) (227). These can cause phospholipid degradation by hydrolysing acyl ester and phosphodiester bonds respectively (228).

This has the potential to destabilise the cellular membrane leading to a reduced cell viability (228).

Ureaplasmas are thought to be commensals of the lower reproductive tract in women. In support of this, they can quite often be found in the lower reproductive tract of sexually active women. The percentage has been shown to range between 40% (229) and 80% (230). The more common of the two is *U. parvum* (231). Further evidence comes from the report that women presenting with symptoms of lower genital tract infections have similar colonization rates of *Ureaplasma* spp with women of the control group with no infection (231). However, this is not always the case as *Ureaplasmas* have been shown to be able to cause infections of the female reproductive system. In particular, there are reports associating them with infection of both the vagina (232) and the cervix (233), as well as urinary tract infections (234) (235) and bacterial vaginosis (236). What determines why this happens in some women and not in others has not been elucidated yet.

Importantly, the presence of *Ureaplasmas* in the lower reproductive tract has been recognized as a potential risk factor for adverse pregnancy outcomes including preterm delivery. Vaginal colonization with *U. parvum* was found to be an independent risk factor for preterm birth or late abortion with an OR of 3 (237). The same study examined other genital *Mycoplasmas* but none of them was associated with the above outcomes (237). Although not in the same study, *U. urealyticum* has also been described as a risk factor for preterm delivery (238). Similar to the vagina, colonization of the endocervix with the *Ureaplasma* spp was also associated with preterm delivery in women presenting with preterm labour and intact membranes (239). As further support of this association, a quantitative approach has been also studied. The study found that women that had increased titres of *U. urealyticum* in the vagina were at increased risk of preterm birth (240). This was not the case for women colonized with low titres (240). Despite being a strong candidate as a risk factor for PTB, lower reproductive tract colonization with *Ureaplasma* spp cannot actually predict PTB (241). The reason for this is the high proportion of women than deliver normally at term despite having their vagina or cervix colonized with *Ureaplasmas* (242).

Despite normally colonizing the female lower reproductive tract, the *Ureaplasma* spp have also the potential to ascend to the upper reproductive tract as they have also been found in tissues such as the endometrium and the fallopian tubes (243) (244). In most cases they are not causing any inflammation, however they possess the capacity to cause an infection, which is more often subclinical in nature (245).

Quite crucial to the association between *Ureaplasma* spp and PTB is the fact that these bacteria are also considered to be causing chorioamnionitis, the infection implicated to 40-70% of all preterm births (246). The first study that described the potential link was back in 1975 and used culture methods on swabs from the infants' ears, throat, umbilicus, external genitalia and the perineum. They found a significant association between fetal colonization with *Ureaplasma* spp and histological lesions in the placenta that were consistent with chorioamnionitis (247). Later, the presence of *Ureaplasma* spp in the fetal serum and the fetal cerebrospinal fluid were also associated with chorioamnionitis (248). Their isolation in these compartments could potentially imply a role in cases of intraventricular haemorrhage as well. The results are also similar when examining the presence of *Ureaplasmas* in the cord blood, as an association with chorioamnionitis, PROM and earlier gestation has been noticed (249).

Most studies that have addressed this question have chosen to examine the presence of *Ureaplasma* spp either in the amniotic fluid or the placenta. High titres of *Ureaplasma* spp in the amniotic fluid have been found to be associated with higher incidence of both intra-amniotic inflammation (250) and histological chorioamnionitis (251).

Consistent with the findings in the other tissues and body fluids, placental colonization with *Ureaplasma* spp is associated with histological chorioamnionitis and low birth weight (252). This has been described in different gestational ages. The presence of *Ureaplasma* spp was found to increase the risk for histologically confirmed chorioamnionitis and intra-amniotic inflammation in moderate and late preterm births (253). This is also the case for extremely preterm deliveries (254). In these instances, chorioamnionitis is also increased risk of intraventricular haemorrhage and subsequent brain lesions (254) as well as chronic lung disease (255).

From a pathophysiological perspective, studies in animal models have shown that *Ureaplasmas* can stimulate the mechanistic pathways that are implicated in infection/inflammation-induced preterm birth. Specifically, intrauterine infection with *U. urealyticum* has been shown to increase the protein expression of TLR2 and the important TLR co-factor CD14 (256), which is also found upregulated in the amniotic fluid of women infected with *Ureaplasma* spp (257). In a sheep model of intra-amniotic infection, administration of *U. parvum* can mount an inflammatory response that is characterised by increased expression of the proinflammatory cytokines IL-1b, IL-6 and IL-8 in the chorion and the amnion (258) as well as the fetal lung (259).

Studies in non-human primates further are also consistent with the above findings. IL-6 and IL-8 were increased in the amniotic fluid and the fetal lung of pregnant baboons 2-3 days post-intra-amniotic inoculation with *U. urealyticum* (260). After administration of *U. parvum* to rhesus monkeys, a mild inflammatory response is observed with upregulation of TNFα, CXCL-8 and CCL-8 (261). In another study on non-human primates, intra-amniotic administration of *U. parvum* to pregnant rhesus monkeys was found to elicit an inflammatory response that resulted in a significant increase of IL-1a, IL-1b, IL-6, IL-8 and TNFα in the amniotic fluid after 2-3 days (262). This study also reported increased amniotic fluid levels of the prostaglandins E$_2$ and F$_{2a}$ and increased activity of MMP-9 (262). These resulted in increased uterine contractions as measured by the intrauterine pressure changes and ultimately led to preterm delivery (262).

Overall, these data highlight the importance of *Ureaplasma* spp as microorganisms commonly associated with preterm delivery. This is in large due to their role as causative agents of chorioamnionitis, the most common antecedent of preterm birth. Furthermore, the *Ureaplasma*-induced pathophysiology during pregnancy is compatible with the mechanisms involved in inflammation-induced PTB. Therefore, the *Ureaplasma* spp are clinically relevant bacteria for preterm birth.

1.9 The role of the cervix

As discussed before, the cervix constitutes one of the three components of the parturition process. However, its role during pregnancy extends well beyond parturition itself.

1.9.1 The cervix during pregnancy

During the course of gestation, the cervix remains closed and firm in order to support and keep the conceptus within the uterus. At the same time, it undergoes progressive remodelling that ultimately leads to parturition related changes, effacement and dilatation.

Remodelling of the cervix is divided into four phases. These phases overlap with one another and are termed softening, ripening, dilation and postpartum repair. Cervical softening is a long procedure that spans across the whole of gestation and is characterised by a progressive increase in tissue distensibility that can be clinically assessed in the first trimester of pregnancy. The main feature of cervical softening is the change in the structure of collagen, the most abundant protein of the cervical extracellular matrix. This is characterised by a decrease in the formation of cross-links between collagen fibres (263). An important reason for this is the decrease in the expression of the key enzymes thrombospondin 2 and tenascin C, which are involved in the cross-link formation (264). The end result is a gradual increase in collagen solubility and a subsequent loss in tensile tissue strength in the absence of an increase in tissue hydration.

In contrast with the long and progressive nature of cervical softening, ripening and dilation occur very rapidly at the end of pregnancy. They thus overlap to a great extent as the ripening process allows maximum compliance of the cervical tissue, something that facilitates dilation to allow the fetus to pass through. This maximum compliance is achieved by an increase in the diameter of the collagen fibres and their in-between spacing (265).

Finally, timely recovery of the cervix postpartum is essential to maintain protection from potential environmental threats. The tissue repair process initiated results in increased cross-linking of collagen fibrils to promote return of the cervix to the pre-pregnancy state (266).

1.9.2 Barrier function against infection

By being located between the uterus and the vagina, the cervix is what separates the uterine content from the bacteria-rich vaginal environment. To exert its role in safeguarding pregnancy, the cervix forms both a physical and a functional barrier against infections that could potentially be detrimental to pregnancy by leading to preterm birth and other complications. Central to these, is the role of the cervical epithelium.

Physical barrier

The cervical epithelium is divided into two parts: the columnar endocervical and the stratified squamous ectocervical epithelium. The physical part of the barrier to infections is achieved by a precise regulation of the expression of specific proteins that participate in inter- and intra-cellular adhesions. Among these proteins are tight junction proteins, adherens junction proteins and desmosomes (267) (268). In particular, the mouse cervix expresses the tight junction proteins claudin 1 and claudin 2. During pregnancy, the expression of the tight junction protein claudin 1 in the mouse cervical epithelium progressively increases (269). At the same time, the expression of claudin 2 decreases in a similar fashion (269). This phenotype is characterised by a much more efficient barrier function with increased tightness between the adjacent cells (270). Loss of claudin function has been shown to compromise the epithelial barrier (271).

Other junction proteins expressed in the cervix include occludin (272) (273), zona occludens (274) and junctional adhesion molecule-A (JAM-A) (275). Specific microRNAs that target the expression of these proteins can be expressed during pregnancy (276) (277). Importantly, a study on cervical smears found that women that

went on to deliver preterm had an increased expression of miR-43 and miR-45 earlier during gestation (278). These microRNAs target JAM-A and could thus compromise the epithelial barrier function of the cervix to increase susceptibility to PTB (279). It has also been found that inappropriate differentiation of the cervical epithelial cells of the mouse results in loss of the barrier function and increased preterm birth rates after vaginal administration of *E.coli* (280).

Functional barrier

The epithelium also plays a major part in the functional barrier of the cervix during pregnancy. Cervical epithelial cells can sense a bacterial infection, as they have been shown to express TLRs, in particular TLR2 and TLR4 (281). They can also secrete proinflammatory cytokines and chemokines to stimulate the immune response (282). In addition, the epithelial cells participate in the effector mechanisms of innate immunity by secreting antimicrobial peptides. In particular, they can secrete Secretory Leukocyte Protease Inhibitor (SLPI) (283), Elafin (284) (283), and LL-37 (285). A study in mice reported that the expression of TLRs and the expression and function of antimicrobial peptides can be diminished by a viral infection (286). This could lead to a disruption of the functional arm of the cervical barrier function and increase susceptibility to infection-induced preterm birth. Overall, these data suggest that cervical epithelial cells have an important role in the innate immunity of the cervix and therefore the whole pregnancy.

Cervical mucus and plug

Cervical epithelial cells also have a pivotal role on the formation of the mucosal barrier of the cervix by secreting significant amounts of mucus. During pregnancy, the epithelial cells secrete a much thicker mucus that forms a plug. This thick layer of mucus ends up filling the cervical canal and sealing off the uterine cavity. Thus, another important layer of physical protection is added by the cervix during pregnancy.

In addition, the mucus plug has some unique immunological properties that are crucial to the functional barrier function of the cervix during pregnancy. Innate immune mechanisms are in place in the cervical mucus plug. Various antimicrobial factors can

be found into the mucus including SLPI, lysozyme, calprotectrin, lactoferrin and human β-defensin 1 (HBD-1) (287) (288). Furthermore, the proinflammatory cytokines IL-1b, IL-6, IL-8 and TNFα have been found to be present in the cervical mucus (289) (290). Levels of proinflammatory cytokines like IL-18 in the mucus plug are not associated with the levels in the amniotic fluid (291). This is indicative of the fact that the cervix is a separate compartment that has to respond to infectious challenges distinctively. Among these cytokines, IL-6 in particular has shown potential as a biomarker for pregnancy complications. Increased levels of IL-6 on cervical secretions are associated with chorioamnionitis. In addition, they have been associated with PPROM (292). Finally, several studies have found an association between IL-6 and preterm delivery (292) (293) (294). As its levels are only moderately predictive of preterm birth, it has limited use as biomarker (295). However, this is still reflective of the role of the cervix as an immunological barrier to infection.

Factors of the highly-specialized adaptive immune response are also present in the mucus plug. The immunoglobulins IgA, IgG and IgM can be found in abundance within the mucus plug (296). This is a specific adaptation to pregnancy as the levels of IgA and IgG are actually much higher in the mucus plug compared to the mucus from non-pregnant women (296). Also, the IgA levels in the cervical mucus plug are much higher than their respective serum levels in pregnant women (297).

These antimicrobial properties of the mucus plug have been proven *in vitro*. Cervical mucus plugs from healthy pregnant women can completely inhibit the growth of bacteria such as *Staphylococcus saprophyticus*, *E.coli*, *Pseudomonas aeruginosa* and Group B *Streptococcus* (298).

1.9.3 Cervical epithelial injury

Iatrogenic cervical injury has also been associated with preterm birth and as a potential cause of cervical insufficiency. Procedures that damage the cervix are commonly performed for the treatment of cervical intraepithelial neoplasia. This is a pre-cancerous state of the cervical epithelium that in some cases evolves into invasive cervical cancer. Excisional procedures like cold knife conisation, laser conisation and

large loop excision of the transformation zone (LLETZ) (also termed loop electrosurgical excision procedure-LEEP) are used to remove the lesions once the diagnosis is confirmed (299).

All excisional procedures have been consistently associated with a subsequent preterm delivery. Laser conisation and LLETZ were reported to increase the risk for PPROM in a retrospective cohort study from a colposcopy clinic in New Zealand by 2.7- (95% CI, 1.3-5.6) and 1.9-fold (95% CI, 1.0-3.8) respectively (300). A population based cohort study from Norway found that cervical conisation treatments had a relative risk of 4.4 for extremely preterm delivery, a risk of 3.4 for very preterm delivery and a risk of 2.5 for late preterm delivery (301). A smaller but still significant risk of preterm birth after conisation treatments was also reported in a cohort study from England, where the relative risk was 1.19 (95%CI, 1.01-1.41) Similar were the findings for LLETZ from another population based cohort study from Denmark, which identified a relative risk of 2.07 (95% CI, 1.88-2.27) among women that were treated with the procedure (302).

Secondary analyses that took place confirmed the above findings. A secondary analysis on pregnant women participating in multicentre studies and randomized for treatment interventions in London found an increased risk for preterm delivery both before and after 34 weeks gestation in women previously treated with LLETZ (303). The relative risk was 2.71 (95% CI, 1.63-4.52) (303). A systematic review and meta-analysis found that both cold knife conisation and LLETZ are significantly associated with a subsequent preterm birth (304). The relative risks were 2.59 (95% CI, 1.80-3.70) and 1.70 (95% CI, 1.24-2.35) respectively (304). These findings were in agreement with a later systematic review and meta-analysis that reported an increased risk of preterm delivery in women previously treated with excisional procedures compared to the control group (RR 1.96, 95% CI 1.46-2.64) (305).

What these procedures have in common is the fact that they remove a part of the epithelium along with the underlying stroma. As described earlier, the importance of the cervical epithelium in the barrier function of the cervix against infection is

paramount. However, no satisfactory explanation has been provided for the association between excisional procedures and preterm birth.

1.10 Animal models of Preterm Birth

Despite the growing body of literature that provides new insights into the pathophysiology of preterm birth, the incidence of the syndrome has not changed substantially over the past decades. This may reflect the fact that our current understanding of the mechanisms implicated in preterm birth is incomplete. Due to a series of ethical and practical restrictions, mechanistic studies in humans are difficult.

From an ethical perspective, human samples cannot be collected at predefined time points to ensure optimal experimental design. Also, experiments can only be performed *ex vivo* or *in vitro*, making it hard to link any intervention with the pregnancy outcome. Practical restrictions include the limited number of human tissues that can be readily available for research purposes. With the exception of the placenta and the fetal membranes, the other reproductive and fetal tissues cannot be collected as a whole from humans. More tissues become available in the case of caesarean sections, but still not as a whole. For example, decidual samples are usually collected only from the superficial layers and myometrial samples are usually collected from the upper flap of the lower transverse incision through the uterine wall (306). This makes the effort to extrapolate the findings very difficult. Overall, these limitations have necessitated the use of animal models for an in-depth study of the preterm birth pathophysiology. Different species have been used in preterm birth research and, despite their limitations, each has significantly contributed to our current understanding.

1.10.1   Sheep

Historically, sheep has been the first animal model to contribute to the basic understanding of the mechanisms of parturition. The size of sheep is closer to humans compared with most other animal models. Importantly, the fetal weight of the sheep at birth is very similar to the fetal weight of humans (307). Such is also the size of the

litter as the sheep usually have 1-2 fetuses per pregnancy. The gestational length at an average of 147 days is also closer to the human average of 280 days than any other model that has been studies, with the exception of non-human primates (308). The development of surgical techniques that enabled catheterization of intrauterine compartments was crucial for the widespread use of this model (308).

The use of sheep has been pivotal for the current understanding of the endocrinology of parturition. The studies that identified the role of the fetal Hypothalamus-Pituitary-Adrenal (HPA) axis were first conducted in sheep. In particular, it was first reported 50 years ago that a continuous and prolonged administration of Adrenocorticotropic hormone (ACTH) to fetal lambs mid- to late- gestation induces preterm delivery within one week (309). Administration of cortisol to the fetus yielded similar results (309). The same group also found that glucocorticoids administered to the fetus can induce preterm birth in sheep (310).

From the maternal side, it was found in sheep that a single administration of estradiol benzoate induces delivery within 48 hours (311). Studies in sheep also helped establish the role of prostaglandin F_{2a} as a potential agent to stimulate myometrial contractions (312). This prostaglandin was also shown to be able to induce preterm birth, albeit at lower rates compared to glucocorticoids such as flumethasone (FLU) (313). An increased in the levels of prostaglandin F_{2a} is achieved by a shift in the hormonal balance with towards a decrease in progesterone activity with a concurrent increase in estradiol levels, which initiates labour (314). When continuously administered prostaglandin E_2 can cause preterm birth in sheep as well, by activating the fetal HPA axis (315). Collectively, these data were crucial helped to clarify the series of hormonal events leading to the onset of labour. Briefly, increased ACTH secretion from a mature fetal HPA axis stimulates corticosteroid secretion from the fetal adrenal gland. The increased cortisol secretion, along with promoting maturation of the fetal lung it stimulates the placental conversion of progesterone to estrogen. This increases the levels of prostaglandins in the process of a pro-labour phenotype acquisition (316).

When studying the mechanisms of infection-mediated preterm birth, the sheep model has also been valuable. The big gestational length allows for samples to be collected at various time points and it also potentiates the study of the effect of chronic exposure to infectious stimuli. However, creating a sheep model of infection-induce preterm birth has been very challenging. Intravenous infusion of LPS derived from *Salmonella typhimurium* can has been shown to cause birth within 28 hours (317). Still, this model does not satisfactorily recapitulate the most clinically relevant case of intrauterine infection. Intra-amniotic administration of *E. coli*-derived LPS has also been reported to induce preterm delivery, in this case within 72 hours (318). Yet, this is not the case in most studies that have been performed so far. In fact, despite the initiation of a potent inflammatory response at the gestational tissues, preterm birth was not achieved after administration of either intra-amniotic (319) (320) or extra-amniotic LPS (319) (321) or live *U. parvum* (322).

On the positive side, this allows for the study of the effects of infectious agents to the fetus to be examined *in utero* and at different time points, since preterm delivery does not occur. However, the very fact that bacterial products and live bacteria cannot consistently induce preterm birth restricts the use of sheep as a clinically relevant model to study infection-mediated preterm delivery. In addition, the sheep's immune system is not very well characterised and there is a shortage of available molecular tools to develop proper mechanistic studies (308). Lastly, practical reasons such as the requirement for large landholdings and specialized storage facilities further limits the use of this model.

1.10.2   Non-human primates

The species more closely related to humans, is the nonhuman primates. Pregnancy in this species resembles human pregnancy much closer compared to sheep or rodents (323). The gestational length of around 170 days which is longer than any other PTB model and the singleton pregnancies which are usually the case, are two features of the species alignment (324). They also possess a unicornuate uterus like humans (323).

As in sheep, the biotechnology tools necessary for catheterisation of the intrauterine compartments have been fully developed (325) (326) (118).

Nonhuman primates have been an invaluable model for the *in vivo* study of uterine electrophysiology during pregnancy. It was first found that cynomolgus monkeys have synchronous uterine contractions at the third trimester that could resemble those observed in humans (327). Based on this knowledge of the uterine contraction pathways, potential tocolytic drugs have been tested in nonhuman primates. As in humans, oxytocin induces preterm labour in cynomolgus monkeys (328). The oxytocin receptor antagonists Barusiban and Atosiban are highly efficient in reducing oxytocin-induced uterine contractions and can delay the onset of labour and therefore prolong the pregnancy (328). However, they were ineffective in stopping normal labour (329).

The pathways of infection-induced preterm birth have also been studied in non-human primates. The first model was described in the rhesus monkeys where an intra-amniotic administration of live Group B *Streptococci* resulted in significant increases in the levels of the proinflammatory cytokines TNFα, IL-1a and IL-6 in the amniotic fluid (330). This was then followed by an increase in the levels of prostaglandins E_2 and F_{2a} which resulted in an increase in myometrial contractility (330). The end result was delivery within 28 hours of the inoculation (330). The same research group then took this model one step closer to recapitulating the more clinically relevant scenario of ascending infection by administering the Group B *Streptococci* in the choriodecidual space instead (331). This resulted in intra-amniotic inflammation with the same features that were described before (331). When high bacterial doses were administered, this was followed by microbial invasion of the amniotic fluid and an even more robust inflammatory response that led to preterm labour (331). In a following study, the administration of the antibiotic ambicillin could not reverse the intra-amniotic proinflammatory phenotype induced by Group B *Streptococci* despite eradicating the infection (332). This is in line with observations in humans rendering the antibiotics incapable of delaying preterm birth. However, when they targeted the inflammatory response by using the COX inhibitor indomethacin plus dexamethasone

at the same time as targeting the bacteria by ampicillin, they managed to delay the onset of labour (332).

The same series of events can also be induced by the cytokines IL-1b and TNFα (333) (334). On the other hand, IL-6 and IL-8 could not stimulate the same pathway, indicating that they most likely have a bystander role in triggering inflammation-mediated preterm birth (334). Similar to the live bacterial infection, the IL-1b-mediated uterine contractions could be prevented by pre-treatment with indomethacin. This further confirms the validity of the perceived pathway of infection-associated preterm delivery in this model (335).

LPS administered intra-amniotically can also induce the cytokine and prostaglandin milieu that has been associated with preterm birth in rhesus monkeys (336). This effect has been shown to be alleviated by the use of a TLR-4 antagonist, indicating the central role of TLRs in this process (336).

Overall, nonhuman primates have some outstanding features that make them suitable for investigating preterm birth mechanisms. On top of anatomical resemblance and the common pregnancy characteristics with humans, they also appear to share the same pathophysiological pathways that lead to infection-mediated preterm birth. However, their use in parturition research has been limited. The main reason is the high financial costs associated with their research use, as they require specialized facilities and care. In addition, they sometimes exhibit aggressive behaviour and can thus only be handled by specialized personnel. This results in only a few selected centres worldwide being able to meet the above requirements. Consequently, the vast majority of researchers has focused on the use of the much more pragmatic alternative of rodent models.

1.10.3   Rodents

Despite their drawbacks as a model, rodents are overall the most extensively used species in parturition research. These drawbacks include massive anatomical differences such as the size difference and the presence of a bicornuate uterus (337). Their very small size in particular is a huge barrier in trying to study individual

intrauterine compartments as can be done in sheep and nonhuman primates. This is further intensified by the much bigger litter size compared to humans. The size varies depending on the strain and can range from 7 to 20 pups per dam (338). In addition, different mouse strains can respond differently to the same stimuli, something that makes the attempt to extrapolate relatively hard even for the same species. Also, the very short gestational length of approximately 20 days is both very far from the human length and does not allow for the study of chronic conditions and effects in a rigorous manner (306). Nevertheless, the very short rodent gestation can also pose a significant advantage as it allows for a much bigger number of experiments to be conducted within the timeframe. It also allows for quicker acquisition of sufficient numbers to ensure validity of the results obtained.

Perhaps the most substantial difference between the rodent and human parturition relates to its hormonal regulation. In rodents, the main source of progesterone during pregnancy is the corpus luteum (339), whereas in humans the placenta takes over from the corpus luteum at around 8 to 10 weeks of gestation (340). Importantly, a systemic progesterone withdrawal precedes and is necessary for the onset of term parturition in rodents (341). In humans, progesterone levels do not drop at the end of pregnancy and rather a functional withdrawal of progesterone has been described (342) (343). However, in infection-induced preterm birth using *E. coli* in mice, progesterone withdrawal is not necessary for preterm delivery to occur (344). Furthermore, exogenous progesterone supplementation cannot rescue preterm delivery induced by either bacterial products (345) or live bacteria (344). Thus, the fundamental difference of absolute versus functional progesterone withdrawal appears to be less relevant in the context of infection-mediated preterm birth.

Rats

The use of rodent models and especially mice has been particularly important on the field of infection-related preterm birth. Rats have been useful for establishing the role of prostaglandins in labour processes as it was first found in a rat model that the administration of prostaglandin F_{2a} can stimulate myometrial contractions *in vivo*

(346). The main disadvantage of the use of rats is the absence of a consistent model of infection/inflammation-induced preterm birth. There are reports that both systemic, after intraperitoneal injection (347), and intrauterine, after catheterisation (348), administration of LPS can significantly shorten the timing of delivery. However, other studies either reported much lower preterm birth rates (349) or even failure to induce preterm birth at all (350). In line with these findings, intrauterine administration of live *E. coli* bacteria also failed to cause preterm delivery in rats (351). Therefore, the use of the much more consistent mouse models of preterm birth has been widely adopted.

Mice

In this context, mice have the significant advantage of having a well-studied immune system that is very similar to the human (323). The mouse immune system can be genetically manipulated, something that offers the ability to dissect specific pathways involved in the parturition mechanisms (323). For example, it was found that mice lacking the prostaglandin F_{2a} receptor cannot go into labour, highlighting the importance of this mediator for the parturition process (352). These findings were also confirmed by knocking out the prostaglandin synthase COX-1, which accounts for much of PGF_{2a} production (353) (354). The COX-1 deficient mice exhibited delayed parturition (353). Studies in KO mice helped elucidating mechanisms involved in the hormonal and biochemical events that stimulate labour. For instance, KO of the cannabinoid receptor 1 (CB1) disrupts the progesterone/estrogen balance leading to a pro-labour phenotype that results in preterm birth (355). Also, a K^+ channel with an important function in parturition was identified (small conductance calcium activated K^+ channel isoform 3) in by genetic manipulation. Mice overexpressing this channel demonstrated failed parturition (356) and were also resistant to preterm birth induction by LPS and mifepristone (RU486) (357), suggesting its down-regulation is necessary for labour to occur. Finally, chemical ablation of the myometrial gap junction Cx-43 resulted in pregnancy prolongation, indicating the crucial role of this protein for the parturition process (358).

Mouse KO models were also crucial for studying the mechanisms underlying infection/inflammation-induced preterm birth. KO of the TLR signalling downstream adaptor molecule MyD88 protected mice from preterm delivery caused by intrauterine injection of *E.coli*, while their wildtype (WT) delivered prematurely (359). This finding suggested that PTB induced by *E.coli* or its products depends upon TLR signalling. This was not the case for the IL-1b receptor, as mice deficient in it were vulnerable to preterm labour induction by an intrauterine *E. coli* administration (360). Such a finding is likely to reflect the redundancy of the cytokine network in intrauterine infection.

Specific pathways through which the inflammatory response secondary to bacterial infection could stimulate myometrial contractions were identified using mouse KO models. The phosphodiesterase PDE4 is involved in regulation of inflammation and smooth muscle contractility and the inhibition of its action in mice prevents LPS-induced preterm labour (361). Furthermore, inhibition of the Rho/Rho-kinase pathway which is involved in myometrial contractions also managed to stop preterm LPS-stimulated preterm delivery (362). Both of these finding support a role for the respective pathway in the pathophysiology of infection-mediated preterm birth and suggest potential therapeutic targets.

1.10.3.1.1   *Mouse models of infection/inflammation-induced preterm birth*

These many advantages that the mouse has as a model led many groups to the effort of creating mouse models of preterm birth. The first one was described back in 1991 and involved the subcutaneous administration of IL-1b which resulted in preterm delivery in all treated mice (116). Since then, different bacteria and bacterial products have been utilised. The use of LPS is perhaps the most widespread in mouse models of preterm birth. The first study managed to induce PTB via intraperitoneal administration of LPS (363). Later studies also managed to induce preterm birth by administering LPS in the intrauterine compartment, either by open laparotomy (364) or using ultrasound guidance to guide the injection (170). There is also a study reporting induction of preterm labour after intravaginal inoculation of LPS (365).

Other bacterial products have also been used in mouse models of PTB. LTA, a product of gram-positive bacteria was shown to induce preterm delivery after intraperitoneal injection, although not as effectively as LPS (366). In addition, co-administration of the TLR2 agonist peptidoglycan (PGN) and the TLR3 agonist polyinosinic:cytidilic acid [poly(I:C)] in the uterus also stimulated preterm birth in a mouse model (367). Another study managed to induce preterm delivery by stimulating another family of PRRs, the intracellular Nod-like receptors (NLRs) (368). In particular, they reported that an intraperitoneal injection of the Nod1 agonist γ-D-glutamyl-meso-diaminopimelic acid (iE-DAP) results in preterm birth within 24 hours (368).

Different bacterial have also been used in preterm mouse birth models. Firstly, an intrauterine injection of *E.coli* after open laparotomy resulted in delivery within 48 hours (306). Later studies used other bacteria as well. Intravaginal administration of *Chlamydia trachomatis* on day 5 during mouse gestation resulted in preterm delivery on days 15 to 16 (369). However, none of the above bacteria have been strongly associated with preterm birth in humans. Another study reported the induction of preterm birth in mice after intravenous administration of *Fusobacterium nucleatum* (370). This is an oropulmonary pathogen that has been associated with preterm birth in humans (371). This model tries to recapitulate the concept of preterm birth caused by periodontitis that leads to intrauterine infection via hematogenous dissemination. Although, clinically relevant, it does not mimic the most clinically relevant scenario of ascending infection of vaginal bacteria through the cervix.

1.10.3.1.2   Other models of preterm birth

Several mouse models of preterm birth that used non-infectious stimuli have also been described. The most widely used among them involves the subcutaneous injection of the progesterone receptor antagonist RU486 (372). Systemic progesterone withdrawal is essential for parturition to occur in mice, albeit not in humans. The effect of alcohol was also examined. A study found that repeated alcohol administration via oral gavages resulted in increased rates of preterm delivery (373). This was achieved through the upregulation of prostaglandins E and F_{2a} (373). Intraperitoneal injection of

prostaglandin F_{2a} alone was shown to induce preterm birth in a different study (374). The uterine smooth muscle relaxation function of nitric oxide (NO) was also investigated in a study which reported that a subcutaneous injection with the NO inhibitor N^G-nitro-L-arginine methyl esther (L-NAME) caused preterm birth (375). Similarly, the peptide neuromedin B which is thought to stimulate smooth muscle contraction in the urogenital and gastrointestinal tract, could cause preterm birth after intraperitoneal administration (376). Another model used an intra-amniotic injection of the lung surfactant SP-A, which is produced only by a mature fetal lung, to induce preterm delivery identifying its crucial role in the endocrinology of parturition (377).

Sterile inflammation models have also been established in the context of preterm birth. In particular, both intrauterine administration of fetal fibronectin (378) and intra-amniotic injection of the damage-associated molecular pattern (DAMP) high-mobility group box 1 (HMGB1) (379) can cause preterm delivery in mice.

1.10.4   The need for a new model

The above-mentioned models and their successors have substantially contributed to our current understanding of preterm birth and its underlying mechanisms. However, as discussed earlier, the preterm birth rates have not significantly reduced and the current therapeutic options are very limited. This is an indication of the fact that our current knowledge is not sufficient to effectively tackle the problem. To this end, the development of new and more clinically relevant models is of paramount importance. Most current models use either bacterial products but not live bacteria, or bacteria that are not clinically relevant, or an administration route that is not reflective of the current consensus of ascending infection.

In addition, the role of the cervix in the mouse models of preterm birth has been underappreciated. To our knowledge, no mouse model of cervical damage during pregnancy has been described. To this end, an aim of this thesis was to create and characterise a mouse model of cervical damage during pregnancy. For this purpose, the surfactant Nonoxynol-9 (N-9) was identified as potent damage inducer candidate.

1.11 Nonoxynol-9

Nonyl-phenoxy-polyethoxy-ethanol or Nonoxynol-9 (N-9) belongs to the family of isononyl-phenyl-polyoxyethylene ethers. It is a non-ionic surfactant, meaning that its chemical structure consists of a hydrophobic and a hydrophilic group, the latter having no electrical charge. It has been extensively used as a spermicidal agent in various contraceptive methods, such as condoms or cervical barrier methods.

NONOXYNOL-9

$$CH_3-(CH_2)_8-\langle O \rangle-(OCH_2CH_2)_9-OH$$

(Nonylphenoxypolyethoxyethanol)
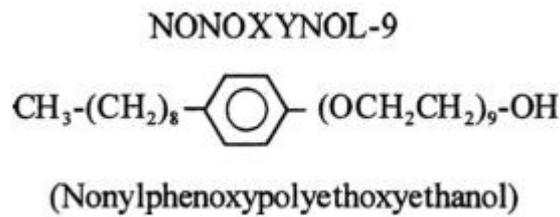
Figure 1.4 Chemical structure of Nonoxynol-9.

Its spermicidal function is based on the molecule's structural affinity to the cell membranes' lipids (380). When N-9 comes in contact with sperm, its molecules start to lyse the cell membranes of spermatozoa, resulting in their detachment, immobilization and ultimately cell death (381). This leads to a complete cessation of sperm motility within 4-6 minutes (382). Eventually, the membranes lose their integrity resulting in sperm death (382). However, the Centres for Disease Control and Prevention (CDC), have recommended against the use of N-9-containing condoms in the absence of evidence from clinical trials that they confer superior protection (383).

The use of N-9 is significantly declining and is now banned from most European counties. This was decided based on the several concerns that have been raised regarding cytotoxicity, especially against epithelial surfaces. Although initially considered to be the safest among spermicides (384), this perception changed when a study in rabbits found that N-9 vaginal application resulted in significant ulceration of the vaginal epithelium (385). Similar findings were also reported in rats, in this case as inflammation in both the vagina and the cervix as acute cervicovaginitis (386). Another study in the same species found that N-9 application results in increased

vaginal epithelial permeability *in vivo* (387). This could potentially imply a decreased epithelial protection against infection.

Studies in nonhuman primates further confirmed the above findings. A single N-9 vaginal application on pigtailed macaques caused irritation of the lower reproductive tract with erythematous lesions as observed by colposcopy (388). A different study found that a single application can cause significant epithelial damage with whole sheets of vaginal epithelia identified in the vaginal lavage fluid (389). The same study also reported large infiltrations of neutrophils and macrophages in the vaginal lumen (389). The cervical epithelium was found to be even more susceptible to epithelial disruption, especially after repeated exposures to N-9 (390).

More recently, mouse studies have reported similar results. The first one found that a single vaginal application of N-9 results in significant disruption of the cervical epithelium that is apparent at 2 hours post-administration and reaches the maximum toxicity levels at 8 hours post-administration (391). The vaginal epithelium had only minor disruptions (391). A later study reported identical findings and also found that N-9 application resulted in significant infiltration of monocytes and tissue resident macrophages in the cervical stroma (392).

Overall, these data confirm that N-9 is an agent of high cytotoxicity against epithelial cells *in vivo* and is also a potent stimulator of an inflammatory response. Importantly, a higher selectivity if these effects towards the cervix as opposed to the vagina has been suggested. However, all these studies have been conducted in non-pregnant animals. This means that the effects of N-9 during pregnancy, particularly with regards to its potential interplay with an ascending infection, have not been studied.

1.12 Summary

Preterm birth is a worldwide healthcare problem as it represents the leading cause of neonatal mortality and morbidity. Despite extensive research in the field, the incidence of preterm birth remains steady over the past decades. At the same time, no proper etiological treatment for preterm birth has been found. This is reflective of the fact that

our current understanding of the disease mechanisms is not sufficient and makes the need for new approaches using clinically relevant models all the more necessary.

The most common cause of spontaneous preterm birth is an intrauterine infection with bacteria that reside in the vagina, the most common of which is the *Ureaplasma* species. The cervix stands between the vagina and the uterus to form a physical and functional barrier that protects the uterine content from ascending infection with vaginal bacteria. This protective function largely depends on the presence of a healthy cervical epithelium. Human data have shown cervical epithelial damage after excisional procedures to be associated with an increased risk for preterm delivery but without any satisfactory mechanistic explanation. The surfactant N-9 has also been shown to cause cervical epithelial damage in various models but its effects during pregnancy remain unknown.

1.13 Hypothesis

The hypothesis of the study presented in this thesis is that Nonoxynol-9:

i)   damages the cervical epithelium
ii)   facilitates ascending infection and
iii)   predisposes to preterm birth.

1.14 Aims

To address this hypothesis, the aims that were set were:

- To investigate the effect of N-9 on cervical epithelial cells *in vitro*.
- To create and characterise a mouse model of cervical epithelial damage during pregnancy using N-9.
- To examine whether N-9-induced cervical epithelial damage during pregnancy facilitates ascending infection with *Ureaplasma parvum*.
- To determine whether *Ureaplasma parvum* can mount an inflammatory response in maternal and fetal tissues and that could lead to preterm birth.

Chapter 2   Materials and Methods

2.1 Cell culture

2.1.1 End1/E6E7 cells

End1/E6E7 ATCC CRL-2615^{TM} (ATCC, Manassas, VI, USA) are immortalized human endocervical cells, isolated from a 43-year-old premenopausal woman that had undergone hysterectomy for endometriosis (393). Immortalisation was made possible by transducing a retroviral vector expressing the HPV16 oncogenes E6 and E7 (LXSN-16E6E7) (393). These proteins have been shown to help human epithelial cells increase their proliferative capacity and avoid cell senescence (394) (395) (396). End1/E6E7 cells were cultured in Keratinocyte Serum-free Medium (Gibco, ThermoFischer Scientific, Paisley, UK) supplemented with $CaCl_2$ (1:5000), Epidermal Growth Factor (EGF) (0.1 ng/ml; Gibco, ThermoFischer Scientific) and Bovine Pituitary Extract (BPE) (0.05 mg/ml; Gibco, ThermoFischer Scientific). Cells were incubated at 37°C in a humid incubator with 5% CO_2 in the air and grown in T75 flasks with media changing every 2-3 days until they reached 80-90% confluence.

2.1.2 HeLa cells

HeLa are human malignant epithelial cells derived from an epidermoid carcinoma of the cervix (397). HeLa cells (ATCC) were cultured in Dulbeco's Modified Eagle Medium (DMEM) supplemented with 10% v/v heat-inactivated Fetal Bovine Serum (FBS), 0.1 mM non-essential amino acids, 1.0 mM sodium pyruvate, 10 mM (4-(2-hydroxyethyl)-1-piperazineethanesulfonic acid or HEPES and 100 U/mL penicillin/streptomycin (ThermoFisher Scientific, Waltham, MA, USA). Cells were incubated at 37°C in a humid incubator with 5% CO_2 in the air and grown in T75 flasks with media changing every 2-3 days until they reached 80-90% confluence.

2.1.3 HESC cells

HESC are immortalized human fibroblast stromal cells obtained from an adult female with myomas (398). HESC cells were cultured in DMEM supplemented with 15% v/v

heat-inactivated FBS, 0.1 mM non-essential amino acids, 1.0 mM sodium pyruvate, 10 mM (4-(2-hydroxyethyl)-1-piperazineethanesulfonic acid or HEPES and 100 U/mL penicillin/streptomycin. Cells were incubated at 37° in a humid incubator with 5% CO_2 in the air and grown in T75 flasks with media changing every 2-3 days until they reached 80-90% confluence.

2.1.4 Swan 71 cells

Swan 71 cells are immortalized human first trimester trophoblast cells (399). Swan 71 cells were cultured in Dulbeco's Modified Eagle Medium: Nutrient Mixture F-12 (DMEM/F12) supplemented with 10% v/v FBS, 0.1 mM non-essential amino acids, 1.0 mM sodium pyruvate, 10 mM 4-(2-hydroxyethyl)-1-piperazineethanesulfonic acid or HEPES and 100 U/mL penicillin/streptomycin. Cells were incubated at 37° in a humid incubator with 5% CO_2 in the air and grown in T75 flasks with media changing every 2-3 days until they reached 80-90% confluence.

2.1.5 Mycoplasma testing

All cell lines were routinely monitored for the presence of mycoplasma using the MycoAlert™ Mycoplasma Detection Kit (Lonza, Basel, Switzerland). This assay is used to detect the presence of enzymes that are released from lysed mycoplasmas. Addition of the enzymes' MycoAlert™ substrate results in the conversion of adenosine diphosphate (ADP) to adenosine triphosphate (ATP). The ATP level can be measured before and after MycoAlert™ is added. ATP levels are proportionate to the presence of mycoplasmal enzymes.

The assay was performed by Dr Forbes Howie, following the protocol described below (Specialised Assay Service, University of Edinburgh).

Cells were seeded at 1.5×10^5 cells/ml (3×10^5 cells in 2 ml) in 6-well plates and cultured in 10% FBS DMEM, omitting P/S and G418, for 48 h. An aliquot of medium was removed and centrifuged at 200g for 5 min to remove cell debris and 100 μl of supernatant was collected for analysis. The MycoAlert™ reagent was then added in an equal volume of 100 μl and the samples were incubated for 5 min at room temperature. The first luminescence reading was then taken on a FLUOstar OPTIMA (BMG

Labtech, Ortenberg, Germany). Then, 100µl MycoAlert™ substrate was added to the sample, followed by a 10-min incubation at room temperature. The luminescence was then read again and the ratio between the two readings was calculated. Ratios greater than 1.2 suggested mycoplasma contamination.

2.2 *Ureaplasma* spp culture

2.2.1 Ureaplasma urealyticum

Ureaplasma urealyticum ATCC 27618 (ATCC, Manassas, VA, USA) was cultured in SP4 Broth with urea (Hardy Diagnostics, Santa Monica, CA, USA). The key aspect of *Ureaplasma* growth in medium is the conversion of urea to ammonium ions, which increases the pH of the growth medium from pH=6.2 to pH>9, resulting in a colour change from yellow to dark pink. The SP4 Broth with urea contains 1.0 g/L urea. Culture of the bacteria was performed at the Reproductive Immunology Unit, Yale University School of Medicine.

Using a 96-well plate, 20µl of *Ureaplasma urealyticum* ATCC 27618 were added to 180µl of SP4 Broth in the top well of a given column. The rest of the wells in that column were filled with 180µl of SP4 Broth each. 10-fold serial dilutions of the 1st well's bacterial concentration were created across the column by transferring 20µl from the 1st well to the 2nd, from the 2nd to the 3rd etc. Depending on the volume of *Ureaplasma urealyticum* needed, several columns could be used in each 96-well plate. Plates were sealed with adhesive tape and incubated at 37°C in a humidified cell culture incubator with ambient CO_2 overnight. The following morning, the last 2 wells from each column showing pH change consistent with the threshold of detection based on colour change (dark pink) were pooled with the 2 subsequent wells that did not reach this threshold (yellow). The pooled aliquots were returned to a humidified cell culture incubator with ambient CO_2 and left to incubate for 3-4 h in order to form a homogeneous population in log phase growth. Following this incubation period, aliquots were frozen and stored in -80ºC.

2.2.2 *Ureaplasma parvum*

Luciferase expressing HPA5 *Ureaplasma parvum* serovar 3 was donated by Dr Brad Spiller from Cardiff University. The bacteria expresses NanoLuc, a luciferase engineered by Promega (Madison, WI, USA), coming from the deep sea shrimp *Oplophorus gracilirostris* (400). Upon administration of the NanoLuc imidazopyrazinone substrate called furimazine, glow-type luminescence is produced (400).

The same culture method as for *U. urealyticum* was used. *Ureaplasma parvum* was cultured in Ureaplasma Selective Medium (USM) (Mycoplasma Experience ltc, Surrey, UK). Bacteria were shipped to Edinburgh as individual aliquots in dry ice and were stored in -80°C until use.

2.2.3 Determination of *Ureaplasma* concentration

Determination of *Ureaplasma* concentration is based on the culture method and utilizes the colour change visual detection resulting from the pH change. It is expressed in Colour Changing Units per ml (CCU/ml).

Using a 96-well plate, 20µl of *Ureaplasma urealyticum* of unknown concentration were added to 180µl of SP4 Broth in the top well of a given column. The rest of the wells in that column were filled with 180µl of SP4 Broth each. 10-fold serial dilutions of the 1st well's bacterial concentration were created across the column by transferring 20µl from the 1st well to the 2nd, from the 2nd to the 3rd etc. Plates were sealed with adhesive tape and incubated at 37°C in a humidified cell culture incubator with ambient CO_2 overnight. After 48 h, the last well from each column showing pH change consistent with the threshold of detection based on colour change (dark pink) represented 1 Colour Changing Unit (CCU). As this well was a 10-fold dilution of the previous one, the previous well represented 10 CCU. Consequently, if n number of wells in the column showed pH change consistent with the threshold of detection based on colour change (dark pink) and the last well represented 1 CCU, the top well

containing 20µl of the *Ureaplasma* of unknown concentration represents 10^{n-1} CCU. In this case, the initial concentration is 5×10^{n} CCU/ml.

2.3 MTT metabolic activity assay

To assess the effect of N-9 on End1/E6E7 cells' viability, a metabolic activity assay was performed. The assay uses the yellow tetrazolium dye 3-(4,5-dimethylthiazol-2-yl)-2,5-dyphenyltetrazolium or MTT, which is being processed in the mitochondria of metabolically active cells into an insoluble purple formazan by the enzyme succinate dehydrogenase. In this case, the metabolic activity of a cell population is directly proportionate to the cell viability of the population.

80-90% confluent End1/E6E7 cells were transferred to 96-well plates (2×10^{5} cells/ml) and allowed to set for 48 h in Growth medium (200 µl/well). After 48 h supernatant was discarded and N-9 or vehicle control was added to the wells (200 µl; 2, 4, 8, 16, 32, 64, 128, 256, 512 µg/ml in Growth medium; AbCam, Cambridge, UK). Cells were incubated in N-9 for various time points (30 min, 1, 2, 4, 24 h). After that, supernatant was discarded and 200 µl of Growth medium was added to each well. This was then followed by adding 10 µl of MTT (5 mg/ml; ThermoFisher Scientific, Waltham, MA, USA) in each well and left to incubate for 4 h. Supernatant was then discarded and 100 µl of Acidified Isopropanol (4M HCl 1:100 in Isopropanol; Sigma-Aldrich, Poole, UK) was added in each well as a solubilizing agent. Solution was mixed in a shaking platform for 20 min and absorbance was read at 540mm. Four independent experiments were conducted.

2.4 In vitro cell permeability assay

1. Endothelial cells are seeded into the inserts and cultured until complete monolayer formation occurs

Receiver plate well

Semi-permeable membrane pre-coated with collagen

Permeability insert

Seeded cells

Cell monolayer formation

2. Cells are treated with permeability modulator of choice.

Permeability treatment

Cell monolayer

3. The permeability treatment is removed, then FITC-dextran is added to the semi-permeable insert coated with an endothelial monolayer.

FITC-dextran

Treated cell monolayer

4. FITC-dextran permeates the treated cell monolayer into the plate well. The resulting fluorescence in the plate well is measured and used as an indicator of the extent of monolayer permeability.

FITC-dextran

Treated cell monolayer

Figure 2.1 *In vitro* permeability assay principle. Adapted from (401).

The semi-permeable membranes of specialised inserts (MilliporeSigma, Burlington, MA, USA) were first hydrated at RT for 15 min with 250 µl of Growth medium. Then, 200 µl of medium was removed and 200 µl of End1/E6E7 cell suspension was added to each insert (2.5 x10^6 cells/ml in Growth medium). They were left to incubate for 72 h. Supernatant was discarded and N-9 or vehicle control was added to the wells (200 µl; 3, 10, 30, 100 µg/ml) and left to incubate for 2 h. Supernatant was discarded and 500 µl of Growth medium was added to the receiver wells. A Fluorescein-tagged dextran solution was added to the inserts (150 µl; 1:40 in Growth medium; MilliporeSigma) for 1 h, protected from light, at RT. Following this, dextran permeation was stopped by removing the inserts from the receiver wells. Medium in the receiver wells was thoroughly mixed and 100µl out of each well was transferred to a 96-well opaque plate. Five independent experiments were conducted. Fluorescence intensity of the medium in the receiver wells was measured in a CLARIOstar multimode microplate reader at 485 mm excitation/535 mm emission wavelengths (BMG Labtech, Ortenberg, Germany).

Inserts that were removed to stop permeation were placed in a new receiver wells. A cell stain solution (Part # 20294; MilliporeSigma) was added to the inserts (100 µl) for 20 min at RT. Following this, the cell stain solution was removed and inserts and receiver wells were washed x2 with PBS.

Images were taken on a Leitz Labovert inverted brightfield microscope (Leitz, Wetzlar, Germany) using an AxioCam ICc 1 camera (Carl Zeiss AG, Oberkochen, Germany).

2.5 Human cytokine proteomic array

2.5.1 Principle

The assay uses selected capture antibodies against human cytokines that have been spotted in duplicate on nitrocellulose membranes. Samples are mixed with a cocktail of biotinylated detection antibodies and then incubated with the membranes. Streptavidin- Horseradish peroxidase (HRP) and a chemiluminescence-based

detection system are used resulting in light production that can be quantified using light detectors.

2.5.2 Kit reagents

Table 2-1 Human cytokine proteomic array kit reagents (R&D Systems)

Array Buffer 4 (Part #895022)	Buffered protein base with preservatives
Array Buffer 5 (Part #895876)	Buffered protein base with preservatives
Wash Buffer Concentrate (Part #895003)	Concentrated solution of buffered surfactant with preservatives
Detection Antibody Cocktail (Part #898261)	
Streptavidin-HRP (Part #893019)	
Chemi Reagent 1 (Part #894287)	Stabilised hydrogen peroxide with preservative
Chemi Reagent 2 (Part #894288)	Stabilised luminol with preservative

2.5.3 Assay procedure

Supernatants (200 µl each) from 4 different experiments were pooled after centrifugation to get rid of the debris. Each membrane was blocked with 2 ml of Array Buffer 4 for 1 h on a rocking platform shaker making sure the membrane is rocking end to end.

To prepare the sample/detection antibody mix, samples were first diluted by adding up to 1 ml of each sample to 0.5 ml of Array Buffer 4 in separate tubes. Final volume was adjusted to 1.5 ml with Array Buffer 5. Then, 15 µl of reconstituted Human Cytokine Array Detection Antibody Cocktail was added to each prepared sample. Mix was left

to incubate at room temperature for 1 h. Array Buffer 4 was then aspirated and sample/antibody mix was added. Mix was left to incubate with the membrane overnight at 2-8 °C on a rocking platform. After overnight incubation, membranes were carefully removed and placed in individual plastic containers with 20 ml of 1X Wash Buffer. Each membrane was washed with 1X Wash Buffer for 10 min on a rocking platform shaker for a total of three washes.

Streptavidin-HRP was prepared in Array Buffer 5 according to the dilution factor on the vial label. Membranes were incubated in Streptavidin-HRP for 30 minutes at room temperature on a rocking platform shaker. Each membrane was then washed with 1X Wash Buffer for 10 min on a rocking platform shaker for a total of three washes. Each membrane was then placed on the bottom sheet of the plastic sheet protector with the identification number facing up. 1 ml of the prepared Chemi Reagent Mix (1:1 Chemi Reagent 1: Chemi Reagent 2) was added on top of each membrane and allowed to spread evenly. Membranes were left to incubate for 1 min. Chemiluminescence signal was read in a LI-COR Odyssey Fc (LI-COR Biotechnology, Lincoln, NE, USA).

2.6 DuoSet Enzyme-linked immunosorbent assay (ELISA)

2.6.1 ELISA solutions preparation

Table 2-2 Generic ELISA reagents

Preservatives	Methylisothiazolone (20%, 2 g)
	Bromonitrodioxane (20%, 2 g)
	Dimethylsulfoxide (DMSO, 5 ml)
	Dimethylformamide (DMF, 5 ml)

Dry coat solution	Polyvinyl pyrollidone (20%, 2 g)
	Bovine serum albumin (BSA, 0.5%; 5 g)
	Ethylenediaminetetraacetic acid (EDTA, 5 mM; 1.68 g)
	Tris base (50 mM; 6.05 g)
	Preservatives (0.1%; 1 ml)
ELISA Buffer	Tris base (100 mM; 12.11 g)
	Sodium chloride (NaCl, 0.9%; 9 g)
	EDTA (2 mM; 0.744 g)
	BSA (0.5%; 5 g)
	Phenol red solution (0.03%; 300 μl)
	TWEEN 20 (0.03%; 300 μl)
	Preservatives (1ml)
	Deionized H_2O (800 ml)
Wash Buffer (x20)	NaCl (0.9%; 360 g)
	Tris base (10 mM; 48.4 g)
	TWEEN 20 (0.05%; 20 ml)
	dH_2O (1.7 L)
	pH adjusted to 7.5
	Buffer made to 2 L

Substrate Buffer	Sodium acetate anhydrous (100 nM; 4.1 g)
	Preservatives (0.1%; 0.5 ml)
	dH_2O (405 ml)
	pH adjusted to 6
	Buffer made to 500 ml
Solution A	3, 3', 5, 5'- Tetramethylbenzidine (TMB; 0.3%; 0.3 g)
	DMF (100 ml)
Solution B	Urea hydrogen peroxide (0.5%; 0.5 g)
	Sodium acetate buffer (50 mM; 100 ml)
Stop solution	Sulfuric acid (2N H_2SO_4)

2.6.2 DuoSet ELISA reagents

Table 2-3 DuoSet IL-6 and IL-8 ELISA reagents (R&D Systems)

Capture Antibodies

Mouse anti-human IL-6 (R&D Systems, Abington, UK)	1:120 in PBS
Mouse anti-human IL-8 (R&D Systems)	1:120 in PBS

Detection Antibodies

Biotinylated goat anti-human IL-6 (R&D Systems)	1:60 in ELISA buffer
Biotinylated goat anti-human IL-8 (R&D Systems)	1:60 in ELISA buffer
Streptavidin HRP	1:40 in ELISA buffer

2.6.3 Assay procedure

96-well plates werecoated with the following capture antibodies: anti-human IL-6 and anti-human IL-8 (100μl/well; 1:120 in PBS). Plates were seal-covered and incubated overnight at 5°. The following day, plate contents were discarded and the plate was blot-dried on tissue. 100μl of Dry Coat Solution was added to each well and left to incubate for 1 h. After this, contents were discarded, plates were blot-dried and left to air-dry at RT for 3-4 hours. Plates were then washed x4 in Wash Buffer and blotted dry in tissue. A 7-point standard curve was created by adding 100μl/well of a solution with known cytokine concentration and diluting it 2-fold across the plate's column (top standard 600pg/ml for IL-6 and 2000pg/ml for IL-8 serially diluted 2-fold in ELISA Buffer). All samples were in duplicates. The plate was sealed and incubated overnight at 5°C. The following day, contents were discarded and plates were washed x4 in Wash Buffer and blotted dry. 100μl of detection antibody (1:60 in ELISA Buffer for all 3 cytokines) was added to each well and the plates incubated for 1° at RT under gentle agitation. After this, well contents were discarded and plates were washed x4 in Wash Buffer and blotted dry. 100μl of a Streptavidin-HRP solution was added to each well (1:40 in ELISA Buffer) and plates incubated for 20 min at RT under gentle agitation and protected from direct sunlight. Well contents were then discarded and plates were washed x4 in Wash Buffer and blotted dry. 100μl of the substrate solution (for a full plate: 10 ml Substrate buffer + 1 ml Solution A + 1 ml Solution B) was then added to each well and incubated for 20 min at RT. The reaction was stopped and colour development was quenched by adding 50μl of the Stop solution to each well.

The colour absorbance was then immediately read at 450 nm using the Softmax Pro software and plate reader (Molecular Devices, Sunnyvale, CA, USA).

2.7 Protein quantification assay

Total secreted protein is directly proportionate to the total number of cells. To quantify total protein, a colorimetric microplate assay was performed.

All samples were cell culture supernatants collected from the experiment described in section 2.1.4. Using a 96-well plate, 5 µl of each sample or Radioimmunoprecipitation Assay Buffer (RIPA Buffer) (Bio Rad, Hercules, CA, USA) used as blank were added per well. A 7-point standard curve was created by adding 100µl/well of a solution with known protein concentration (1.37mg/ml serially diluted in RIPA Buffer) (Bio Rad). 25 µl of "Working Reagent A" were added to each well (20 µl of Reagent S to each 1ml of Reagent A needed for the assay, Bio Rad). After this, 200 µl or Reagent B (Bio Rad) were added to each well and plates were left to incubate on bench for 15 min. The colour absorbance was then read at 650 nm using the Softmax Pro software and plate reader (Molecular Devices, Sunnyvale, CA, USA).

2.8 LDH cytotoxicity assay

LDH is present in all cell membranes and, upon damage, it is released by the damaged cells in the Growth medium. This assay utilizes the ability of LDH to oxidize lactate and generate NADH, which then reacts with WST resulting in yellow colour production. Colour intensity is directly correlated with the cell number lysed.

All samples were cell culture supernatants collected from the experiment described in section 2.1.4. Using a 96-well plate, 10 µl of each sample or Growth medium used as negative control were added per well. 100 µl of LDH Reaction Mix (200 µl of WST Substrate Mix in 10 ml of LDH Assay Buffer for every 100 reactions) (BioVision, Milpitas, CA, USA) was then added to each well and incubated for 30 min at room temperature. To stop colour development, 10 µl of Stop Solution (BioVision) were added in each well and mixed thoroughly. The colour absorbance was then read at 450

nm using the Softmax Pro software and plate reader (Molecular Devices, Sunnyvale, CA, USA).

2.9 Bio-Plex cytokine assay

To measure secreted cytokines in cell culture supernatant, the Bio-Plex Pro^{TM} Human Cytokine, Chemokine and Growth Factor Magnetic Bead-Based Assay was used (Bio Rad, Hercules, CA, USA). This assay utilizes 6.5µm magnetic beads to capture the cytokines of interest. Biotinylated detection antibodies are then added to the mix. The addition of Streptavidin-Phycoerythrin (PE) results in light emission after sample excitation that allows for cytokine quantification against a standard curve. The experiment was performed by Mrs Paulomi Aldo at Yale University School of Medicine.

A standard flat-bottom 96-well plate was first pre-wet with 100 µl/well Bio-Plex Assay Buffer (Bio Rad) and then vacuum-filtered. The vacuum pressure was set to 2 inches Hg. The bottom of the plate was then blotted on tissue.

50 µl of Working Bead Solution (25-fold dilution of the Anti-cytokine Bead Stock Solution in Bio-Plex Assay Buffer A, Bio Rad) was then added to each well. Before being added, the Working Bead Solution was vortexed for 20 sec. The plate was then vacuum-filtered and blotted on tissue. Plate was then washed x2 with 100 µl of Bio-Plex Wash Buffer/per well (Bio Rad).

A 7-point standard curve was created by adding 50µl/well of a standard solution reconstituted in tissue culture media and diluting it 4-fold across a plate's column (top standard 32,000 pg/ml, low standard 0.2 pg/ml). 50 µl from each sample was then added in appropriate wells (each sample was tested in duplicate). The plate was covered with foil and samples and standards were incubated at room temperature for 30 min in a shaking platform. Initially, the shaking frequency was slowly ramped up to 1,100 rpm and the plate was then shaken for 30 sec. After this, the speed was reduced

to 300 rpm for the remainder of the incubation time. Plate sealer was then removed and the plate was washed x3 with 100 μl of Bio-Plex Wash Buffer/per well.

25 μl of the Detection Antibody Mixture was then added to each well (10-fold dilution of the Detection Antibody Mix Stock Solution in Bio-Plex Detection Antibody Diluent, Bio Rad). The plate was covered with foil and samples and standards were incubated at room temperature for 30 min in a shaking platform. Initially, the shaking frequency was slowly ramped up to 1,100 rpm and the plate was then shaken for 30 sec. After this, the speed was reduced to 300 rpm for the remainder of the incubation time. Plate sealer was then removed and the plate was washed x3 with 100 μl of Bio-Plex Wash Buffer/per well.

50 μl of Streptavidin-PE Working Solution was then added to each well (100-fold dilution of the Streptavidin-PE Stock Solution in Bio-Plex Assay Buffer, Bio Rad). The plate was covered with foil and samples and standards were incubated at room temperature for 30 min in a shaking platform. Initially, the shaking frequency was slowly ramped up to 1,100 rpm and the plate was then shaken for 30 sec. After this, the speed was reduced to 300 rpm for the remainder of the incubation time. Plate sealer was then removed and the plate was washed x3 with 100 μl of Bio-Plex Wash Buffer/per well.

To resuspend the beads, 125 μl of Bio-Plex Assay Buffer was then added to each well. Plate was covered with an adhesive plate sealer and the bottom of the plate was thoroughly blotted. The plate was then shaken on a platform shaker. The shaking frequency was slowly ramped up to 1,100 rpm and the plate was then shaken for 30 sec. Plate sealer was then removed and the plate was read in a Bio-Plex Reader ((100 beads/region in a volume of 50 μl in the low Photomultiplier Tube (PMT)) (Bio Rad).

2.10 RNA extraction

2.10.1   RNA extraction from cells

Cells were lysed using Buffer RLT (Qiagen Ltd., Maryland, USA) with beta-mercaptoethanol (β-ME; Sigma-Aldrich). They were then further lysed by being

repeatedly passed through a blunt 20-gauge needle (0.9mm diameter; BD Microlance™) in an RNase-free syringe (BD Plastipak™). An RNAeasy mini kit (Qiagen) was used to extract total RNA with the solutions supplied. EtOH (70%) was added to the homogenised lysate (v/v) and mixed well by pipetting. Each sample was then added to an RNeasy mini spin column within a 2 ml collection tube for RNA extraction. All samples were centrifuged for 15 sec at 8000 x g (10, 000 rpm). Each column was then washed with 350 μl Buffer RW1 under centrifugation for 15 sec at 8000 x g (10, 000 rpm) to remove carbohydrates and proteins. To eliminate genomic DNA contamination, a DNase digestion step was performed by adding 10 μl DNase I stock, in 70 μl Buffer RDD (Qiagen), directly onto the spin column membrane for each sample. Samples were then incubated for 15 min at room temperature. Each column was then washed with 350 μl Buffer RW1 under centrifugation for 15 sec at 8000 x g (10,000 rpm). To remove residual salts, samples were washed twice with Buffer RPE under centrifugation at 8000 x g (10, 000 rpm) for 15 sec and 2 min, respectively. A final centrifugation step was performed for 1 min at full speed to eliminate any possible Buffer RPE carryover. RNA was eluted from the spin column membrane using 30 μl RNase-free H2O under centrifugation for 1 min at 8000 x g (10,000 rpm). Extracted RNA was stored at -80°C until further use.

2.10.2   RNA extraction from tissue

Placental tissue was lysed in 1ml TRI reagent® (Sigma-Aldrich) with one sterile 5 mm stainless steel bead (Qiagen) per Eppendorf/sample. The tissue was lysed at 25Hz using a Tissue Lyser II (Qiagen), 2x3 min, with tubes rotated half way through. The samples were then incubated for 15 min at room temperature. Following this, they were centrifuged at 14, 000 x g for 10 minutes at 4°C. The supernatant was then transferred to a 2 ml phase-lock tube (5-PRIME, Hamburg, Germany) and 200 μl of 1-bromo-3-chloropropane (BCP; Sigma-Aldrich) were added to each sample. Samples were shaken for 15 sec, incubated for 10 min at room temperature and then centrifuged at 14, 000 x g for 15 min at 4°C. The upper aqueous phase was transferred to a new 2ml Eppendorf and 550μl of 70% EtOH was added. Each sample was then added to an RNeasy mini spin column within a 2ml collection tube for RNA extraction. All

samples were centrifuged for 15 sec at 8000 x g (10, 000 rpm). Each column was then washed with 350 μl Buffer RW1 under centrifugation for 15 sec at 8000 x g (10, 000 rpm) to remove carbohydrates and proteins. To eliminate genomic DNA contamination, a DNase digestion step was performed by adding 10μl DNase I stock, in 70 μl Buffer RDD (Qiagen), directly onto the spin column membrane for each sample. Samples were then incubated for 15 min at room temperature. Each column was then washed with 350 μl Buffer RW1 under centrifugation for 15 sec at 8000 x g (10,000 rpm). To remove residual salts, samples were washed twice with Buffer RPE under centrifugation at 8000 x g (10, 000 rpm) for 15 sec and 2 min, respectively. A final centrifugation step was performed for 1 minute at full speed to eliminate any possible Buffer RPE carryover. RNA was eluted from the spin column membrane using 30μl RNase-free H2O under centrifugation for 1 minute at 8000 x g (10,000 rpm). Extracted RNA was stored at -80°C until further use.

2.10.3   RNA quantification

Nucleic acid concentration was quantified by measuring sample absorbance at 260nm on a NanoDrop ONE (ThermoFisher Scientific, Waltham, USA). RNA absorbs at 260nm, while protein contaminants absorb closer to 280nm. RNA purity is determined by the 260:280 ratio. Acceptable 260:280 ratios were between 1.8 and 2.1.

2.11 Reverse transcription (RT)- cDNA preparation

2.11.1   RNA extract from cells

Total RNA was reverse transcribed using the iScript^{TM} cDNA Synthesis kit (Bio Rad). An RT mastermix was prepared on wet ice. This included the following reagents; 5X iScript Reaction Mix, iScript RT enzyme and Nuclease-free H2O. RNA (300ng/μl) was added to the mastermix and pipetted gently to mix, then centrifuged at 10,000 rpm for 30 seconds to remove any air bubbles. A "no reverse transcriptase" control was included, omitting the enzyme, to control for genomic DNA contamination. A "no template" control, omitting the RNA, was included to control for general contamination of reagents. A G-Storm GS1 Thermal Cycler (G-Storm, Somerset, UK)

was set to perform the following cycles; 25°C for 5 minutes, 42°C for 30 minutes, 85°C for 5 minutes, then held at 4°C. Samples were stored at -20°C until required for quantitative real time polymerase chain reaction (qRT-PCR) analysis.

Table 2-4 Reverse transcription reagents

Reagent	Volume (μl) per sample for each reaction
5x iScript Reaction Mix	4
iScript Reverse Trascriptase	1
Nuclease-free H_2O	x
RNA template (up to 1 μg Total RNA)	x
Total Volume	20

2.11.2   RNA extract from mouse tissues

Total RNA was reverse transcribed using the High Capacity cDNA Reverse Transcription kit (Applied Biosystems, Life Technologies, ThermoFisher Scientific). A 2X RT mastermix was prepared on wet ice. This included the following reagents; 10X RT buffer, 25X deoxyribonucleotide triphosphates (dNTPs), 10X random primers, RNase inhibitor, MultiScribe™ RT enzyme and RNA-free H2O. RNA (300 ng/μl) was added to the mastermix and pipetted gently to mix, then centrifuged at 10,000 rpm for 30 seconds to remove any air bubbles. A "no reverse transcriptase" control was included, omitting the enzyme, to control for genomic DNA contamination. A "no template" control, omitting the RNA, was included to control for general contamination of reagents. A G-Storm GS1 Thermal Cycler (G-Storm, Somerset, UK) was set to perform the following cycles; 25°C for 10 minutes, 37°C for

120 minutes, 85°C for 5 minutes, then held at 4°C. Samples were stored at -20°C until required for quantitative real time polymerase chain reaction (qRT-PCR) analysis.

Table 2-5 Reverse transcription reagents

Reagent	Volume (µl) per sample for 2x RT Mastermix
10x RT Buffer	2
25x dNTPs	0.8
10x Random primers	2
RNase inhibitor	1
MultiScribe™ RT enzyme	1
RNA-free H_2O	3.2
RNA (300ng)	10
Total volume	20

2.12 Quantitative Real-time Polymerase Chain Reaction (qRT-PCR)

2.12.1   *In vitro* experiments

To quantify the mRNA expression of specific genes of interest, qRT-PCR was performed using predesigned iTaq™ universal SYBR® Green supermix assay (Bio Rad). All samples and controls were added in duplicate in a 96-well PCR plate (Applied Biosystems). A reagent mixture was prepared with iTaq™ universal SYBR Green supermix, forward and reverse primers, cDNA sample and Nuclease-free H_2O. In addition to the cDNA samples, wells containing the following controls were

included; "no reverse transcriptase", "no template" and finally a H$_2$O-only control, replacing cDNA, to determine any reagent contamination. Plates were sealed with optical adhesive film (MicroAmp®, Applied Biosystems) and then centrifuged at 500 x g for 1 minute. All qRT-PCR analyses were performed on a CFX Connect^{TM} Real-Time PCR System. The instrument was set to perform the following cycles: 95°C for 30 seconds, then 95°C for 15 seconds and 60°C for 30 sec, repeated for 40 cycles. Target gene expression was normalised for RNA loading using the housekeeping gene *GAPDH*. The expression in each sample was calculated relative to a calibrator sample (vehicle-treated cells) using the $2^{-\Delta\Delta}$ threshold cycle (CT) method of analysis.

Table 2-6 iTaq^{TM} Universal SYBR® Green assay reagents

Reagent	Volume (µl) per sample for each reaction
iTaq^{TM} Universal SYBR® Green supermix (x2)	10
Forward and reverse primers (500 nM)	x
cDNA template (100ng)	x
Nuclease-free H$_2$O	x
Total Volume	20

Table 2-7 Primers for qRT-PCR (*in vitro* experiments)

Gene	Forward(5'-3')	Reverse(5'-3')
Tlr1	AAAAGAAGACCCTGAGGGCC	TCTGAAGTCCAGCTGACCCT
Tlr2	CAAATGACGGTACATCCACG	GGGTAAATCTGAGAGCTGCG

Tlr3	AACAGCATCAAAAGAAGCAGAAA	AAACATTCCTCTTCGCAAACAG
Tlr4	GACAACCTCCCCCTTCTCAACC	ATAGTCCAGAAAAGGCTCCCAG
Tlr6	AGAACTACATCGCTGAGC	CTGAAACTCACAATAGGATGG
Tlr7	TGTGGTTTGTCTGGTGGGTTA	CCACACATCCCAGAAATAGAGG
Tlr9	CAGCAGCTCTGCAGTACGTC	AAGGCCAGGTAATTGTCACG

2.12.2   Mouse experiments

To quantify the mRNA expression of specific genes of interest, qRT-PCR was performed using predesigned TaqMan gene expression assays from Applied Biosystems. All samples and controls were added in duplicate in a 384-well PCR plate (Applied Biosystems). A reagent mixture was prepared and 14 μl was added to each well, together with 1 μl of cDNA sample. In addition to the cDNA samples, wells containing the following controls were included; "no reverse transcriptase", "no template" and finally a H_2O-only control, replacing cDNA, to determine any reagent contamination. Plates were sealed with optical adhesive film (MicroAmp®, Applied Biosystems) and then centrifuged at 500 x g for 1 min. All qRT-PCR analyses were performed on an Applied Biosystems 7900HT instrument set to perform the following cycles; 50°C held for 2 minutes, 95°C held for 10 minutes, then 95°C for 15 seconds and 60°C for 1 minute, repeated for 40 cycles. Target gene expression was normalised for RNA loading using *β-actin* (ACTB VIC, Mouse: 4352341E, Applied Biosystems). Previous studies from our laboratory found this endogenous gene to be consistent during late pregnancy in the mouse (170). The expression in each sample was

calculated relative to a calibrator sample (vehicle control) using the $2^{-\Delta\Delta}$ threshold cycle (CT) method of analysis.

Table 2-8 Taqman gene expression assay reagents (Applied Biosystems)

Reagent	Volume (µl) per sample for TaqMan reagent mixture
TaqMan Universal Master Mix II	7.5
Primer/probe or *β-actin*	0.75
Nuclease-free H_2O	5.75

Table 2-9 Taqman gene expression assays

Gene	Species	Code
TNFa	Mouse	Mm99999068_m1
Il1b	Mouse	Mm00434228_m1
Cxcl1	Mouse	Mm04207460_m1
Cxcl2	Mouse	Mm00436450_m1
Il6	Mouse	Mm00446190_m1
Tlr1	Mouse	Mm00446095_m1
Tlr2	Mouse	Mm01213946_g1
Tlr6	Mouse	Mm02529782_s1

Tlr9	Mouse	Mm00446193_m1
β-actin	Mouse	Mm00607939_s1
UreC*	*Ureaplasma parvum*	*Provided by Dr Brad Spiller

2.13 Experimental procedures

2.13.1 N-9 effect on cytokine secretion by End1/E6E7 cells

80-90% confluent End1/E6E7 cells were put in 12-well plates (1 ml; 2 x10^5 cells/ml in Growth medium) and left to incubate for 48 h. Following this, supernatants were discarded and N-9 (1 ml; 4 μg/ml in Growth medium) or vehicle control was added to the wells and left to incubate for 2 h. After this, supernatants were discarded, cells were washed x2 in PBS and Lipopolysaccharide (LPS O111:B4) (1 ml; 1 μg/ml in Growth medium: Sigma-Aldrich, St Louis, MO, USA) or vehicle control was added to the cells and left to incubate for 24 h (**Fig 2.2**). For all experiments the *E. coli* LPS serotype O111:B4 was used in line with the *in vivo* experiments described below. At the end of this time point, supernatants were collected and stored at -20ºC until further use and cells were frozen at -20ºC. Four different independent experiments were performed.
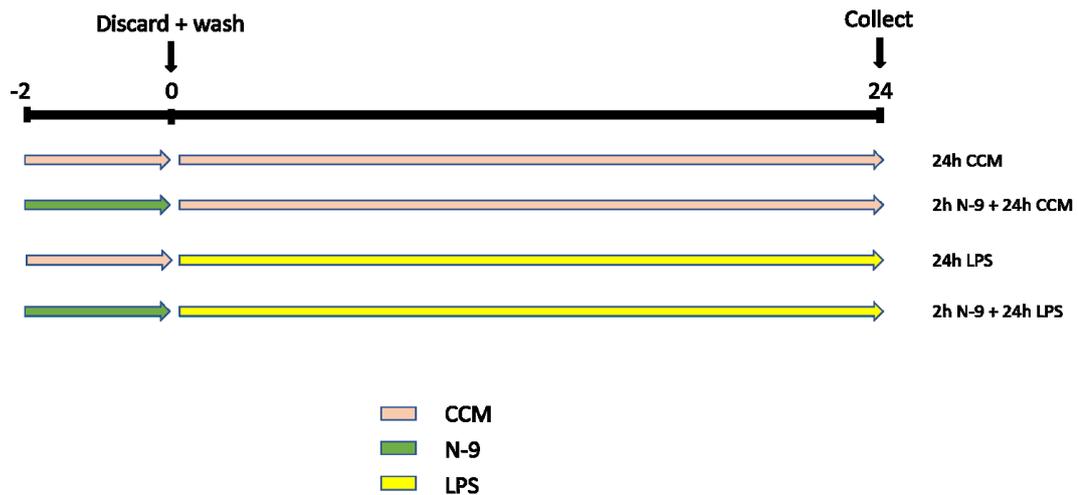
Figure 2.2 Experimental outline. Effect of N-9 on basal and LPS-stimulated cytokine secretion by End1/E6E7 cells.

Cytokine levels were determined using the human cytokine proteomic array and ELISA. Ideal N-9 concentration was decided by assessing the viability at the end of the experiment using MTT and LDH assays. To take the reduced cell viability in the N-9 treated groups into account when assessing the N-9 effect on cytokine secretion, the cytokine concentrations found using ELISA were normalized against the concentration of total secreted protein.

2.13.2   Effect of *Ureaplasma urealyticum* infection on HeLa and HESC cells' wound healing capacity

Confluent HeLa and HESC were transferred to 24-well ImageLock plates (Essen BioSciences, Ann Arbor, MI, USA) ($5x10^4$ and $1x10^5$ cells/ml in 500 µl of Growth medium per well for HeLa and HESC respectively) and allowed to set for 48 h. Following this, an artificial wound was created across the wells by scratching the cells with a pipette tip using a standardized semi-manual system (**Fig 2.3**). Growth medium was then discarded and the cells were then washed x2 with PBS. Cells were then treated either with *Ureaplasma urealyticum* (5µl/well; $5x10^7$ CCU/ml in SP4 Broth)

or with vehicle control (10μl/well of SP4 Broth) and the plates were placed in an IncuCyte ZOOM system (Essen BioSciences) to monitor the wound closure. The plates were scanned every 2h for 48h.
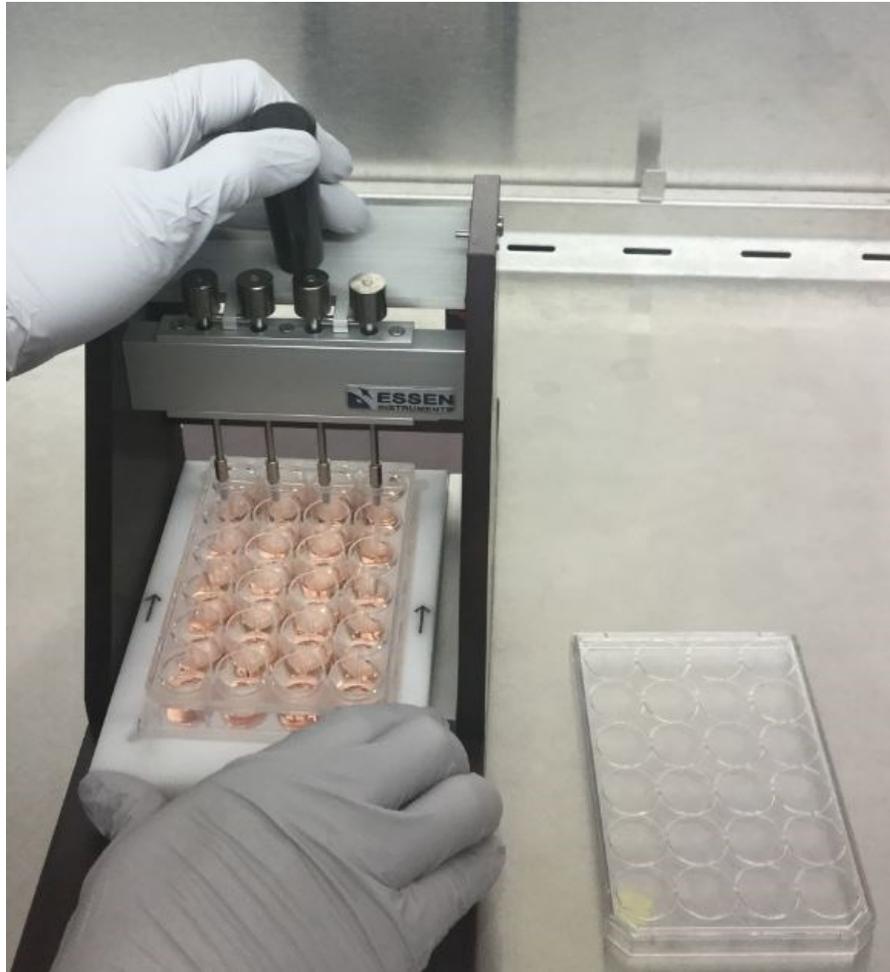
Figure 2.3 Semi-manual system used for the Wound Healing Assay

2.13.3 Effect of N-9 on *Ureaplasma parvum* growth

To examine the effect of N-9 on *Ureaplasma parvum* growth, the Minimum Inhibitory Concentration (MIC) of N-9 was determined using an adaptation of a previously described microdilution technique (402). MIC is the lowest concentration of an antimicrobial substance that will inhibit the visible growth of a microorganism after a given incubation time.

Using a 96-well plate, an N-9 gradient was created from 1024 µg/ml to 1 µg/ml across the plate columns, the last column being N-9 free for unrestricted growth comparison (180µl of each N-9 concentration/per well). 20 µl of *Ureaplasma parvum* from the overnight culture of unknown CCU was added to each well in the columns A1 to A12 (1:10 dilution). A 10-fold dilution curve of bacteria was then titrated at 90 degrees across the N-9 gradient. Plates were sealed with adhesive tape and incubated at 37°C in a humidified cell culture incubator with ambient CO_2 for 48 h, at which time color change within the growth control had ceased. The MIC was defined as the lowest concentration of antibiotic that prevented a color change after 48 h when read at 10^4 CCU (relative to growth in the antibiotic-free medium). USM (with and without antibiotics) was also incubated in the absence of added *Ureaplasma* isolates to serve as a negative color-changing control.

2.14 Animal studies

All animal studies were performed under UK Home Office License 70/8927 (PPL) to Professor Jane Norman and in accordance with the UK Animals (Scientific Procedures) Act of 1986. All researchers that carried out procedures as part of this thesis were Personal License holders (PIL). Practical training was provided by the Establishment's designated trainers until the PIL holder was signed off as competent to perform the relevant procedure unsupervised. Before each experiment, an Experimental Request Form (ERF) was submitted for review by the Named Veterinary Surgeon (NVS). ERF approval was a prerequisite for ordering mice to be used in an experiment.

Virgin female C57Bl/6J mice aged 5-7 weeks were obtained from Charles Rivers Laboratories (Margate, UK). Mice were acclimatized for at least 7 days prior to any further experimental action. Upon mice arrival and until the start of each experiment, mice were housed in groups of 5-6 per cage and provided with food and water. Timed mating and vaginal copulatory plug checks of the animals were performed by the Animal Facility technicians, Mrs Carrie Owen and Mr Michael Dodds. During each

experiment, pregnant mice were housed in individual cages and were closely monitored either in person at least twice a day, or by CCTV. They were checked for signs of delivery and severity endpoints as defined by the PPL. Temperature (19-23°C) and humidity (~55%) were tightly controlled, with constant 12-hour light/dark cycles.

Animals were euthanized using methods permitted in the Schedule 1 of the UK Animals Scientific Procedures Act of 1986. In particular, dams were sacrificed by the inhalation of rising concentrations of CO_2 in a sealed chamber and death was confirmed be cervical dislocation. Pups were sacrificed by cervical dislocation. For all the experiments described below, embryonic day 1 (D1) of mouse pregnancy was defined by the presence of a vaginal copulatory plug.

2.14.1 Mouse model of cervical damage during pregnancy using N-9

In the morning of D17 of pregnancy, mice were anaesthetized using inhalational isoflurane (5% for induction of anaesthesia, 2.5% for maintenance) and a pipette was used for intravaginal administration of either N-9 ((60 μl; 2%, 5%, 10% v/v in PBS or PBS (60 μl)). Mice were randomly assigned to each group. Care was taken to avoid spillage of treatment outside the vagina. Mice were allowed to recover from anaesthesia on a piece of tissue. Maintenance of treatment in the vagina after recovery from anaesthesia was assessed by observing potential leakage on the tissue. Only minor leakage incidents were observed. Following successful recovery, mice were put in individual cages for 8 h. During this period, they were checked in person twice per day for signs of potential adverse effects. At 8 h post-treatment, mice were culled by Schedule 1 procedures (CO_2 asphyxiation followed by cervical dislocation) for tissue collection (**Fig 2.4**). Pups were culled by Schedule 1 (cervical dislocation followed by decapitation).
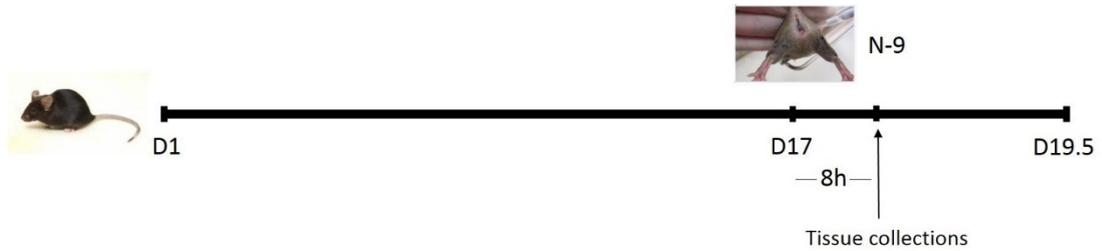
Figure 2.4 Mouse model of cervical damage assessment experimental outline.
Pregnant C57Bl/6 mice were administered 60 µl of 2%, 5%, 10% N-9 or PBS control
intravaginally in the morning of D17 of gestation. 8 h post-administration, mice were
sacrificed for tissue collections to assess the effect of N-9-induced damage.

Tissue collection and processing

The vagina, the cervix and part of the uterus were collected as a single tube-like
tissue and, after the surrounding fat was trimmed off, it was immediately transferred
to 4% v/v Paraformaldehyde (polymeric formaldehyde) (PFA) for fixation. Tissue
samples were fixed overnight in 4% PFA overnight (ON). Following fixation, tissue
samples were stored in 70% v/v Ethanol. Samples were then made into paraffin
blocks by a specialist technician, Mr Garry Menzies.

2.14.2   Mouse model of cervical damage using N-9 and vaginal inflammation using LPS

In the morning of D17 of pregnancy, mice were anaesthetized using inhalational
isoflurane (5% for induction of anaesthesia, 2.5% for maintenance) and a pipette was
used for intravaginal administration of either N-9 and Lipopolysaccharide (LPS) ((60
µl; 10% v/v N-9 and 100 µg LPS O111:B4 (Sigma-Aldrich) in sterile PBS) or N-9
alone (60 µl; 10% v/v N-9 in sterile PBS) or LPS alone (60 µl; 100µg in sterile PBS)
or 60 µl sterile PBS alone. For all experiments the *E. coli* LPS serotype O111:B4 was
used. This was recently showed to be the most potent in inducing preterm birth in mice
when administered intrauterine (403). Mice were randomly assigned to each group.
Care was taken to avoid spillage of treatment outside the vagina. Mice were allowed
to recover from anaesthesia on a piece of tissue. Maintenance of treatment in the vagina

after recovery from anaesthesia was assessed by observing potential leakage on the tissue. Only minor leakage incidents were observed. Following successful recovery, mice were put in individual cages to monitor the time to delivery. During this period, they were checked in person twice per day for signs of potential adverse effects.

In a different set of experiments, in the afternoon of D16 of pregnancy, mice were anaesthetized using inhalational isoflurane (5% for induction of anaesthesia, 2.5% for maintenance) and a pipette was used for intravaginal administration of either N-9 (60 µl; 10% v/v N-9 in sterile PBS) or 60 µl sterile PBS alone. Mice were randomly assigned to each group. 16 h later, in the morning of D17, mice were anaesthetized using inhalational isoflurane (5% for induction of anaesthesia, 2.5% for maintenance) and a pipette was used for intravaginal administration of either LPS O11:B4 (1 mg in 60 µl sterile PBS) or 60 µl sterile PBS alone. Following successful recovery from anaesthesia, mice were put in individual cages to monitor the time to delivery. During this period, they were checked in person twice per day for signs of potential adverse effects.
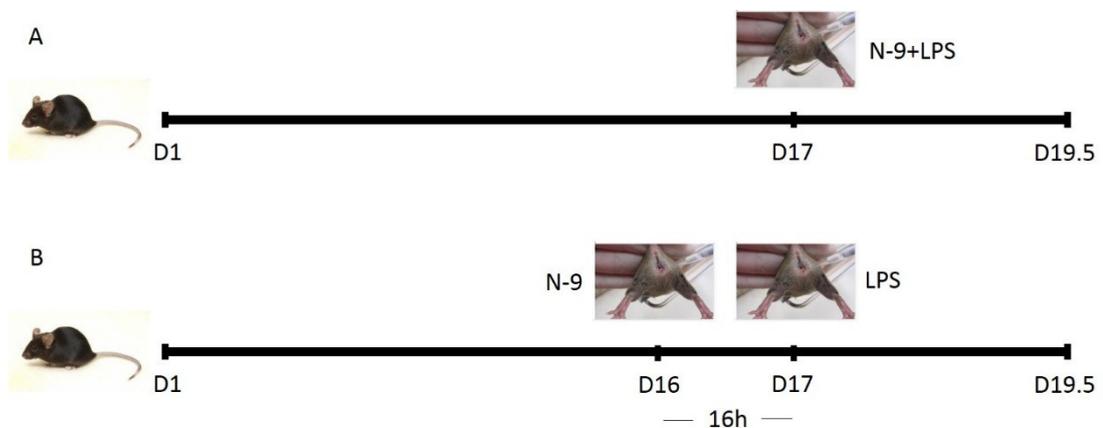
Figure 2.5 Effect of N-9-induced cervical damage and vaginal LPS on timing of delivery. Pregnant C57Bl/6 mice were administered 60 µl of a solution containing 10% N-9 and 100 µg of LPS, or10% N-9 alone or 100 µg LPS or PBS control intravaginally in the morning of D17 of gestation (**A**). Alternatively, mice were administered 60 µl of a solution containing 10% N-9 or PBS control intravaginally in the afternoon of D16 of gestation and this was followed by intravaginal administration

of 60 μl of either 1mg LPS or PBS control 16h later, in the morning of D17 of gestation (**B**). Timing of delivery after the above treatment schemes was monitored using CCTV cameras.

2.14.3 Mouse model of cervical damage-mediated ascending infection with *Ureaplasma parvum*

To assess the effect of N-9-induced cervical damage on facilitating ascending vaginal infection with *Ureaplasma parvum*, *in vivo* bioluminescence imaging and amniotic fluid cultures for the presence of *Ureaplasma parvum* were performed. Bioluminescence imaging allows for optical detection and quantification of the Nanoluc-expressing bacteria after administration of the Nanoluc substrate, Furimazine, in a highly specific and non-invasive manner. Amniotic fluid cultures for the presence of *Ureaplasma parvum* allow for the detection and quantification of live and growing bacteria within the amniotic fluid.

In the afternoon of D16 of pregnancy, mice were anaesthetized using inhalational isoflurane (5% for induction of anaesthesia, 2.5% for maintenance) and a pipette was used for intravaginal administration of either N-9 (60 μl; 10% v/v N-9 in sterile PBS) or 60 μl sterile PBS alone. Mice were randomly assigned to each group. 16 h later, in the morning of D17, mice were anaesthetized using inhalational isoflurane (5% for induction of anaesthesia, 2.5% for maintenance) and a pipette was used for intravaginal administration of either *Ureaplasma parvum* (10^8 CCU/ml in 40 μl of USM) or 40μl USM alone. Following successful recovery from anaesthesia, mice were put in individual cages. During this period, they were checked in person twice per day for signs of potential adverse effects. 24 h later, in the morning of d18, mice were anaesthetized to undergo *in vivo* bioluminescence imaging. After imaging was complete, a Norwegian Formula Deep Moisture Body Lotion was applied to the shaved abdomen to allow for quicker wound healing (Neutrogena, Los Angeles, USA). Following successful recovery from anaesthesia, mice were put in individual cages to

monitor the time to delivery. During this period, they were checked in person twice per day for signs of potential adverse effects.

Mice that had not delivered any of their pups 48 h after the administration of either *Ureaplasma parvum* or vehicle control, in the morning of D19, were deemed term and were sacrificed for tissue collections using Schedule 1 methods (CO_2 asphyxiation followed by cervical dislocation). Term pups that were culled by cervical dislocation followed by decapitation. Mice that had delivered at least 1 of their pups before 48 h after the d17 administration, were deemed preterm. Preterm mice were culled using Schedule 1 methods (CO_2 asphyxiation followed by cervical dislocation). Preterm pups were culled by cervical dislocation followed by decapitation.
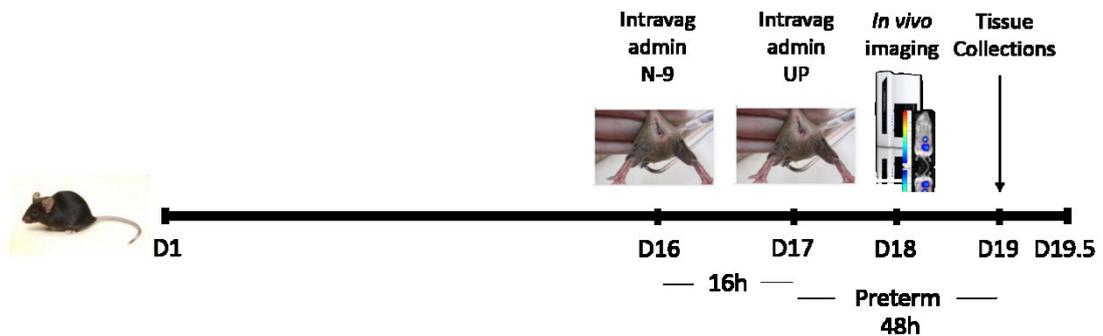
Figure 2.6 Effect of N-9-induced cervical damage on ascending infection with *Ureaplasma parvum* during pregnancy. Pregnant C57Bl/6 mice were administered 60 μl of 10% N-9 or PBS control intravaginally in the afternoon of D16 of gestation. This was then followed by intravaginal administration of 40 μl of *Ureaplasma parvum* in Ureaplasma medium (USM) or USM alone 16 h later, in the morning of D17. Mice underwent *in vivo* bioluminescence imaging 24 h later, in the morning of D18. Mice that had not delivered by the morning of D19 were sacrificed for tissue collections.

Tissue collection and processing

The following tissues were collected and snap-frozen in dry ice from all term dams: vaginal flush (60 μl of PBS were flushed into the vagina right after the mouse was culled) and cervix. 4 pups were chosen for tissue collections from each term dam, 2 from each horn: the one closest to the cervix (proximal) and the one furthest from the

cervix (distal). The following tissues were collected and snap-frozen in dry ice from all term pups: amniotic fluid, placenta, uterus, fetal membranes, and fetal lung. Unless used immediately, tissues were stored in -80°C.
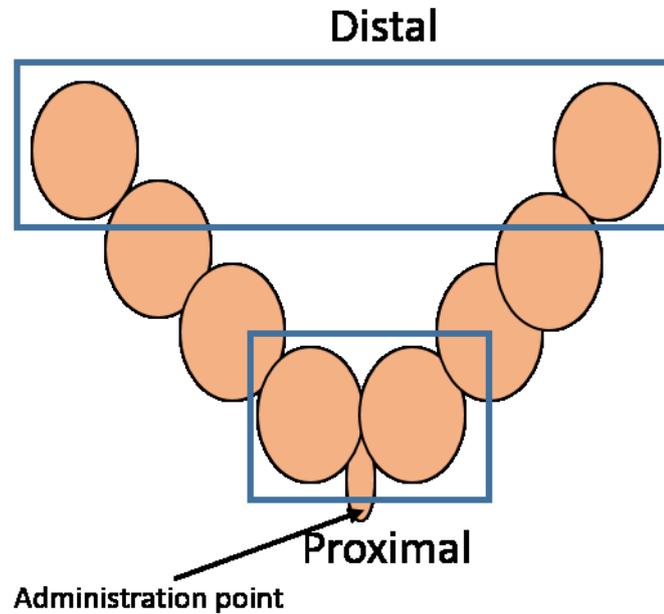
Figure 2.7 Tissue collection strategy. From each term mouse, tissues were collected from 4 different pups: The ones in both horns that were closest to the cervix (Proximal) and the ones in either horn than were furthest from the cervix (Distal).

2.14.4   Time to delivery

Following recovery from anaesthesia, individual cameras were placed at each cage and mice were recorded using a digital video recorder. Time to delivery was calculated as the number of hours from the time of intravaginal administration until delivery of the first pup.

2.14.5   Proportion of live-born pups

Following delivery of the first pup and after recording the timing of delivery, mice were left in the cage for a further 24 h to deliver the rest of the pups. The proportion of live pups was then calculated for each mouse by dividing the number of live pups by the total number of pups and being presented as a percentage. Any live pups still

within the uterine horns 24 h after the first pup was delivered were not considered as live-born, as they had not been through labour.

2.15 *In vivo* Bioluminescence imaging

Mice were anaesthetized using inhalational isoflurane (2.5% for induction of anaesthesia, 2.5% for maintenance). To minimize signal interference through absorbance, scattering or diffraction of light by the mouse fur, mice abdomens were shaved before imaging. 100 µl of the Nanoluc substrate Furimazine (Nano-Glo Live Cell Assay System) were injected intraperitoneally (Promega, Madison, WI, USA). Mice were placed in a PhotonIMAGER^{TM} OPTIMA for optical imaging (Biospace Lab, Nesles-la-Vallee, France). The PhotonIMAGER^{TM} OPTIMA uses a photon counting technology based on intensified Charge-Coupled Devices (CCDs). This allows real-time display of the bioluminescence signal and recording of kinetics information.

Imaging started right after Furimazine administration. The following imaging parameters have been used:

Table 2-10 Parameters for *in vivo* bioluminescence imaging

Software	Photo Acquisition (Biospace Lab, Nesles-la-Vallee, France)
Cryostat temperature	-25ºC
Stage temperature	37ºC
Aperture	50mm f/1.2
Stage height	560mm
Field of view	210x158mm
Image size	313.40371875 x 234.546203125 mm

Pixel size	169.133145574744 x 168.616968457944 μm
Acquisition mode	BLI Bioluminescence (61 ms per frame)
Illumination power	10-20%
Acquisition time	10:00 min
Quantification Units	ph/s/cm^2/sr

2.15.1   Imaging analysis

Imaging analysis was performed using the M3 Vision software (Biospace Lab, Nesles-la-Vallee, France). The same elliptical ROI was drawn around the area that corresponded to each mouse's abdomen, including the lower abdomen and the cervix. Since the Photo Acquisition software allows the display of signal kinetics, quantification analysis was performed during a time frame where the signal intensity was in the plateau phase for each of the ROIs on display.

Quantification unit was photons per second per centimeter square per steradian (ph/s/cm^2/sr). This unit normalizes for differences in the mice size and position on the stage as well as the time frame used for the quantification analysis.

2.16 Amniotic fluid cultures

Detection and quantification of *Ureaplasma parvum* in amniotic fluid samples from D19 of pregnancy followed the principles described earlier.

Using a 96-well plate, 15μl of amniotic fluid were added to 135μl of USM in the top well of a given column. The rest of the wells in that column were filled with 135μl of USM each. 10-fold serial dilutions of the 1st well's bacterial concentration were created across the column by transferring 15μl from the 1st well to the 2nd, from the 2nd

to the 3rd etc. Plates were sealed with adhesive tape and incubated at 37°C in a humidified cell culture incubator with ambient CO_2 overnight. After 48 h, the last well from each column showing pH change consistent with the threshold of detection based on colour change (dark pink) represented 1 Colour Changing Unit (CCU). As this well was a 10-fold dilution of the previous one, the previous well represented 10 CCU. Consequently, if n number of wells in the column showed pH change consistent with the threshold of detection based on colour change (dark pink) and the last well represented 1 CCU, the top well containing 15μl of amniotic fluid of unknown *Ureaplasma parvum* concentration represents 10^{n-1} CCU.

2.17 Cervical damage assessment

To assess tissue damage, the following tissue processing and analysis strategy was decided (**Fig 2.8**): For each mouse, 3 consecutive longitudinal 5μm-thick sections from 3 different levels (L1, L2, L3) would be used for morphological damage, inflammatory infiltrations and mitotic activity analysis respectively. Each level would be 50μm deeper than the preceding one. This strategy allows for potential differences in the damage severity across different parts of the vagina and the cervix to be taken into account.
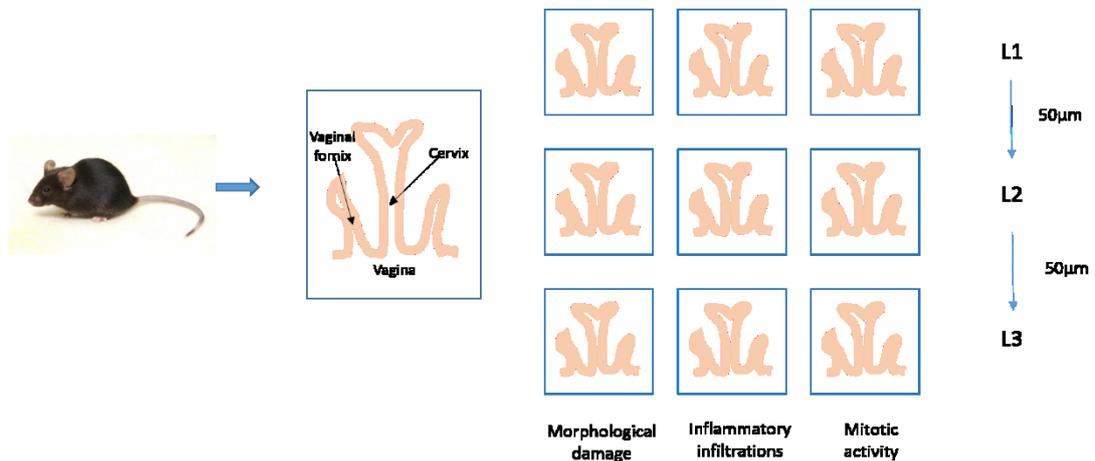
Figure 2.8 Tissue processing and analysis strategy for the cervical damage model. At each of the 3 levels (L1, L2, and L3) one section would be used for morphological damage analysis, one for inflammatory infiltrations analysis and one for mitotic

activity analysis. L2 would be 50μm deeper than L1 and L3 would be 50μm deeper than L2.

2.18 Alcian Blue/Periodic Acid Schiff (AB/PAS) staining

AB/PAS special staining was used to stain the mucus-producing epithelial cells of the mouse vagina and cervix. This would allow to identify subtle changes in the integrity of the epithelial layers of both tissues. Alcian Blue pH 2.5 imparts a blue colour to the acidic mucins and other carboxylated or weakly sulphated acid mucosubstances. The periodic acid Schiff (PAS) reaction is then used to stain basement membranes, glycogen and neutral mucosubstances pink to red. Mixtures of neutral and acidic mucosubstances will appear purple due to positive reactions with both Alcian Blue and PAS. The AB/PAS special stain was performed by the Shared University Research Facilities (SuRF) team of the University of Edinburgh according to their standard protocols.

2.18.1   Deparaffinisation and rehydration

For deparaffinization, slides were immersed 2x5 min in Xylene (Cell Path Ltd, Newtown, UK). This was followed by progressive rehydration of the samples through a sequential immersion in 100%, 95%, 80%, 70% Ethanol, for 20 sec each.

2.18.2   Staining

Following rehydration, slides were immersed in 1% Alcian Blue for 10 min. Slides were then washed under running cold tap water for 10 min. Following this, slides were rinsed in deionized H_2O and were then oxidized in an acquous solution of 0.5% periodic acid for 10-20 min. Slides were then washed under running cold tap water for the same length of time. After a rinse in deionized H_2O, slides were treated with Schiff's reagent for the same length of time. Slides were then washed under running cold tap water for the same length of time.

2.18.3 Counterstain

Slides were immersed in Harris' Haematoxylin for 30 sec. After a 5-min wash under running tap water, slides were placed in Scott's Tap Water Substitute until sections were blue. Slides were then dehydrated through a sequential immersion in 70%, 80%, 95%, 100% Ethanol followed by 2x5 min in Xylene. Mounting media (ThermoFischer Scientific, UK) mounting medium was added to the slides. All slides were sealed with cover slips.

2.19 Immunohistochemistry

Immunohistochemistry was used to localize polymorphonuclear neutrophils in the epithelium and stroma of the cervix and vagina. It was also used to localize proliferating cells, being in the active phases of the cell cycle, within the cervix basement membrane.

2.19.1 Deparaffinisation and rehydration

For deparaffinization, slides were immersed 2x5 min in Xylene (Cell Path Ltd, Newtown, UK). This was followed by progressive rehydration of the samples through a sequential immersion in 100%, 95%, 80%, 70% Ethanol, for 20 sec each. Slides were then left for 5 min under running tap water to further remove residual ethanol.

2.19.2 Antigen retrieval

For antigen unmasking, Heat-Induced Epitope Retrieval (HIER) using a Pressure Cooker was performed. Slides were put in a plastic slide holder containing 300 ml of Sodium Citrate Buffer (10mM Sodium Citrate, pH 6.0 in distilled H_2O, Sigma-Aldrich, St Louis, USA). The slide holder was then placed in an InstantPot IP-LUX60 6L/6.33Qt Pressure Cooker containing 500ml of distilled H_2O (InstantPot, Ottawa, Canada). The slides were left in the Pressure Cooker for approximately 20 min until boiling temperature was reached, the pressure was then released and the slides were left for a further 20 min to cool down.

Upon return of the samples temperature to room temperature, slides were washed 1x5 min in distilled H_2O on a rocker platform at 35 revolutions/min. This was followed by 1x5 min wash in 1% Tris-buffered saline (TBS) on a rocker platform at 35 revolutions/min (Sigma-Aldrich, St Louis, USA).

2.19.3 Blocking

On every slide, a circle was drown around each tissue section using a 5mm hydrophobic PAP pen for immunostaining (Sigma-Aldrich, St Louis, USA), to confine reagent incubation around the tissue.

To block the endogenous peroxidase activity of the samples, slides were immersed in 300ml of a Hydrogen Peroxide (H_2O_2) blocking solution and left to incubate for 30 min on a rocker platform at 35 revolutions/min (10% H_2O_2 in methanol). This was then followed by 2x5 min washes in TBS on a rocker platform.

To prevent non-specific binding of antibodies to tissue or to Fc receptors, 100 µl of a blocking solution was applied on each sample. The blocking solution was a 20% v/v non-immune normal goat serum (NGS) (primary antibodies were raised in different species) and 5% w/v Bovine Serum Albumin (BSA) in PBS (Sigma-Aldrich, St Louis, USA). Samples were left to incubate in a dark humidified chamber to minimize reagent evaporation.

2.19.4 Primary antibodies incubation

To identify polymorphonuclear neutrophils, the following primary antibody preparation was used: Purified rat anti-mouse Ly-6G (Lymphocyte antigen 6 complex, locus G) (1:500 in blocking solution, Biolegend, San Diego, USA). To identify proliferating cells, 100 µl of the following primary antibody preparation was applied on a different set of slides: rabbit anti-Ki67 (ab15580, 1:1000 in blocking solution, Abcam, Cambridge, UK). One section per slide was used as negative control, where blocking solution alone was applied. Samples were left to incubate overnight in a dark humidified chamber at 4ºC. After overnight incubation, slides were washed 1x5 min

in TBS-Tween (0.05% v/v Tween in TBS, Sigma-Aldrich, St Louis, USA) and 2x5 min in TBS on a rocker platform.

In slides where an anti-Ly-6G primary antibody was applied, 100 μl of the following Horseradish Peroxidase (HRP)-conjugated secondary antibody preparation was applied: ImmPRESS HRP Anti-Rat IgG (Vector Laboratories, Burlington, USA). In slides where an anti-Ki67 primary antibody was applied, 100 μl of the following Horseradish Peroxidase (HRP)-conjugated secondary antibody preparation was applied: ImmPRESS HRP Anti-Rabbit IgG (Vector Laboratories, Burlington, USA). Slides were left to incubate with the above-mentioned secondary antibody preparations for 1 h. This was then followed by slides being washed 1x5 min in TBS-Tween and 2x5 min in TBS on a rocker platform.

2.19.5 Chromogenic detection

As the secondary antibody used was conjugated with the enzyme HRP, the substrate used was 3,3'- diaminobenzidine (DAB). DAB is a soluble organic substrate that is converted by HRP to an insoluble brown product, localized at the sites of epitope expression. Slides were incubated with 100 μl of DAB solution until brown colour development for a maximum of 2 min. Colour development was stopped by placing the slides in deionized H_2O.

2.19.6 Counterstain

Slides were immersed in Harris' Haematoxylin (Cell Path Ltd, Newtown, UK) for 5 min. Slides were then washed under running cold tap water and put in 0.3% acid alcohol (Cell Path Ltd, Newtown, UK) for 2-3 sec to differentiate. After another wash slides were put in Scott's tap water (Cell Path Ltd, Newtown, UK) for 30 sec to stop differentiation. Slides were then dehydrated through a sequential immersion in 70%, 80%, 95%, 100% Ethanol followed by 2x5 min in Xylene. Mounting media (ThermoFischer Scientific, UK) mounting medium was added to the slides. All slides were sealed with cover slips (Cell Path Ltd, Newtown, UK).

2.20 Light microscopy imaging

Imaging of the samples was performed using a Zeiss Axio Scan.Z1 Slide Scanner (Carl Zeiss AG, Oberkochen, Germany). Imaging analysis was performed using Zeiss ZEN Blue software (Carl Zeiss AG, Oberkochen, Germany).

2.21 Statistical analysis

All statistical analyses were performed using GraphPad Prism version 7 (GraphPad, San Diego, CA, USA). Data in graphs are presented as dot plots. Error bars represent standard deviation (SD). Data in text are presented as mean± standard error of the mean (SEM). Observation of data points and D' Agostino- Pearson omnibus normality test were used to assess normality of the sample distributions. For normally distributed groups the following tests were used: Unpaired or paired Student's *t* test was used to compare means of two groups. One way analysis of variance (ANOVA) was used to compare more than two groups. Dunnett's *post hoc* test was used to compare multiple groups to a control group. Holm-Sidak test was used to analyse sets of P values between multiple groups. For groups that did not follow a Gaussian distribution the following tests were used: Mann-Whitney test to compare the means of two groups. Kruskal-Wallis test to compare the means between 3 or more groups. Percentages were compared by Fisher's exact test. Inter-rater reliability was assessed using weighted Cohen's kappa.

Gene expression analysis was performed on DDCt values. Two way ANOVA was used to determine statistical significance in the presence of two variables. This was followed by *post hoc* Dunnett's test in cases where statistically significant results were yielded for the particular variable. Spearman's correlation coefficient was used to determine correlation in gene expression studies. A P-value less than 0.05 was considered statistically significant.

Chapter 3   Effects of Nonoxynol-9 and *Ureaplasma* spp on cervical epithelial cells *in vitro*

3.1 Introduction

The uterine cervix has a key role in maintaining a healthy pregnancy. It provides structural support to the uterine content throughout gestation and at the same time undergoes progressive remodelling to acquire the necessary distensibility that will allow safe passage of the fetus during labour. Importantly, it forms a physical and functional barrier to protect the fetus from external insults, such as a bacterial infection. This is particularly important given that an ascending infection of vaginal bacteria through the cervix is the most common precursor of preterm birth, the leading cause of neonatal mortality and morbidity worldwide (3) (16).

The cervical epithelium is an important component of the barrier function of the cervix during pregnancy. In humans, the cervical epithelium consists of two parts: the endocervical single-layer columnar epithelium which is proximal to the uterus and the ectocervical multi-layered squamous epithelium that is proximal to the vagina. To maintain an effective physical barrier, the cervical epithelium strictly regulates the temporal expression of tight and gap junction proteins (269) and desmosomes (268). This ensures selective pericellular epithelial permeability of useful substances such as nutrients while excluding harmful bacteria. In addition, the cervical epithelium forms a functional immunological barrier against infection. Cervical epithelial cells express Toll-like receptors and are thus able to sense a microbial challenge (268). Upon pathogen recognition, the epithelium can stimulate the innate and adaptive immune response by secreting proinflammatory cytokines and chemokines (282). Epithelial

cells also participate in the effector mechanisms of the adaptive immunity by secreting antimicrobial peptides such as SLPI (288), Elafin (284) and LL-37 (285). The importance of a healthy cervical epithelium could be clinically demonstrated by the fact that excisional procedures for the treatment of CIN like cone biopsy or LLETZ, that remove part of the epithelium and the underlying stroma, significantly increase the risk for preterm delivery (304) (305). However, the underlying mechanisms remain elusive.

Nonoxynol-9 is a non-ionic surfactant that has been extensively used as a component of spermicides due to its ability to solubilize and disrupt the plasma membrane of spermatozoa (404) (405). However, it is also highly cytotoxic for epithelial cells of the reproductive tract (406). Although it has been shown to cause significant epithelial damage *in vivo* (407) (408) (409), its effects during pregnancy have not been studied yet.

Among the bacteria that have been associated with preterm birth, the most common ones belong to the *Ureaplasma* spp, namely *U. parvum* and *U. urealyticum* (410). These bacteria have been shown to cause chorioamnionitis that predisposes to PTB (253). In addition, they can cause significant fetal injury with disruption of the fetal brain development (411). As *Ureaplasmas* are considered commensals of the vagina, they need to break through the cervical barrier to cause an intrauterine infection. However, whether the cervical epithelium can mount an effective immune response against *Ureaplasmas* is not known.

The work described in this chapter investigated the effects of Nonoxynol-9 on cervical epithelial cells *in vitro*. We hypothesized that N-9 treatment could compromise both the physical and the functional barrier function of the cervical epithelium. Furthermore, we assessed the capacity of cervical epithelial cells to sense an infection with *U. urealyticum* and respond by producing proinflammatory cytokines and chemokines. The hypothesis was that cervical epithelial cells could recognize *U. urealyticum* through TLRs and that this recognition could only cause a mild inflammatory response.

3.2 Results

3.2.1 N-9 reduces the viability of endocervical End1/E6E7 epithelial cells

To assess the effect of N-9 on the viability of endocervical End1/E6E7 cells, a metabolic activity assay using MTT assay was performed. MTT assesses the metabolic activity of the cells which directly proportionate to the cell viability. Different doses of N-9 were used (0, 2, 4, 8, 16, 32, 64, 128, 256, 512 µg/ml in Cell Culture Medium-CCM) and for different time points (30 min, 1, 2, 4, 24 h). At the end of each incubation period, MTT assays were performed. The metabolic activity for each group of cells was expressed as a percentage of the metabolic activity of the untreated cells.

A clear trend was identified (**Fig 3.1**). The low doses of N-9 (2, 3, 8 µg/ml) had only minimal effects on the endocervical cells' viability, as they resulted in the cells demonstrating 80-90% of the metabolic activity of the vehicle-treated cells for all incubation times (**Fig 3.1**).

Similarly, the high N-9 doses (128, 256, 512 µg/ml) almost completely abolished the cells' metabolic activity to less than 20% of the vehicle-treated cells for all time points (**Fig 3.1**).

The medium N-9 doses of 16 µg/ml and more so 32 and 64 µg/ml exhibited time-dependent trends (**Fig 3.1**). The 16 µg/ml dose started with 81.15±3.18% metabolic activity of the vehicle-treated cells after 30 min incubation, to drop to 68.35±6.4% at 24 h. More dramatic were the changes with the other two dosages. At 32 µg/ml, N-9 resulted in the metabolic activity being 81.2±7.34% of the vehicle-treated after 30 min which gradually dropped to only 12.05±1.69% at 24 h. The 64 µg/ml dose leads to a metabolic activity of 66.28±8.8% of vehicle-treated cells at 30 min but then follows a steep drop to 26.88±3.26% at 1 h and below 20% for all incubation times after this (**Fig 3.1**).
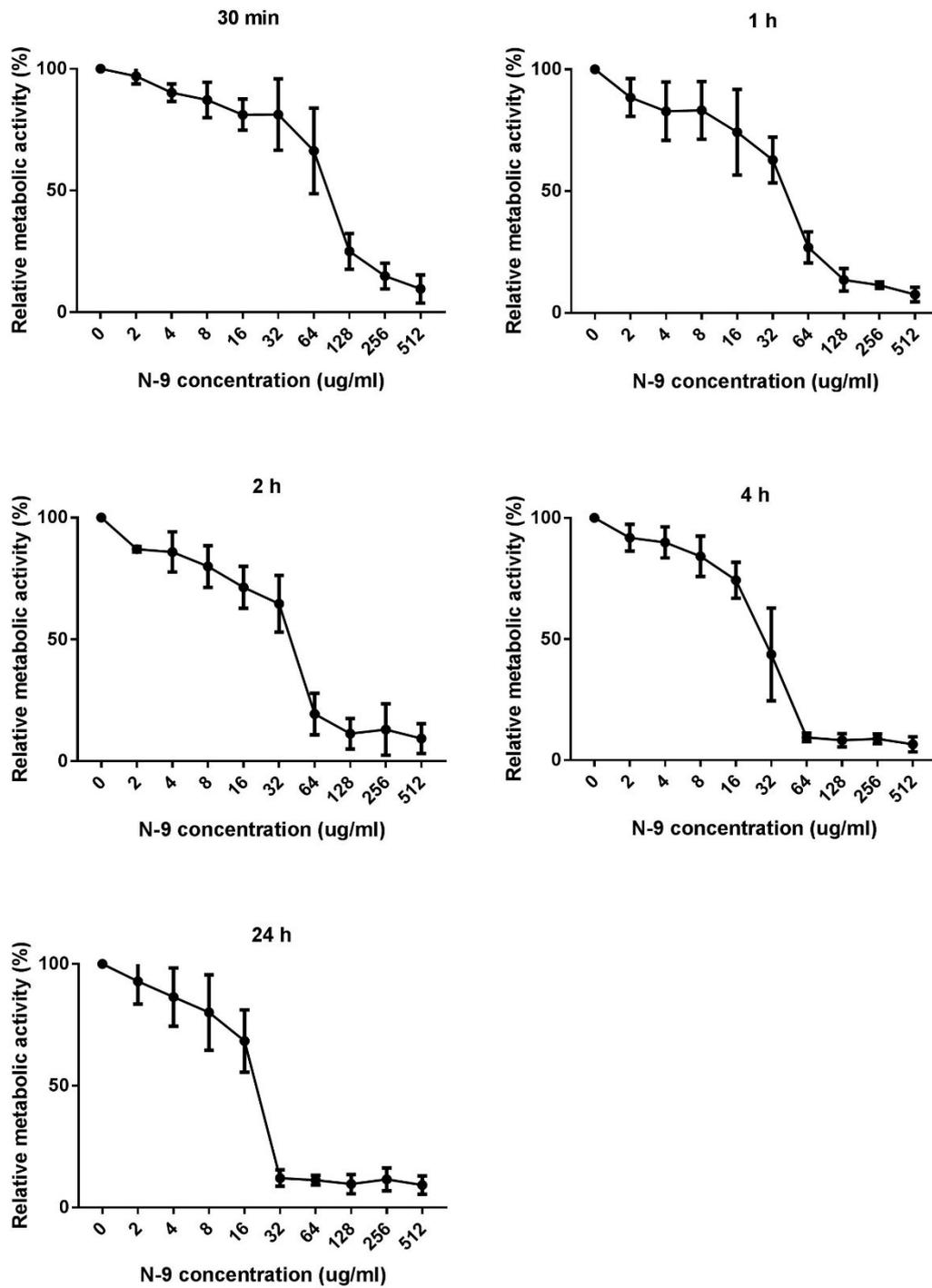
Figure 3.1 Treatment of endocervical cells (End1/E6E7) with N-9 results in decreased cell metabolic activity in a dose- and time-dependent manner. End1/E6E7 cells were incubated with various N-9 concentrations (0, 2, 4, 8, 16, 32,

64, 128, 256 and 512 μg/ml) for 30min, 1h, 2h, 4h and 24h. Metabolic activity indicating cell viability was determined by an MTT assay and is expressed relative to that of the untreated cells. Four independent experiments were conducted. Error bars indicate *SD*.

3.2.2 N-9 compromises the physical barrier function of an endocervical End1/E6E7 monolayer

To assess whether N-9 treatment could compromise the physical barrier function of the cervical epithelium, an *in vitro* permeability assay was performed on a monolayer of End1/E6E7 cells. After different N-9 treatments (0, 3, 10, 30, 100 μg/ml) for 2 h, a FITC-Dextran solution was administered and the fluorescence intensity (F. I.) was measured at the other side of the monolayer (receiver well) (**Fig 3.2**).

The low doses of N-9 (3, 10 μg/ml) had no effect on the epithelial barrier function as they resulted in practically the same F. I. values (412.2 ± 41.27 units and 452.1 ± 26.44 units respectively) as the vehicle-treated cells (441.8 ± 48.5 units). They also had no effect on the monolayer confluence as observed by microscopy (**Fig 3.2**).

The medium (30 μg/ml) and high (100 μg/ml) doses compromised the epithelial barrier function as they significantly increased the F. I. in the receiver well compared to both the untreated cells and the ones treated with the low doses. The medium dose increased the F. I to 968.9 ± 139.3 units ($P < 0.05$ for 30 μg/ml *vs* 0, 3 and 10 μg/ml). The high dose increased the F. I. to 1424 ± 207.1 units ($P < 0.001$ for 100 μg/ml *vs* 0, 3 and 10 μg/ml). Under the microscope, both treatments disrupted the continuity of the epithelial cell monolayer (**Fig 3.2**).
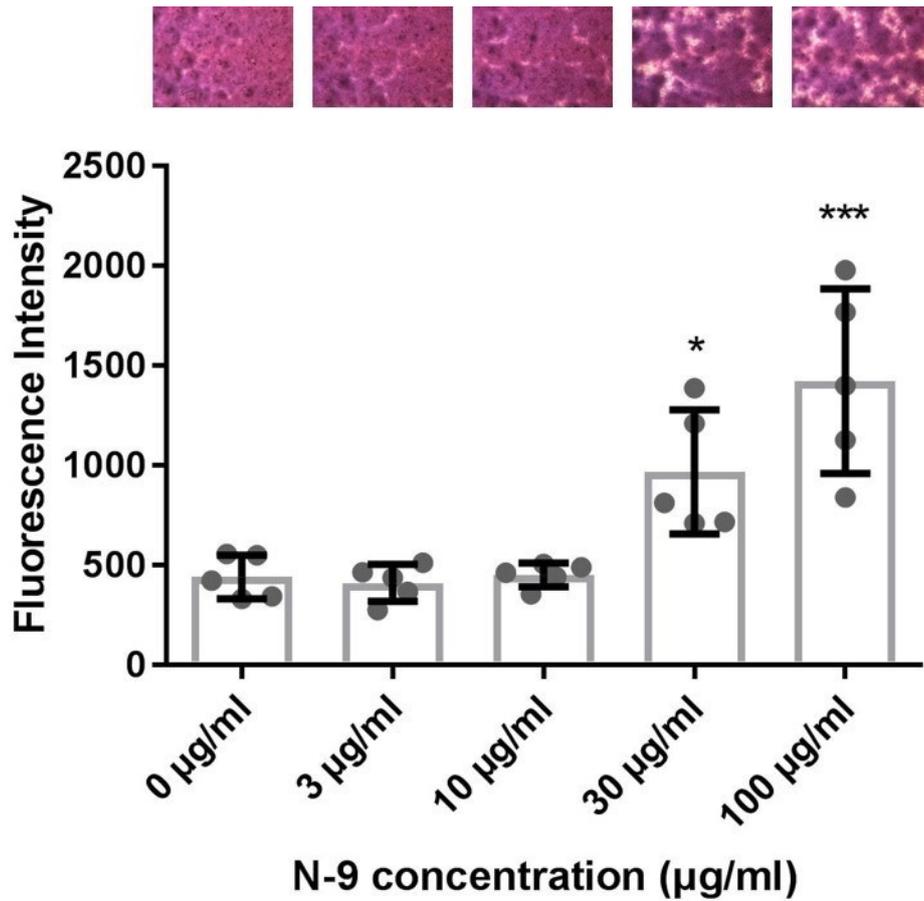
Figure 3.2 Medium and high doses of N-9 result in compromised epithelial barrier function of endocervical (End1/E6E7) cells. Confluent End1/E6E7 cells were seeded at 500,000 cells per insert for 72 hours in growth medium. Following this period, the monolayers were treated with different concentrations of N-9 diluted in growth medium (0 µg/ml, 3 µg/ml, 10 µg/ml, 30 µg/ml and 100 µg/ml) for 2 hours. A FITC-Dextran solution was added to the inserts for 1 hour and the fluorescence intensity (F. I.) of the receiver wells was measured using CLARIOstar multimode microplate reader. High N-9 concentrations (30 and 100 µg/ml) resulted in higher F. I. of the respective receiver wells compared to low N-9 concentrations (0, 3 and 10 µg/ml), indicating increased epithelial permeability. Five independent experiments were conducted. Error bars indicate *SD*. Statistical significance was assessed using 1-way ANOVA with Dunnett's multiple comparisons test against the 0 µg/ml group (*P<0.05 for 30 µg/ml *vs.* 0, 3 and 10 µg/ml, ***P<0.001 for 100 µg/ml *vs.* 0, 3, and 10 µg/ml).

3.2.3 N-9 has no effect on the ability of endocervical End1/E6E7 cells to secrete proinflammatory cytokines and chemokines

To assess whether N-9 could compromise the functional epithelial barrier to infection by disrupting the ability of the epithelial cells to secrete proinflammatory cytokines basally and upon LPS-stimulation, End1/E6E7 cells were pre-treated with N-9 for 2 h and then treated with Growth medium (CCM) or LPS only.

Identification of the proper N-9 dose

As shown in Chapter 3.2.1 (**Fig 3.1**), after 2 h of N-9 treatment, the N-9 dose that results in an acceptable 50% cytotoxicity is 40 µg/ml. For this experiment, after the 2-hour N-9 treatment, a 24-hour treatment with either CCM or LPS followed. To take into account the possibility of a prolonged N-9 effect even after it is removed from the treatment, we tried two lower doses of N-9 as well (0.4 and 4 µg/ml). At, the end of each experiment, the cell viability was assessed by MTT assay and the findings were validated with a cytotoxicity LDH assay.

The high pre-treatment dose of 40 µg/ml N-9 followed by either CCM or LPS led to extremely low viability (2.09±0.32% and 2.44±0.53% respectively) relative to the control treatment as assessed by the MTT assay (**Fig 3.3A**). Similar were the cytotoxicity findings of the LDH assay (**Fig 3.3B**).

The low pre-treatment dose of 0.4 µg/ml N-9 followed by either CCM or LPS led to a viability of 91.89±1.71% and 88.15±1.89% relative to the control treatment respectively, using the MTT assay (**Fig 3.3A**). The cytotoxicity levels of the above treatments in the LDH assay mirrored the MTT findings. This dose of N-9 followed by CCM resulted in 9.23±3.1% cytotoxicity and the N-9 followed by LPS to 3.87±0.95% cytotoxicity relative to cytotoxicity of the highest dose of N-9 (**Fig 3.3B**).

Finally, the medium dose of 4 µg/ml N-9 followed by either CCM or LPS led to a viability of 74.2±4.02% and 75.48±3.88% of the control treatment respectively, using the MTT assay (**Fig 3.3A**). Again the cytotoxicity findings mirrored the viability ones

with 23.94±9.52% and 20.62±10.07% of the highest dose of N-9 respectively (**Fig 3.3B**).

As the highest dose of N-9 was proven very toxic and the lowest dose had only a minimal effect, the dose of 4 µg/ml was chosen for subsequent experiments.

Another important finding is that LPS itself does not reduce cell viability as confirmed by both the MTT and the LDH assay (**Fig 3.3A, B**).
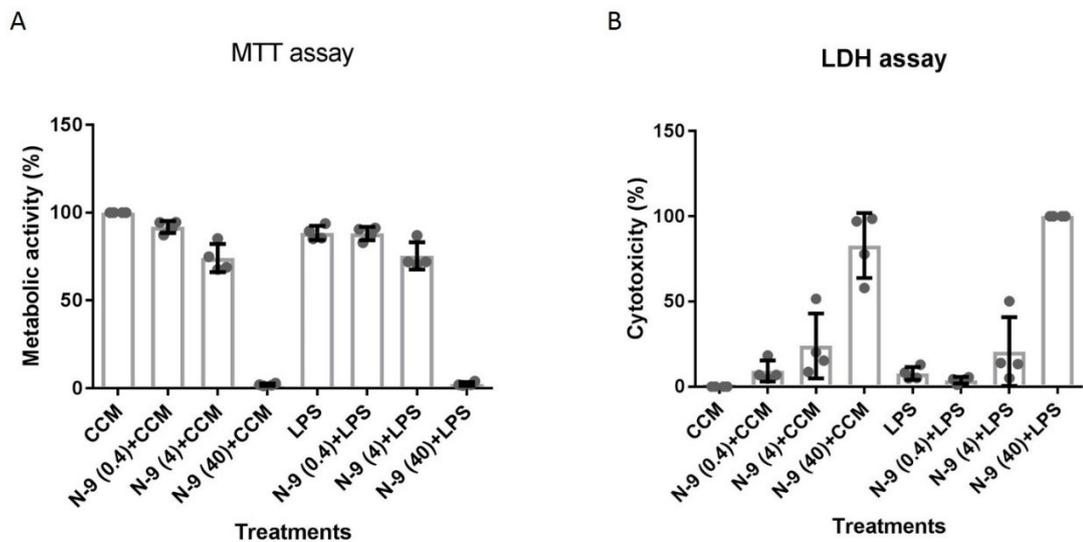
Figure 3.3 N-9 pre-treatment at 4 µg/ml for 2 h affects the viability of End1/E6E7 cells but without exceeding the 50% cytotoxicity limit. Confluent End1/E6E7 cells were seeded at 200,000 cells per well for 48 hours in growth medium. Following this, cells were treated with 3 doses of N-9 diluted in Cell Culture Medium (CCM) (0.4 µg/ml, 4 µg/ml and 40 µg/ml) for 2 hours followed by a further 24 h either with 1 µg/ml LPS in CCM or CCM alone. N-9 at 0.4 µg/ml has no effect on End1/E6E7 cells' viability and at 40 µg/ml results in acceptably low levels of viability as assessed by metabolic activity (**A**) and cytotoxicity (**B**) levels, relative to those of untreated cells (CCM alone). N-9 at 4 µg/ml affects viability but without exceeding the 50% cytotoxicity limit.

Protein analysis

To identify proinflammatory cytokines and chemokines secreted by the End1/E6E7 cells that could have been affected by the treatments, a human cytokine proteomic array was performed on pooled cell culture supernatants from experimental repeats.

The array identified that the following cytokines and chemokines are secreted: IL-6, IL-8, CXCL-1 and CXCL-10. All of them are upregulated with LPS treatment compared to CCM treatment (**Fig 3.4A**).

To examine whether 4 μg/ml N-9 pre-treatment could affect the ability of the End1/E6E7 cells to secrete cytokines, ELISA was performed on cell culture supernatants from the same experiments. IL-6 and IL-8 were chosen for further investigation.

Pre-treatment with N-9 did not change the levels of basal IL-6 secretion by End1/E6E7 cells after 24 hours in CCM (374.9±68.68 and 394.5±56.53 pg/ml without and with pre-treatment respectively). Similarly, N-9 pre-treatment had no effect in the LPS-stimulated secretion of IL-6 either (286.3±18.73 and 239.1±34.71 pg/ml without and with pre-treatment respectively) (**Fig 3.4B**).

The same results were also found for the levels of IL-8. No difference by N-9 pre-treatment was noticed at a basal level (374.9±68.68 and 394.5±56.53 pg/ml without and with pre-treatment respectively) or after LPS stimulation (4,243±260.6 and 4,050±309.7 pg/ml without and with pre-treatment respectively) (**Fig 3.4D**).

To take into account the N-9-induced cytotoxicity that resulted in smaller population of cells, the amount of total protein concentration in the cell culture supernatants was determined using a protein assay. The levels of IL-6 and IL-8 determined by ELISA were subsequently expressed and graphed as a percentage of the total protein produced by each group of cells. Similar to the previous findings, no change in the expression levels of IL-6 (**Fig 3.4C, E**) and IL-8 was noticed, either basally or after LPS stimulation.
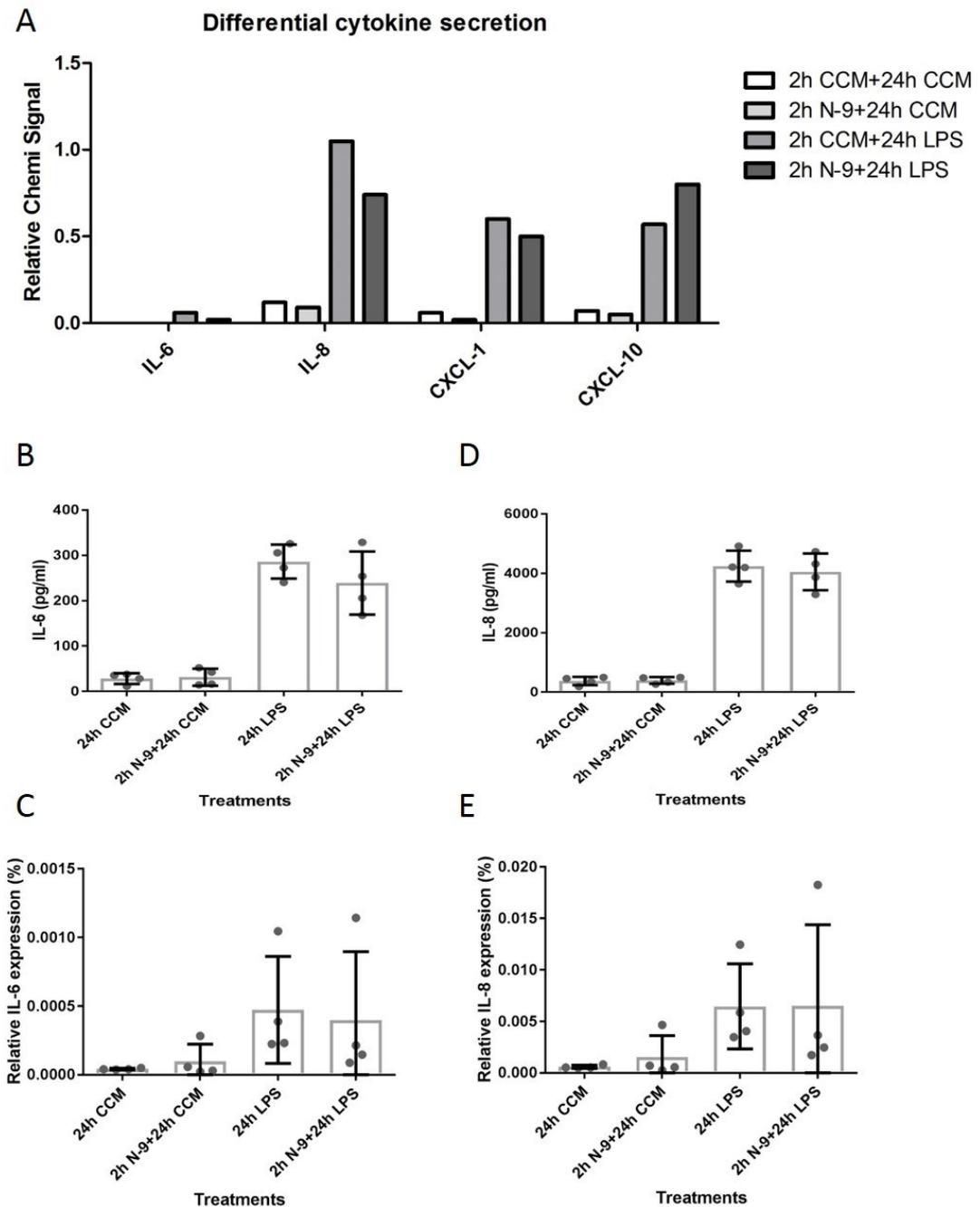
Figure 3.4 N-9 pre-treatment has no effect on the ability of End1/E6E7 cells to secrete proinflammatory cytokines basally and after LPS stimulation. Confluent End1/E6E7 cells were seeded at 200,000 cells per well for 48 hours in growth medium. Following this, cells were treated with 4 µg/ml N-9 in CCM or CCM alone for 2 h and then with CCM alone or 1 µg/ml LPS in CCM. No effect on IL-6, IL-8, CXCL-1 and

CXCL-10 levels was found as assessed using a cytokine array (**A**). No effect was found on IL-6 and IL-8 absolute levels as assessed by ELISA (**B, D** respectively) or levels relative to total protein as assessed by ELISA and total protein assay (**C, E** respectively) (Unpaired *t*-test with Welch's correction).

3.2.4 *Ureaplasma urealyticum* effect on TLR gene expression on HeLa cells

While ascending to the uterus, the bacteria most commonly associated with PTB first come in contact with the cervical epithelium. To identify whether an infection with *Ureaplasma urealyticum* could result in upregulation of TLRs by cervical epithelial cells, HeLa cells were treated with 10^7 CCU/ml *U. urealyticum* for 24 h. The gene expression of TLR1, TLR2, TLR3, TLR4, TLR6, TLR7 and TLR9 relative to the vehicle-treated cells were analysed by qPCR.

The expression of the TLRs examined did not demonstrate any statistically significant changes between cells treated with *U. urealyticum* and those treated with the vehicle control USM (**Fig 3.5**).
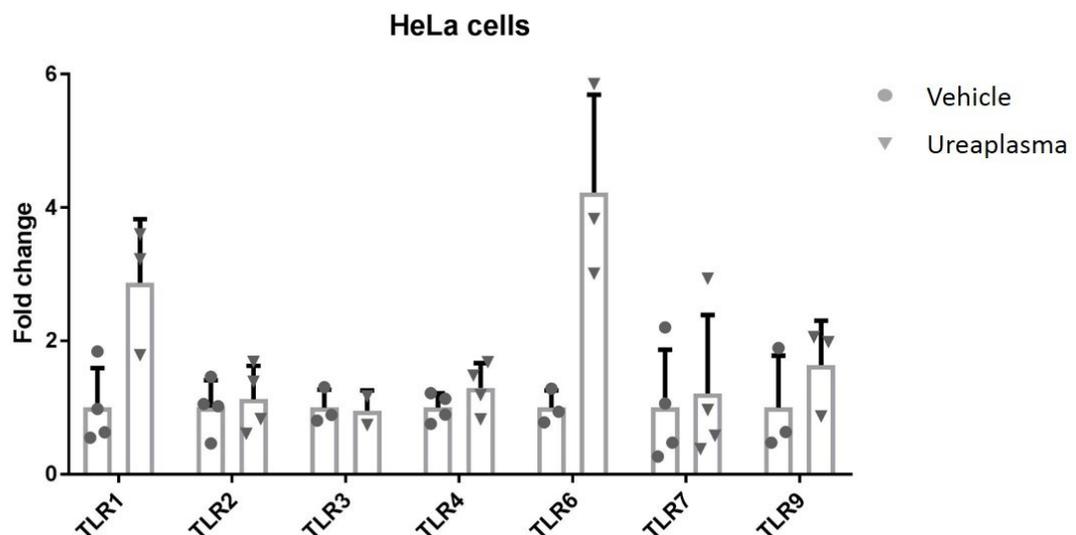
Figure 3.5 *Ureaplasma urealyticum* **infection of HeLa cells does not result in significant changes of TLRs mRNA levels.** Confluent HeLa cells were seeded at 100,000 cells per well for 48 hours in growth medium. Following this, cells were treated either with *Ureaplasma urealyticum* (10^7 CCU/ml in USM) or with vehicle control (USM alone) for 24 h. Quantitative Real-Time PCR showed no changes in the mRNA expression of TLRs in cells infected with *Ureaplasma urealyticum.* Error bars represent *SD*. Statistical significance was determined using the Holm-Sidak method on DDCt values.

3.2.5 *Ureaplasma urealyticum* effect on cytokine and chemokine secretion on HeLa cells

To assess whether HeLa cells could respond to an infection with *U. urealyticum* by secreting proinflammatory cytokines and chemokines, a Luminex multiplex assay on cell culture supernatants after 24-h treatment with with 10^7 CCU/ml *U. urealyticum* or USM was performed. A panel of 17 cytokines and chemokines was examined.

Luminex assay revealed 9 of these cytokines (IL-6, IL-8, GM-CSF, INFγ, IP-10, MCP-1, MIP-1b, RANTES and TNFa) are secreted by the HeLa cells but their levels are not altered in the presence of an infection with *U. urealyticum* (**Fig 3.6**).
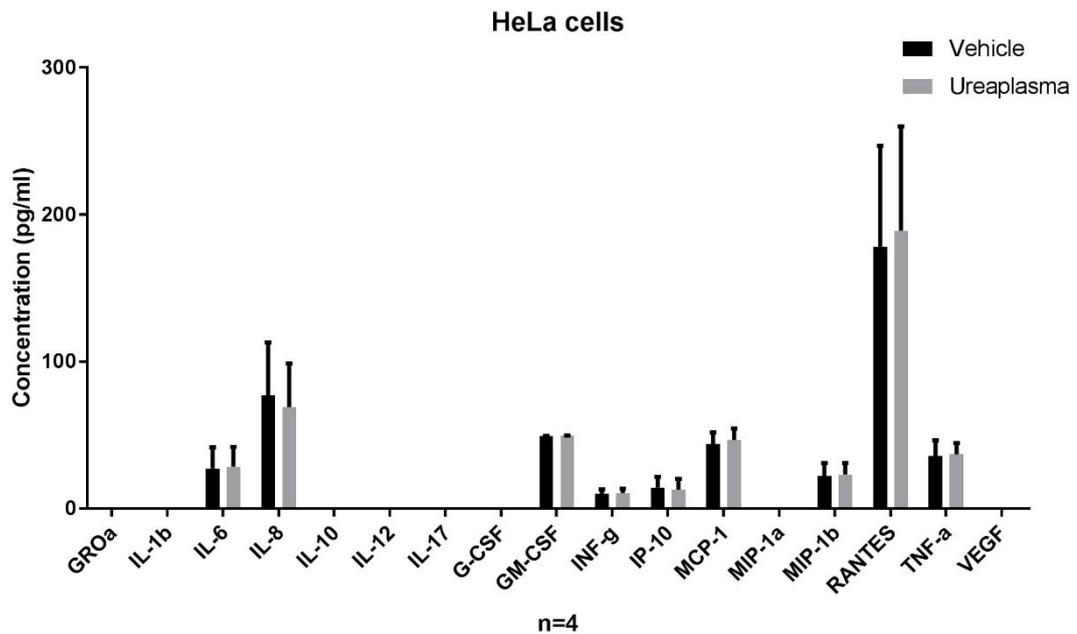
Figure 3.6 ***Ureaplasma urealyticum* infection of HeLa cells has no effect on the levels of secreted proinflammatory cytokines**. Confluent HeLa cells were seeded at 100,000 cells per well for 48 hours in growth medium. Following this, cells were treated either with *Ureaplasma urealyticum* (10^7 CCU/ml in USM) or with vehicle control (USM alone) for 24 h. A Luminex assay showed no difference in the levels of secreted proinflammatory cytokines with *Ureaplasma urealyticum* infection. Statistical significance was determined using the Holm-Sidak method.

3.2.6 *Ureaplasma urealyticum* effect on TLR gene expression on HESC cells

If the physical epithelial barrier is compromised, the bacteria can then be exposed to the underlying stroma. To identify whether an infection with *Ureaplasma urealyticum* could result in upregulation of TLRs by endometrial stromal cells that closely resemble cervical stromal cells, HESC cells were treated with 10^7 CCU/ml *U. urealyticum* for 24 h. The gene expression of TLR1, TLR2, TLR3, TLR4, TLR6, TLR7 and TLR9 relative to the vehicle-treated cells were analysed by qPCR.

No significant changes were found in the gene expression of TLRs following treatment with *U. urealyticum* (**Fig 3.7**).
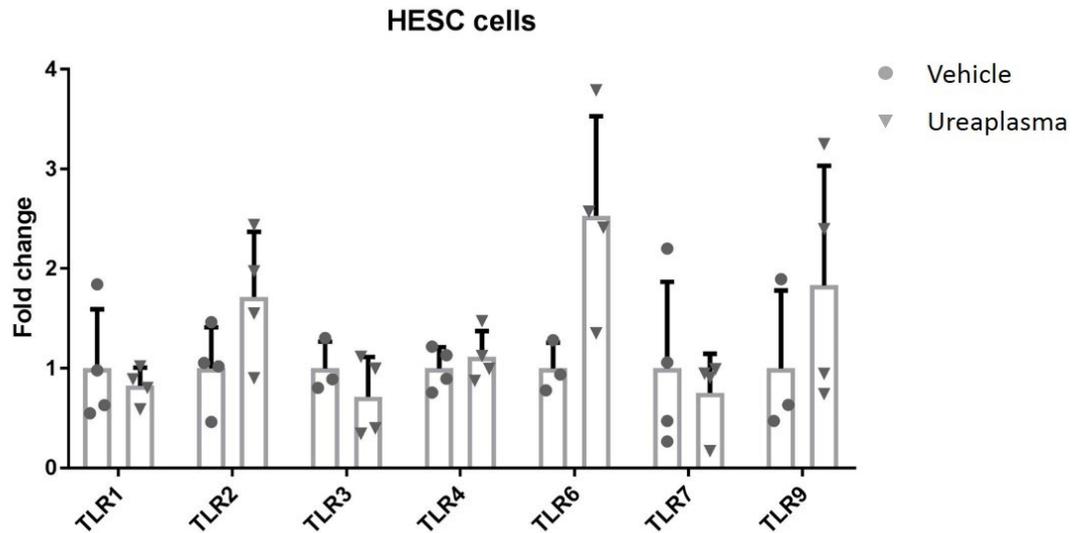
Figure 3.7 *Ureaplasma urealyticum* **infection of HESC cells does not result in significant changes of TLRs mRNA levels.** Confluent HeLa cells were seeded at 100,000 cells per well for 48 hours in growth medium. Following this, cells were treated either with *Ureaplasma urealyticum* (10^7 CCU/ml in USM) or with vehicle control (USM alone) for 24 h. Quantitative Real-Time PCR showed no changes in the mRNA expression of TLRs in cells infected with *Ureaplasma urealyticum*. Error bars represent *SD*. Statistical significance was determined using the Holm-Sidak method on DDCt values.

3.2.7 *Ureaplasma urealyticum* effect on cytokine and chemokine secretion on HESC cells

To assess whether HESC cells could respond to an infection with *U. urealyticum* by secreting proinflammatory cytokines and chemokines, a Luminex multiplex assay on cell culture supernatants after 24-h treatment with with 10^7 CCU/ml *U. urealyticum* or USM was performed. A panel of 17 cytokines and chemokines was examined.

Luminex assay revealed 8 of these cytokines (GROa, IL-8, G-CSF, GM-CSF, INFγ, MCP-1, MIP-1b and TNFa) are secreted by the HeLa cells but their levels are not altered in the presence of an infection with *U. urealyticum* (**Fig 3.8**).
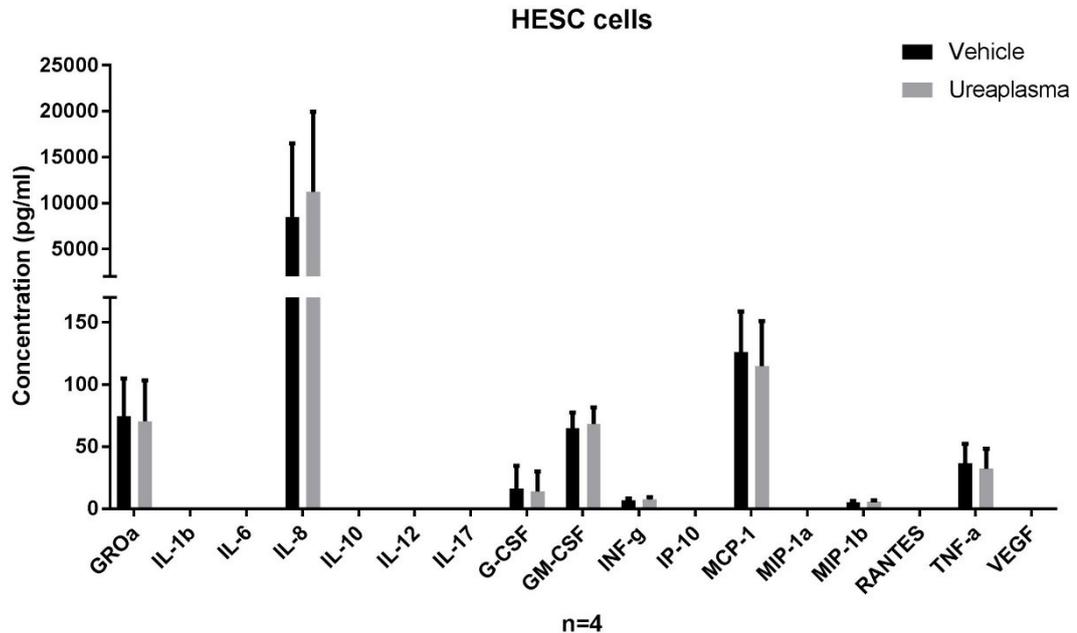
Figure 3.8 *Ureaplasma urealyticum* **infection of HESC cells has no effect on the levels of secreted proinflammatory cytokines.** Confluent HeLa cells were seeded at 200,000 cells per well for 48 hours in growth medium. Following this, cells were treated either with *Ureaplasma urealyticum* (10^7 CCU/ml in USM) or with vehicle control (USM alone) for 24 h. A Luminex assay showed no difference in the levels of secreted proinflammatory cytokines with *Ureaplasma urealyticum* infection. Statistical significance was determined using the Holm-Sidak method.

3.2.8 *Ureaplasma urealyticum* effect on wound healing capacity of HeLa cells

It is the hypothesis of this thesis that cervical damage predisposes to ascending infection. In the case of cervical damage, vaginal bacteria ascending to the uterus will encounter a damaged cervical epithelium. To assess the effect of *U. urealyticum* on

the wound healing capacity of cervical epithelial cells, an artificial wound was created on a HeLa cells' monolayer and wound closure efficiency was examined in the presence of infection for 48 h.

24 h after the wound was created the cell density in the wound area relative to the cell density outside the wound are was significantly lower for the cells that were infected with *U. urealyticum* (24.02±3.47% for *Ureaplasma vs* 29.42±2.84% for vehicle, P=0.0135). Similar were the findings 48 h after the wound was created (25.68±3.62% for *Ureaplasma vs* 31.95±3.099% for vehicle, P=0.0111) (**Fig 3.9A, B**).

During the whole 48 h, the relative wound density of the *Ureaplasma*-treated cells was consistently lower than the vehicle-treated cells (**Fig 3.9C**).
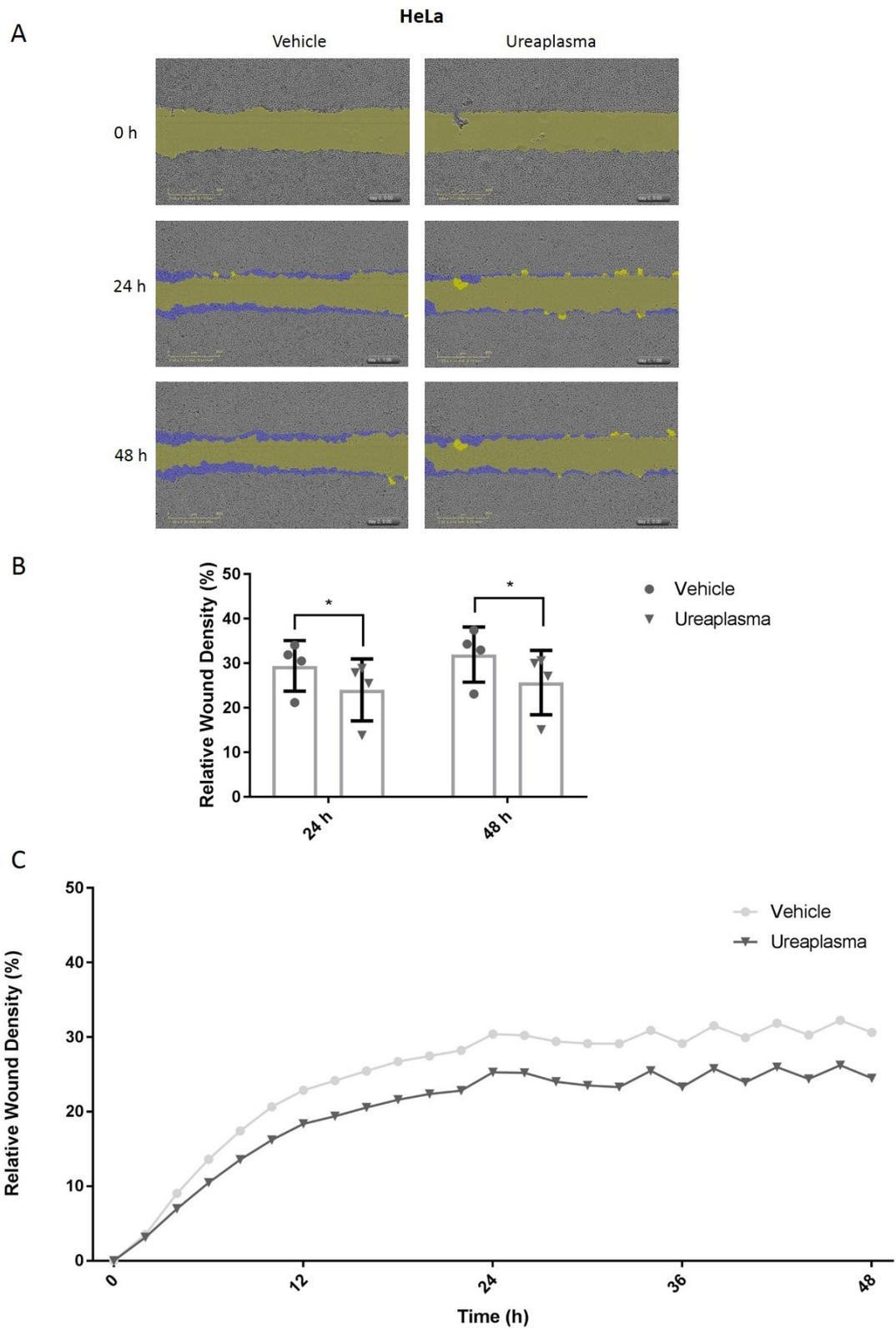
Figure 3.9 *Ureaplasma urealyticum* **infection diminishes the wound healing capacity of HeLa cells.** Confluent HeLa cells were seeded at 50,000 cells per well for 48 hours in growth medium. Following this, an artificial wound was created using a 10µl pipette tip (**A**, yellow). Cells were treated either with *Ureaplasma urealyticum* (10^7 CCU/ml in USM) or with vehicle control (USM alone) and the closure of the artificial wound (**A**, blue) was monitored every 2 h using the IncuCyte Zoom system. *Ureaplasma urealyticum* infection results in a significantly decreased relative wound density compared to vehicle control at 24 and 48 h (**B**). Curves comprising all time points for Vehicle and *Ureaplasma* (**C**) (each data point is an average of n=4 experimental repeats). Error bars represent *SD*. Statistical significance was determined using a paired *t*-test (*P<0.05 for *Ureaplasma vs.* vehicle at 24 and 48 h).

3.2.9 *Ureaplasma urealyticum* effect on wound healing capacity of HESC cells

In the case of cervical damage, vaginal bacteria ascending to the uterus will encounter an underlying cervical stroma as well. To assess the effect of *U. urealyticum* on the wound healing capacity of stromal cells, an artificial wound was created on a HESC cells' monolayer and wound closure efficiency was examined in the presence of infection for 48 h.

24 h after the wound was created there was no difference in the relative wound density between infected and uninfected cells (28.35±3.18% for *Ureaplasma vs* 30.8±3.15% for vehicle). However, at 48 h, the *Ureaplasma*-infected cells had a significantly lower relative wound density compared to the vehicle-treated cells (44.94±2.22% for *Ureaplasma vs* 51.49±3.32% for vehicle, P=0.012) (**Fig 3.10A, B**).

During the 48 h-monitoring of the wound, the relative wound density of the *Ureaplasma*-treated cells was similar to that of the vehicle-treated cells for the first 28 h. After this, infected cells had a consistently lower relative wound density compared to the uninfected ones (**Fig 3.10C**).
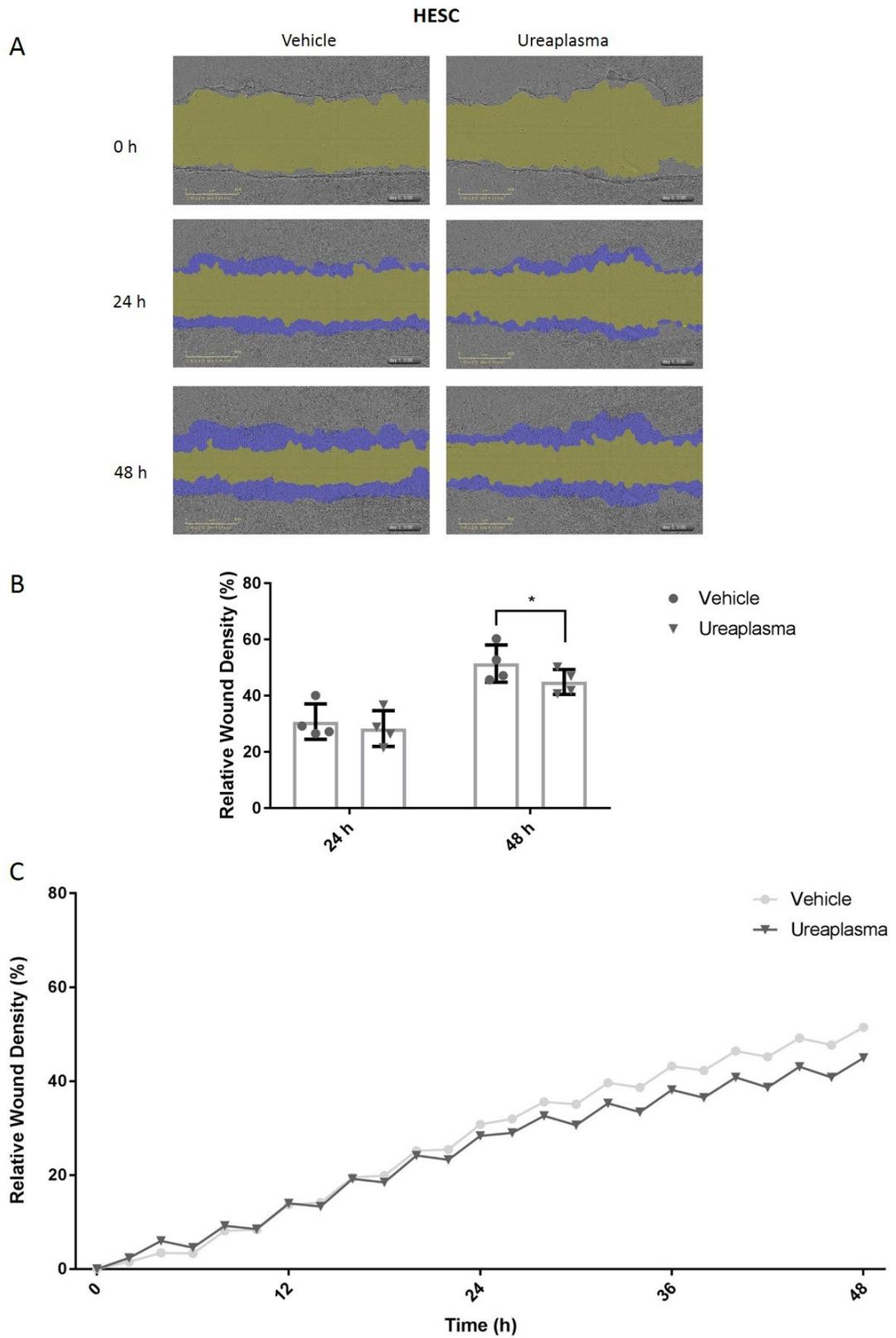
Figure 3.10 *Ureaplasma urealyticum* infection diminishes the wound healing capacity of HESC cells. Confluent HESC cells were seeded at 50,000 cells per well for 48 hours in growth medium. Following this, an artificial wound was created using a 10μl pipette tip (**A**, yellow). Cells were treated either with *Ureaplasma urealyticum* (10^7 CCU/ml in USM) or with vehicle control (USM alone) and the closure of the artificial wound (**A**, blue) was monitored every 2 h using the IncuCyte Zoom system. *Ureaplasma urealyticum* infection results in a significantly decreased relative wound density compared to vehicle control at 48 h (**B**). Curves comprising all time points for Vehicle and *Ureaplasma* (**C**) (each data point is an average of n=4 experimental repeats). Error bars represent *SD*. Statistical significance was determined using a paired *t*-test (*P=0.012 for *Ureaplasma vs.* vehicle at 48 h).

3.2.10 *Ureaplasma urealyticum* effect on TLR gene expression on Swan 71 cells

The *Ureaplasma* spp have been associated with histological chorioamnionitis with placental lesions. To identify whether an infection with *Ureaplasma urealyticum* could result in upregulation of TLRs by trophoblast cells, Swan 71 cells were treated with 10^7 CCU/ml *U. urealyticum* for 24 h. The gene expression of TLR1, TLR2, TLR3, TLR4, TLR6, TLR7 and TLR9 relative to the vehicle-treated cells were analysed by qPCR.

Among the TLRs that were examined, TLR9 demonstrated a statistically significant increase in its gene expression levels relative to the cells treated with the vehicle USM. In particular, TLR9 expression increased by 1.8±0.05-fold relative to USM (P=0.049 for *Ureaplasma vs* vehicle) (**Fig 3.11**).
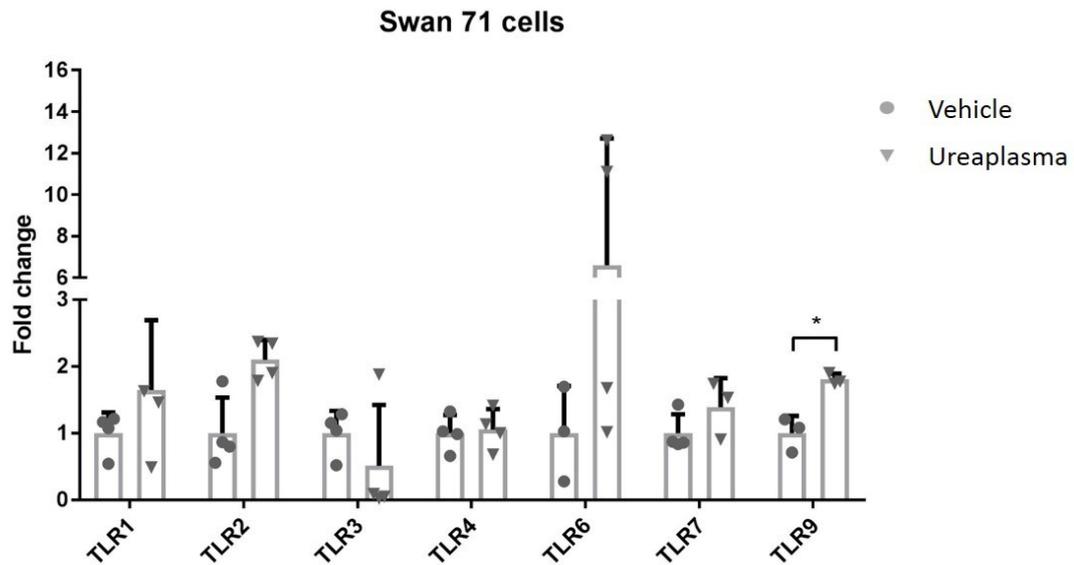
Figure 3.11 ***Ureaplasma urealyticum* infection of Swan 71 cells results in a significant up-regulation of TLR9 mRNA levels.** Confluent Swan 71 cells were seeded at 100,000 cells per well for 48 hours in growth medium. Following this, cells were treated either with *Ureaplasma urealyticum* (10^7 CCU/ml in USM) or with vehicle control (USM alone) for 24 h. Quantitative Real-Time PCR revealed a statistically significant increase in the mRNA expression of TLR9 in cells infected with *Ureaplasma urealyticum.* Error bars represent *SD*. Statistical significance was determined using the Holm-Sidak method on DDCt values (adjusted P=0.049 for TLR9).

3.2.11 *Ureaplasma urealyticum* effect on cytokine and chemokine secretion on Swan 71 cells

To assess whether Swan 71 cells could respond to an infection with *U. urealyticum* by secreting proinflammatory cytokines and chemokines, a Luminex multiplex assay on cell culture supernatants after 24-h treatment with with 10^7 CCU/ml *U. urealyticum* or USM was performed. A panel of 17 cytokines and chemokines was examined.

Luminex assay revealed 9 of these cytokines (GROa, IL-6, IL-8, G-CSF, GM-CSF, INFγ, IP-10, MCP-1, MIP-1a, MIP-1b, RANTES and TNFa) are secreted by the HeLa cells but their levels are not altered in the presence of an infection with *U. urealyticum* (**Fig 3.12**).
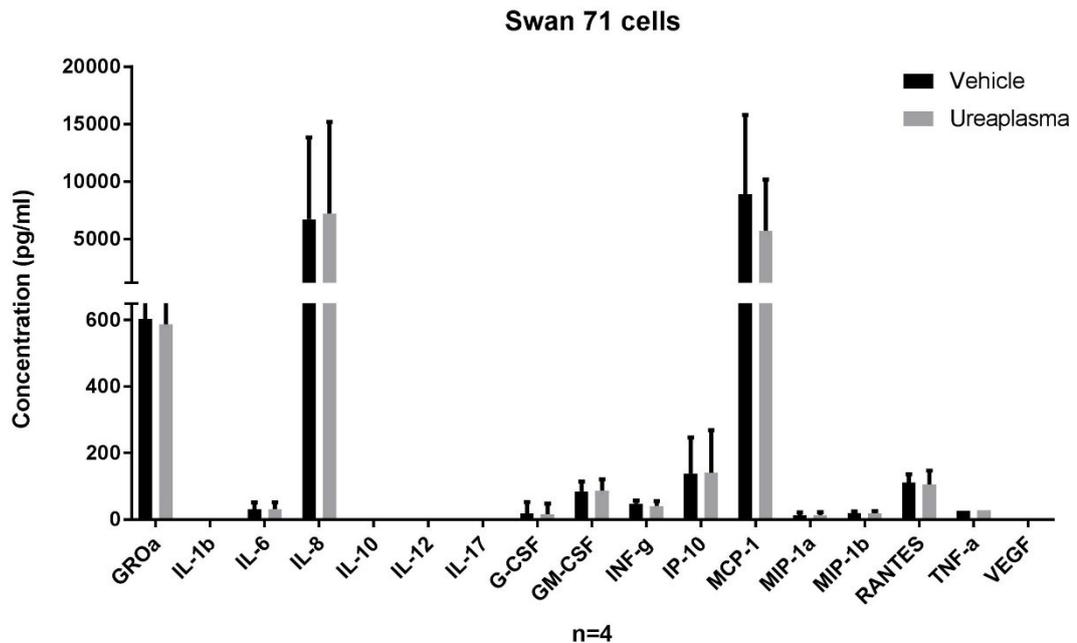
Figure 3.12 *Ureaplasma urealyticum* infection of Swan 71 cells has no effect on the levels of secreted proinflammatory cytokines. Confluent HeLa cells were seeded at 100,000 cells per well for 48 hours in growth medium. Following this, cells were treated either with *Ureaplasma urealyticum* (10^7 CCU/ml in USM) or with vehicle control (USM alone) for 24 h. A Luminex assay showed no difference in the levels of secreted proinflammatory cytokines with *Ureaplasma urealyticum* infection. Statistical significance was determined using the Holm-Sidak method.

3.3 Discussion

The cervical epithelium is key for the barrier function of the cervix during pregnancy as it protects from ascending infection with vaginal bacteria. Cervical epithelial injury

increases the risk for preterm delivery. The surfactant N-9 has been shown to cause epithelial damage in the lower reproductive tract, however its effects during pregnancy have not been studied. In the first part of this chapter we examined whether N-9 could disrupt the physical and functional epithelial barrier against infection by endocervical cells *in vitro*.

Firstly, we assessed the effect of N-9 on the endocervical cells' viability. Using a metabolic activity MTT assay, we found that N-9 decreased the cells' viability in dose- and time-dependent manner. The low N-9 doses (below 10 µg/ml) had no effect on the cells' viability while the high doses (above 100 µg/ml) practically resulted in killing all the cells. The intermediate doses of 16, 32 and 64 µg/ml had an effect that was intensified with increased incubation times. These findings are in complete agreement with two previous studies. At first, D'Cruz *et al.* used the same assay to find a very similar viability trendline after 24-hours treatments with N-9 (412). Shortly after, Fichorova *et al.* found using the closely related MTS (3-(4,5-dimethylthiazol-2-yl)-5-(3-carboxymethoxyphenyl)-2-(4-sulfophenyl)-2H-tetrazolium) assay that N-9 cytotoxicity levels for End1/E6E7 cells start at 8 µg/ml (413). These results helped define the cytotoxicity thresholds that were crucial for the design of subsequent experiments.

To assess the effect of N-9 on the physical barrier function of the cervical epithelium, we used an *in vitro* permeability assay. This assay provides a direct indication of permeability by quantifying the movement of FITC-Dextrans through a monolayer. We found that high (100 µg/ml) and medium (30 µg/ml) doses of N-9 are able to disrupt the continuity of an endocervical cells' monolayer and thus increase their epithelial permeability. This is in agreement with *in vivo* studies in the rat (387) and the rabbit (409) showing an increase in the permeability of the vaginal epithelium after N-9 application. In humans, N-9 was also shown to increase the permeability of the vaginal (414) as well as the rectal epithelium (415). Low doses of N-9 (3 and 10 µg/ml) did not have the same effect. In these cases, the monolayer was intact and the permeability remained unchanged. Therefore, the permeability was increased only after disruption of the continuity of the monolayer as a result of administering

cytotoxic N-9 doses. This suggests that N-9 can compromise the barrier function of the cervical epithelium only in doses that are high enough to mediate epithelial cytotoxicity. Since N-9 can integrate in the cell membranes due to its characteristic chemical structure as a surfactant, it is plausible to assume that it could also increase the permeability even without demonstrating its cytotoxic effect. However, N-9 has probably no effect in the cell adhesion properties of endocervical cells. This is because when the monolayer was intact, even in the presence of low doses of N-9, the permeability was stable.

Next, we investigated the effect of N-9 on the functional barrier of the cervical epithelium by assessing whether it could disrupt the ability of endocervical cells to secrete proinflammatory cytokines and chemokines basally and upon 24 h LPS stimulation. Using further viability and cytotoxicity assays, we determined that a low dose of 4 µg/ml N-9 was ideal for a 2 h pre-treatment of the cells before administering growth medium or LPS for a further 24 h. This treatment scheme resulted in around 75% viability at the end of the experiment, indicating that it did have an effect on the cells which was totally attributable to N-9 as LPS alone resulted in practically 100% viability. An intermediate dose of 40 µg/ml N-9 resulted in 0% viability at the end of the treatment scheme. Our previous results using the same dose for 2 h without an extra 24 h of further non-cytotoxic treatments showed a viability of around 75%. Taken together, these findings suggest that N-9 has a prolonging cytotoxic effect that continues even after its removal from the culture medium.

Using a cytokine proteomic array, we found no effect of 4 µg/ml N-9 pre-treatment in the levels of IL-6, IL-8, CXCL-1 and CXCL-10 after 24 h of treatment either with culture medium only or with LPS. The findings for IL-6 and IL-8 were also confirmed using ELISA. Since the N-9 pre-treatment at this dose results in about 25% cytotoxicity, we quantified the total protein using a protein assay and expressed the levels of IL-6 and IL-8 as a percentage of this. As the total secreted protein is directly proportional to the amount of viable cells in each well, this allowed us to normalise for the cytotoxic effect of N-9. After normalisation, the levels of IL-6 and IL-8 were almost identical between samples pre-treated with 4 µg/ml N-9 and those treated with

vehicle. Therefore, N-9 had no effect on the ability of these cells to secrete cytokines and chemokines. N-9 itself has been shown to increase the secretion of IL-1a, IL-1b and IL-8 (413). However, in our experiments we tried to assess the N-9 potential as a damage inducer that could predispose to infection. This is why the cells were pre-treated with N-9 and then, after removal of the medium, treated with LPS. In conclusion, we found that the functional barrier of the cervical epithelium against infection is not compromised by N-9.

Ascending infection with vaginal bacteria is the most common cause of preterm birth (113). Among the bacteria implicated in preterm birth, the most common ones belong to the *Ureaplasma* spp (410). In the second part of this chapter, we assessed whether *Ureaplasma urealyticum* could stimulate cervical cells to initiate an inflammatory response. This set of experiments were performed during the visit of the author of this thesis at Yale University School of Medicine. Initial attempts to grow End1/E6E7 cells were proven unsuccessful. Given the time constraints, the use of HeLa cells was decided instead. HeLa cells are derived from an epidermoid carcinoma of the cervix (397) and therefore less representative of the normal cervical epithelial physiology compared to End1/E6E7 cells who were isolated from a healthy cervix (393). However, they both come from the same tissue and they both avoid cell senescence, HeLa being naturally immortal and End1/E6E7 being immortalised by transfection with the Human Papilloma Virus 16 (HPV16) oncogenes E6 and E7.

During ascending infection the first cells that come in contact with *Ureaplasma* spp are the cervical epithelial cells. We infected HeLa cells with *U. urealyticum* and assessed potential changes in the expression of TLRs at the mRNA level. TLR1, TLR2, TLR6 and TLR9 have been implicated in the mechanism of entry of the *U. parvum* in amniotic epithelial cells (223) (224). However, here we found no statistically significant changes. In addition, we found that there was no difference in the levels of an array of secreted cytokines and chemokines in the supernatant of infected and uninfected cells, as assessed by a Luminex assay. This suggests that TLR pathways were not stimulated by the infection and there was no overall inflammatory response.

The working hypothesis of this thesis is that cervical epithelial damage predisposes to ascending infection with *Ureaplasma* spp. Upon epithelial injury, the cervical stroma gets exposed to the infectious stimuli. As a cervical stromal cell line is not readily available, we used the closely related endometrial stromal cell line HESC to assess if these cells can react to an infection with *U. urealyticum* by stimulating inflammation. Similar to the HeLa cells we found no changes in TLRs gene expression and no effect on cytokine secretion after a 24 h-infection, indicating an absence of an inflammatory response.

Ureaplasma spp have been described as causative agents of chorioamnionitis that can cause placental lesions (416). Here we tested whether an infection with *U. urealyticum* could result in an inflammatory response by the trophoblast cell line Swan 71. A minimal yet statistically significant 2-fold upregulation was noticed only for TLR9, with no significant changes in the gene expression of the other TLRs. Taking into account the minimal effect along with the absence of any effect on cytokine secretion, it is most likely that this observation does not represent a result of biological significance. Still, there was again no effect on the levels of secreted cytokines.

Taken together, data on TLR gene expression and secreted cytokine protein levels suggest that *U. urealyticum* does not stimulate an inflammatory response by these cells. This can be explained by both the low virulence of the microorganism and the limited capacity of these cells to acquire a strong inflammatory phenotype compared to immune cells.

To simulate cervical damage *in vitro*, we created an artificial wound at the bottom of a well containing HeLa or HESC cells. We found using a wound healing assay that infection with *U. urealyticum* diminishes the wound healing capacity of both HeLa and HESC cells. This is a reasonable finding as infection of a wound is known to prolong the wound closure or maintain chronicity of the damage (417). However, this is the first time such a report is made about the *Ureaplasma* spp. This is particularly important and could have implications on preterm birth mechanisms as cervical

damage is associated with PTB and *Ureaplasma* spp are the most common bacteria isolated from the amniotic fluid of preterm deliveries.

In summary, the results from the first part of this chapter demonstrate the capacity of N-9 to compromise the barrier function of the cervical epithelium due to its cytotoxicity against cervical epithelial cells. We therefore describe an *in vitro* model of cervical epithelial damage and identify N-9 as a solid damage inducer that could be tested *in vivo* to generate our proposed model of cervical damage during pregnancy. This is the focus of the next chapter. Data from the second part suggest that *U. urealyticum* does not stimulate a robust inflammatory response by non-immune cells from the reproductive tissues. However, it can negatively affect the ability of epithelial and stromal cells to close the wound, as in the event of cervical damage.

Chapter 4   Generation and characterisation of a new mouse model of cervical epithelial damage during pregnancy using Nonoxynol-9

4.1 Introduction

The mouse represents a valuable model for the study of preterm birth mechanisms. In parturition research, mouse models of PTB have been extensively used since their establishment. Various models have been described including PTB induced in the absence of inflammation, by sterile inflammation or by infections/inflammatory stimuli. Representative examples of the above models include the progesterone receptor antagonist RU486 (372), the DAMP HMGB1 (379) and the gram (-) bacterial product LPS (364). Most models use the administration of LPS.

Cervical damage has also been associated with PTB. Specifically, excisional procedures that remove part of the cervical epithelium and the underlying stroma significantly increase the risk for preterm delivery by at least 100% (304) (305). However, this association has not been studied in experimental models. To our knowledge, no model of cervical damage during pregnancy to study its role in PTB has been described so far.

The surfactant N-9 has been used as a spermicidal component for decades. It was also considered a potential topical microbicide against sexually transmitted diseases (STDs) (406). After a large Randomised Clinical Trial (RCT) found that N-9 actually increased the risk for HIV transmission (418), its safety profile has been evaluated in preclinical animal models.

Experiments in these models revealed significant irritation of the cervical and vaginal mucosa in non-pregnant rabbits and rats (419). Other studies reported an important disruption of the continuity of the epithelial layers with a significant submucosal oedema (420). Acute inflammation was also described in the rats (407).

In non-pregnant mice, a single application of N-9 was also found to cause disruption of the cervical and vaginal epithelium, resulting in complete sloughing of the former 8 h post-administration (391). Single N-9 administration for consecutive days was shown to diminish the cervical toxicity observed compared to a single administration of like duration (392).

Studies in non-human primates that more closely resemble the human anatomy and physiology yielded similar results. Using colposcopy, the examination of the lower genital tract in this species revealed significant irritation with signs of acute inflammation (390). This involved the presence of neutrophils and macrophages (389). Epithelial disruption was made apparent through the presence of whole sheets of epithelial cells in the vaginal fluid (389).

In humans, erythematous irritation after vaginal application of N-9 is observed, both in the vagina and the cervix (421). Once-daily applications for a few days result in significant irritation and inflammation but not in epithelial disruption (422). After multiple daily applications, cervical and vaginal epithelial disruption was observed by colposcopy in a significant percentage of women (423). These abnormalities have been shown to be dose-dependent (424).

Findings from preclinical and clinical models agree that N-9 can cause significant damage in the lower reproductive tract. However, its effects during pregnancy have not been studied yet.

The work described in the first part of the previous chapter found that N-9 can compromise the barrier function of endocervical cells *in vitro*. These data, along with data from non-pregnant animals and humans described above, suggest that N-9 could be used to establish a mouse model of cervical damage during pregnancy. The aim of

this chapter is to develop and characterise this model using N-9 and then assess its effects on timing of delivery and pup survival.

4.2 Results

To generate a mouse model of cervical damage during pregnancy, timed pregnant mice were treated on D17 with 3 different doses of N-9 (2%, 5% and 10% v/v in PBS) for 8 h. Tissues were collected to be analysed for signs of damage using histological methods.

4.2.1 Effect of vaginal N-9 on cervical epithelial morphology during pregnancy

To assess the effect of N-9 on cervical epithelial tissue integrity, AB/PAS staining was used to identify the epithelial cells of the cervix based on their ability to produce mucins.

To quantify the disruptions of the epithelial morphology caused by N-9, a new histopathological epithelial injury score was developed. This involved two different features: Epithelial morphology and area involved. Three different morphologies were described and scored: *Intact morphology* was given 1 point, *Disturbance* was given 2 points and *Sloughing* was given 3 points. Representative images can be seen (**Fig 4.1A**). For *Disturbance* and *Sloughing* only, the area involved was also described and scored: *less than 10%* of the total surface area was given 0 points, *10% to 50%* of the total surface was given 1 point and *more than 50%* was given 2 points (**Fig 4.1A**). The total score for each section was Morphology+ Area involved.

All three N-9 doses resulted in a significantly increased epithelial injury score. The 2% N-9 was scored at 4.033 ± 0.36 (P=0.0043), the 5% N-9 at 3.89 ± 0.29 (P=0.0265) and the 10% N-9 at 4.42 ± 0.48 (P=0.0033) compared to 1.54 ± 0.36 for the PBS control (**Fig 4.1B**).
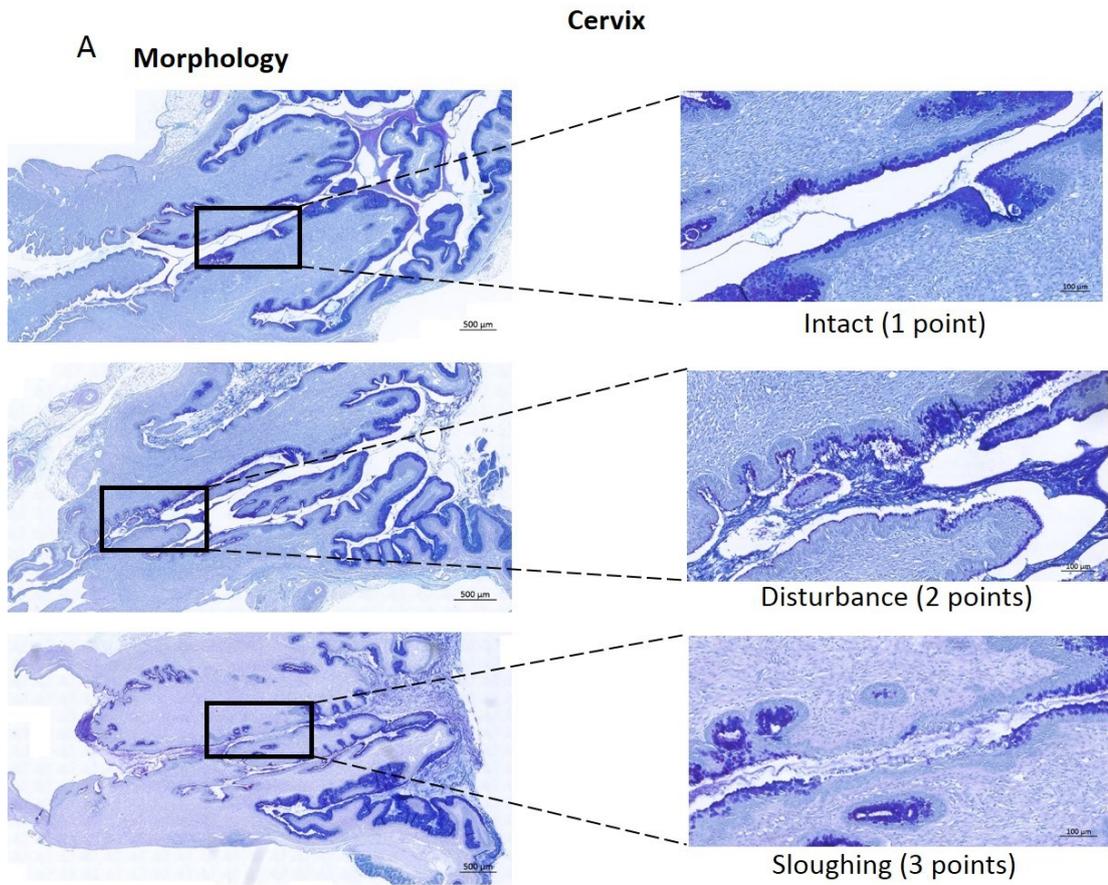
Cervix

A **Morphology**

Intact (1 point)

Disturbance (2 points)

Sloughing (3 points)

Area involved (for disturbance/sloughing only):

<10%   (0 points)

10-50% (1 point)

50%<   (2 points)

B
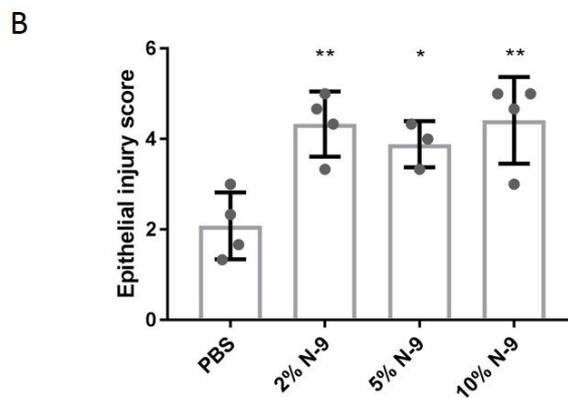
Figure 4.1 Intra-vaginal N-9 disrupts cervical epithelial morphology during pregnancy in a mouse model. In the morning of D17 of gestation, mice received either N-9 (2%, 5% or 10% in PBS) or PBS control via intravaginal inoculation. 8 h later mice were sacrificed for tissue collections. Cervical tissue sections were stained with AB/PAS and a morphological damage scoring system was used to assess epithelial damage (**A**). N-9 significantly damages the morphology of the cervical epithelium during pregnancy (**B**). Error bars indicate *SD*. Statistical significance was assessed using 1-way ANOVA with Dunnett's multiple comparisons test against PBS group (**P<0.005 for 2% N-9 and 10% N-9 *vs*. PBS, *P<0.05 for 5% N-9 *vs*. PBS).

All samples were assessed by two independent assessors who were blinded to treatment allocation. Inter-observer reliability was calculated (Weighted Cohen's kappa=0.952) (**Table 4-1**).

Table 4-1 Inter-rater reliability for the assessment of Morphological epithelial damage in the cervix. Numbers in bold represent the scores given by the assessors. The other numbers represent the amount of samples that were given each score combination.

		Assessor A				
		1	**2**	**3**	**4**	**5**
Assessor B	**1**	5	0	0	0	0
	2	0	2	1	0	0
	3	0	0	9	1	0
	4	0	0	1	11	0
	5	0	0	0	0	15

Weighted Cohen's kappa=0.952

4.2.2 Effect of vaginal N-9 on vaginal epithelial morphology during pregnancy

The same epithelial injury score was also utilised to assess the effect of N-9 in the vaginal epithelial integrity. Representative images of *Intact morphology*, *Disturbance* and *Sloughing* for the vaginal epithelium can be seen in **Fig 4.2A**.

As in the cervix, all three N-9 doses resulted in a significantly increased epithelial injury score. The 2% N-9 was scored at 4.08 ± 0.37 (P=0.0075), the 5% N-9 at 3.56 ± 0.95 (P=0.0434) and the 10% N-9 at 4.42 ± 0.37 (P=0.0033) compared to 1.54 ± 0.36 for the PBS control (**Fig 4.2B**).

Vagina

A Morphology

Intact (1 point)

Disturbance (2 points)
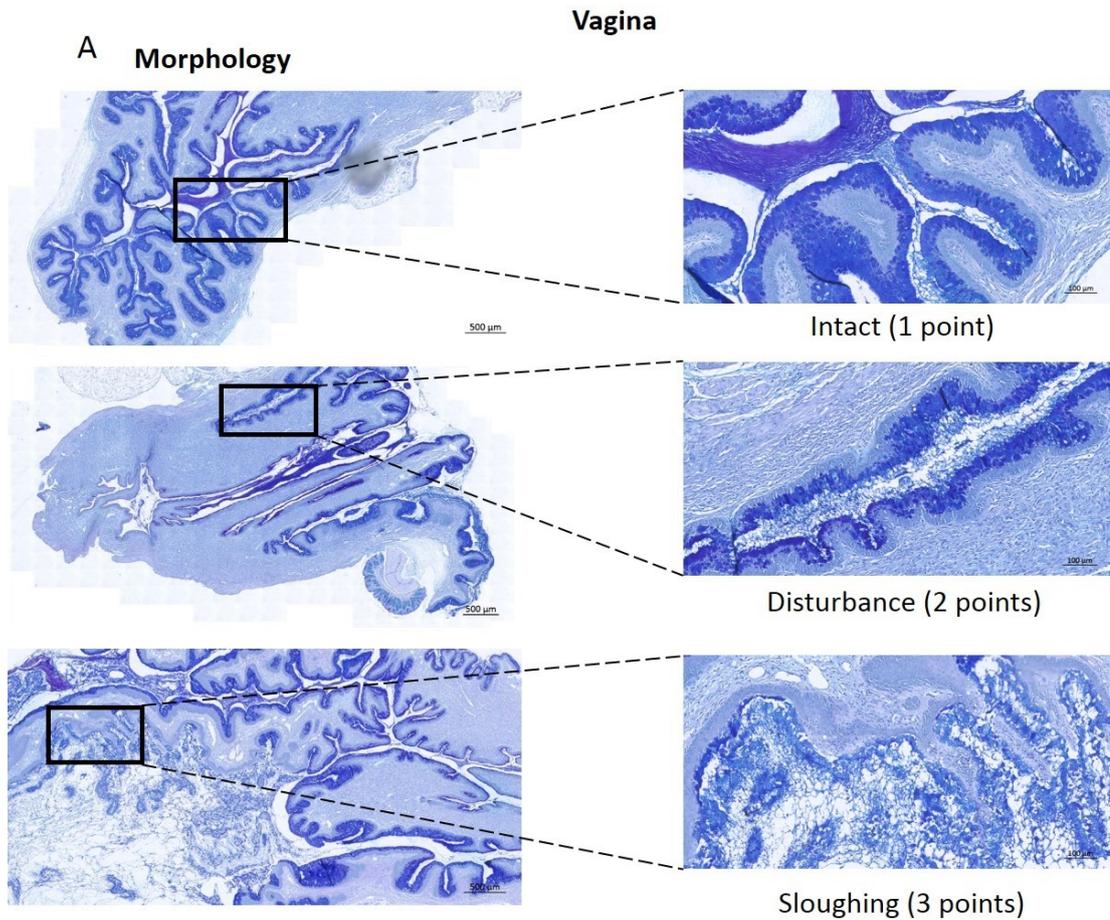
Sloughing (3 points)

Area involved (for disturbance/sloughing only):

<10%   (0 points)

10-50% (1 point)

50%<   (2 points)

B
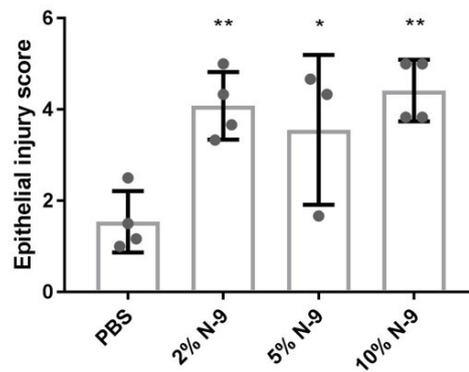
Figure 4.2 Intra-vaginal N-9 disrupts the vaginal epithelial morphology during pregnancy in a mouse model. In the morning of D17 of gestation, mice received either N-9 (2%, 5% or 10% in PBS) or PBS control via intravaginal inoculation. 8 h later mice were sacrificed for tissue collections. Vaginal tissue sections were stained with AB/PAS and a morphological damage scoring system was used to assess epithelial damage (**A**). N-9 significantly damages the morphology of the vaginal epithelium during pregnancy (**B**). Error bars indicate *SD*. Statistical significance was assessed using 1-way ANOVA with Dunnett's multiple comparisons test against PBS group (**P<0.005 for 2% N-9 and 10% N-9 *vs*. PBS, *P<0.05 for 5% N-9 *vs*. PBS).

All samples were assessed by two independent assessors who were blinded to treatment allocation. Inter-observer reliability was calculated (Weighted Cohen's kappa=0.774) (**Table 4-1**).

Table 4-2 Inter-rater reliability for the assessment of Morphological epithelial damage in the vagina. Numbers in bold represent the scores given by the assessors. The other numbers represent the amount of samples that were given each score combination.

		Assessor A				
		1	**2**	**3**	**4**	**5**
Assessor B	**1**	6	2	2	0	0
	2	2	0	0	0	0
	3	0	0	4	3	0
	4	0	0	0	9	4
	5	0	0	0	1	11

Weighted Cohen's kappa=0.774

4.2.3 Cervical infiltration of polymorphonuclear neutrophils after vaginal N-9 administration during pregnancy

Upon tissue injury as the one described in the previous section, an inflammatory response is initiated and neutrophils are among the first immune cells to arrive on site. To assess neutrophil infiltrations following N-9 administration, Ly6G immunohistochemistry on tissue sections was performed.

To allow for accurate quantification of these infiltrations, a new neutrophil infiltration score assessing both the epithelium and the sub-epithelial stroma was described. For the epithelium: *No epithelial infiltrations* were given 0 points, infiltrated area *0% to 10%* of the total surface area was given 1 points, infiltrated area *10% to 50%* of the total surface area was given 2 points and *more than 50%* was given 3 points (**Fig 4.3A**). For the sub-epithelial stroma: An average of *0-1 neutrophils* per field of interest (FOI) was given 1 point, an average of *1-3 neutrophils* per FOI was given 2 points and *more than 3 neutrophils* per FOI were given 3 points (**Fig 4.3B**). Representative images can be seen (**Fig 4.3A, B**). The total score for each section was Epithelium+ Sub-epithelial stroma.

The highest dose of 10% N-9 resulted in a significantly increased neutrophil infiltration score in the cervix of pregnant mice (3.75±0.75, P=0.0147) compared to PBS control (1±0) (**Fig 4.3C**). The 2% N-9 (2.75±0.75, P=0.1234) and the 5% N-9 (1.33±0.33, P=0.962) doses did not demonstrate statistically significant differences compared to the control group (**Fig 4.3C**).
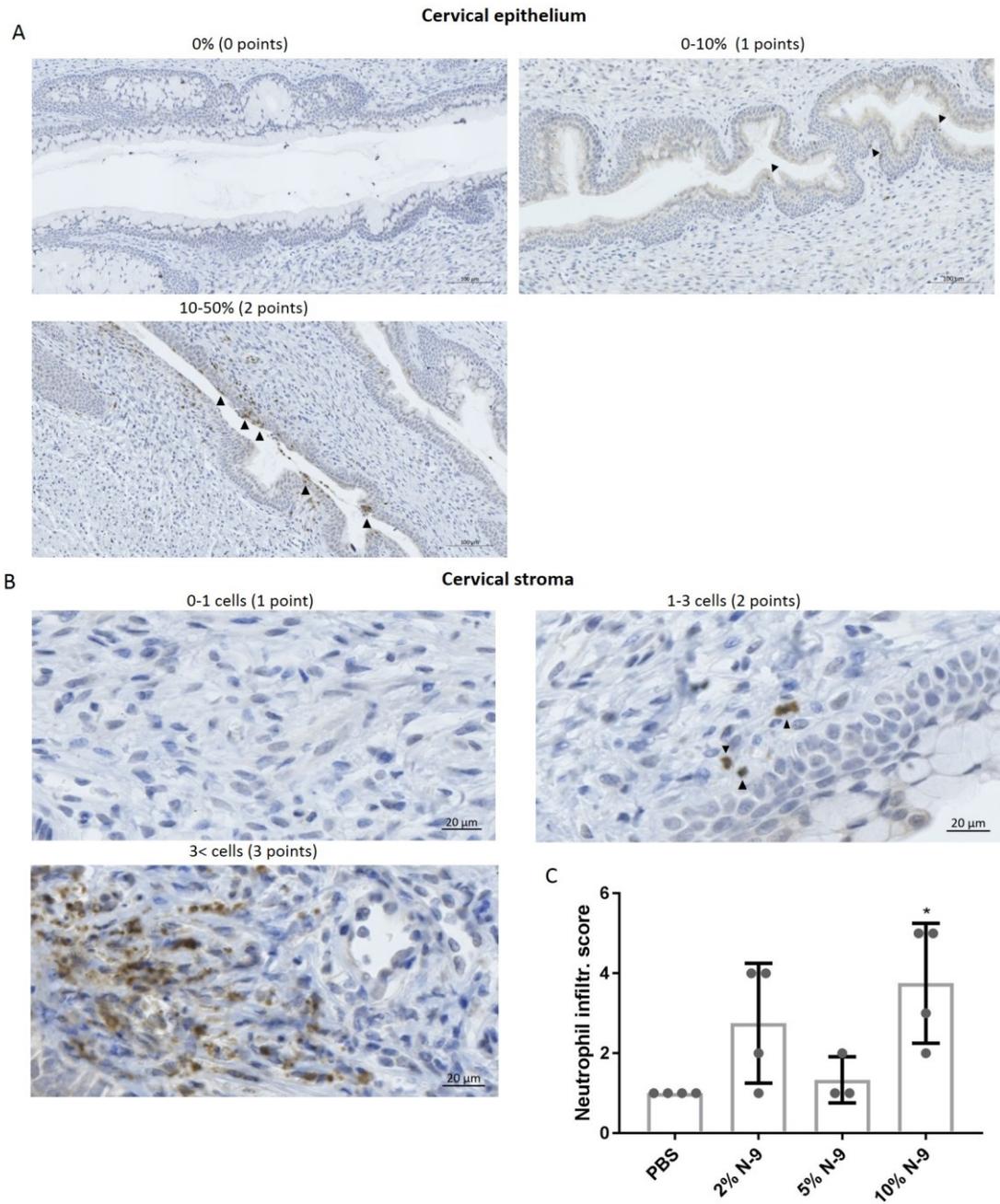
Figure 4.3 Intra-vaginal N-9 results in polymorphonuclear neutrophils infiltrations in the cervix during pregnancy in a mouse model. In the morning of D17 of gestation, mice received either N-9 (2%, 5% or 10% in PBS) or PBS control via intravaginal inoculation. 8 h later mice were sacrificed for tissue collections. Anti-Ly6G immunohistochemistry on cervical tissue sections was used to assess the presence of neutrophils. A neutrophil infiltration scoring system was used to quantify

the presence of neutrophils in the cervical epithelium (**A**) and stroma (**B**), the total score being the sum of the two. 10% N-9 significantly increased the neutrophil infiltrations in the cervix (**C**). Arrowheads indicate positively stained cells. Error bars indicate *SD*. Statistical significance was assessed using 1-way ANOVA with Dunnett's multiple comparisons test against PBS group (*P<0.05 for 10% N-9 *vs*. PBS).

All samples were assessed by two independent assessors who were blinded to treatment allocation. Inter-observer reliability was calculated (Weighted Cohen's kappa=0.874) (**Table 4-3**).

Table 4-3 Inter-rater reliability for the assessment of neutrophil infiltrations in the cervix. Numbers in bold represent the scores given by the assessors. The other numbers represent the amount of samples that were given each score combination.

		Assessor 1					
		1	**2**	**3**	**4**	**5**	**6**
Assessor 2	**1**	6	1	0	0	0	0
	2	1	1	1	0	0	0
	3	0	0	1	0	0	0
	4	0	0	0	2	0	0
	5	0	0	0	0	2	0
	6	0	0	0	0	0	0

Weighted Cohen's kappa=0.874

4.2.4 Vaginal infiltration of polymorphonuclear neutrophils after vaginal N-9 administration during pregnancy

The same neutrophil infiltrations score was also utilised to assess the effect of N-9 in the vaginal tissue. Representative images of all conditions for the vaginal epithelium and sub-epithelial stroma can be seen in **Fig 4.4A, B**.

Similar to the finding in the cervix, the highest dose of 10% N-9 resulted in a significantly increased neutrophil infiltration score in the vagina of pregnant mice (5.5±0.5, P=0.0032) compared to PBS control (1.25±0.25) (**Fig 4.4C**). In addition, the dose of 2% N-9 resulted in a significantly increased score as well when compared to PBS control (4.75±0.63, P=0.0115) (**Fig 4.4C**). The 5% N-9 (3.67±1.45, P=0.1046) dose showed no statistically significant changes (**Fig 4.4C**).
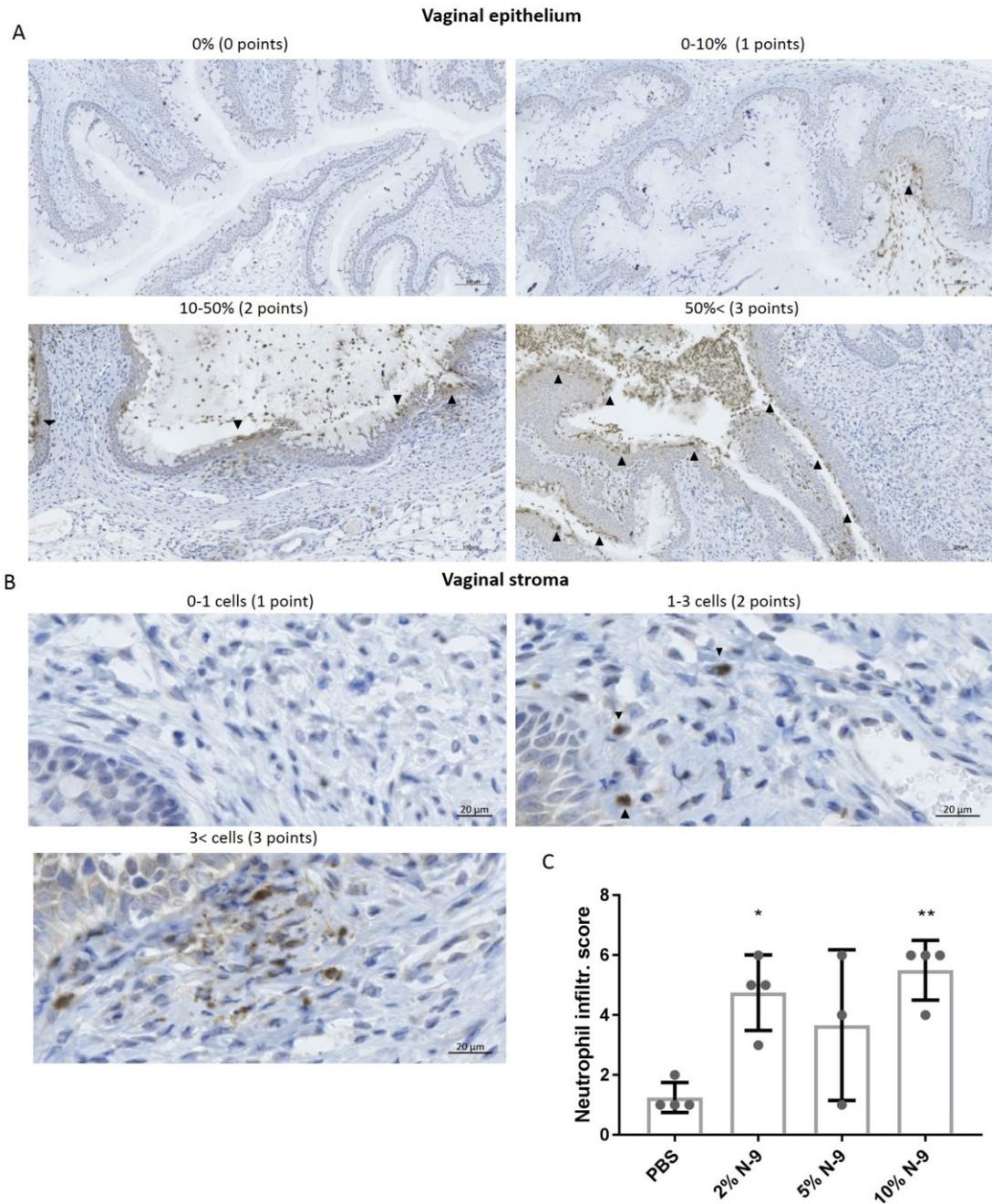
Figure 4.4 Intra-vaginal N-9 results in polymorphonuclear neutrophils infiltrations in the vagina during pregnancy in a mouse model. In the morning of D17 of gestation, mice received either N-9 (2%, 5% or 10% in PBS) or PBS control via intravaginal inoculation. 8 h later mice were sacrificed for tissue collections. Anti-Ly6G immunohistochemistry on vaginal tissue sections was used to assess the presence of neutrophils. A neutrophil infiltration scoring system was used to quantify

the presence of neutrophils in the vaginal epithelium (**A**) and stroma (**B**), the total score being the sum of the two. N-9 significantly increased the neutrophil infiltrations in the vagina (**C**). Error bars indicate *SD*. Statistical significance was assessed using 1-way ANOVA with Dunnett's multiple comparisons test against PBS group (**P<0.005 for 10% N-9 *vs.* PBS, *P<0.05 for 2% N-9 *vs.* PBS).

All samples were assessed by two independent assessors who were blinded to treatment allocation. Inter-observer reliability was calculated (Weighted Cohen's kappa=0.849) (**Table 4-4**).

Table 4-4 Inter-rater reliability for the assessment of neutrophil infiltrations in the vagina. Numbers in bold represent the scores given by the assessors. The other numbers represent the amount of samples that were given each score combination.

		Assessor 1					
		1	**2**	**3**	**4**	**5**	**6**
Assessor 2	**1**	4	0	0	0	0	0
	2	0	0	1	0	0	0
	3	0	0	0	1	0	0
	4	0	0	0	0	2	0
	5	0	0	0	0	2	0
	6	0	0	0	0	1	4

Weighted Cohen's kappa=0.849

4.2.5 Increased proliferation of the basal cells of the cervical epithelium during pregnancy after vaginal N-9 administration

As a response to tissue injury, an epithelial regeneration process is initiated, characterised by increased proliferation of the basal cells. To assess whether N-9 treatment resulted in increased epithelial regeneration as an indirect indication of epithelial damage, Ki67 immunohistochemistry was performed on cervical tissues.

The percentage of proliferating cells at the basal layer of at least 1mm of the cervical epithelium was quantified. Representative images are shown on **Fig 4.5A**.

All three doses of N-9 significantly increased the percentage of proliferating cells at the basal layer of the cervical epithelium compared to PBS control. The 2% N-9 dose resulted in $42.21\pm2.96\%$ of the cells being positively stained (P=0.0437); the 5% N-9 dose resulted in $43.94\pm2.66\%$ being positively stained (P=0.0298); and the 10% N-9 dose resulted in $50.46\pm3.47\%$ being positively stained (P=0.0011), whereas the percentage of proliferating cells for the PBS control was $31.73\pm1.2\%$ (**Fig 4.5B**).
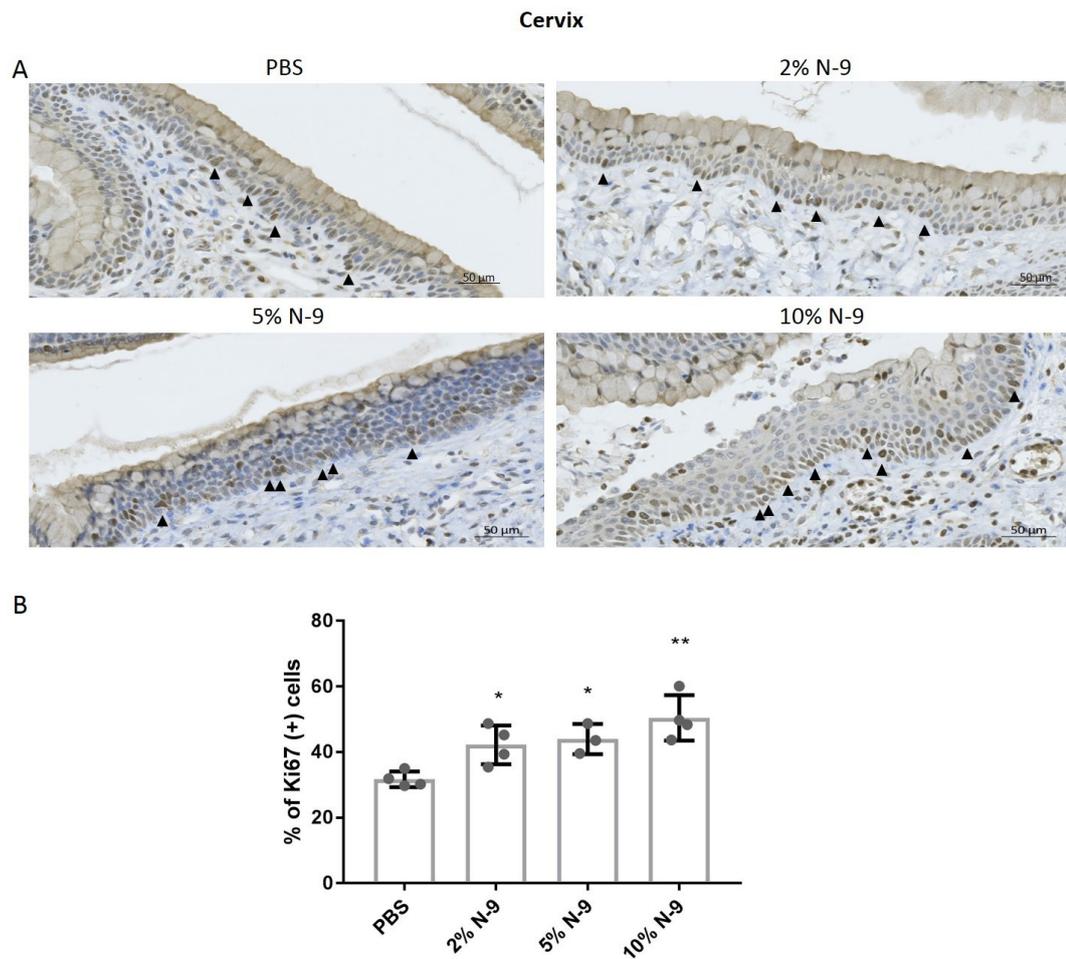
Figure 4.5 Intra-vaginal N-9 results in increased proliferation of the basal cells of the cervical epithelium during pregnancy in a mouse model. In the morning of D17 of gestation, mice received either N-9 (2%, 5% or 10% in PBS) or PBS control via intravaginal inoculation. 8 h later mice were sacrificed for tissue collections. Anti-Ki67 immunohistochemistry on cervical tissue sections was used to assess cellular proliferation at the basal layer of the cervical epithelium. Representative images are shown (**A**). The percentage of Ki-67 positive cells was calculated across an area covering at least 1mm of the basal layer. N-9 significantly increases cellular proliferation at the cervix basal layer (**B**). Error bars indicate *SD*. Statistical significance was assessed using 1-way ANOVA with Dunnett's multiple comparisons test against PBS group (**P<0.005 for 10% N-9 *vs*. PBS, *P<0.05 for 2% N-9 and 5% N-9 *vs*. PBS).

4.2.6 No change on cell proliferation at the basal layer of the vaginal epithelium during pregnancy after vaginal N-9 administration

In the vagina, the percentage of proliferating cells at the basal layer of at least 1mm of the epithelium was quantified. Representative images are shown on **Fig 4.6A**.

None of the three doses of N-9 significantly increased the percentage of proliferating cells at the basal layer of the vaginal epithelium compared to PBS control-treated animals. The percentage of proliferating cells in the basal layer was 85.31±2.16% for mice treated with 2% N-9, 84.56±4.17 for mice treated with 5% N-9 and 86.08±2.64 for mice treated with 10% N-9 (**Fig 4.6B**). In PBS-treated animals, the respective proportion was79.58±1.9%.
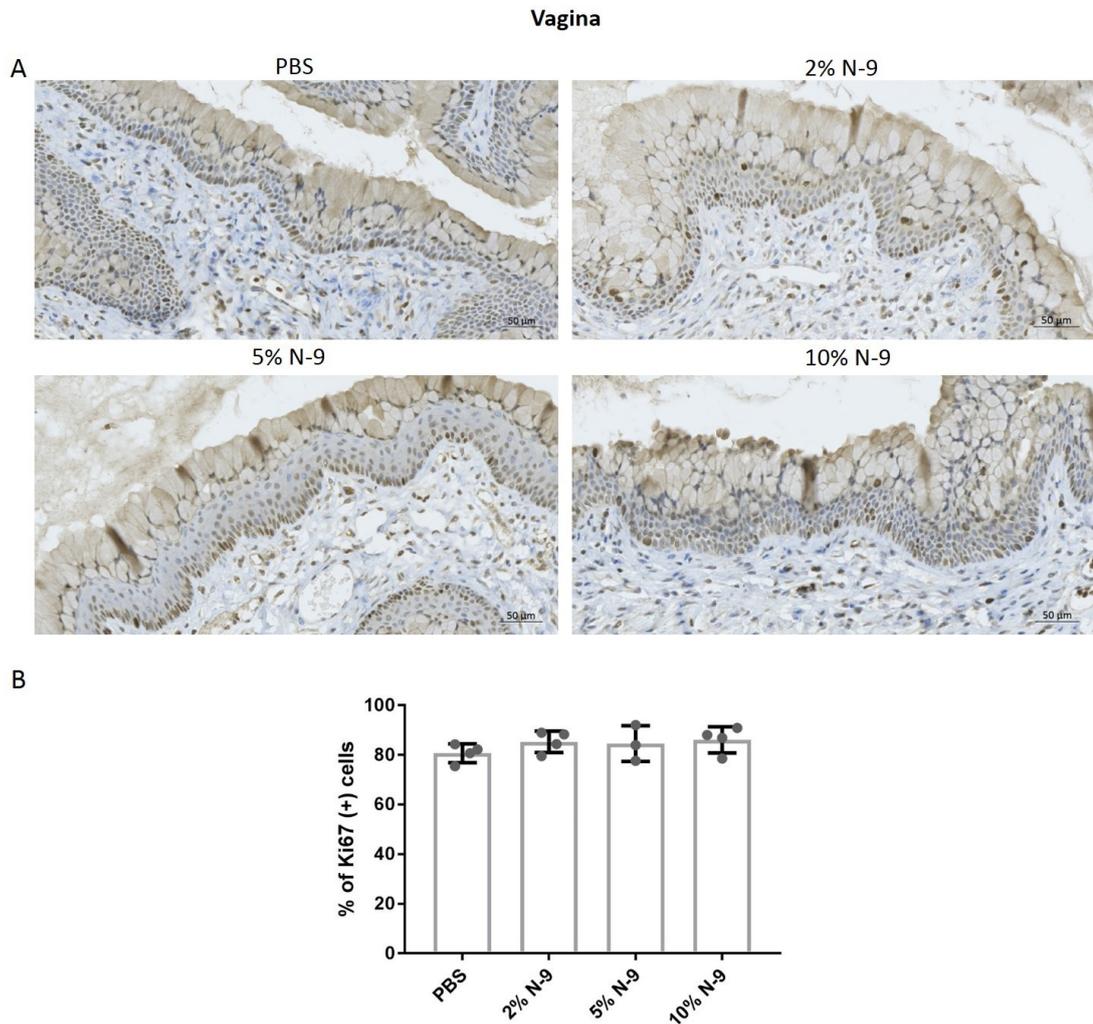
Vagina

Figure 4.6 Intra-vaginal N-9 has no effect on cell proliferation of the basal cells of the vaginal epithelium during pregnancy in a mouse model. In the morning of D17 of gestation, mice received either N-9 (2%, 5% or 10% in PBS) or PBS control via intravaginal inoculation. 8 h later mice were sacrificed for tissue collections. Anti-Ki67 immunohistochemistry on vaginal tissue sections was used to assess cellular proliferation at the basal layer of the vaginal epithelium. Representative images are shown (**A**). The percentage of Ki-67 positive cells was calculated across an area covering at least 1mm of the basal layer. N-9 has no effect on cellular proliferation at the vaginal basal layer (**B**). Error bars indicate *SD*. Statistical significance was assessed using 1-way ANOVA with Dunnett's multiple comparisons test against PBS group.

4.2.7 The effects of N-9-induced epithelial damage on timing of delivery and pup survival

To assess whether N-9-induced cervicovaginal epithelial damage could result in preterm delivery and whether there would be any effect on pup survival, a time-to-delivery experiment was conducted. On D17 of pregnancy, timed pregnant mice were given an intravaginal inoculation of the three N-9 doses that were used for generating and characterising the model as shown before. A further dose of 40% v/v N-9 was also used to generate a dose response. Timing of delivery of the first pup post-administration was monitored using CCTV. The percentage of pups born alive was calculated for each mouse.

None of the administered doses had any effect on timing of delivery. Mice treated with PBS delivered at an average of 57.93±2 hours post-administration. Mice treated with 2% N-9 delivered 60.05±4.97 hours post-administration. Those treated with 5% N-9 delivered 58.1±3.58 hours post-administration. The ones that received 10% N-9 delivered 64.34±4.18 hours post-administration. Finally, mice treated with the highest dose of 40% N-9 delivered 68.3±3.66 hours post-administration (**Fig 4.7A**).

There was also no effect on the percentage of live born pups for any of the N-9 groups. As expected, the average percentage of live born pups for all mice treated with PBS 98±2%. The percentages for the N-9 treated mice were 97.8±2.2%, 98±2%, 96.75±2.14% and 90.6±6.49 for 2% N-9, 5% N-9, 10% N-9 and 40% N-9 respectively (**Fig 4.7B**).
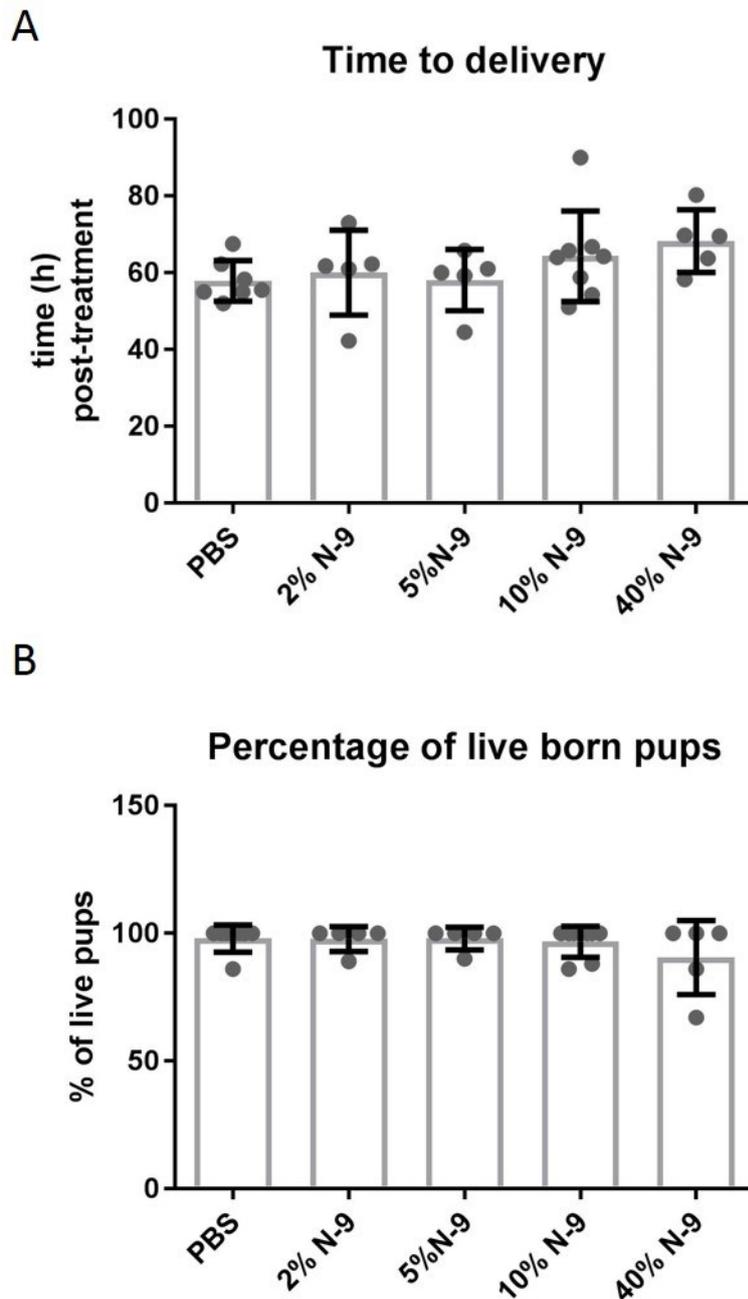
Figure 4.7 Cervical damage caused by intra-vaginal N-9 does not affect timing of delivery and pup survival in a mouse model of cervical damage during pregnancy. In the morning of D17 of gestation, mice received either N-9 (2%, 5%, 10% or 40% in PBS) or PBS control via intravaginal inoculation. Time to delivery was calculated from the moment of intravaginal inoculation until the delivery of the first pup. N-9 had

no effect on timing of delivery (1-way ANOVA with Dunnett's multiple comparisons test against 0% N-9) (**A**). Percentage of live born pups for each mouse was calculated by dividing the number of live pups delivered by the total number of pups. N-9 had no effect on pup survival (1-way ANOVA with Dunnett's multiple comparisons test after arcsine transformation of proportions against 0% N-9) (**B**). Error bars represent *SD*.

4.3 Discussion

Cervical epithelial damage has been shown to increase the risk for preterm delivery in humans (304). However, no mechanisms underpinning this association have been suggested. It is our hypothesis that cervical epithelial damage predisposes to ascending infection with vaginal bacteria. To address this hypothesis, the aim of creating a mouse model of cervical epithelial damage during pregnancy was set. In the previous chapter, we identified the surfactant N-9 to be a potent inducer of cervical epithelial damage *in vitro*. The work in this chapter describes the establishment and characterisation of a new mouse model of cervical epithelial damage during pregnancy using N-9.

N-9 was administered intravaginally in day 17 of the mouse gestation. N-9 has been used as a spermicidal component for female-controlled contraception for decades. The N-9 doses that we tried in this mouse model (2%, 5%, 10% v/v) represent the whole pharmacological spectrum that has been applied in humans (2-12%). To quantify the extent of damage, we described a new scoring system. This system took into account the morphology of the epithelium after N-9 application and the extent of the damaged area. We found that N-9 caused a significant disruption of the cervical epithelial morphology 8 hours post-administration with all three doses. This disruption involved the presence of extensive areas of disturbance and complete sloughing of the epithelial layers. This findings are in agreement with reports from non-pregnant animal models and humans. Significant damage in the lower reproductive tract with epithelial disruption and shedding after vaginal application of N-9 has been found in mice (391), rats (407), rabbits (425) and non-human primates (390). In addition, the detrimental

effects of N-9 appear to extend outside the epithelium of the lower reproductive tract. Specifically, it has been shown to cause exfoliation of the rectal epithelium with exposure of the underlying stroma in mice (426) (427), rhesus monkeys (390) and humans (428).

A significant disruption with all three doses of N-9 was also found in the vaginal epithelium of pregnant mice. The extent of damage was similar to that found in the cervical epithelium. Catalone *et al.* and Lozenski *et al.* reported that the damage in the vagina was minimal compared to the cervix (391) (392). Data from rabbits also suggest that the cervical epithelium is more susceptible to N-9-induced damage (420). However, the explanation for rabbits lies in the fact that, similar to humans, the vaginal epithelium consists of multiple layers of squamous cells, whereas the cervical canal only has a simple columnar epithelium (429). Columnar cells have been shown to be more susceptible to the N-9 cytotoxicity (409). Therefore, the vaginal epithelium is more protected compared to the cervical. In mice though, the epithelium of the lower reproductive tract is continuous from the vagina to the uterus and consists of multiple layers of squamous cells (430). More layers are seen in the vaginal epithelium, which might explain the differences observed in other non-pregnant mouse models. Progesterone treatment has been shown to induce a columnar mucus-producing phenotype in the entire cervicovaginal epithelium (406). The very high pregnancy levels of progesterone during the course of pregnancy, as in our model, ensure this phenotype is consistent across the vaginal and cervical epithelium. Our AB/PAS staining confirms the abundance of mucins within the epithelial cells of both the cervix and the vagina. Thus, both epithelia are susceptible to N-9 cytotoxicity.

Using immunohistochemistry, we found that N-9 treatment also leads to polymorphonuclear neutrophil populations infiltrating the epithelium and the sub-epithelial stroma in both the cervix and the vagina. To quantify the extent of the infiltrations, we developed another scoring system. This system systematically assessed the presence of neutrophils in both the epithelium and the sub-epithelial stroma. The effect was stronger with the highest N-9 dose of 10% v/v. This was in fact the only dose that yielded statistically significant results both in the cervix and the

vagina using our scoring system. However, the clear effect of the highest dose was enough proof of the inflammatory infiltrations not to require an increase in sample size.

These findings are consistent with an early immune response to tissue injury as neutrophils are among the first immune populations to arrive on site. Therefore, these data constitute a further indication of the extent of damage caused by N-9 in our model. They are also in line with other histological findings in mice (391). Apart from infiltrating the epithelial tissue, high levels of neutrophils after N-9 application have also been detected in vaginal secretions from mice (389) and pigtailed macaques (388). In addition to confirming the extent of N-9-induced damage, the finding that N-9 can cause neutrophil recruitment in the cervix is important. This could have implications in cervical damage-induced preterm birth mechanisms as the influx of neutrophils into the cervix secondary to intrauterine LPS administration can induce premature cervical ripening in mice (431).

To further investigate the functional effects of N-9-mediated damage in the cervix and the vagina, we used immunohistochemistry to determine the percentage of proliferating cells across the basement membrane of the cervix. All three doses of N-9 resulted in a statistically significant increase in the proportion of proliferating cells. This increased proliferation of the cells in the basement membrane is characteristic of an epithelial regeneration process as a response to acute tissue injury. Catalone *et al.* reported that the epithelium of the cervix in non-pregnant mice is completely regenerated within 24 hours of the original insult (391). In our model, this seems unlikely given the extent of damage observed 8 hours post-application. However, it does suggest that an epithelial regeneration process is in place in response to the damage exerted by N-9. In addition, it provides further evidence that validates our mouse model and confirms the suitability of N-9 as an epithelial damage inducer.

In the vaginal epithelium, we found no increase in the percentage of proliferating cells in the basement membrane. The vast majority of the cells were proliferating in all groups including mice that only received the vehicle treatment. The proportion for the

control group in the vagina was around 80% as opposed to 30% in the cervix. As the vaginal epithelium has substantially more epithelial layers, it is likely that in any given time more cells in the basement membrane are proliferating in order for the cells in the apical part to be promptly replaced. High rates of proliferating cells in the basal layer of the vaginal epithelium late during the mouse pregnancy have been reported before (432). Estrogen is known to stimulate this proliferation in non-pregnant mice and the increased levels of estrogen during late pregnancy could have accounted for our observation (433). Another factor implicated in increasing vaginal cell proliferation is relaxin, the secretion of which by the corpus luteum is also increased during late pregnancy in the mouse (434). This means that even if there would have been increases in the proliferation of basal cells due to tissue injury, these would not be identified because of the high percentage of the cells that are already proliferating.

Collectively, these experiments confirmed that N-9 significantly damages the cervicovaginal epithelium during pregnancy. From the features of damage that we assessed, morphological damage and neutrophil infiltrations could have resulted in preterm delivery. However, we found no effect of N-9-induced damage on the timing of delivery or pup survival. An even higher dose of 40% N-9 was used in these experiments to ensure coverage of the whole spectrum, even outside the pharmacological limits. Akgul *et al.* found that loss of Hyaluronic acid (HA) in the cervix results in epithelial disorganisation (280). This is not sufficient to cause preterm birth on its own (280). It rather predisposes to preterm delivery induced by *E. coli* (280). This is in line with our finding that N-9-induced morphological damage does not cause PTB. In addition, we found that the neutrophil infiltrations induced by N-9 are again not sufficient to cause PTB. Timmons *et al.* suggested that neutrophils are not necessary for cervical ripening to occur in the mouse and are physiologically recruited on site in preparation for postpartum repair (435). Still, the activation of immune pathways appears to be sufficient to induce preterm cervical ripening in mice (436). In our damage model, the neutrophils recruited are targeting the epithelium as part of the tissue repair process secondary to N-9 application. Hence, they have no

effect on the main bulk of the stroma and are therefore incapable of inducing premature cervical ripening and a subsequent preterm birth.

In summary, data from this chapter reveal that N-9 causes significant damage in the morphology of the cervicovaginal epithelium. This initiates a tissue repair process that is characterised by neutrophil infiltrations and increased proliferation in the basement membrane of the epithelium. However, this damage is not sufficient to cause preterm delivery and has no effect on pup survival. Overall, we describe and characterise for the first time a mouse model of cervical epithelial damage during pregnancy using N-9.

Chapter 5 The effect of cervical epithelial damage on ascending infection and preterm birth

5.1 Introduction

Preterm birth is a syndrome that has been associated with a diverse range of etiologies (56). Among them, the most common one affecting at least 25-40% of pregnancies is infection (437). In addition, intrauterine infection is the only condition for which a causality link has been established and the underlying pathophysiology is well studied.

There are several routes through which microorganisms can access the uterine cavity and cause an intrauterine infection. By ascending from the vagina and through the cervix; by disseminating haematogenously and through the placenta; by retrograde spread from the abdominal cavity and through the fallopian tubes; or by accidental dissemination during invasive medical procedures (196). The bacteria most commonly isolated from the amniotic fluid of women delivering preterm are are common to those which are also present in the vagina. Therefore, the most common route of intrauterine infection is believed to be the ascending pathway of vaginal bacteria through the cervix.

Ureaplasmas are the bacteria most frequently associated with preterm birth, and are commonly present in the amniotic fluid of preterm deliveries, as they can be detected in more than 40% of patients with preterm labour or PPROM (438). In addition, they are associated with potential adverse pregnancy outcomes in the absence of preterm delivery. These adverse outcomes include chorioamnionitis (416), fetal brain injury (411) and pulmonary disease (439) (440). *Ureaplasmas* are divided into two species: *U. urealyticum* and *U. parvum*. The latter is considered to be the more prevalent of the

two in the case of PTB, and is considered to be an independent risk factor for PTB (231). Despite the rate of around 40% of *Ureaplasma* infection in early preterm birth studies, a causal link is hard establish in humans, as a significant number of women with positive *Ureaplasma* cultures have normal pregnancy outcomes (242). One potential explanation is the low virulence of these bacteria. Further evidence on the mechanisms of infection during pregnancy is needed to establish the role of *Ureaplasma* spp as PTB-triggering microorgnanisms.

The cervical epithelium has a pivotal role in protecting against ascending infection during pregnancy (282). It has been shown that excisional procedures that damage the cervix by removing part of the epithelium and the underlying stroma significantly increase the risk for preterm delivery (304) (305), but the association has not been explained yet. A potential explanation could involve a compromise of the barrier function after cervical damage that could increase the risk for an ascending infection.

In the previous chapter, we established and characterised a new mouse model of cervical epithelial damage during pregnancy using the surfactant Nonoxynol-9. We also found that N-9-induced cervical damage per se does not cause preterm birth. Thus, the aim of the work described in this chapter is to address whether cervical damage could predispose to ascending inflammation and/or infection.

Intra-vaginal administration of LPS has previously been shown to induce preterm delivery (365). However, it is not clear if this is achieved by LPS only causing intrauterine inflammation or by causing vaginal inflammation that propagates to reach the intrauterine compartment. In addition, our group did not manage to replicate this finding before, with mice delivering normally at term after vaginal LPS administration (170). Therefore, we hypothesized that N-9-induced cervical epithelial damage and inflammation would boost LPS-induced inflammation in the vagina to induce preterm birth after co-administration of both substances. We also tested the hypothesis that loss of the epithelial barrier function by N-9 pre-treatment would facilitate preterm birth induced by a subsequent LPS intra-vaginal administration.

The effect of cervical epithelial damage on ascending infection and preterm birth 167

Ureaplasma parvum, the most clinically relevant bacteria for preterm birth, was also used to model ascending infection. We hypothesized that N-9-induced cervical epithelial damage would facilitate ascending infection with *U. parvum*. We also sought to investigate the capacity of *U. parvum* to mount an inflammatory response in fetal and maternal tissues.

5.2 Results

In the previous chapter, the establishment and characterisation of a mouse model of cervical damage using N-9 was described. Among the three different doses of N-9 that were tested, the one resulting in statistically significant epithelial injury as assessed by our scoring systems was the 10% N-9 v/v. Therefore, this was the dose of choice used in all subsequent experiments.

5.2.1 Co-administration of N-9 and LPS has no effect on timing of delivery or pup survival

To assess whether the added inflammatory effects induced by co-treatment of N-9 and LPS could result in preterm delivery and whether there would be any effect on pup survival, a time-to-delivery experiment was conducted. On D17 of pregnancy, timed pregnant mice were given an intravaginal inoculation of a formulation of N-9 and LPS. Timing of delivery of the first pup post-administration was monitored using CCTV. The percentage of pups born alive was calculated for each mouse. The experimental outline can be seen in Materials and Methods (**Fig 2.5A**).

Co-treatment with N-9 and LPS had no effect on timing of delivery. Mice treated with it delivered at an average of 70±6.06 hours post-administration compared to the ones treated with PBS control who delivered at 56.5±1.22 hours post-administration (P=0.0636). There was also no effect on timing of delivery for mice treated with either N-9 or LPS only, compared with PBS vehicle control only. Mice treated with N-9 alone or LPS alone delivered at 64.34±4.18 and 65.25±2.85 hours post-administration respectively (**Fig 5.1A**).

Co-administration of N-9 and LPS had also no effect on the pup survival. Mice in this group exhibited an average pup survival of 93.4±6.6% compared to 98±2% for mice treated with PBS control. Again, there was also no effect on pup survival for mice treated with N-9 or LPS alone. The former had an average pup survival of 96.75±2.14% while the latter had an average pup survival of 94.33±3.81% (**Fig 5.1B**).
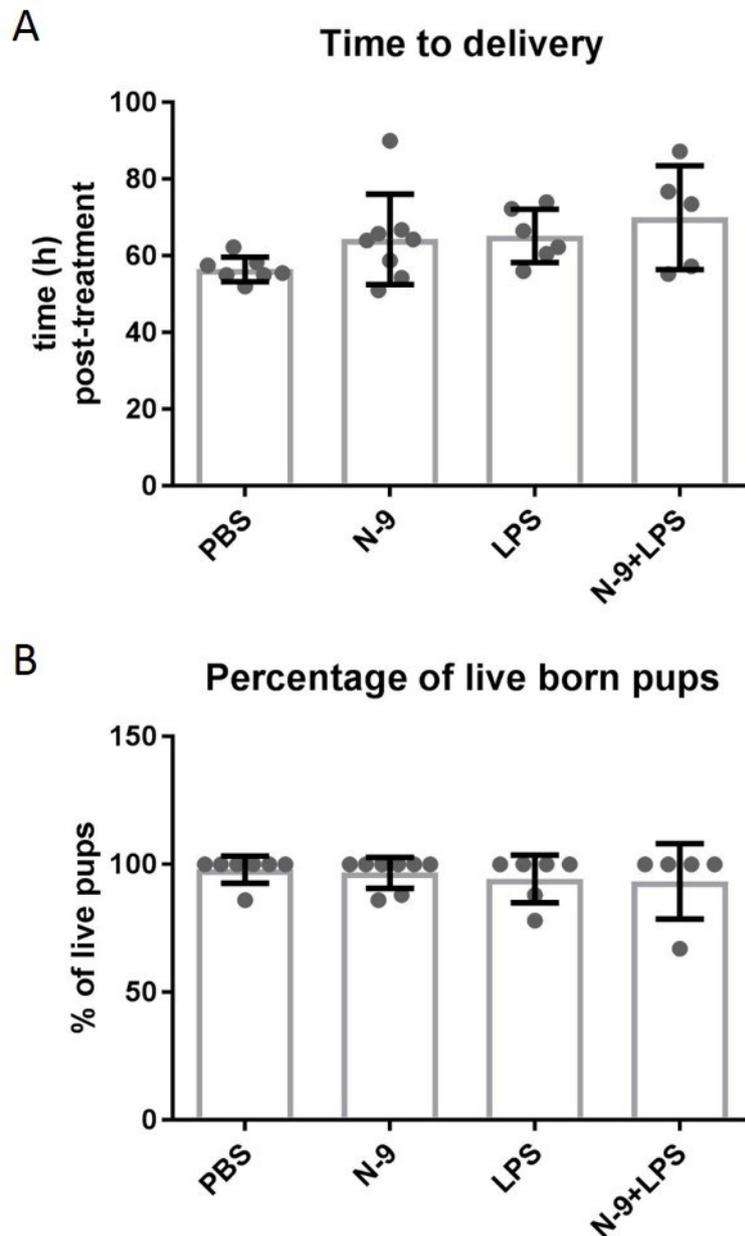
Figure 5.1 The combination of intra-vaginal N-9 with LPS does not affect timing of delivery and pup survival in a mouse model of cervical damage during pregnancy. In the morning of D17 of gestation, mice received either 10% N-9 in PBS or 100 μg/ml LPS in PBS or 10% N-9 and 100 μg/ml LPS in PBS or PBS control via intravaginal inoculation. Time to delivery was calculated from the moment of intravaginal inoculation until the delivery of the first pup. N-9 and LPS either alone or combined had no effect on timing of delivery (**A**). Percentage of live born pups for

each mouse was calculated by dividing the number of live pups delivered by the total number of pups. N-9 and LPS either alone or combined had no effect on pup survival (**B**). Statistical significance was assessed using 2-way ANOVA. Error bars represent *SD*.

5.2.2 N-9 pretreatment induced cervical damage does not facilitate vaginal LPS-induced preterm delivery and has no effect on pup survival

To investigate whether cervical damage induced by pretreatment with N-9-induced could facilitate vaginal LPS-induced preterm birth, another time-to delivery experiment was performed. In the afternoon of D16 of pregnancy, timed pregnant mice were given an intravaginal inoculation of N-9 and 16 hours later they were administered with vaginal LPS. Timing of delivery of the first pup post-administration was monitored using CCTV. The percentage of pups born alive was calculated for each mouse. The experimental outline can be seen in Materials and Methods (**Fig 2.5B**).

The administration of N-9 followed by LPS had no effect on timing of delivery. Mice treated with this scheme delivered at an average of 64.34±4.18 hours post-administration compared to the ones treated with PBS control who delivered at 57.93±2 hours post-administration. There was also no effect on timing of delivery for mice treated with either N-9 followed by PBS control or PBS control followed by LPS. Mice treated with the former combination delivered at 60.05±4.97 hours post-administration. Mice treated with the latter delivered at and 58.1±3.58 hours post-administration (**Fig 5.2A**).

N-9 followed by LPS had also no effect on the pup survival. Mice in this group had an average pup survival of 66.45±14.59% compared to 87.5±10.03% for mice treated with PBS controls only. Again, there was also no effect on pup survival for mice

treated with N-9 or LPS alone. The former had an average pup survival of 95.6±2.36% while the latter had an average pup survival of 75.21±9.9% (**Fig 5.2B**).
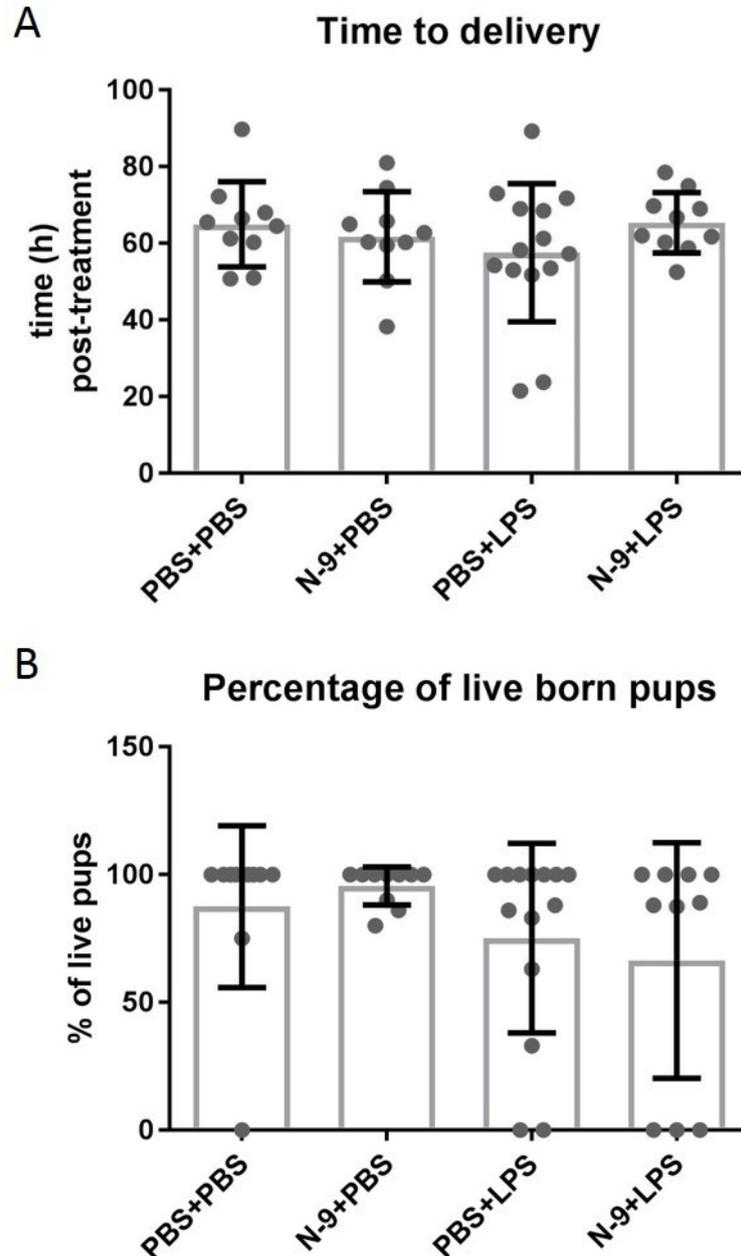
Figure 5.2 Cervical damage caused by intra-vaginal N-9 does not facilitate intra-vaginal LPS-induced preterm birth and has no effect on pup survival. In the afternoon of D16 of gestation, mice received either 10% N-9 in PBS or PBS control via intravaginal inoculation. 16 h later, in the morning of D17 of gestation, mice

The effect of cervical epithelial damage on ascending infection and preterm birth 172

received either 1 mg/ml LPS in PBS or PBS control via intravaginal inoculation. Time to delivery was calculated from the moment of intravaginal inoculation until the delivery of the first pup. N-9 and LPS either alone or combined had no effect on timing of delivery (**A**). Percentage of live born pups for each mouse was calculated by dividing the number of live pups delivered by the total number of pups. N-9 and LPS either alone or combined had no effect on pup survival (**B**). Statistical significance was assessed using 2-way ANOVA. Error bars represent *SD*.

5.2.3 N-9 is more cytotoxic against endocervical cells than against Ureaplasma parvum

N-9 has been shown to be cytotoxic against a wide range of bacteria (441) (442) (443) (444) and against epithelial cells (413). Our *in vivo* experimental design to test the hypothesis that cervical epithelial damage predisposes to ascending infection with *U. parvum* involved the sequential administration of N-9 followed by *U. parvum* 16 h later. First, we sought to determine the relative cytotoxicity of N-9 against cervical epithelial cells and *U. parvum*. To assess whether N-9 is more cytotoxic against endocervical cells or against *U. parvum*, both of them were treated with various N-9 concentrations for 48 hours and their ability to survive and grow was assessed by an MTT assay and colour changing assessment respectively.

Determination of the minimum N-9 cytotoxic dose against End1/E6E7

An MTT assay after 48 h of treatment with various doses of N-9 (0, 1, 2, 4, 8, 16, 32, 64, 128, 256, 512, 1024 µg/ml in Growth medium) revealed that the dose of 32 µg/ml was the minimum dose that completely abolished the cells' metabolic activity (**Fig 5.3**).

The effect of cervical epithelial damage on ascending infection and preterm birth 173
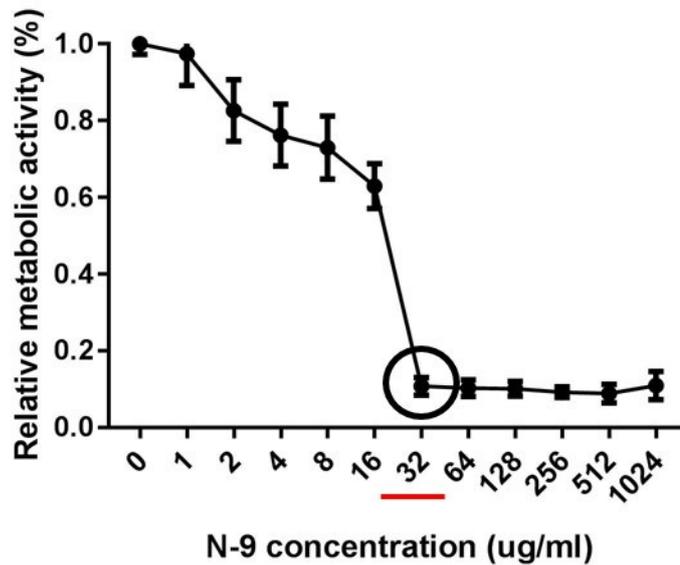
Figure 5.3 Determination of minimum N-9 concentration that stops endocervical End1/E6E7 cells' growth after 48 hours. End1/E6E7 cells were incubated with various N-9 concentrations (0, 2, 4, 8, 16, 32, 64, 128, 256 and 512 µg/ml) for 48h. Metabolic activity indicating cell viability was determined by an MTT assay and is expressed relative to that of the untreated cells. The minimum N-9 concentration that stops End1/E6E7 growth is 32 µg/ml. Error bars indicate *SD*.

Determination of the minimum N-9 cytotoxic dose against *Ureaplasma parvum*

U. parvum bacteria were allowed to grow in the presence of various doses of N-9 (0, 1, 2, 4, 8, 16, 32, 64, 128, 256, 512, 1024 µg/ml in Ureaplasma selective medium) and the microplate assay based on colour change indicative of bacterial growth was used to determine the lowest dose of N-9 that inhibited *U. parvum* growth. The minimum cytotoxic dose was found to be 128 µg/ml (**Fig 5.4**).
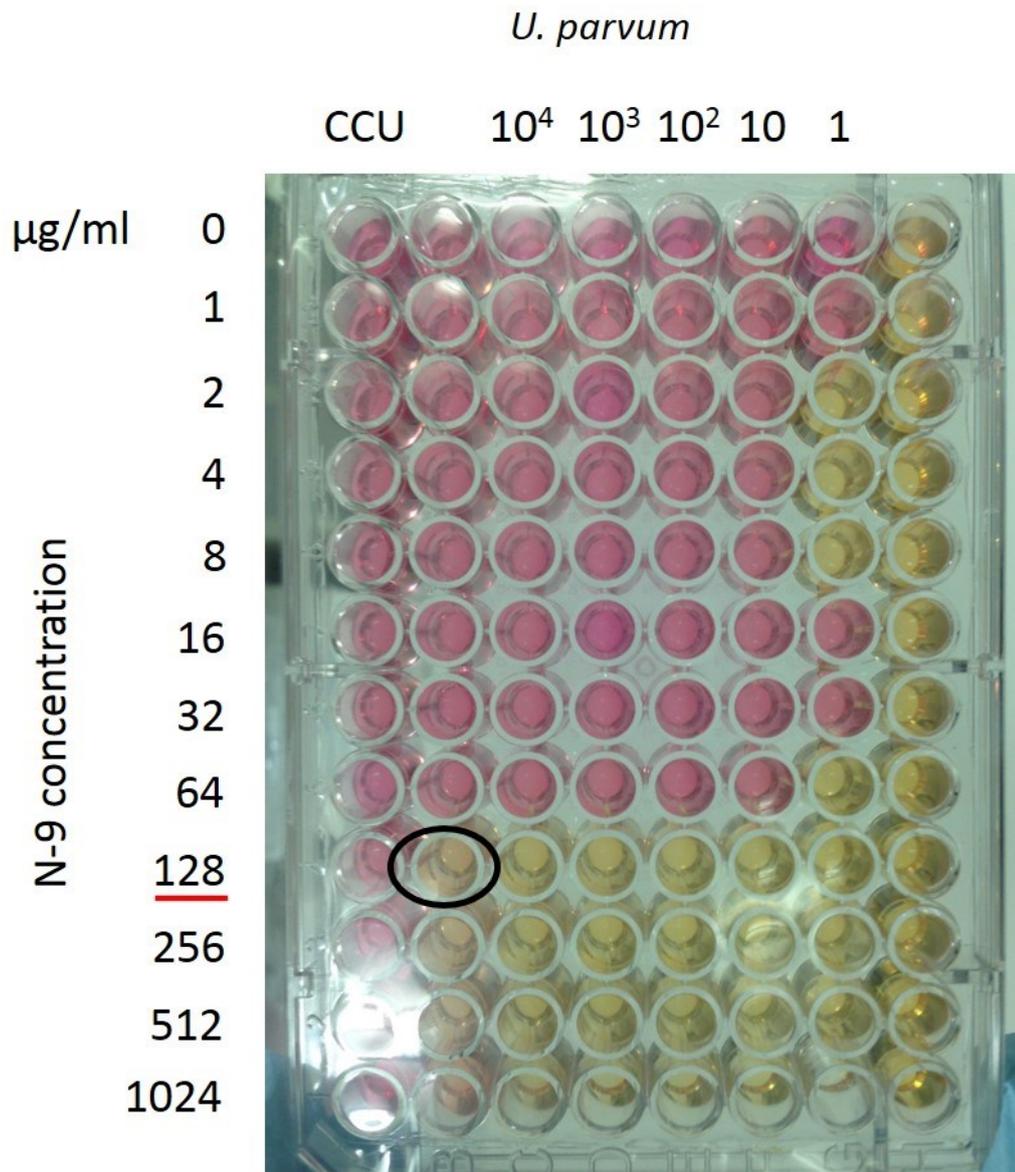
Figure 5.4 Determination of minimum N-9 concentration that stops *Ureaplasma parvum* growth after 48 hours. The 96-well plate contains an N-9 gradient from 1024 µg/ml to 1 µg/ml. Pink wells indicate growth and yellow wells indicate no growth of *Ureaplasma parvum (UP)* after 48 h. The minimum N-9 concentration that stops *UP* growth is 128 µg/ml.

5.2.4 N-9-induced cervical damage facilitates ascending infection with *Ureaplasma parvum* during pregnancy

To investigate whether N-9-induced cervical damage could facilitate ascending infection with *U. parvum*, a bioluminescent strain of the bacteria was used. In the afternoon of D16 of pregnancy, timed pregnant mice were given an intravaginal inoculation of 10% N-9 or PBS control. Sixteen hours later they were vaginally administered with *U. parvum* or Ureaplasma selective medium (USM) control. Twenty-four hours later, in the morning of D18, optical *in vivo* bioluminescence imaging was performed to assess the presence of *U. parvum* in the upper reproductive tract. The experimental outline can be seen in Materials and Methods (**Fig 2.6**). Bioluminescence signal (BLI) was quantified in pre-drawn regions of interest (ROI) that covered the whole mouse abdomen. A representative image is shown (**Fig 5.5A**).

Mice treated with control treatments (PBS+USM) exhibited only background levels of BLI (706±48 counts). Such was the case for that received the cervical damage treatment but were not administered with *U. parvum* (N-9+USM) (734±55 counts) (**Fig 5.5B**).

N-9 induced cervical damage facilitated ascending infection with *U.* parvum. Among mice that were given *U. parvum*, those that were previously treated with N-9 (N-9+UP) exhibited a significantly higher BLI signal ($61,2x10^3 \pm 25,7x10^3$ counts; P=0.0245) compared to those that received a control treatment for cervical damage (PBS+UP) ($9,5x10^3 \pm 7,4x10^3$ counts) (**Fig 5.5B**).
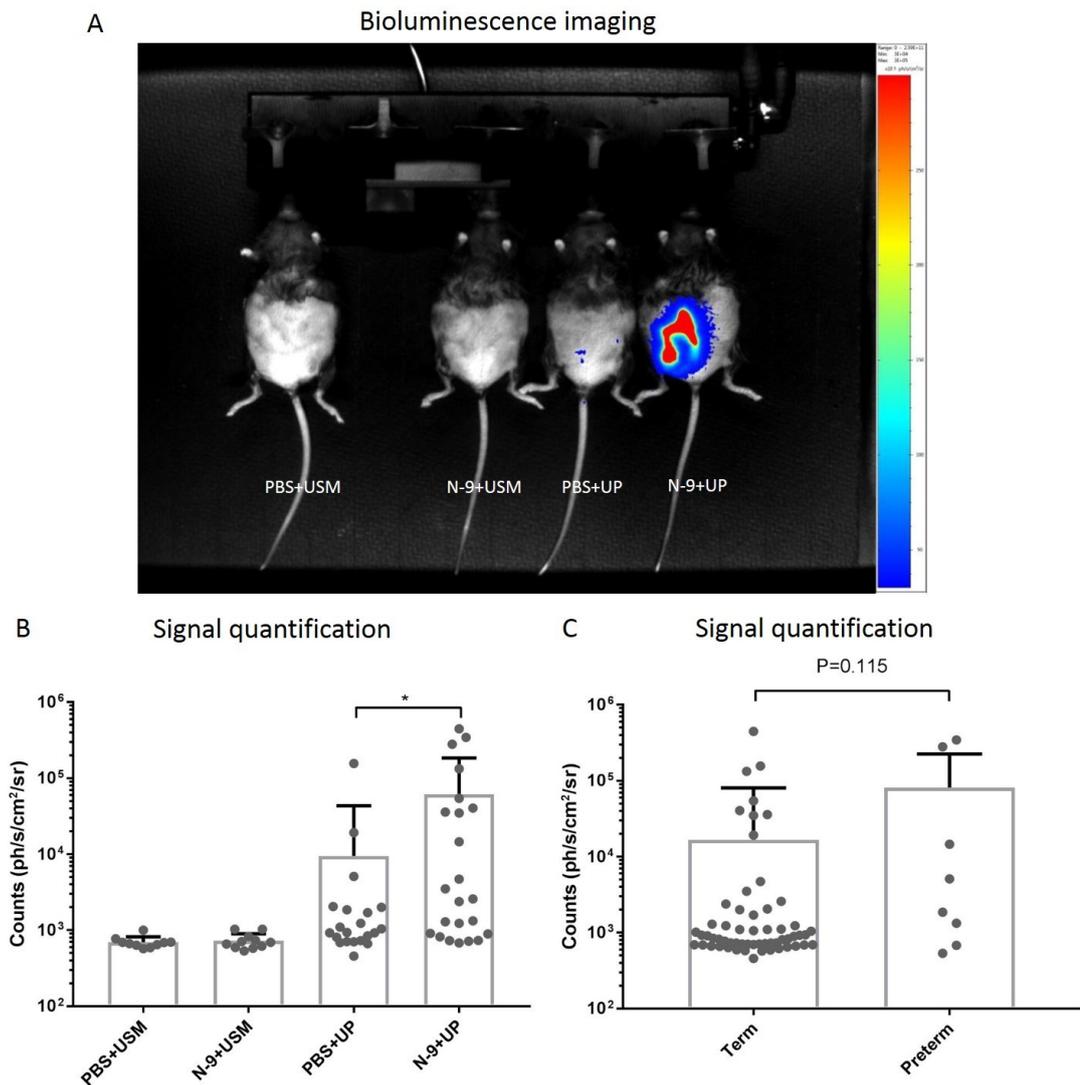
Figure 5.5 Cervical damage caused by N-9 results in increased bioluminescence signal in the upper reproductive tract after vaginal infection with luciferase-expressing *Ureaplasma parvum* during pregnancy. In the afternoon of D16 of gestation, mice received either 10% N-9 in PBS or PBS control via intravaginal inoculation. 16 h later, in the morning of D17 of gestation, mice received either luciferease-expressing *Ureaplasma parvum* (UP) in Ureaplasma Selective Medium (USM) or USM control via intravaginal inoculation. 24h later, in the morning of D18, the luciferase substrate Furimazine was injected intraperitoneally to allow *UP* localisation. A representative image is shown (**A**). Bioluminescence signal was quantified in a region of interest (ROI) covering each mouse's abdomen.

Bioluminescence signal coming from luciferase-expressing *UP* was significantly increased in mice that have been pre-treated with N-9 compared to PBS controls (**B**). No difference was found between bioluminescence signal on mice that delivered preterm compared to those that delivered at term (**C**). Error bars indicate *SD*. Statistical significance was assessed using a non-parametric Mann-Whitney test for PBS+UP *vs.* N-9+UP (*P=0.0245) and Term *vs.* Preterm (P=0.115).

5.2.5 N-9 pre-treatment results in higher *Ureaplasma parvum* titres in the amniotic fluid

To assess the capacity of *Ureaplasma parvum* to establish an infection at the administration site and whether this is affected by pre-treatment of the site with N-9, vaginal flushes with PBS were performed 48 hours post-administration. *U. parvum* titres were quantified in the returned solution. To further investigate the level to which cervical epithelial damage facilitates ascending infection, *Ureaplasma parvum* titres were measured in the amniotic fluid from sites located both proximally and distally to the cervix 48 hours post-administration of *Ureaplasma parvum*.

Ureaplasma parvum can grow in the vagina of pregnant mice either pre-treated with N-9 (N-9+UP) or not (PBS+UP). The bacterial titres in the vaginal flushes for the 2 groups were similar ($1.3x10^6 \pm 7x10^5$ CCU/15ul of vaginal flush for PBS+UP; $1.1x10^6 \pm 7x10^5$ CCU/15ul of vaginal flush for N-9+UP) (**Fig 5.6**).

Pre-treatment with N-9 was again shown to facilitate ascending infection with *U. parvum*. At a site proximal to the cervix, *Ureaplasma parvum* titres were statistically significantly higher in the amniotic fluid of mice pre-treated with N-9 ($2.2x10^6 \pm 7x10^5$ CCU/15ul of amniotic fluid; P=0.0356) compared to those pre-treated with PBS control ($7.2x10^4 \pm 3.7x10^4$ CCU/15ul of amniotic fluid) (**Fig 5.6**).

Similarly, the same statistically significant trend was noticed at a site distal to the cervix with higher bacterial titres in the amniotic fluid of N-9 pre-treated mice

$(2.2 \times 10^6 \pm 8.10^5$ CCU/15ul amniotic fluid; P=0.0466) compared to the PBS control pre-treated ones $(3.7 \times 10^3 \pm 2.8 \times 10^3$ CCU/15ul of amniotic fluid) (**Fig 5.6**).
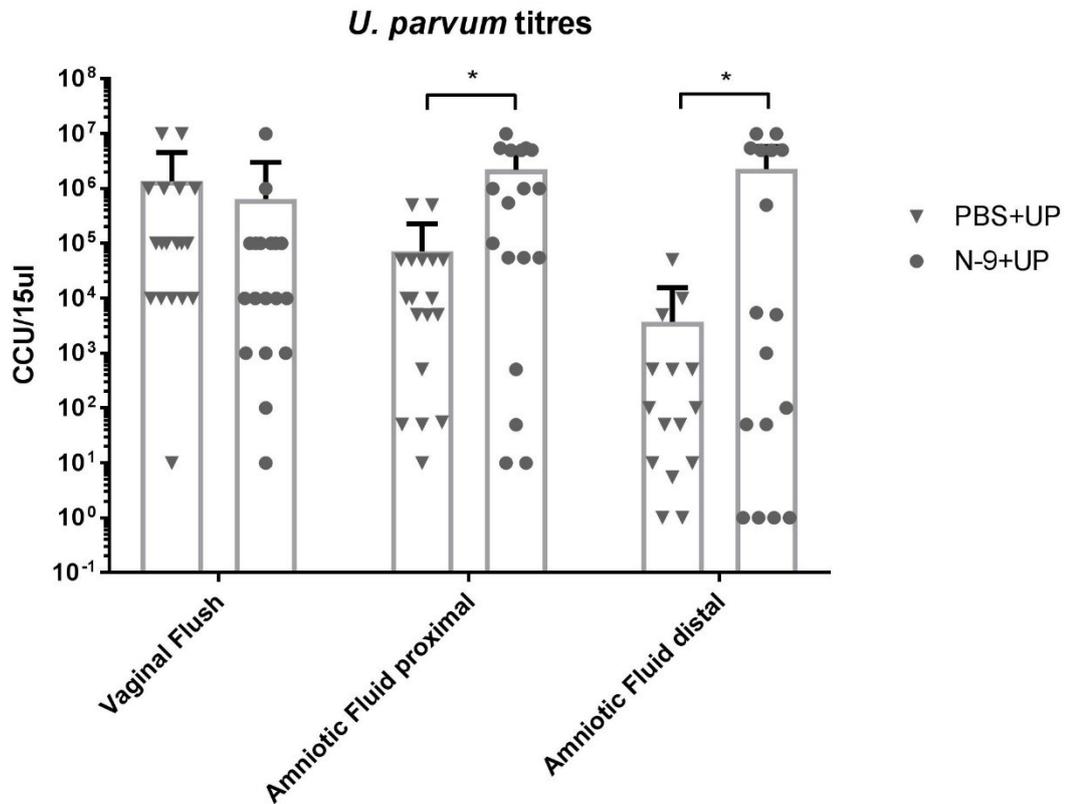
Figure 5.6 Cervical damage caused by N-9 results in higher *Ureaplasma parvum* titres in the amniotic fluid of pregnant mice after vaginal *U. parvum* administration. In the afternoon of D16 of gestation, mice received either 10% N-9 in PBS or PBS control via intravaginal inoculation. 16 h later, in the morning of D17 of gestation, mice received either *Ureaplasma parvum* (UP) in Ureaplasma Selective Medium (USM) or USM control via intravaginal inoculation. 48 h after *U. parvum* administration, vaginal flushes and amniotic fluid (AF) from proximal and distal sites were cultured in USM and *Ureaplasma parvum* titres were calculated using the microplate method. There was a significant increase in *UP* titres at the proximal sites and a trend increase at the distal sites in the amniotic fluid of mice pre-treated with N-9. For AF proximal and distal, each dot in the dot plot represents the average of left and right horn for each mouse at either site. Error bars indicate *SD*. Statistical

significance was assessed using unpaired *t*-test with Welch's correction on the log-transformed values of *Ureaplasma parvum* titres for PBS+UP *vs.* N-9+UP at all three sites (*P<0.05; P=0.0356 for Amniotic Fluid proximal, P=0.0466 for Amniotic Fluid distal).

5.2.6 N-9 pre-treatment results in a higher copy number of the *U. parvum* gene *Urease C* in the upper reproductive tract

To assess whether cervical damage could facilitate ascending infection with *U. parvum* that results in tissue invasion and/or colonisation, the copy number of the *U. parvum*-derived gene *Urease C* was quantified in the placenta, uterus, fetal membranes and fetal lung 48 hours after administration using qPCR.

Once again, results consistently supported that cervical damage facilitated ascending infection. Pre-treatment with N-9 followed by *U. parvum* administration resulted in a significantly higher *UreC* copy number in the placenta (29,490±5,037 copies) and the fetal membranes (48,270±7,716 copies) at a site proximal to the cervix compared to pre-treatment with PBS control (10,386±2,862 copies for placenta; 22,602±8,623 copies for fetal membranes) (P=0.0093 for placenta; P=0.048 for fetal membranes). The same trend was noticed in these two tissues at the distal site (12,894±4,420 *vs* 4,820±871 for placenta; 43,253±12,036 *vs* 14,522±6,725 for fetal membranes), although statistical significance was not reached (**Fig 5.7A, C**).

Similarly, the N-9+UP group demonstrated a higher *UreC* copy number in the uterus both proximally (6,382±1,785 copies) and distally (5,566±2,402 copies) to the cervix compared to the PBS+UP group (3,857±1,646 copies for proximal; 3,129±1,384 copies for distal). The differences observed were not statistically significant (**Fig 5.7B**).

The same trend for *UreC* gene copy number was followed in the fetal lung at the proximal site, albeit at a much lower copy number (333.8±190.1 copies for N-9+UP

vs 218.8±108.2 copies for PBS+UP). No difference was observed at the distal site (**Fig 5.7D**).
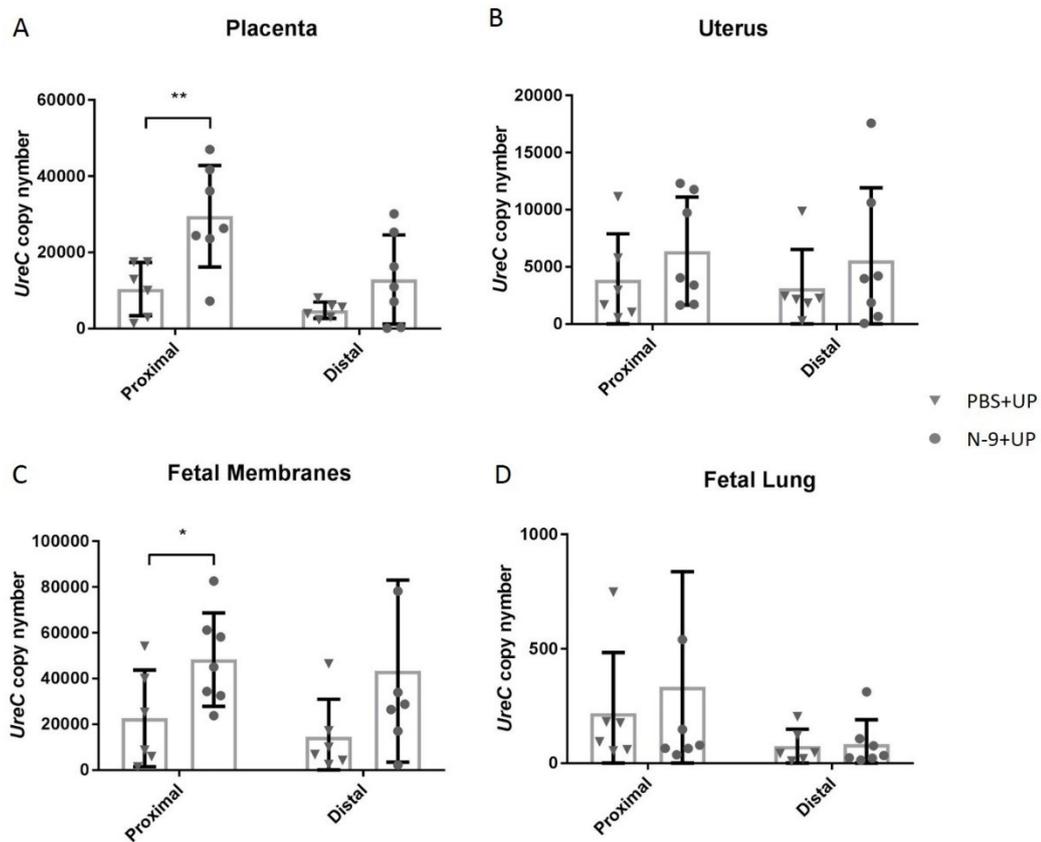
Figure 5.7 Cervical damage caused by N-9 results in a higher copy number of the *Ureaplasma parvum*-derived gene *Urease C* in the placenta, uterus and fetal membranes after vaginal *U. parvum* administration. In the afternoon of D16 of gestation, mice received either 10% N-9 in PBS or PBS control via intravaginal inoculation. 16 h later, in the morning of D17 of gestation, mice received either *Ureaplasma parvum* (UP) in Ureaplasma Selective Medium (USM) or USM control via intravaginal inoculation. 48 h after *U. parvum* administration, tissues were collected and gene expression of *UreC* was analysed using qPCR. In mice pre-treated with N-9, there was a significant increase in *UreC* copy number at the proximal sites of the placenta and the fetal membranes and a trend increase in all other tissues and sites. No difference was observed at the distal site of the fetal lung. Each dot in the dot plot represents the average of left and right horn for each mouse at either site. Error

The effect of cervical epithelial damage on ascending infection and preterm birth 181

bars indicate *SD*. Statistical significance was assessed using unpaired *t*-test for PBS+UP *vs.* N-9+UP in all 4 tissues and at both sites (*P=0.048 for N-9+UP *vs* PBS+UP at the fetal membranes' proximal site, **P=0.0093 for N-9+UP *vs* PBS+UP at the placental proximal site).

5.2.7 Increased preterm birth rates in mice treated with N-9 followed by ascending infection with *Ureaplasma parvum*

C57Bl/6 mice normally deliver at around 60 hours after the morning of D17 of gestation. Timings of delivery of all control mice that were used in previous experiments is shown on **Fig 5.8**. Delivery occurs 60.45±1.76 hours post-administration, 95% Confidence Intervals (CI) [56.81, 64.08] (**Fig 5.8**). No mice delivered before 48 hours post-administration.
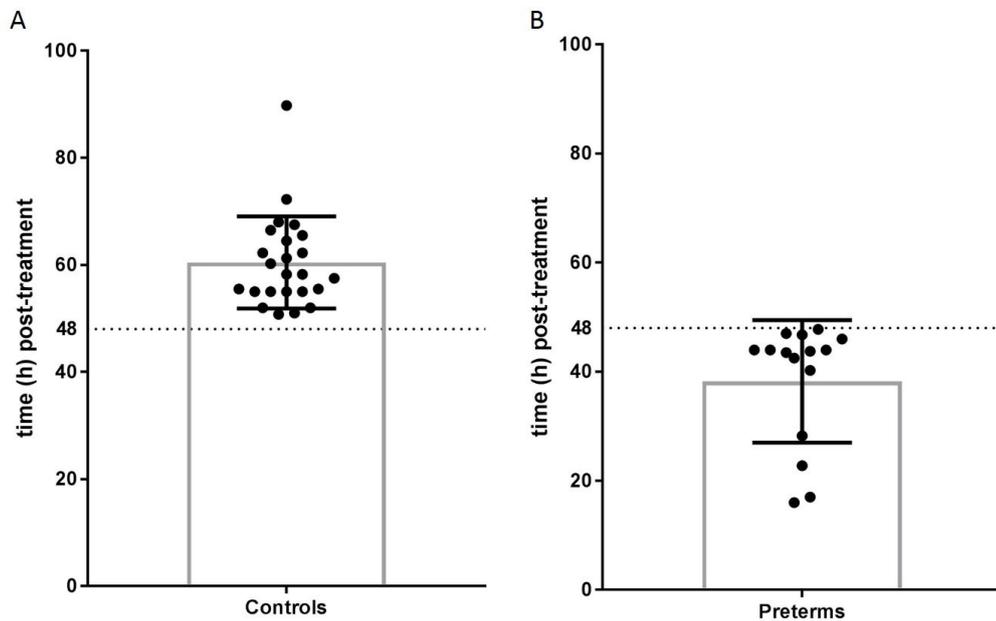
Figure 5.8 C57Bl/6 mice normally deliver at around 60 hours after the morning of D17 of gestation. Data from all experiments conducted in the previous chapters using control-treated animals (**A**). No mice delivered before 48 hours post-administration (**A**). Timing of delivery of mice that delivered preterm using the 48-hour threshold in subsequent experiments are also depicted (**B**).

To assess whether ascending infection with *U. parvum* facilated by N-9-induced cervical damage can cause PTB, a time threshold at 48 hours post *U. parvum* administration was set up. Delivery of the first pup before 48 hours after *U. parvum* administration deemed the respective pregnancy to be called preterm.

N-9 pre-treatment followed by *U. parvum* administration (N-9+UP) resulted in significantly increased PTB rates. 10/36 (28%) mice in this group delivered prematurely (P=0.0104) as opposed to 0/19 (0%) in the group that received control treatments only (PBS+USM) (**Fig 5.9**). Only 1/16 (6%) of mice treated with N-9 but without *Ureaplasma parvum* (N-9+USM) delivered preterm (P=0.4571). Mice that were infected with *U. parvum* but without prior N-9 treatment (PBS+UP) exhibited a 13% preterm birth rate (4/31; P=0.1476). None of these groups differed significantly from the group that received the control treatments only (**Fig 5.9**). Total numbers and percentages can be seen on **Table 5-1**.
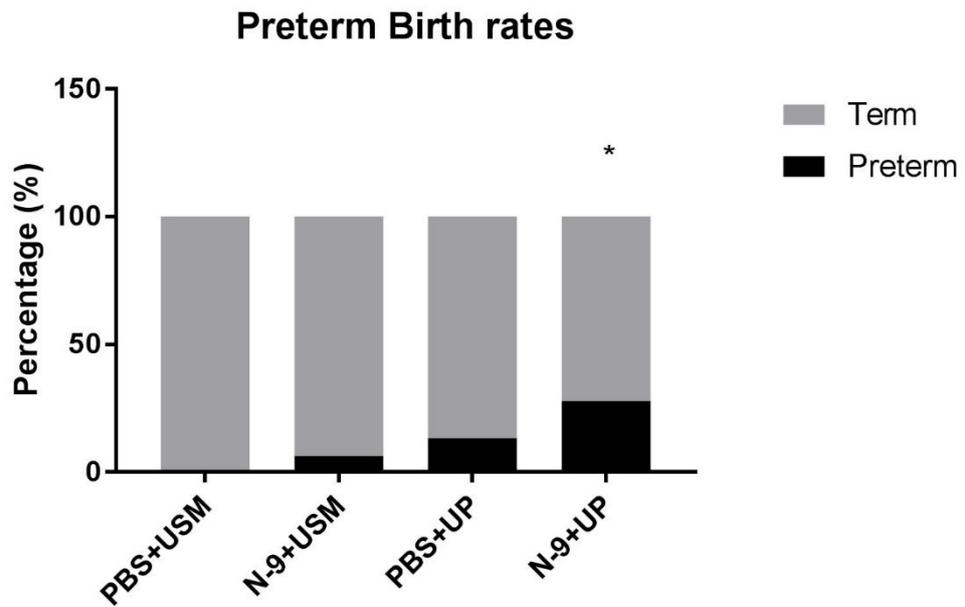
Figure 5.9 Cervical damage caused by N-9 facilitates a significant increase in preterm birth rates after vaginal infection with *Ureaplasma parvum.* In the afternoon of D16 of gestation, mice received either 10% N-9 in PBS or PBS control via intravaginal inoculation. 16 h later, in the morning of D17 of gestation, mice received either *Ureaplasma parvum* (UP) in Ureaplasma Selective Medium (USM) or USM control via intravaginal inoculation. Preterm birth was defined as delivery of the first pup before 48 completed hours from the moment of the D17 inoculation. The combination of N-9-induced cervical damage and *Ureaplasma parvum* infection resulted in a significant increase in preterm birth rates compared to controls. Statistical significance was assessed using Fisher's exact test (*P=0.0104 for PBS+USM *vs.* N9+UP).

Table 5-1 Preterm birth rates in mice after cervical damage and/or vaginal infection with *Ureaplasma parvum.*

PBS+USM	N9+USM	PBS+UP	N9+UP
0/19 (0%)	1/16 (6%)	4/31 (13%)	10/36 (28%)

The effect of cervical epithelial damage on ascending infection and preterm birth 184

5.2.8 Inflammatory gene response in the placenta following vaginal infection with *Ureaplasma parvum*

To assess whether ascending infection with *U. parvum* facilitated by cervical damage could mount an inflammatory response in the reproductive tract during pregnancy, maternal and fetal tissues from the previous experiment were collected 48 h after vaginal *U. parvum* administration that was preceded by cervical damage or control. As defined in the previous section, these mice were deemed term. Changes in the gene expression of proinflammatory cytokines and TLRs were examined using RT-qPCR. The analysis was performed both at the proximal and at the distal site.

Proinflammatory cytokine gene expression in the placenta

Infection with *U. parvum* but not damage with N-9 was a statistically significant source of variation in the expression of *Tnfa* (P<0.0001 for proximal, P=0.0141 for distal)*, Il1b* (P<0.0001 for proximal and distal)*, Cxcl1* (P<0.0001 for proximal, P=0.0004 for distal) *and Cxcl2* (P<0.0001 for proximal and distal) both at the proximal and at the distal site. No interaction between the two independent variables was detected. No differences were found for *Il-6*.

At the proximal site, the genes *Tnfa, Il1b, Cxcl1* and *Cxcl2* were significantly upregulated in the two groups infected with *U. parvum* (N-9+UP, PBS+UP) compared to the vehicle-treated group (PBS+USM). For the N-9+UP group, *TNFa* expression increased by 2.35±0.3-fold, *Il1b* increased 10.71±2.59-fold, *Cxcl1* increased 3.82±0.48-fold and *Cxcl-2* increased 61.3±12.26-fold. For the PBS+UP group, *TNFa* expression increased by 1.85±0.32-fold, *Il1b* increased 7.27±1.56-fold, *Cxcl1* increased 3.26±0.57-fold and *Cxcl2* increased 39.01±12.83-fold. *Il6* levels did not change. No differences were found for the group that received N-9 but not *U. parvum* (N-9+USM). All changes can be seen in **Table 5-2** and **Fig 5.10**.

At the distal site, the genes *Il1b* and *Cxcl2* were significantly upregulated in the two groups infected with *U. parvum* (N-9+UP, PBS+UP) compared to the vehicle-treated group (PBS+USM). For the N-9+UP group, *Il1b* increased 4.14±0.87-fold and *Cxcl-2*

increased 29.79±8.04-fold. For the PBS+UP group *Il1b* increased 2.64±0.39-fold and *Cxcl-2* increased 8.51±1.41-fold. *Tnfa, Cxcl1* and *Il6* levels did not change. No differences were found for the group that received N-9 but not *U. parvum* (N-9+USM). All changes can be seen in **Table 5-2** and **Fig 5.10**.

The changes for *Il1b, Cxcl1* and *Cxcl2* were significantly higher at the proximal site compared to the distal. *Tnfa* followed the same trend without reaching statistical significance (**Fig 5.10**).

A significant correlation was noticed between the copy number of the *Urease C* gene derived from *U. parvum* and the increase in the expression of *Tnfa* (r=0.51, P=0.0072), *Il1b* (r=0.72, P<0.0001), *Cxcl1* (r=0.71, P<0.0001) and *Cxcl2* (r=0.78, P<0.0001).

Table 5-2 Inflammatory cytokine gene changes in the placenta after vaginal administration of *Ureaplasma parvum* preceded by cervical damage or control treatments (*P<0.05, **P<0.01, ***P<0.001, ****P<0.0001).

	N-9+USM		PBS+UP		N-9+UP	
	Fold change relative to PBS+USM					
	Proximal	Distal	Proximal	Distal	Proximal	Distal
Tnfa	1.02	0.93	1.85**	1.33	2.35****	1.76
Il1b	0.94	0.94	7.27****	2.64*	10.71****	4.14**
Cxcl1	1.06	0.77	3.26****	1.79	3.82****	1.7
Cxcl2	1.3	1.29	39.01****	8.51***	61.3****	29.79****
Il6	0.75	0.97	1.74	1.69	1.51	1.65

A *Tnfa*

B *Il1b*

C *Cxcl1*
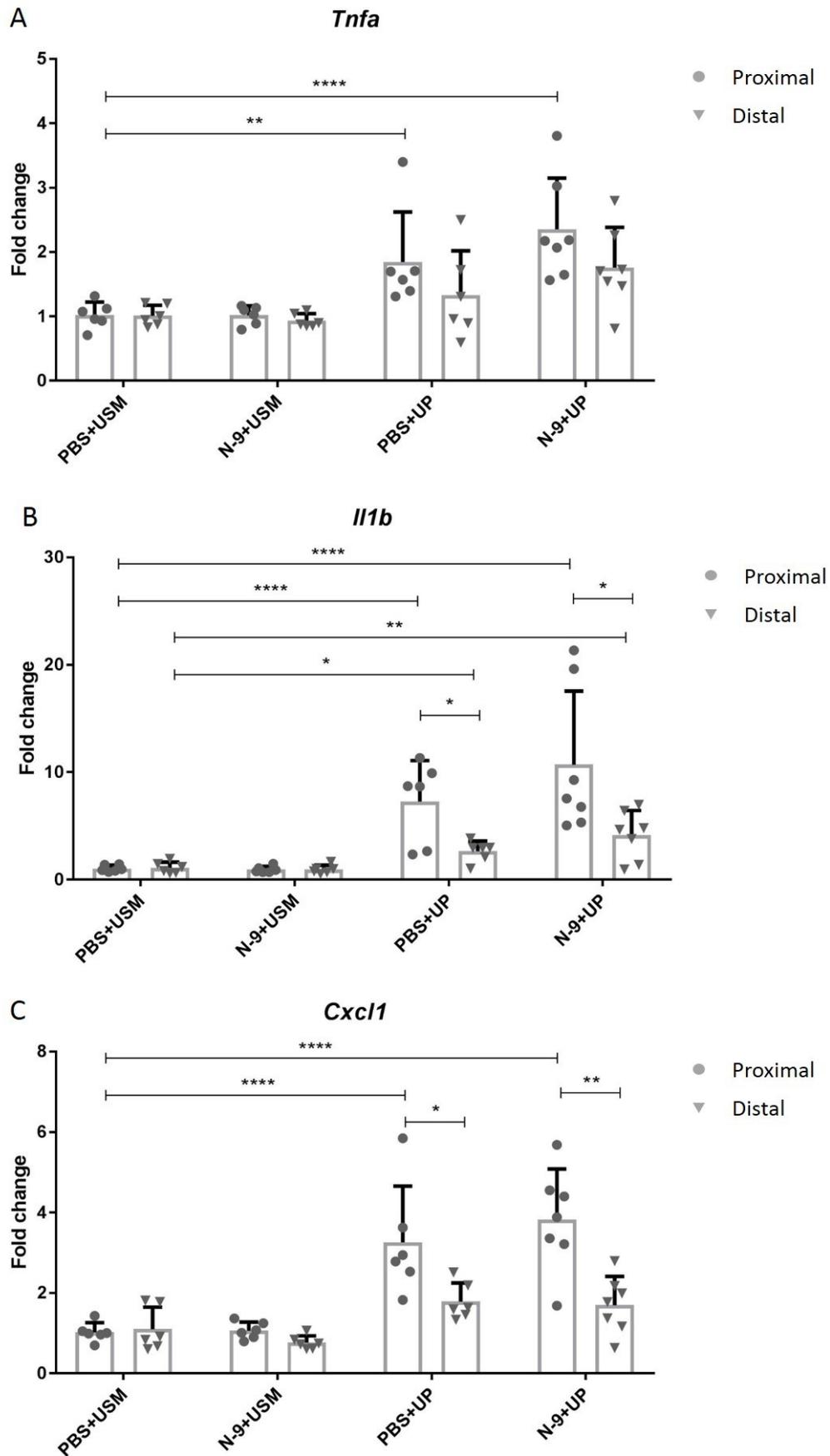
Figure 5.10 *Ureaplasma parvum* **infection causes significant upregulation of proinflammatory genes in the placenta of pregnant mice.** In the afternoon of D16 of gestation, mice received either 10% N-9 in PBS or PBS control via intravaginal inoculation. 16 h later, in the morning of D17 of gestation, mice received either *Ureaplasma parvum* (UP) in Ureaplasma Selective Medium (USM) or USM control via intravaginal inoculation. Tissues were collected 48 h later and analysed using RT-qPCR. Mice that were infected had an increase in the mRNA levels of *Tnfa* (**A**), *Il1b* (**B**), *Cxcl1* (**C**) and *Cxcl2* (**D**) compared to vehicle-treated controls. The effect was

stronger at the proximal site. Error bars indicate *SD*. Statistical significance of the treatment effect was assessed using 2-way ANOVA with *post hoc* Dunnett's multiple comparisons test on the DDCt values against the PBS+USM group for the proximal and distal site. Statistical significance for the site effect was assessed unpaired *t*-test for Proximal *vs* Distal for each treatment group. (*P<0.05, **P<0.01, ***P<0.001, ****P<0.0001). In collaboration with MSc student Gabriella Sammut Demarco.

Toll-like receptors gene expression in the placenta

Infection with *U. parvum* but not damage with N-9 was a statistically significant source of variation in the expression of *Tlr1* (P=0.0336 for proximal, P=0.0346 for distal) and *Tlr2* (P<0.0001 for proximal, P=0.0016 for distal). No interaction between the two independent variables was detected. No differences were found for *Tlr6* and *Tlr9*.At the proximal site, *Tlr2* was significantly upregulated in the two groups infected with *U. parvum* (N-9+UP, PBS+UP) compared to the vehicle-treated group (PBS+USM). For the N-9+UP group, *Tlr2* expression increased by 2.22±0.13-fold. For the PBS+UP group, *Tlr2* expression increased by 2.03±0.34-fold. The levels of *Tlr1* also increased by 1.98±0.41-fold but only for the N-9+UP group. Levels of the other TLRs did not change. No differences were found for the group that received N-9 but not *U. parvum* (N-9+USM). All changes can be seen in **Table 5-3** and **Fig 5.11**.

At the distal site, *Tlr2* was significantly upregulated only in the group infected with *U. parvum* and preceded by cervical damage (N-9+UP) compared to the vehicle-treated group (PBS+USM). In this case, *Tlr2* expression increased by 1.72±0.21-fold. Levels of the other TLRs did not change. No differences were found for the group that received N-9 but not *U. parvum* (N-9+USM) or *U. parvum* but not N-9. All changes can be seen in **Table 5-3** and **Fig 5.11**.

No differences were detected between the proximal and the distal site (**Fig 5.11**).

A significant correlation was noticed between the copy number of the *Urease C* gene derived from *U. parvum* and the increase in the expression of *Tlr1* (r=0.66, P=0.0002), *Tlr2* (r=0.70, P<0.0001), *Tlr6* (r=0.45, P=0.0219) and *Tlr9* (r=0.42, P=0.0323).

Table 5-3 TLR gene changes in the placenta after vaginal administration of _Ureaplasma parvum_ preceded by cervical damage or control treatments (*P<0.05, ***P<0.001, ****P<0.0001).

	N-9+USM		PBS+UP		N-9+UP	
	Fold change relative to PBS+USM					
	Proximal	Distal	Proximal	Distal	Proximal	Distal
Tlr1	1.06	1.03	1.2	1.18	1.98*	1.38
Tlr2	1.19	1.07	2.03***	1.49	2.22****	1.72*
Tlr6	1.23	1	1.17	0.83	1.12	0.86
Tlr9	0.91	0.95	0.9	0.85	1.17	0.97

A

Tlr1

B

Tlr2

C

Tlr6
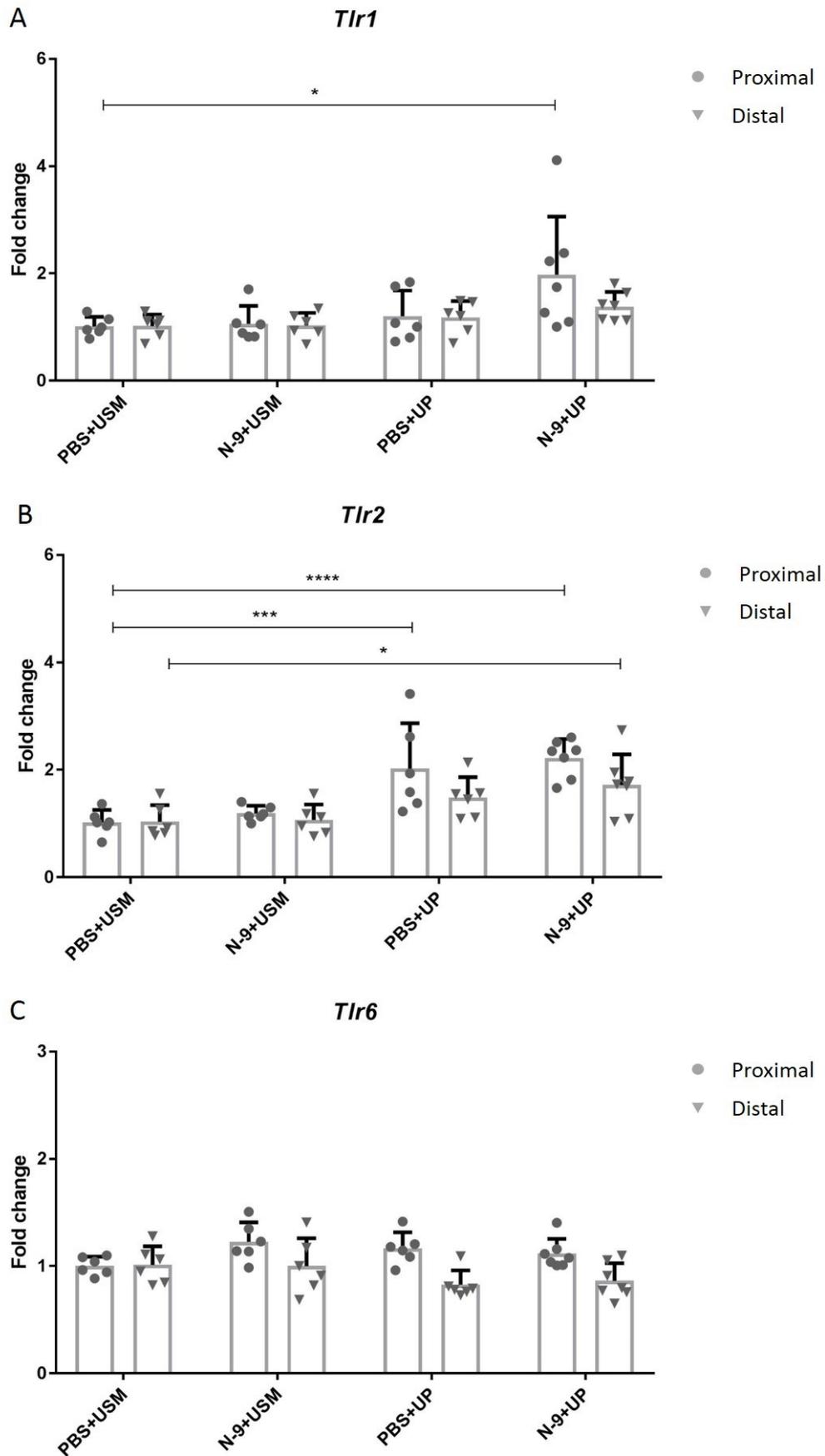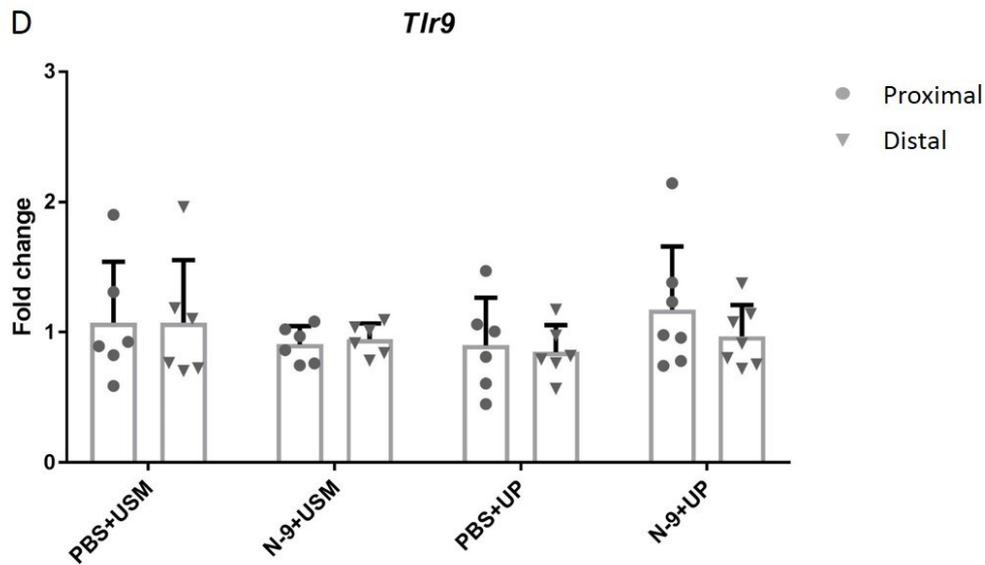
Figure 5.11 *Ureaplasma parvum* **infection causes significant upregulation of TLR2 gene expression in the placenta of pregnant mice.** In the afternoon of D16 of gestation, mice received either 10% N-9 in PBS or PBS control via intravaginal inoculation. 16 h later, in the morning of D17 of gestation, mice received either *Ureaplasma parvum* (UP) in Ureaplasma Selective Medium (USM) or USM control via intravaginal inoculation. Tissues were collected 48 h later and analysed using RT-qPCR. Mice that were infected had an increase in the mRNA levels of *Tlr2* (**B**) and those that were pre-treated with N-9 followed by *U. parvum* also had an increase in *Tlr1* (**A**) mRNA at the proximal site compared to vehicle-treated controls. There was no site effect. Error bars indicate *SD*. Statistical significance of the treatment effect was assessed using 2-way ANOVA with *post hoc* Dunnett's multiple comparisons test on the DDCt values against the PBS+USM group for the proximal and distal site. Statistical significance for the site effect was assessed unpaired *t*-test for Proximal *vs* Distal for each treatment group. (*$P<0.05$, ***$P<0.001$, ****$P<0.0001$). In collaboration with MSc student Gabriella Sammut Demarco.

5.2.9 Inflammatory gene response in the uterus following vaginal infection with *Ureaplasma parvum*

Proinflammatory cytokine gene expression in the uterus

Infection with *U. parvum* but not damage with N-9 was a statistically significant source of variation in the expression of *Tnfa* (P<0.0001 for proximal, P=0.0086 for distal)*, Il1b* (P<0.0001 for proximal, P=0.0042 for distal)*, Cxcl1* (P<0.0001 for proximal, P=0.002 for distal) *and Cxcl2* (P<0.0001 for proximal, P=0.0017 for distal) both at the proximal and at the distal site. No interaction between the two independent variables was detected. No differences were found for *Il-6*.

At the proximal site of the uterus, the genes *TNFa, Il1b, Cxcl1* and *Cxcl2* were significantly upregulated in the two groups infected with *U. parvum* (N-9+UP, PBS+UP) compared to the vehicle-treated group (PBS+USM). For the N-9+UP group, *TNFa* expression increased by 6.46±0.73-fold, *Il1b* increased 7.2±0.98-fold, *Cxcl1* increased 9.11±1.87-fold and *Cxcl-2* increased 24.32±6.19-fold. For the PBS+UP group, *TNFa* expression increased by 2.87±0.63-fold, *Il1b* increased 3.66±1.27-fold, *Cxcl1* increased 7.54±2.5-fold and *Cxcl-2* increased 14.46±4.88-fold. No differences were found for the group that received N-9 but not *U. parvum* (N-9+USM). All changes can be seen in **Table 5-4** and **Fig 5.12**.

At the distal site, the genes *TNFa, Cxcl1* and *Cxcl2* were significantly upregulated in only in the N-9+UP compared to the vehicle-treated group (PBS+USM). For the N-9+UP group, *TNFa* expression increased by 5.47±1.95-fold, *Cxcl1* increased 7.63±3.22-fold and *Cxcl-2* increased 11.66±5.64 -fold. No differences were found in the other two groups. All changes can be seen in **Table 5-4** and **Fig 5.12**.

Although a trend difference was noticed when comparing the site effect, this only reached significance in the case of *Il1b* for the N-9+UP group (**Fig 5.12**).

A significant correlation was noticed between the copy number of the *Urease C* gene derived from *U. parvum* and the increase in the expression of *Tnfa* (r=0.76, P<0.0001)*, Il1b* (r=0.79, P<0.0001)*, Cxcl1* (r=0.80, P<0.0001) and *Cxcl2* (r=0.84, P<0.0001).

Table 5-4 Inflammatory cytokine gene changes in the uterus after vaginal administration of *Ureaplasma parvum* preceded by cervical damage or control treatments (*P<0.05, **P<0.01, ***P<0.001, ****P<0.0001).

	N-9+USM		PBS+UP		N-9+UP	
	Fold change relative to PBS+USM					
	Proximal	Distal	Proximal	Distal	Proximal	Distal
Tnfa	1.5	1.6	2.87**	2.33	6.46****	5.47**
Il1b	0.81	1.04	3.66**	2.29	7.2****	4.06
Cxcl1	0.86	1.16	7.54***	4.15	9.11***	7.63*
Cxcl2	0.79	1.29	14.46****	3.72	24.32****	11.66**
Il6	0.94	1.08	0.83	1.82	0.8	0.83

A

Tnfa

B

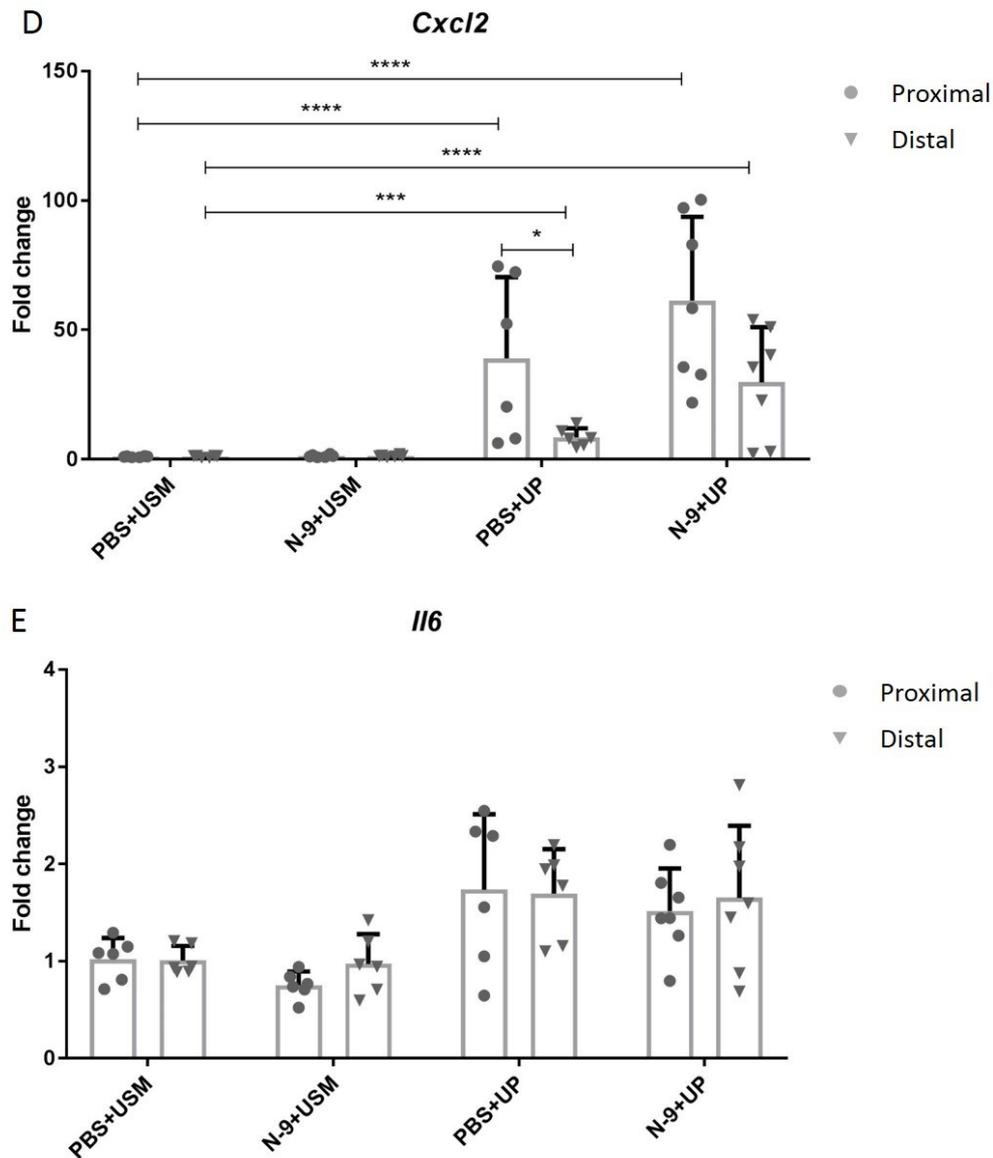**_Il1b_**

C

Cxcl1
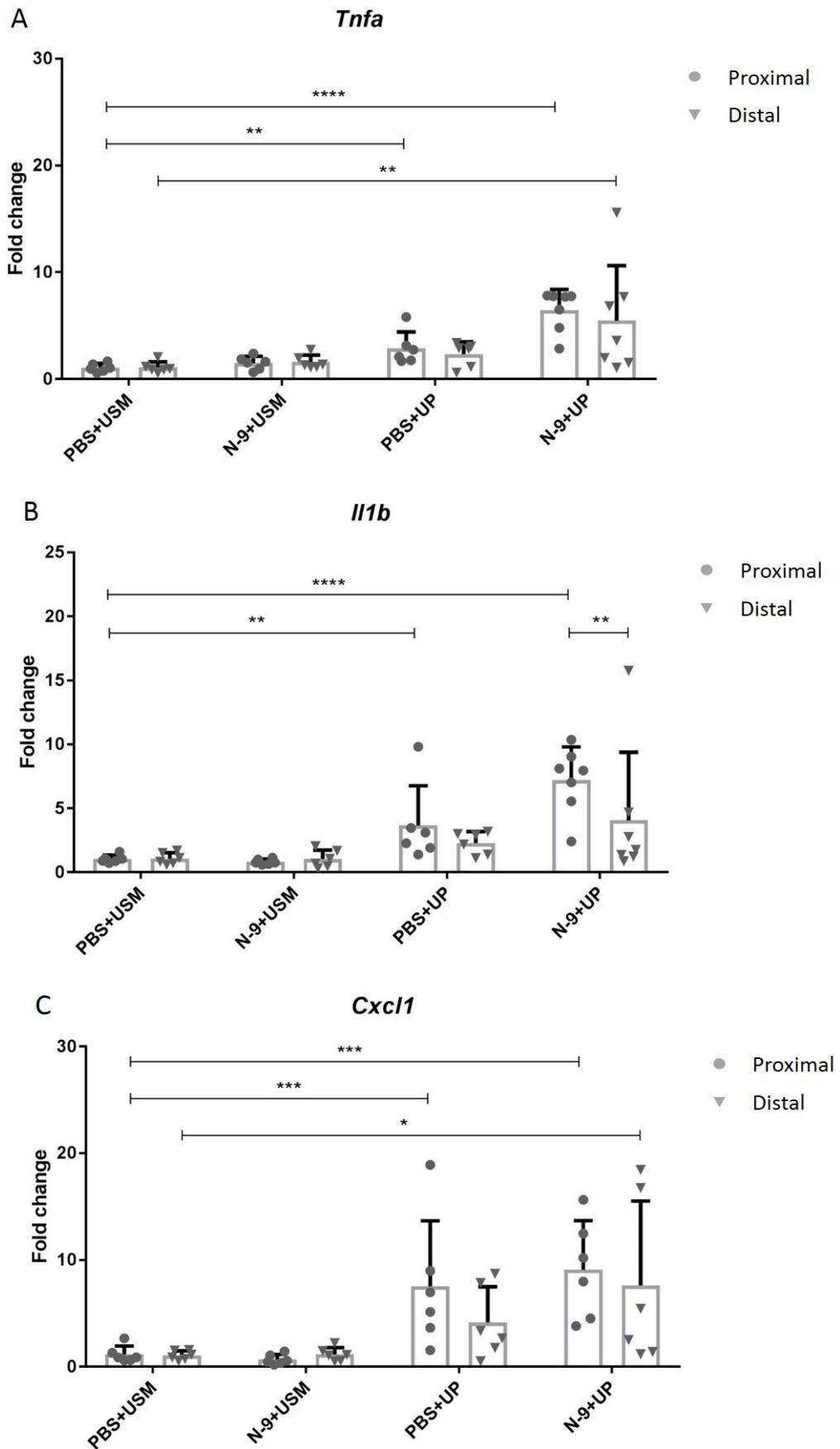
Figure 5.12 *Ureaplasma parvum* **infection causes significant upregulation of proinflammatory genes in the uterus of pregnant mice.** In the afternoon of D16 of gestation, mice received either 10% N-9 in PBS or PBS control via intravaginal inoculation. 16 h later, in the morning of D17 of gestation, mice received either *Ureaplasma parvum* (UP) in Ureaplasma Selective Medium (USM) or USM control via intravaginal inoculation. Tissues were collected 48 h later and analysed using RT-qPCR. Mice that were infected had an increase in the mRNA levels of *Tnfa* (**A**), *Il1b* (**B**)*, Cxcl1* (**C**) and *Cxcl2* (**D**) compared to vehicle-treated controls. The effect was

stronger at the proximal site. Error bars indicate *SD*. Statistical significance of the treatment effect was assessed using 2-way ANOVA with *post hoc* Dunnett's multiple comparisons test on the DDCt values against the PBS+USM group for the proximal and distal site. Statistical significance for the site effect was assessed unpaired *t*-test for Proximal *vs* Distal for each treatment group. (*P<0.05, **P<0.01, ***P<0.001, ****P<0.0001). In collaboration with MSc student Gabriella Sammut Demarco.

Toll-like receptor gene expression in the uterus

Infection with *U. parvum* but not damage with N-9 was a statistically significant source of variation in the expression of *Tlr2* (P=0.041 for proximal, P=0.028 for distal). No interaction between the two independent variables was detected. No differences were found for *Tlr1, Tlr6* and *Tlr9*.

Statistically significant upregulations were only noted for the *Tlr2* gene and for the group were *U. parvum* administration was preceded by N-9 administration. At the proximal site, *Tlr2* expression increased by 2.67±0.4-fold for the N-9+UP group. Levels of the other TLRs did not change for this group. No changes were noticed for the PBS+UP group. No differences were found for the group that received N-9 but not *U. parvum* (N-9+USM). All changes can be seen in **Table 5-5** and **Fig 5.13**.

At the distal site, *Tlr2* was significantly upregulated only in the group infected with *U. parvum* and preceded by cervical damage (N-9+UP) compared to the vehicle-treated group (PBS+USM). *Tlr2* expression increased by 2.47±0.51-fold. Levels of the other TLRs did not change. No differences were found for the group that received N-9 but not *U. parvum* (N-9+USM) or *U. parvum* but not N-9. All changes can be seen in **Table 5-5** and **Fig 5.13**.

No differences were detected between the proximal and the distal site (**Fig 5.13**).

A significant correlation was noticed between the copy number of the *Urease C* gene derived from *U. parvum* and the increase in the expression of *Tlr2* (r=0.63, P<0.0001).

The effect of cervical epithelial damage on ascending infection and preterm birth 198

Table 5-5 TLR gene changes in the placenta after vaginal administration of *Ureaplasma parvum* preceded by cervical damage or control treatments (*P<0.05, **P<0.01).

|	N-9+USM		PBS+UP		N-9+UP	
	Fold change relative to PBS+USM					
	Proximal	Distal	Proximal	Distal	Proximal	Distal
Tlr1	0.82	1.4	0.88	1.67	1.15	1.6
Tlr2	1.14	1.27	1.57	1.84	2.67**	2.47*
Tlr6	0.94	0.95	0.94	1.08	1.1	0.8
Tlr9	1.08	0.98	1.06	1.1	1.25	1.14

A   *Tlr1*

B   *Tlr2*

C   *Tlr6*
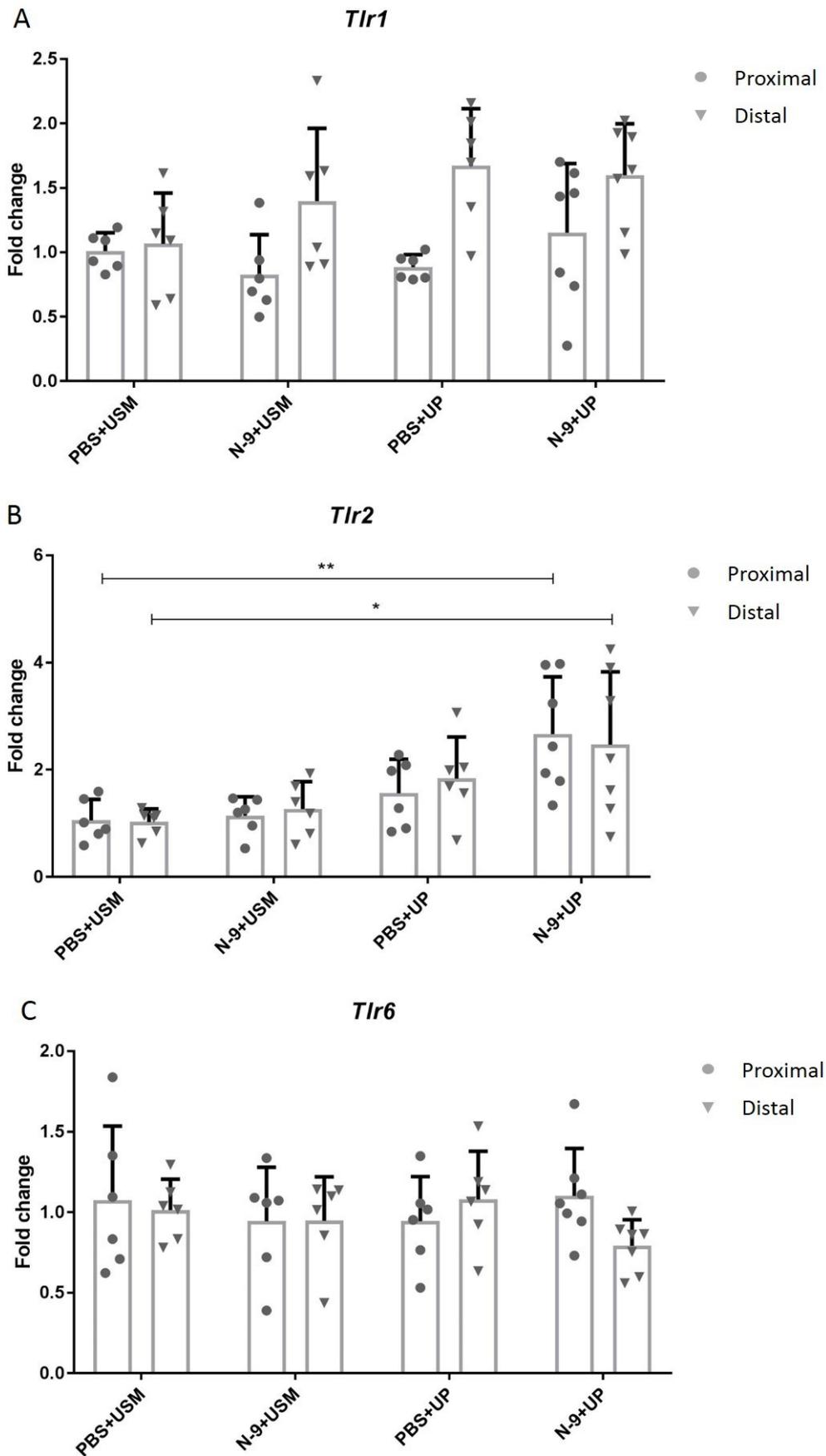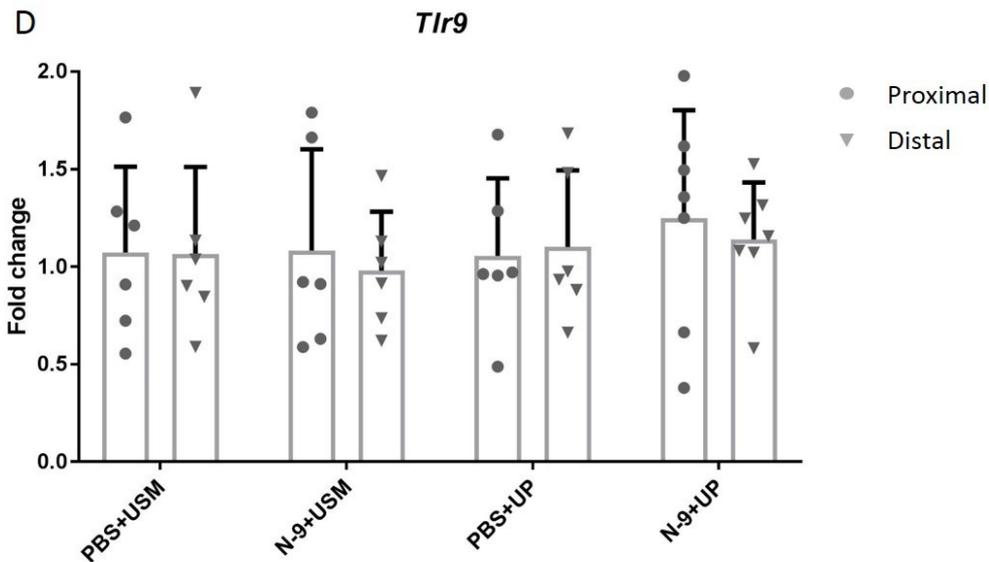
Figure 5.13 *Ureaplasma parvum* **infection causes significant upregulation of TLR2 gene expression in the uterus of pregnant mice.** In the afternoon of D16 of gestation, mice received either 10% N-9 in PBS or PBS control via intravaginal inoculation. 16 h later, in the morning of D17 of gestation, mice received either *Ureaplasma parvum* (UP) in Ureaplasma Selective Medium (USM) or USM control via intravaginal inoculation. Tissues were collected 48 h later and analysed using RT-qPCR. Mice that were infected with UP and had a previously damaged cervix by N-9 had an increase in the mRNA levels of *Tlr2* (**B**) both at a proximal and at a distal site. There was no site effect. Error bars indicate *SD*. Statistical significance of the treatment effect was assessed using 2-way ANOVA with *post hoc* Dunnett's multiple comparisons test on the DDCt values against the PBS+USM group for the proximal and distal site. Statistical significance for the site effect was assessed unpaired *t*-test for Proximal *vs* Distal for each treatment group. (*$P<0.05$, **$P<0.01$). In collaboration with MSc student Gabriella Sammut Demarco.

5.2.10   Inflammatory response in the fetal membranes following vaginal infection with *Ureaplasma parvum*

Proinflammatory cytokine gene expression in the fetal membranes

Infection with *U. parvum* but not damage with N-9 was a statistically significant source of variation in the expression of *Tnfa* (P<0.0001 for proximal, P=0.0006 for distal)*, Il1b* (P<0.0001 for proximal, P=0.0134 for distal)*, Cxcl1* (P<0.0001 for proximal, P=0.0455 for distal) *and Cxcl2* (P<0.0001 for proximal, P=0.0001 for distal) both at the proximal and at the distal site. No interaction between the two independent variables was detected. No differences were found for *Il-6*.At the proximal site of the membranes, the genes *TNFa, Il1b, Cxcl1*and *Cxcl2* were significantly upregulated in the two groups infected with *U. parvum* (N-9+UP, PBS+UP) compared to the vehicle-treated group (PBS+USM). For the N-9+UP group, *TNFa* expression increased by 15.69±3.51-fold, *Il1b* increased 13.38±3.15-fold, *Cxcl1* increased 6.49±1.77-fold and *Cxcl2* increased 63.6±12.51-fold. For the PBS+UP group, *TNFa* expression increased by 14.67±7.99-fold, *Il1b* increased 10.98±3.97-fold, *Cxcl1* increased 5.48±1.35-fold and *Cxcl-2* increased 59.73±32.43-fold. No differences were found for the group that received N-9 but not *U. parvum* (N-9+USM). All changes can be seen in **Table 5-6** and **Fig 5.14**.

At the distal site, the genes *Cxcl2* was significantly upregulated in the two groups infected with *U. parvum* (N-9+UP, PBS+UP) compared to the vehicle-treated group (PBS+USM) and *Tnfa* and *Il1b* were upregulated only in the N-9+UP group. For the N-9+UP group, *TNFa* expression increased by 8.92±3.28-fold, *Il1b* increased 8.6±3.25-fold and *Cxcl-2* increased 28.21±12.67-fold. For the PBS+UP group, *Cxcl-2* increased 6.52±2.15-fold. No differences were found for the group that received N-9 but not *U. parvum* (N-9+USM). All changes can be seen in **Table 5-6** and **Fig 5.14**.

Although a trend difference was noticed when comparing the site effect, this only reached significance in the case of *Cxcl2* for the N-9+UP group (**Fig 5.14**).

A significant correlation was noticed between the copy number of the *Urease C* gene derived from *U. parvum* and the increase in the expression of *Tnfa* (r=0.84, P<0.0001), *Il1b* (r=0.78, P<0.0001), *Cxcl1* (r=0.70, P<0.0001), *Cxcl2* (r=0.87, P<0.0001) and *Il6* (r=0.39, P=0.0059).

Table 5-6 Inflammatory cytokine gene changes in the fetal membranes after vaginal administration of *Ureaplasma parvum* preceded by cervical damage or control treatments (*P<0.05, **P<0.01, ***P<0.001, ****P<0.0001).

	N-9+USM		PBS+UP		N-9+UP	
	Fold change relative to PBS+USM					
	Proximal	Distal	Proximal	Distal	Proximal	Distal
Tnfa	1.09	1.29	14.67***	3.33	15.69****	8.92**
Il1b	0.67	1.35	10.98***	2.93	13.38****	8.6*
Cxcl1	0.94	2.59	5.48**	7.64	6.49***	13.96
Cxcl2	0.79	1.6	59.73****	6.52*	63.6****	28.21***
Il6	1.20	1.26	1.75	1.61	1.71	1.52

The effect of cervical epithelial damage on ascending infection and preterm birth 204
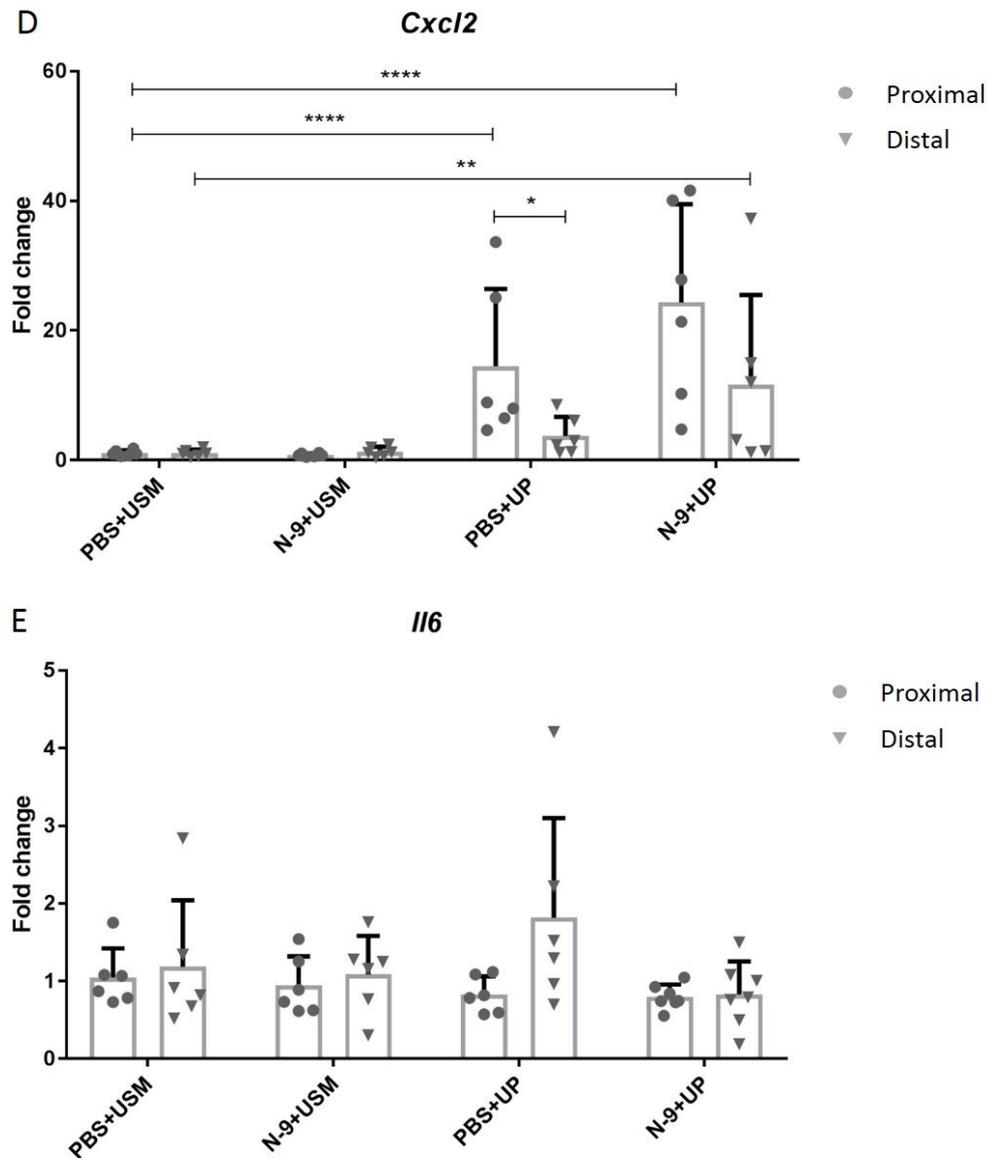
A **Tnfa**

B **Il1b**

C **Cxcl1**
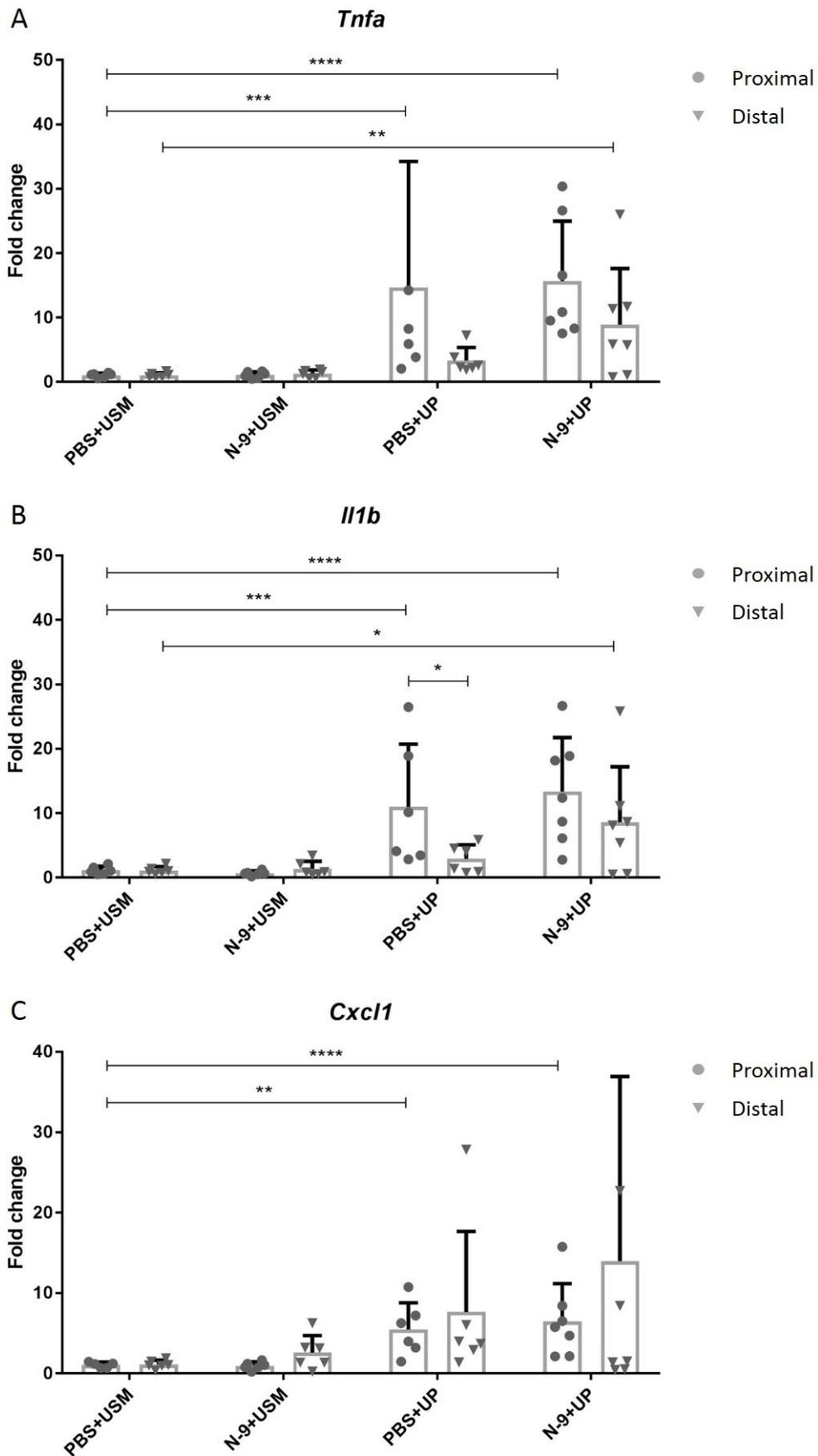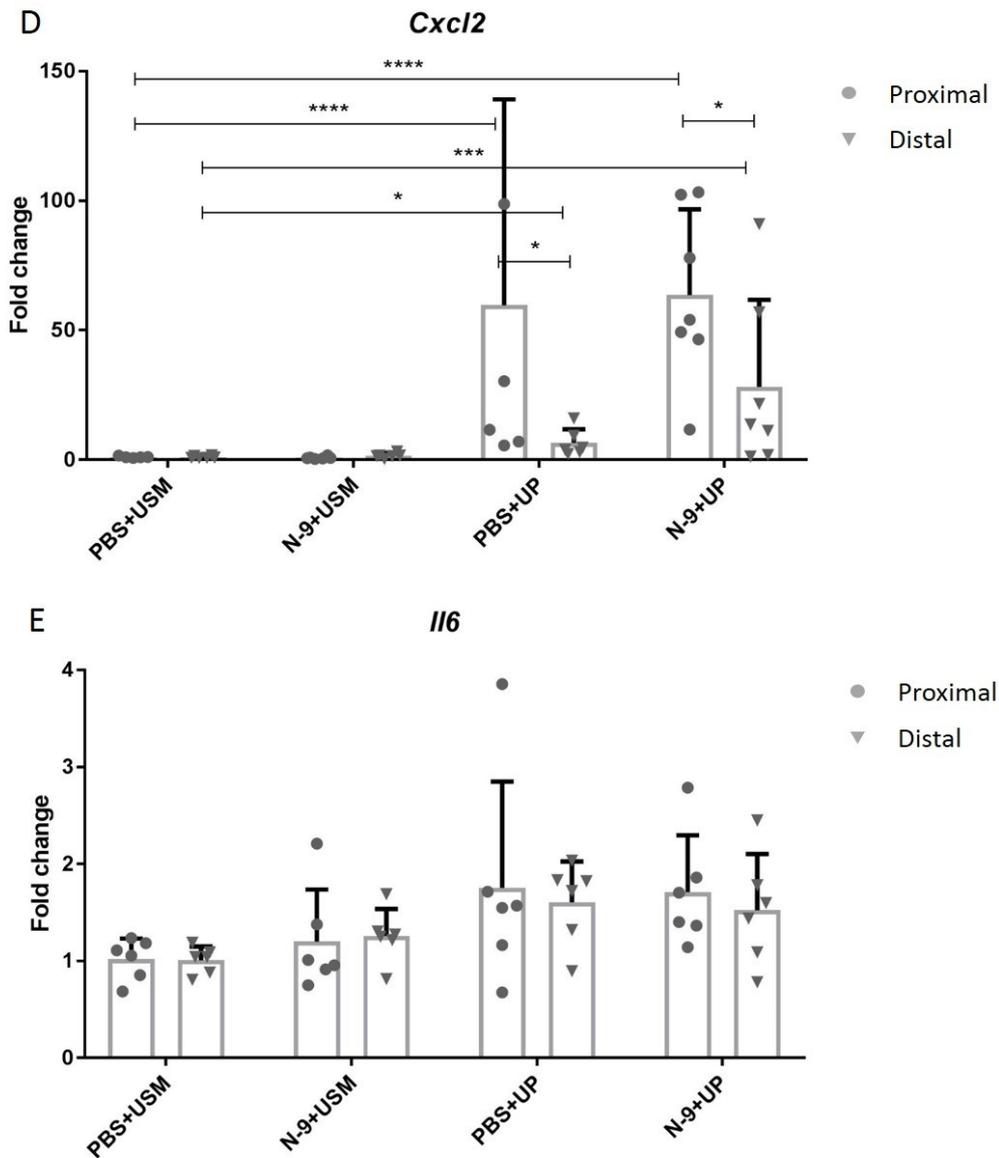
Figure 5.14 ***Ureaplasma parvum* infection causes significant upregulation of proinflammatory genes in the fetal membranes of pregnant mice.** In the afternoon of D16 of gestation, mice received either 10% N-9 in PBS or PBS control via intravaginal inoculation. 16 h later, in the morning of D17 of gestation, mice received either *Ureaplasma parvum* (UP) in Ureaplasma Selective Medium (USM) or USM control via intravaginal inoculation. Tissues were collected 48 h later and analysed using RT-qPCR. Mice that were infected had an increase in the mRNA levels of *Tnfa* (**A**)*, Il1b* (**B**)*, Cxcl1* (**C**) and *Cxcl2* (**D**) compared to vehicle-treated controls. The effect

was stronger at the proximal site. Error bars indicate *SD*. Statistical significance of the treatment effect was assessed using 2-way ANOVA with *post hoc* Dunnett's multiple comparisons test on the DDCt values against the PBS+USM group for the proximal and distal site. Statistical significance for the site effect was assessed unpaired *t*-test for Proximal *vs* Distal for each treatment group. (*P<0.05, **P<0.01, ***P<0.001, ****P<0.0001). In collaboration with MSc student Gabriella Sammut Demarco.

Toll-like receptor gene expression in the fetal membranes

Infection with *U. parvum* but not damage with N-9 was a statistically significant source of variation in the expression of *Tlr2* (P<0.0001 for proximal, P=0.0078 for distal). No interaction between the two independent variables was detected. No differences were found for *Tlr1*, *Tlr6* and *Tlr9*.

At the proximal site, *Tlr2* was significantly upregulated in the two groups infected with *U. parvum* (N-9+UP, PBS+UP) compared to the vehicle-treated group (PBS+USM). *Tlr1* and *Tlr6* were only upregulated in the N-9+UP group. For the N-9+UP group, *Tlr1* expression increased by 2.14±0.5-fold, *Tlr2* expression increased by 5.25±1.03-fold and *Tlr6* expression increased by 1.74±0.13-fold. For the PBS+UP group, *Tlr2* expression increased by 2.91±0.65-fold. Levels of the other TLRs did not change. No differences were found for the group that received N-9 but not *U. parvum* (N-9+USM). All changes can be seen in **Table 5-7** and **Fig 5.15**.

At the distal site, *Tlr2* was significantly upregulated only in the group infected with *U. parvum* and preceded by cervical damage (N-9+UP) compared to the vehicle-treated group (PBS+USM). In this case, *Tlr2* expression increased by 3.52±0.88-fold. Levels of the other TLRs did not change. No differences were found for the group that received N-9 but not *U. parvum* (N-9+USM) or *U. parvum* but not N-9. All changes can be seen in **Table 5-7** and **Fig 5.15**.

No differences were detected between the proximal and the distal site (**Fig 5.15**).

The effect of cervical epithelial damage on ascending infection and preterm birth 207

A significant correlation was noticed between the copy number of the *Urease C* gene derived from *U. parvum* and the increase in the expression of *Tlr1* (r=0.34, P=0.0153)*, Tlr2* (r=0.69, P<0.0001) and *Tlr6* (r=0.36, P=0.0108).

Table 5-7 TLR gene changes in the fetal membranes after vaginal administration of *Ureaplasma parvum* preceded by cervical damage or control treatments (*P<0.05, **P<0.01, ****P<0.0001).

	N-9+USM		PBS+UP		N-9+UP	
	Fold change relative to PBS+USM					
	Proximal	Distal	Proximal	Distal	Proximal	Distal
Tlr1	1.01	1.39	0.98	1.64	2.14*	1.63
Tlr2	1.52	1.75	2.91**	2.03	5.25****	3.52**
Tlr6	1.04	1.33	1.38	1.35	1.74*	1.54
Tlr9	0.91	1.11	0.72	0.98	1.58	1.21

The effect of cervical epithelial damage on ascending infection and preterm birth 208

A *Tlr1*

B *Tlr2*

C *Tlr6*
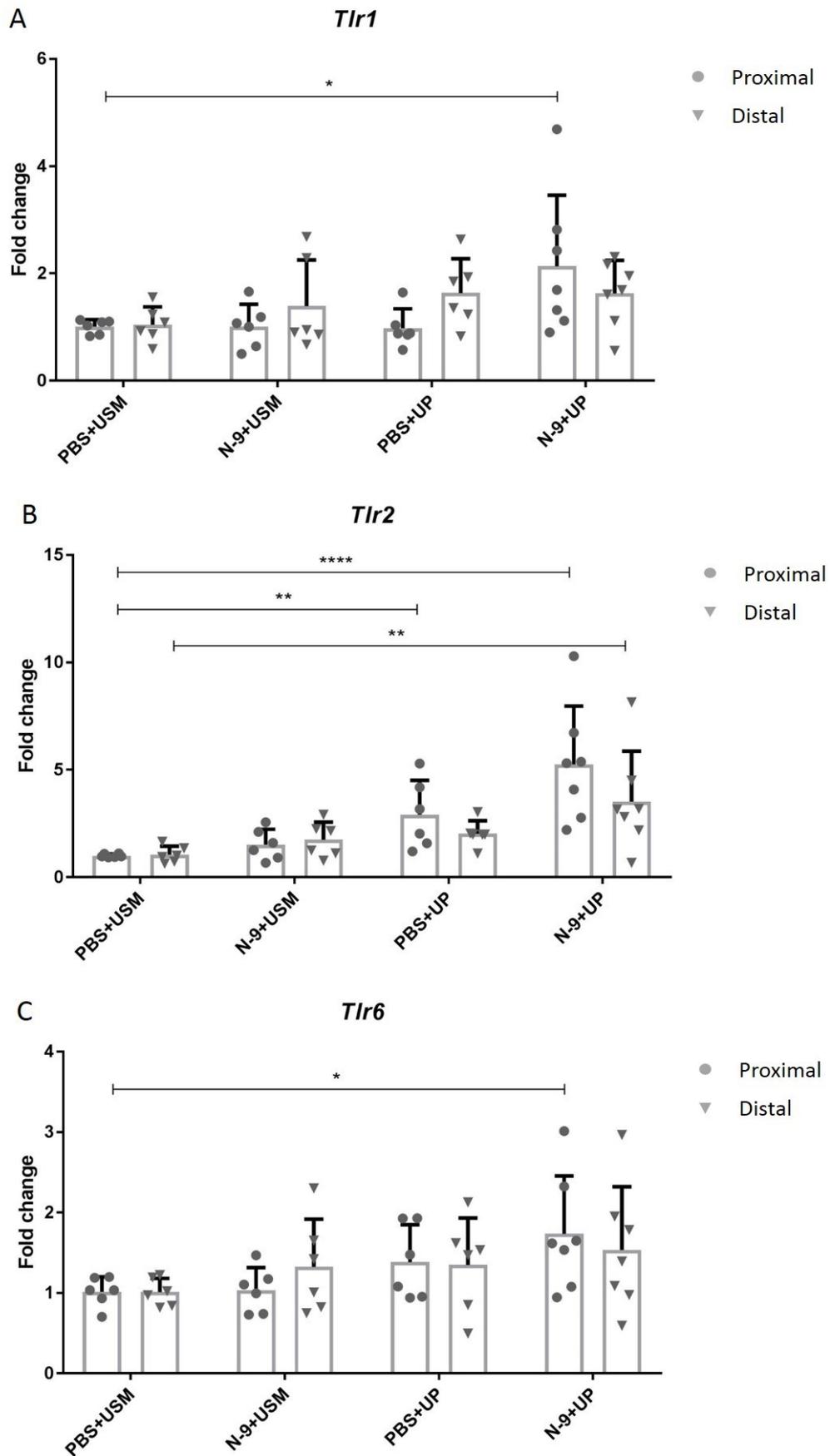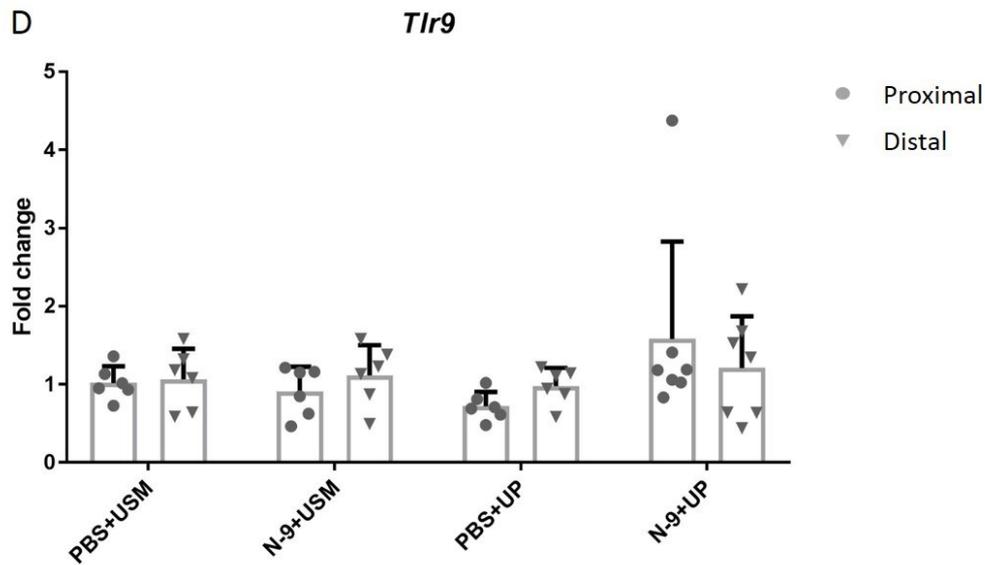
Figure 5.15 *Ureaplasma parvum* **infection causes significant upregulation of TLR2 gene expression in the fetal membranes of pregnant mice.** In the afternoon of D16 of gestation, mice received either 10% N-9 in PBS or PBS control via intravaginal inoculation. 16 h later, in the morning of D17 of gestation, mice received either *Ureaplasma parvum* (UP) in Ureaplasma Selective Medium (USM) or USM control via intravaginal inoculation. Tissues were collected 48 h later and analysed using RT-qPCR. Mice that were infected had an increase in the mRNA levels of *Tlr2* (**B**) and those that were pre-treated with N-9 followed by *U. parvum* also had an increase in *Tlr1* (**A**) and *Tlr6* (**C**) mRNA at the proximal site compared to vehicle-treated controls. There was no site effect. Error bars indicate *SD*. Statistical significance of the treatment effect was assessed using 2-way ANOVA with *post hoc* Dunnett's multiple comparisons test on the DDCt values against the PBS+USM group for the proximal and distal site. Statistical significance for the site effect was assessed unpaired *t*-test for Proximal *vs* Distal for each treatment group. (*P<0.05, ***P<0.001, ****P<0.0001). In collaboration with MSc student Gabriella Sammut Demarco.

5.2.11 Inflammatory gene response in the fetal lung following vaginal infection with *Ureaplasma parvum*

Proinflammatory cytokine gene expression in the fetal lung

In the fetal lung, no change was noticed in the gene expression of any of the above-mentioned cytokines with any of the treatments. Fold changes can be seen in **Table 5-8** and **Fig 5.16**.

The gene copy number of *Urease C* did not correlate with changes in the relative expression of any of the proinflammatory genes.

Table 5-8 Inflammatory cytokine gene changes in the placenta after vaginal administration of *Ureaplasma parvum* preceded by cervical damage or control treatments.

	N-9+USM		PBS+UP		N-9+UP	
	Fold change relative to PBS+USM					
	Proximal	Distal	Proximal	Distal	Proximal	Distal
Tnfa	1.28	1.05	1.04	0.89	1.13	0.74
Il1b	1.26	0.78	1.59	0.82	1.85	0.7
Cxcl1	0.73	0.81	1.07	1.03	0.76	0.79
Cxcl2	1.07	1.33	2.98	1.31	2.59	1.14
Il6	0.71	1.03	0.69	1.33	0.77	1.33

A

Tnfa

B

Il1b

C

Cxcl1

The effect of cervical epithelial damage on ascending infection and preterm birth 212
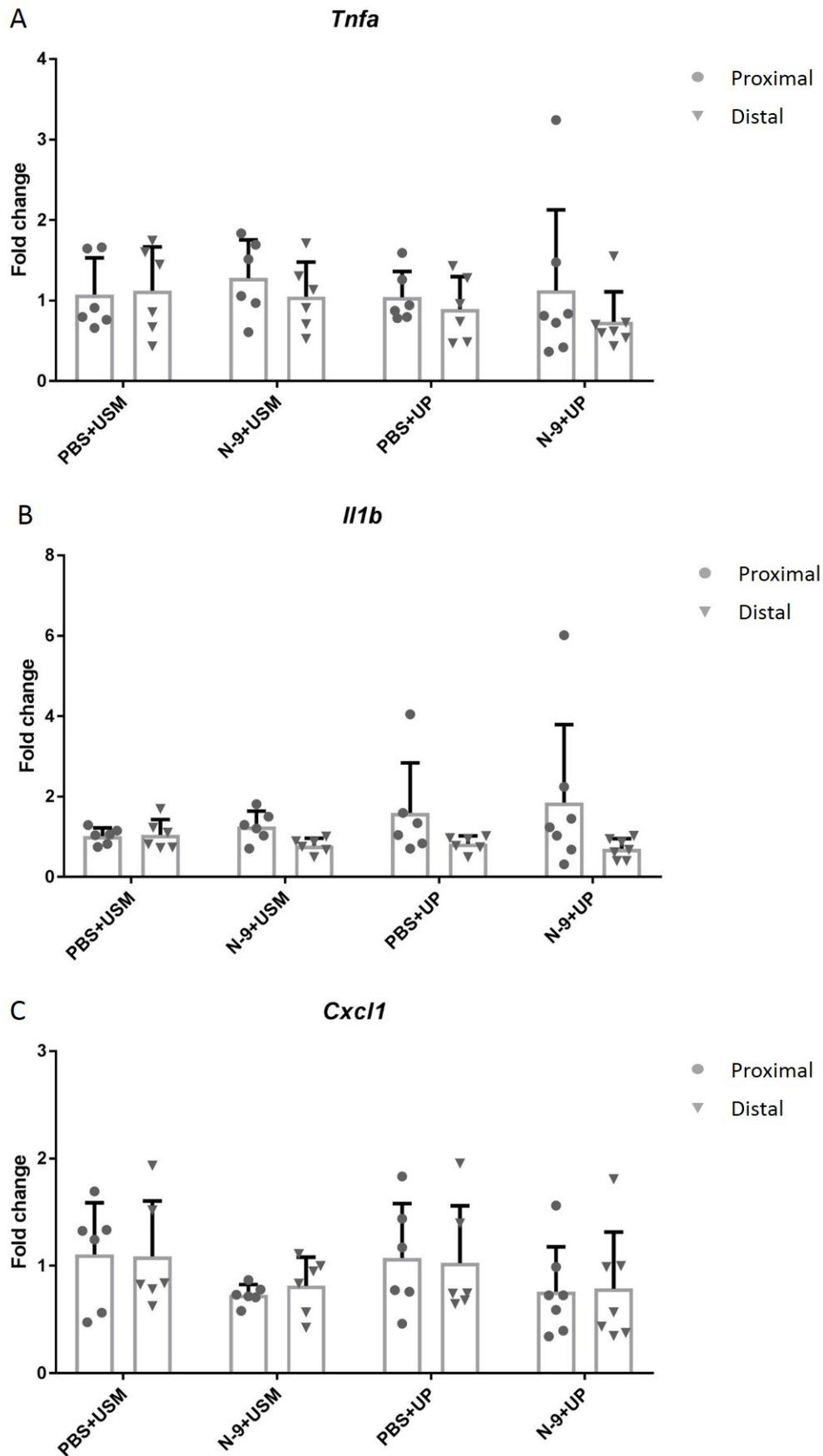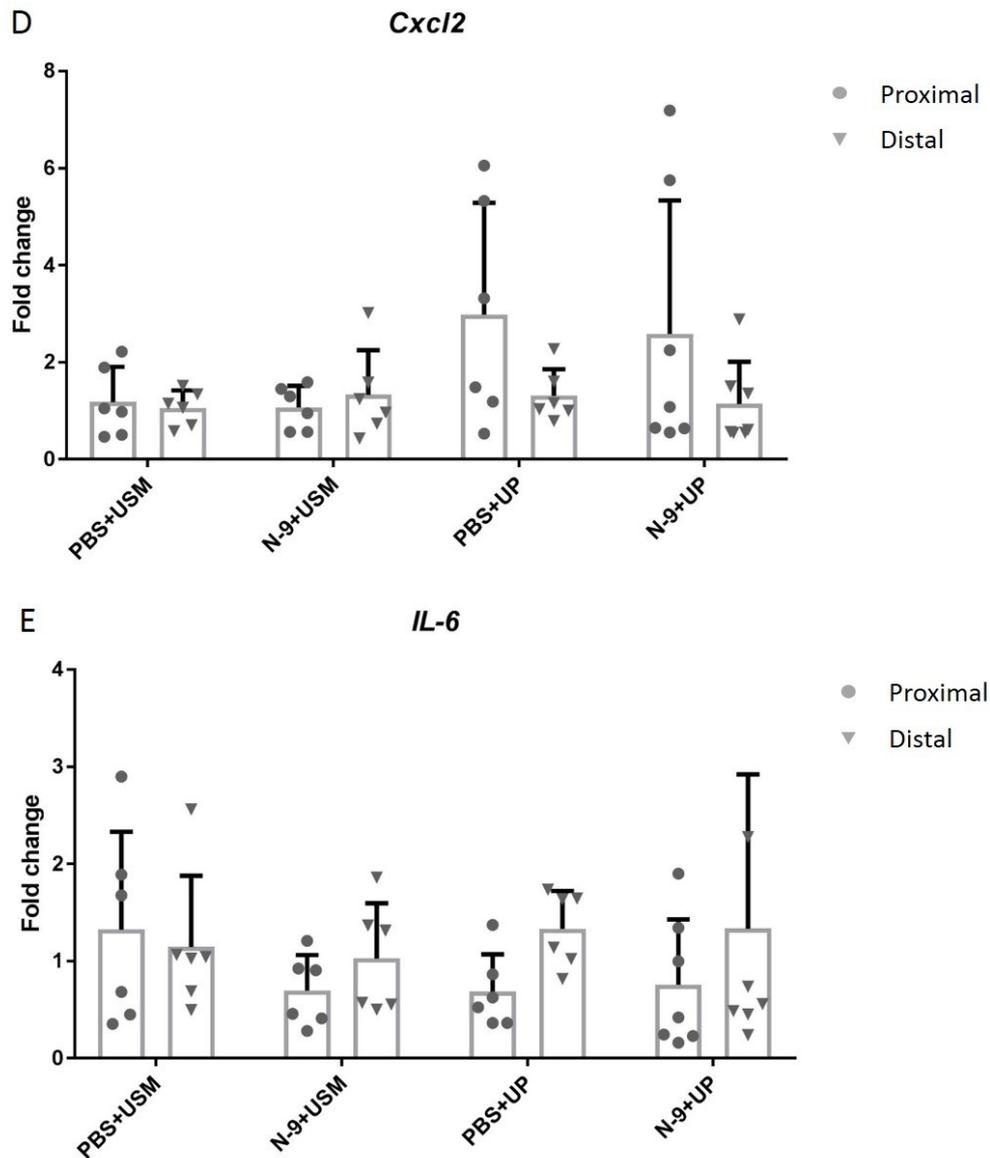
Figure 5.16 *Ureaplasma parvum* infection does not affect the expression of proinflammatory genes in the fetal lung. In the afternoon of D16 of gestation, mice received either 10% N-9 in PBS or PBS control via intravaginal inoculation. 16 h later, in the morning of D17 of gestation, mice received either *Ureaplasma parvum* (UP) in Ureaplasma Selective Medium (USM) or USM control via intravaginal inoculation. Tissues were collected 48 h later and analysed using RT-qPCR. No changes were detected between the different treatments. Error bars indicate *SD*. Statistical significance of the treatment effect was assessed using 2-way ANOVA for the

The effect of cervical epithelial damage on ascending infection and preterm birth 213

proximal and distal site. Statistical significance for the site effect was assessed unpaired *t*-test for Proximal *vs* Distal for each treatment group. (*P<0.05, **P<0.01, ***P<0.001, ****P<0.0001). In collaboration with MSc student Gabriella Sammut Demarco.

As no change was found in the gene expression of proinflammatory cytokines in the fetal lung, gene expression analysis was not performed for TLRs in this tissue.

5.2.12 Correlations between the three methods that demonstrate *Ureaplasma parvum* ascension to the upper reproductive tract

In this chapter we used three different methods to study whether vaginally administered *U. parvum* can ascend to the uterus and whether this is facilitated by prior cervical epithelial damage with N-9. Specifically, 24h hours after *U. parvum* administration, mice that were still pregnant underwent *in vivo* bioluminescence imaging. The following day, 48 hours after *U. parvum* administration, amniotic fluid was cultured for the presence of *U. parvum* and gestational tissues were analysed for gene expression of the *U. parvum*-derived gene, *Urease C.*

A statistically significant moderate correlation was found between the levels of bioluminescence and the amniotic fluid titres the following day (r=0.59, P<0.0001). A further statistically significant strong correlation was found between the levels of bioluminescence and the gene expression of *UreC* in the fetal membranes only (r=0.67, P<0.0001).

The amniotic fluid titres also showed statistically significant moderate correlations with *UreC* gene expression in the fetal membranes (r=0.55, P<0.0001) and the placenta (r=0.47, P=0.0005).

5.3 Discussion

The epithelium is the first line of defence against infectious agents and the cervical epithelium is crucial for the barrier function of the cervix during pregnancy. As cervical epithelial damage has been associated with preterm birth and ascending infection is widely considered as the most common cause of PTB, we hypothesised that cervical epithelial damage predisposes to ascending infection. In the previous chapter we developed and characterised a mouse model of cervical damage during pregnancy using N-9. Here, we utilised this model to address our hypothesis. Since the dose of 10% v/v was consistently shown to cause more significant damage in the cervix compared to the other doses as assessed by our scoring systems, this was the dose of choice for all subsequent experiments. We found that N-9-induced cervical epithelial damage facilitated ascending infection with *Ureaplasma parvum*, leading to increased PTB rates.

First, we examined whether N-9 could facilitate preterm birth induced by vaginally administered LPS. After administering a formulation containing both N-9 and LPS intravaginally, we found the combination treatment to have no effect on the timing of delivery or pup survival. There was also no effect on timing of delivery or pup survival when each of N-9 or LPS were administered alone. In all these experiments, we used the O111:B4 LPS, which is shown to be the most rapid inducer of PTB when administered intrauterine compared to other commonly used serotypes (403). LPS O55:B5 was reported to induce preterm birth when administered intravaginally (365). However, our group did not manage to reproduce this finding. This was also the case for LPS O111:B4 (170). Our results for LPS alone in the current experiments are in line with our previous findings, although they contradict Gonzalez *et al* (365). In addition, our data from the previous chapter that 10% N-9 alone does not induce PTB were successfully replicated here. Our group has previously used as high as 250 μg LPS intravaginally (170). In this case, we used 100 μg LPS, as the potential additive inflammatory effect of N-9 was taken into account. Failure of the co-administration scheme to cause PTB could potentially be due to the fact that by the time N-9 has

The effect of cervical epithelial damage on ascending infection and preterm birth 215

caused substantial epithelial damage, LPS might have already be metabolised to non-toxic levels.

To this end, we pre-treated the mice with N-9 16 hours before LPS administration to examine whether the inflammatory effect of LPS could benefit by being exerted on the ground of an already damaged cervix. Since mice in the previous experiments of co-administration of N-9 and LPS showed no adverse effects, the LPS dose used in this case was very high at 1mg. Still, we found no effect on timing of delivery. The effect on pup survival was again not significant. However, we noticed that there were three mice that demonstrated 100% fetal demise despite delivering at term. This could potentially indicate that the combination of N-9 followed by LPS does initiate an inflammatory response that can propagate to reach the intrauterine compartment. In certain cases, this effect can be potent in inducing fetal death but is still not strong enough to prematurely initiate the labour cascade and this is why these mice deliver at term.

Overall, N-9-induced cervical damage does not appear to promote cervicovaginal inflammation to an extent sufficient enough to induce preterm birth. For the next set of experiments, we investigated its potential to facilitate ascending infection with live *Ureaplasma parvum* bacteria.

To compare the susceptibility of cervical epithelial cells and *U. parvum* to N-9 cytotoxicity, we determined the minimum N-9 dose that resulted in 0% cell viability and completely inhibited bacterial growth respectively. We found N-9 to be much more cytotoxic against endocervical cells than against *U. parvum*. Specifically, the minimum N-9 dose was 128 µg/ml for *U. parvum* while only 32 µg/ml for End1/E6E7 cells after 48 hours incubation time. Similarly, Krebs *et al.* found cervical HeLa cells to be more susceptible to N-9 toxicity compared to HIV virions by a factor of 8 (445). Human lymphocytes were also shown to be more susceptible than HIV virions (446).

Our experimental design had N-9 administered 16 hours before *U. parvum*. When applied in the vagina as an aqueous solution in saline as in our case, the majority of N-9 is absorbed by the cervicovaginal wall within 3-4 hours (447). This means that in

The effect of cervical epithelial damage on ascending infection and preterm birth 216

our experiment, N-9 would first induce cervical damage. Then, by the time of *U. parvum* administration, N-9 would be completely absorbed and thus it would be very unlikely for it to inactivate the bacteria.

Using *in vivo* bioluminescence imaging we found that mice pre-treated with N-9 had a significantly higher BLI signal in their upper reproductive tracts 24 hours after vaginal administration of our NanoLuc-expressing *U. parvum* compared to the ones pre-treated with vehicle control. This finding is supportive of our hypothesis that cervical damage predisposes to ascending infection. Roberts *et al.* also found that N-9 can facilitate a viral infection with HPV16 in non-pregnant mice by disrupting the cervicovaginal epithelium (448). The fact that cervical epithelial damage predisposes to ascending infection with the most clinically relevant bacteria suggests a potential mechanism underlying the higher PTB incidence among women that have undergone excisional treatments of the cervix.

To provide further proof that cervical damage facilitates ascending infection in our model, we quantified the *U. parvum* titres in the amniotic fluid of mice 48 hours after vaginal inoculation. We found *U. parvum* titres to be significantly higher in mice that were pre-treated with N-9 compared to PBS pre-treated controls. This was the case both at a proximal and at a distal site to the cervix. This finding is in agreement with our imaging results and has significant translational importance as it shows that the fetus can also get exposed to infection since it swallows the amniotic fluid. In addition, by culturing the amniotic fluid we identify bacteria that are capable of growing and are therefore able to establish an active infection.

Moreover, we detected significantly higher levels of mRNA expression of the *U. parvum* gene *Urease C* both in the fetal membranes and the placenta at the proximal site of mice pre-treated with N-9 using qPCR. The effect was similar at the distal site as well, although it did not manage to reach statistical significance. Higher levels of *UreC* were also found in the uterus of pre-treated mice, despite the results not being statistically significant. The *UreC* copy number in the uterus was lower than that of the fetal membranes or the placenta. As the whole part of the uterus surrounding each

mouse was analysed, it is likely that levels are artificially low since that majority of the bacteria would probably colonise the decidua. Racicot *et al.* also used qPCR to show that the other *Ureaplasma* species, *U. urealyticum* can ascend to the uterus after vaginal administration and this effect is aided by a viral infection (286).

Furthermore, when examining the preterm birth incidence among mice that had only cervical damage, only infection with *U. parvum*, or both, we found that only the last group had significantly higher PTB rates compared to the group that only received vehicle treatments. This finding highlights the importance of a healthy cervical epithelium for a safe pregnancy outcome. It is also in agreement with a study from Akgul *et al.* which found that inappropriate differentiation of the cervical epithelium increases the risk of PTB induced by an ascending infection with *E. coli* (280). A viral infection of the cervical epithelium was also shown to increase PTB rates after *E. coli* administration (449). The preterm birth incidence in these studies was higher compared to what we found. This is not unexpected as *E. coli* is a much more virulent bacterium than *U. parvum*. Also, the PTB rate of 28% that we found is consistent with the finding that vaginal colonisation with *U. parvum* is an independent risk factor for PTB in humans (237).

Since *U. parvum* does ascend to the upper reproductive tract and can increase the PTB rates, we examined its potential to stimulate an inflammatory response in fetomaternal tissues after vaginal administration using qPCR. We found the gene expression of the cytokines *Tnfa* and *Il1b* and the chemokines *Cxcl1* and *Cxcl2* to be significantly upregulated in the placenta, uterus and fetal membranes of the groups of mice infected with *U. parvum*. *Tnfa* and *Il1b* were shown to be upregulated in mouse peritoneal macrophages that were treated with *U. parvum*-derived lipoproteins, such as MBA (225). They also demonstrated a slight upregulation *in vivo,* in the placentas of mice where *U. parvum* was administered intrauterine after laparotomy (256). These findings are in agreement with a study from von Chamier *et al.* that reported a mild chorioamnionitis after intrauterine administration of *U. parvum* (222). Importantly, we found medium to strong correlations in the increases of these cytokines and chemokines with the copy number of *UreC* produced by *U. parvum* in all three of the

tissues. This further supports a causal role for *U. parvum* in this inflammatory response. Collectively, the gene expression changes observed after vaginal *U. parvum* administration are compatible with an inflammatory pre-labour phenotype. Of note, these experiments were conducted in mice that did not deliver during the 48-hour preterm birth window and were thus deemed term. Consequently, the levels of changes caused by *U. parvum* in these cases were not sufficient to cause PTB.

Trend differences in the expression levels were also identified in mice pre-treated with N-9 compared to those pre-treated with vehicle control. These are reflective of the higher titres of *U. parvum* in the tissues of mice pre-treated with N-9, as N-9 was found in our previous experiments to facilitate ascending infection.

Another important finding was that the increase in the expression of the cytokines and chemokines was higher at the proximal site compared to the distal. This further supports the notion of ascending infection. By being closer to the administration point, tissues at the proximal site were colonised potentially earlier than those at the distal site. This could have allowed more time for the bacteria to establish an infection which led to more significant changes in gene expression of proinflammatory molecules as part of the immune response.

To gain further insights as to which pathway was stimulated by *U. parvum* to result in these proinflammatory gene expression changes, we examined the expression of TLRs in those tissues using qPCR. We found a mild but consistent upregulation in the expression of *Tlr2* in all three tissues and a less consistent increase in *Tlr1* and *Tlr6,* mostly in the fetal membranes. Uchida *et al.* have also found that the proinflammatory changes caused by *U. parvum* in macrophages are mediated by TLR2 (225). Another study, however, found no change in the levels of *Tlr2* or *Cd14* (256). In support of our findings, two other studies suggested a key role of TLR2, both in human amniotic cells (224) and in a human kidney cell line (223). Still, we cannot conclude on the role of TLR2 in the inflammatory response stimulated by *U. parvum* based solely on an upregulation in the gene expression. These studies also described a role for TLR6 (224) and TLR1 (223) respectively, something we also noticed, albeit at a lower extent.

Triantafyllou *et al.* implied that TLR9 can also participate in *U. parvum* recognition by internalising the bacterium as a whole (224). We found no changes in the expression of *Tlr9* in any group and there was no correlation between its relative expression and the levels of *UreC*.

Finally, we assessed whether any changes were caused by *U. parvum* in the fetal lung. No differences were found in the expression of any of the cytokines and chemokines that we tested and found to be increased in the other tissues between infected and sham mice. This is in contrast with a study that found an increase in the levels of IL-1b, IL-6 and CXCL-2 in the fetal lungs after intra-amniotic administration of *U. parvum* (411). This study however was performed on CD-1 mice. While CD-1 fetuses have been shown to be susceptible to *U. parvum* infection, the foetuses of the C57Bl/6 strain that we used are considered to be resistant (222). This was in line with our findings. Given the high *U. parvum* titres that we found in the amniotic fluid, we expected high copy numbers of *UreC* to be found in the fetal lung as the fetuses swallow the amniotic fluid. However, we only found very low copy numbers at levels barely detectable. This was also the finding of von Charmier *et al.* who only detected the bacteria in the intestinal lumen and not the lungs (222). Therefore, *U. parvum* cannot establish an infection at the fetal lungs, something explaining the unchanged levels of the expression of proinflammatory cytokines in our model.

In summary, using our mouse model of cervical damage during pregnancy we provide strong evidence that N-9-induced epithelial damage facilitates ascending infection with *U. parvum*. This leads to increased preterm birth rates. We also report that *U. parvum* can induce an inflammatory response in fetomaternal tissues with increased expression of proinflammatory cytokines and chemokines.

Chapter 6   General Discussion

6.1 Main findings

The cervix is key in protecting pregnancy from ascending infections that can cause preterm birth. The cervical epithelium, in particular, is a major contributor to the physical and functional barrier of the cervix to infection (282). Excisional procedures that damage the cervix by removing part of the epithelium and the underlying stroma have been associated with PTB, but no explanation of this association has been proposed (304) (305). The overarching hypothesis of this thesis is that cervical epithelial injury predisposes to ascending infection. To address this hypothesis we used the surfactant N-9 as an inducer of epithelial damage. N-9 has been shown to cause epithelial damage in the lower reproductive tract of non-pregnant animals and in humans (391) (392) (386) (387) (450) (388). The aims that we set were to: i) investigate the effect of N-9 on cervical epithelial cells *in vitro*, ii) to generate and characterise a mouse model of cervical epithelial damage during pregnancy using N-9 and ii) to investigate the effect of cervical epithelial damage on ascending infection and preterm delivery.

The main findings are summarised below:

- N-9 is cytotoxic against cervical epithelial cells *in vitro* in a dose-dependent manner. Low doses (less than 10 μg/ml) do not have a strong effect, resulting in less than 20% cytotoxicity within 24 hours. High doses (more than 100 μg/ml) rapidly exert 100% cytotoxicity. The effect of the intermediate doses is also time-dependent with cytotoxicity increasing with longer incubation times. At 32 and 64 μg/ml, N-9 cytotoxicity increases from 20% and 30% at 30 minutes respectively, to 90% after 24-hour treatments.

- N-9 compromises the physical barrier function of the cervical epithelium *in vitro* by increasing its permeability through direct cell cytotoxicity.

- N-9 does not affect the ability of cervical epithelial cells to secrete proinflammatory cytokines basally or after LPS stimulation.

- The wound healing capacity of cervical epithelial cells and endometrial stromal cells can be diminished by a concurrent infection with *Ureaplasma urealyticum*.

- N-9 causes cervical epithelial damage in pregnant mice after vaginal administration in late gestation. Features of this damage include severe disruption of the epithelial morphology and infiltrations of polymorphonuclear neutrophils. However, it is not sufficient to cause preterm delivery.

- N-9-induced cervical epithelial damage followed by vaginal administration of high dose of LPS does not cause preterm birth in a mouse model

- N-9-induced cervical epithelial damage facilitates ascending infection with *Ureaplasma parvum*. This is accompanied by an increase in preterm birth rates in a mouse model

- *Ureaplasma parvum* is capable of ascending to the upper reproductive tract and colonise the fetal membranes, the placenta, the uterus and the amniotic fluid. In the first three tissues it can induce an inflammatory response in a mouse model.

6.2 Cervical damage facilitates ascending infection with *Ureaplasma parvum*

We used 3 different methods to identify the presence and quantify the levels of *U. parvum* in the upper reproductive tract. The first was i*n vivo* bioluminescence imaging 24 hours after vaginal administration of the bacteria. The second was by collecting the amniotic fluid 48 hours after administration and then culturing it with Ureaplasma Specific Medium, to detect and quantify a population of actively growing bacteria. The third was by measuring the copy number of the *U. parvum*-derived gene *Urease C* in the fetal membranes, placenta and uterus by qPCR. Previous studies have used PCR (286) or culture-based methods (440) or a combination of the two (261), but this is the first study using three different methods to confirm the presence of *U. parvum*. The use of robust methodoly to address our main question is a strength of the current thesis.

We could detect *U. parvum* in the upper reproductive tract with all three of these methods. Therefore, *U. parvum* can ascend to the uterus during mouse gestation. This is an interesting finding as *Ureaplasmas* are non-motile bacteria. Using *in vivo* imaging, we could determine the presence of *U. parvum* in the upper reproductive tract in some of the mice 24 hours after intravaginal administration. This indicates that *U. parvum* can deploy transport mechanisms that can lead to it ascending in the uterine compartment. These may include the bacteria itself actively moving over epithelial surfaces or passively being moved over. The capacity of other non-motile bacteria such as *Staphylococcus aureus* (451)*, Mycobacterium* spp (452) and a non-motile mutant of *Listeria monocytogenes* (453) to move has also been described. Future studies could investigate potential mechanisms of attachment, detachment and re-attachment by *U. parvum* on epithelial cells. This will help in the design of more effective prevention strategies against pregnancy complications in women colonised by *Ureaplasma* spp.

After quantifying the levels of *U.* parvum, a consistent pattern was identified with all three methods: *U. parvum* was more abundant in the upper reproductive tract of mice that have been pre-treated with N-9. In Chapter 4, we characterised the damage that N-9 causes to the cervical epithelium, which involves significant disturbance and

sloughing. Consequently, these lesions can compromise the barrier function of the cervix to facilitate ascending infection. This finding is supportive of our hypothesis and could represent a potential pathway explaining the increased risk for preterm delivery among women that were treated with excisional procedures.

Different potential mechanisms have been proposed in an effort to explain the epidemiological association between cervical damage-inducing procedures and preterm delivery. These can be broadly divided into three different etiologic factors: impairment of mechanical support (454), decreased protection against infection (455) or both (456). The former is mainly supported by studies reporting that while minimal excisions confer no increased risk of preterm birth, with larger excisions the risk almost doubles (457). The bigger the thickness and the overall volume of cervical tissue excised, the higher the incidence of a subsequent preterm delivery (458). Importantly, this is independent of the interval time between the procedure and conception (457) (459). Current evidence is limited to retrospective cohort studies and as such the validity of these claims is hard to be confirmed. To our knowledge, no studies have been conducted to evaluate whether damage to the cervical epithelium can increase susceptibility to ascending infection.

Our findings support the fact that cervical epithelial injury compromises the barrier function of the cervix to render the uterine content more susceptible to ascending infection with the most clinically relevant bacteria. This suggests a potential mechanism explaining the observation that women with a damaged cervical epithelium are at increased risk for preterm delivery. Our model assesses the effect of the acute phase of cervical epithelial damage characterised by areas of complete epithelial sloughing. As such, the only group of women directly comparable to this scenario would be the ones that conceive very soon after the cervical intervention, a practice that is discouraged by obstetricians. However, our data also have indirect implications for all pregnancies following excisional procedures. A mature cervical epithelium can take up to 7 weeks to cover the affected area (460). This is sufficient time to allow for ascending infection and colonisation of the upper reproductive tract, which can lead to an increased risk of intrauterine infection should a pregnancy occur.

Even after epithelial regeneration, the development of scar tissue has been reported (454). A scarred surface conveying limited protection compared to a healthy epithelium as a result of an excisional treatment could account for an increased risk of ascending infection during pregnancy. Overall, our findings highlight the importance of a healthy epithelium in the protection against microbial invasion.

Apart from the cervical epithelium, the lower reproductive tract has other barriers against infection that could lead to an adverse pregnancy outcome. A beneficial composition of the vaginal microbiome is important in preventing proliferation of potentially pathogenic vaginal microorganisms. A dysbiotic state, as in bacterial vaginosis, has been shown to increase the risk for preterm delivery (461) (462) (463). Another important barrier is the cervical mucus which forms the mucus plug. Mucus from women at high-risk for preterm birth can have altered biophysical properties leading to a reduced capacity to form strong gels (464). It would be interesting for future studies to assess whether disruption of these barriers could also predispose to ascending infection with *Ureaplasma* spp and compare the respective findings with the effect of cervical epithelial damage. This will help for future risk stratification strategies.

6.3 Ascending infection pathway

An interesting observation regarding the pathway of ascending infection can be made when considering the levels of *U. parvum* as assessed by culture and qPCR. At first, bacterial cultures revealed very high titres of *U. parvum* in the amniotic fluid, in a magnitude of about 10^7-10^8 CCU/ml. Next, using qPCR, we found the *UreC* copy number, which is indicative of the *U. parvum* presence, to be higher in the fetal membranes compared to the placenta or the uterus. These apparent higher levels might reflect a pattern that is consistent with the following pathway of ascending infection: From the vagina where it is administered, *U. parvum* passes through the cervix. This is aided by cervical epithelial damage. From there, the bacteria invade the amniotic cavity through a certain region of the fetal membranes. In the amniotic fluid they proliferate rapidly before colonising the fetal membranes and then reaching the

placenta and uterus. This potential pathway of ascending infection was first proposed back in 1961 (465) and is further supported by a human study from Kim *et al* (201). Using qPCR and culture-based methods for general bacterial populations, they found the bacteria to be more abundant on the amniotic fluid than in the fetal membranes (201). Then the genomic DNA copy number was greater in the amnion than in the chorion (201). Thus, bacterial proliferation in the amniotic fluid is likely to precede colonisation of the fetal membranes and subsequent chorioamnionitis. Using detection systems specific for *U. parvum*, we found this to be the case in our study as well. Based on this model of ascending infection, it is likely that *U. parvum* can induce preterm delivery by leading to premature activation and rupture of the fetal membranes. The potential of *U. parvum* to drive PPROM can be studied by assessing its ability to upregulate the expression of prostaglandins and MMPs in the fetal membranes. The other *Ureaplasma* species, *U. urealyticum* was reported to increase the production of PGE$_2$ by human choriodecidual explants *in vitro* (466). In addition, a recent study found that *U. parvum* could stimulate an upregulation in the expression of MMP-9 by both maternal and fetal human monocytes *in vitro* (467). Expanding these findings in an *in vivo* setting will provide further evidence about *U. parvum* pathogenicity with regards to pregnancy complications. The activation status of the MMPs can be examined using zymography. Alternatively, preterm birth induced by *U. parvum* could have premature myometrial contractions as its main feature. Our group has extensive experience using gel contraction assays to examine the pro-contractile potential of different agents. These could be deployed to assess the potency of *U. parvum* as a contraction stimulator.

The much higher *U. parvum* titres in the amniotic fluid compared to the tissues could also be reflective of the composition of the amniotic fluid. The concentration of urea significantly increases in the amniotic fluid during late gestation in the mouse, potentially due to an increase in the fetal urine output (468). *Ureaplasmas* hydrolyse urea to generate virtually 100% of its energy requirements (469). They appear to be the sole bacteria capable of producing ATP via this mechanism. Therefore, the

amniotic fluid late during mouse pregnancy represents an environment that favours the growth of *U. parvum*.

6.4 Inflammatory changes after *Ureaplasma* infection

Inflammatory cytokines are central to the mechanisms of infection/inflammation-induced preterm birth. Levels of several key cytokines and chemokines, such as IL-1b (149), IL-6 (158), IL-8 (161) and TNFa (163) increase in the amniotic fluid after microbial invasion of the amniotic cavity (MIAC) and they can also be used as predictors of intra-amniotic infection (160). In our study, we found *U. parvum* to invade the amniotic cavity after vaginal administration. As the amount of amniotic fluid rapidly decreases during late gestation (470) and our samples were collected on D19, we used all of it for culture-based detection of *U. parvum*. Therefore, we examined the *in situ* gene expression of the cytokines of interest in the fetal membranes, placenta and uterus. We noticed a mild inflammatory response with increases in the gene expression levels of TNFa, IL-1b, CXCL-1 and CXCL-2 correlating with the gene copy number of the *U. parvum*-derived gene *Urease C* in the respective tissues. Previous studies using intrauterine administration of *U. parvum* have reported similar results (222) (256) (225). *In vitro* stimulation of human monocytes by *U. parvum* was also found to cause an increased expression of TNFa, IL-1b and IL-8, the human ortholog of CXCL-1 and CXCL-2 (471). Importantly, our experiments were conducted in term mice, as they had not delivered by the morning of D19 and consequently their tissues were available antenatally. Given the strong correlation between the levels of *U. parvum* and the increase in inflammatory gene expression in these tissues, it can be postulated that in mice that did deliver preterm, higher bacterial levels in the reproductive tissues resulted in a stronger inflammatory response that was potent in inducing preterm delivery. This could be the pathway of *U. parvum*-induced PTB, as these cytokines are known stimulators of the labour-associated prostaglandins E_2 and F_{2a} and their synthesising enzyme COX-2 (181) (174) (175). They can also induce several MMPs (186) (188). Nevertheless, this hypothesis is not backed up by our *in vivo* imaging data as there was no difference in the levels of bioluminescence of mice that ended up delivering preterm compared to those that

delivered at term. However, BLI imaging was performed on D18 so these results are not directly comparable to the qPCR and culture results from D19.

Importantly, by using qPCR, we assessed changes at the gene expression level. This does not necessarily mean that there is an inflammatory response in those tissues. Further studies are required to determine changes of the above-mentioned cytokines at the protein level. This will validate our findings and solidify the role of *U. parvum* as a trigger for preterm birth. In addition, future studies could also assess whether immune cells are recruited in the reproductive tissues after infection with *U. parvum* and determine their activation status. This will provide further information regarding the magnitude of the inflammatory response induced by *U. parvum* in the reproductive tissues and will be important for designing potential etiological treatment strategies.

6.5 Pathway of *Ureaplasma*-induced inflammation

Since we found *U. parvum* to increase the expression of proinflammatory cytokines and chemokines, we sought to identify Pathogen Recognition Receptors (PRRs) that are involved in triggering this response. Using qPCR, we found a significant upregulation in TLR2 gene expression across all tissues where an inflammatory response has been observed, namely the fetal membranes, placenta and uterus. Trend increases were also noticed in the gene expression of TLR1 and TLR6, more so in the fetal membranes. This findings are in agreement with a previous study in mice identifying TLR2 as the receptor activated by MBA (225), the *Ureaplasma* main virulence factor. In addition, studies in human cell lines suggested that TLR1/TL2 (223) and TLR2/TLR6 (224) dimers are involved in the cytokine responses stimulated by *U. parvum*. Activation of TLR2 in mouse macrophages has been shown to elicit a mild inflammatory response (472). This is consistent with our findings that do not represent a robust inflammatory reaction. It is also consistent with the pregnancy outcome in these mice, as none of them delivered preterm.

However, our findings on TLR2 expression are at the gene expression level. Further studies evaluating changes at the protein level are needed to evaluate the role of this receptor in the *Ureaplasma*-induced inflammation in the reproductive tissues during

pregnancy. Future experiments using TLR2 KO mice could identify whether this receptor is necessary for the induction of an inflammatory response by *U. parvum*.

At a molecular level, the key transcriptional events leading to the increased expression of cytokines after *U. parvum* infection should also be assessed. Previous studies have demonstrated that *U. parvum*-derived products can lead to increased cytokine secretion by activating the NFκB pathway via TLR2 (225). NFκB is an important regulator of the inflammatory and pro-contractile pathways leading to preterm birth (473). In addition, the transcription factor Activator ptotein-1 (AP-1) has also been suggested as a key driver of the inflammatory events preceding the onset of labour and a sufficient inducer of preterm labour (474). It would be interesting for future studies to assess whether an infection with *U. parvum* could also activate AP-1 during pregnancy to stimulate the expression of labour-associated genes. Phosphorylation of the AP-1 sub-unit c-Jun results to activation and nuclear translocation of the complex (475). Measuring the levels and localisation of phosphorylated c-Jun after *U. parvum* infection in the uterus by Western blot and immunofluorescence will provide an indication on the activation status of this transcription factor. Chromatin immunoprecipitation (ChIP) in combination with high-throughput sequencing will allow the identification of specific genes (476) stimulated by these transcription factors during pregnancy in relation to *U. parvum* infection. This will help identify potential targets for therapeutic interventions.

6.6 *Ureaplasma* virulence

As we identified that *U. parvum* is able to elicit an inflammatory response in reproductive tissues, it is important to determine its specific virulence factors that could contribute to an adverse pregnancy outcome. In our study, we found the gene copy number of *Urease C* to have a strong positive correlation with the increase in the gene expression of TNFa, IL-1b, CXCL-1, CXCL-2 and TLR2 in the fetal membranes, placenta and uterus. A study by Ligon *et al* found that intravenous administration of *Ureaplasmas* can kill mice within 5 min of the injection (477). This lethal effect can be rescued by administering a urease inhibitor (477). In humans, *Ureaplasma*-derived

urease causes increased precipitation of minerals leading to increased formation of urinary struvite stones and urolithiasis (478). During sheep pregnancy, it has been shown to increase the pH of the amniotic fluid due to increased production of ammonia as part of the urea hydrolysis process (479). This can lead to significant damage in the fetal lung (479). Therefore, urease has the potential to cause adverse pregnancy outcomes.

The *Ureaplasma* multiple-banded antigen (MBA) is also considered a major virulence factor of *Ureaplsama spp*. It can stimulate dimers between TLR2 and TLR1 or TLR6 to activate NFκB leading to the production of proinflammatory cytokines (223) (225). Phospholipase A and phospholipase C have also been suggested as virulence factors, as they can cleave and destabilise the cell membrane phospholipids of the host cells (480). Immunoglobulin A (IgA) protease is also pivotal for *Ureaplasma* spp survival and can contribute to the disease pathogenesis by helping the bacteria escape the mucosal immune surveillance (481) (482) (483). Future studies should focus on identifying the relative contribution of these factors to an adverse pregnancy outcome. One way through which this can be achieved is by genetic manipulation of *Ureaplasma* strains that will elucidate a definitive role for its virulence factors by examining the relative pathogenicity of mutant strains. This will determine candidate molecules that could be targeted for preventing and treating infections with *Ureaplasma* spp that could lead to adverse pregnancy outcomes.

6.7 Summary and conclusions

In conclusion, the findings of this thesis highlight the importance of a healthy cervical epithelium for a healthy pregnancy. We confirmed the potential of the surfactant N-9 as a damage-inducing agent capable of compromising the barrier function of the cervical epithelium *in vitro*. We then used N-9 to establish the first mouse model of cervical epithelial damage during pregnancy that has been described. To quantify the extent of damage caused by N-9 in the epithelial surfaces of the lower reproductive tract, we developed a robust epithelial injury scoring system. This model could be broadly used to study the barrier function of the cervical epithelium.

Finally, using this model we showed that cervical epithelial damage predisposes to ascending infection with *Ureaplasma parvum* from the vagina to the uterus. This causes a mild inflammatory response in the upper reproductive tract and increases preterm birth rates among these mice. We provide evidence that the most clinically relevant bacteria for preterm birth in humans are also capable of causing adverse pregnancy outcomes in the mouse. Further studies are needed to decipher the pathogenetic mechanisms of *Ureaplasma* spp-induced preterm delivery. This will have broad implication in the prevention, proper identification of at-risk individuals and treatment of a series of pregnancy complications.

Chapter 7   References

1.   WHO. WHO: recommended definitions, terminology and format for statistical tables related to the perinatal period and use of a new certificate for cause of perinatal deaths. Modifications recommended by FIGO as amended October 14, 1976. Acta Obs Gynecol Scand [Internet]. 1977;56:247–53. Available from: http://dx.doi.org/10.1016/j.jri.2016.11.008

2.   Kramer MS, Papageorghiou A, Culhane J, Bhutta Z, Goldenberg RL, Gravett M, et al. Challenges in defining and classifying the preterm birth syndrome. Am J Obstet Gynecol [Internet]. 2012;206(2):108–12. Available from: http://dx.doi.org/10.1016/j.ajog.2011.10.864

3.   Blencowe H, Cousens S, Oestergaard MZ, Chou D, Moller AB, Narwal R, et al. National, regional, and worldwide estimates of preterm birth rates in the year 2010 with time trends since 1990 for selected countries: A systematic analysis and implications. Lancet [Internet]. 2012;379(9832):2162–72. Available from: http://dx.doi.org/10.1016/S0140-6736(12)60820-4

4.   Blencowe H, Cousens S, Chou D, Oestergaard M, Say L, Moller A-B, et al. Born too soon: the global epidemiology of 15 million preterm births. Reprod Health [Internet]. 2013;10 Suppl 1(Suppl 1):S2. Available from: http://www.pubmedcentral.nih.gov/articlerender.fcgi?artid=3828585&tool=pmcentrez&rendertype=abstract

5.   Beck S, Wojdyla D, Say L, Betran AP, Merialdi M, Requejo JH, et al. The worldwide incidence of preterm birth: A systematic review of maternal mortality and morbidity. Bull World Health Organ. 2010;88(1):31–8.

6.   Berkowitz GS, Blackmore-Prince C, Lapinski RH, Savitz DA. Risk Factors for Preterm Birth Subtypes. Vol. 9, Epidemiology. 1998. p. 279–85.

7.   Savitz DA, Dole N, Herring AH, Kaczor D, Murphy J, Siega-Riz AM, et al. Should spontaneous and medically indicated preterm births be separated for studying aetiology? Paediatr Perinat Epidemiol [Internet]. 2005;19(2):97–105. Available from: http://doi.wiley.com/10.1111/j.1365-3016.2005.00637.x

8.   Schaaf JM, Mol BWJ, Abu-Hanna A, Ravelli ACJ. Trends in preterm birth: Singleton and multiple pregnancies in the Netherlands, 2000-2007. BJOG An Int J Obstet Gynaecol. 2011;118(10):1196–204.

9.   Dunietz GL, Holzman C, McKane P, Li C, Boulet SL, Todem D, et al. Assisted reproductive technology and the risk of preterm birth among

primiparas. Fertil Steril. 2015;103(4):974–9.

10.   Brown MK, DiBlasi RM. Mechanical ventilation of the premature neonate. Respir Care [Internet]. 2011 Sep 1 [cited 2018 Jul 31];56(9):1298-311; discussion 1311-3. Available from: http://www.ncbi.nlm.nih.gov/pubmed/21944682

11.   Morley CJ. Surfactant treatment for premature babies-a review of clinical trials [Internet]. Vol. 66, Archives ofDisease in Childhood. 1991 [cited 2018 Jul 31]. Available from: https://www.ncbi.nlm.nih.gov/pmc/articles/PMC1590295/pdf/archdisch00893-0079.pdf

12.   Soll RF. Surfactant treatment of the very preterm infant. Biol Neonate [Internet]. 1998 Sep [cited 2018 Jul 31];74 Suppl 1(Suppl. 1):35–42. Available from: http://www.ncbi.nlm.nih.gov/pubmed/9730590

13.   Roberts D, Brown J, Medley N, Dalziel S. Antenatal corticosteroids for accelerating fetal lung maturation for women at risk of preterm birth. Cochrane Database Syst Rev. 2017;1(3):1–273.

14.   Gultom E, Doyle LW, Davis P, Dharmalingam A, Bowman E. Changes Over Time in Attitudes to Treatment and Survival Rate for Extremely preterm Infants (23-27 Weeks ' Gestational Age). Aust N Z J Obs Gynaecol. 1997;37(1):56–8.

15.   Doyle LW, Rogerson S, Chuang SL, James M, Bowman ED, Davis PG. Why do preterm infants die in the 1990s? [Internet]. Vol. 170, Med J Aust. 1999. 528-32 p. Available from: http://journals.lww.com/anesthesia-analgesia/toc/publishahead%5Cnhttp://ovidsp.ovid.com/ovidweb.cgi?T=JS&PAGE=reference&D=emed13&NEWS=N&AN=2015227327

16.   Liu L, Oza S, Hogan D, Perin J, Rudan I, Lawn J, et al. Global, regional, and national causes of child mortality in 2000-2010: an updated systematic analysis. Lancet [Internet]. 2012;385(9966):430–40. Available from: http://dx.doi.org/10.1016/S0140-6736(14)61698-6

17.   Costeloe K, Hennessy E, Gibson AT, Marlow N, Wilkinson AR. The EPICure Study: Outcomes to Discharge From Hospital for Infants Born at the Threshold of Viability. Pediatrics [Internet]. 2000 [cited 2018 Jul 31];106(4):659–71. Available from: www.aappublications.org/news

18.   Saigal S, Doyle LW. An overview of mortality and sequelae of preterm birth from infancy to adulthood. Lancet. 2008;371(9608):261–9.

19.   Oken E, Kleinman KP, Rich-Edwards J, Gillman MW. A nearly continuous measure of birth weight for gestational age using a United States national reference. BMC Pediatr [Internet]. 2003 Dec 8 [cited 2018 Jul 31];3(1):6. Available from: http://bmcpediatr.biomedcentral.com/articles/10.1186/1471-

2431-3-6

20.   Fanaroff AA, Stoll BJ, Wright LL, Carlo WA, Ehrenkranz RA, Stark AR, et al. Trends in neonatal morbidity and mortality for very low birthweight infants. Am J Obstet Gynecol. 2007;196(2).

21.   Mathews TJ, MacDorman MF. Infant mortality statistics from the 2005 period linked birth/infant death data set. Natl Vital Stat Rep. 2008;57(2):1–32.

22.   Doyle LW, Faber B, Callanan C, Freezer N, Ford GW, Davis NM. Bronchopulmonary Dysplasia in Very Low Birth Weight Subjects and Lung Function in Late Adolescence. Pediatrics [Internet]. 2006;118(1):108–13. Available from: http://pediatrics.aappublications.org/cgi/doi/10.1542/peds.2005-2522

23.   Doyle LW, Ford G, Davis N. Health and hospitalisations after discharge in extremely low birth weight infants. Semin Neonatol. 2003;8(2):137–45.

24.   Connor ARO, Stephenson T, Johnson A, Tobin MJ, Ed DLIT, Moseley MJ, et al. Long-Term Ophthalmic Outcome of Low Birth Weight Children With and Without Retinopathy of Prematurity. Pediatr Res. 2014;109(1):12–8.

25.   Saigal S, Stoskopf B, Boyle M, Paneth N, Pinelli J, Streiner D, et al. Comparison of Current Health, Functional Limitations, and Health Care Use of Young Adults Who Were Born With Extremely Low Birth Weight and Normal Birth Weight. Pediatrics [Internet]. 2007;119(3):e562–73. Available from: http://pediatrics.aappublications.org/cgi/doi/10.1542/peds.2006-2328

26.   Marlow N, Wolke D, Bracewell M, Samara M. Neurologic and Developmental Disability at Six Years of Age after Extremely Preterm Birth. N Engl J Med [Internet]. 2005;352(1):9–19. Available from: http://scholar.google.com/scholar?hl=en&btnG=Search&q=intitle:New+engla+nd+journal#0

27.   Hofman PL, Regan, FionaJackson W, Jefferies C, Knight DB, Robinson EM, Cutfield WS. Premature birth and insulin resistance. N Engl J Med. 2005;352(9):939-940; author reply 939-940.

28.   Abitbol CL, Rodriguez MM. The long-term renal and cardiovascular consequences of prematurity. Nat Rev Nephrol [Internet]. 2012;8(5):265–74. Available from: http://dx.doi.org/10.1038/nrneph.2012.38

29.   Wilson-Costello D, Friedman H, Minich N, Fanaroff AA, Hack M. Improved Survival Rates With Increased Neurodevelopmental Disability for Extremely Low Birth Weight Infants in the 1990s. Pediatrics [Internet]. 2005;115(4):997–1003. Available from: http://pediatrics.aappublications.org/cgi/doi/10.1542/peds.2004-0221

30.   Hagberg B, Hagberg G, Beckung E, Uvebrant P. Changing panorama of cerebral palsy in Sweden. VIII. Prevalence and origin in the birth year period

1991–94.pdf. Acta Paediactrica. 2001;90(7):271–7.

31.   Mikkola K, Ritari N, Tomminska V, Salokorpi T, Lehtonen L, Tammela O, et al. Neurodevelopmental Outcome at 5 Years of Age of a National Cohort of Extremely Low Birth Weight Infants Who Were Born in 1996-1997. Pediatrics [Internet]. 2005;116(6):1391–400. Available from: http://pediatrics.aappublications.org/cgi/doi/10.1542/peds.2005-0171

32.   Wood NS, Marlow N, Costeloe K, Gibson AT, Wilkinson AR. Neurologic and Developmental Disability After Extremely preterm birth. N Engl J Med. 2000;343(6):378–84.

33.   Saigal S, Ouden L d., Wolke D, Hoult L, Paneth N, Streiner DL, et al. School-Age Outcomes in Children Who Were Extremely Low Birth Weight From Four International Population-Based Cohorts. Pediatrics [Internet]. 2003;112(4):943–50. Available from: http://pediatrics.aappublications.org/cgi/doi/10.1542/peds.112.4.943

34.   Anderson PJ, Doyle LW. Preterm or With Extremely Low Birth Weight in the 1990s. Pediatrics. 2004;114(1):50–8.

35.   Aylward GP. Neurodevelopmental Outcomes of Infants Born Prematurely. J Dev Behav Pediatr [Internet]. 2005;35(6):394–407. Available from: http://content.wkhealth.com/linkback/openurl?sid=WKPTLP:landingpage&an=00004703-201407000-00007

36.   Phibbs CS, Schmitt SK. Estimates of the Cost and Length of Stay Changes that can be Attributed to One-Week Increases in Gestational Age for Premature Infants. Early Hum Dev. 2006;82(2):85–95.

37.   Ringborg A, Berg J, Norman M, Westgren M. Preterm birth in Sweden : What are the average lengths of hospital stay and the associated inpatient costs ? Acta Paediactrica. 2006;95:1550–5.

38.   Mangham LJ, Petrou S, Doyle LW, Draper ES, Marlow N. The Cost of Preterm Birth Throughout Childhood in England and Wales. Pediatrics [Internet]. 2009;123(2):e312–27. Available from: http://pediatrics.aappublications.org/cgi/doi/10.1542/peds.2008-1827

39.   Behrman RE, Butler AS. Prematurity at birth: Determinants, consequences, and geographic variation. Preterm birth: causes, consequences and prevention. 2007. 772 p.

40.   Chang HH, Larson J, Blencowe H, Spong CY, Howson CP, Cairns-Smith S, et al. Preventing preterm births: Analysis of trends and potential reductions with interventions in 39 countries with very high human development index. Lancet [Internet]. 2013;381(9862):223–34. Available from: http://dx.doi.org/10.1016/S0140-6736(12)61856-X

41.   Gotsch F, Romero R, Erez O, Vaisbuch E, Kusanovic JP, Mazaki-Tovi S, et

al. The preterm parturition syndrome and its implications for understanding the biology, risk assessment, diagnosis, treatment and prevention of preterm birth. J Matern Neonatal Med. 2009;22(May):5–23.

42.   Teixeira J, Rueda BR, Pru JK. Uterine stem cells [Internet]. StemBook. Harvard Stem Cell Institute; 2008 [cited 2018 Jul 31]. Available from: http://www.ncbi.nlm.nih.gov/pubmed/20614602

43.   Carlin A, Alfirevic Z. Physiological changes of pregnancy and monitoring. Best Pract Res Clin Obstet Gynaecol [Internet]. 2008 Oct 1 [cited 2018 Jul 31];22(5):801–23. Available from: https://www.sciencedirect.com/science/article/pii/S1521693408000837

44.   Challis JRG, Matthews SG, Gibb W, Lye SJ. Endocrine and paracrine control of birth at term and preterm. Endocr Rev [Internet]. 2000;21(January):514–50. Available from: http://www.ncbi.nlm.nih.gov/pubmed/11041447

45.   Bourne GL. The microscopic anatomy of the human amnion and chorion. Am J Obstet Gynecol [Internet]. 1960 Jun 1 [cited 2018 Jul 31];79(6):1070–3. Available from: http://linkinghub.elsevier.com/retrieve/pii/0002937860905123

46.   Bryant-Greenwood GD. The extracellular matrix of the human fetal membranes: Structure and function. Placenta [Internet]. 1998 Jan 1 [cited 2018 Jul 31];19(1):1–11. Available from: https://www.sciencedirect.com/science/article/pii/S0143400498900923

47.   MA E. Color atlas of life before birth: normal fetal development. [Internet]. Chicago Illinois Year Book Medical Publishers 1983.; 1983 [cited 2018 Jul 31]. Available from: https://www.popline.org/node/417330

48.   Perry JS. The mammalian fetal membranes. J Reprod Fertil [Internet]. 1981 Jul 1 [cited 2018 Jul 31];62(2):321–35. Available from: http://www.ncbi.nlm.nih.gov/pubmed/7252917

49.   Parry S, Strauss JF. Premature Rupture of the Fetal Membranes. N Engl J Med. 1998;338(10):663–70.

50.   Ferenczy A, Winkler B. Anatomy and Histology of the Cervix. In: Blaustein's Pathology of the Female Genital Tract [Internet]. New York, NY: Springer New York; 1987 [cited 2018 Jul 31]. p. 141–57. Available from: http://link.springer.com/10.1007/978-1-4757-1942-0_5

51.   Blaustein A, Kurman RJ. Blaustein's pathology of the female genital tract [Internet]. Springer; 2002 [cited 2018 Jul 31]. 1391 p. Available from: https://books.google.co.uk/books?hl=en&lr=&id=tuKGMxGRKa8C&oi=fnd&pg=PA207&dq=cervix+anatomy&ots=ec2yoJcMzT&sig=mb8eKzVALUiiFvuJxrEJ6oKb2z4#v=onepage&q=cervix anatomy&f=false

52.   Odeblad E. The Functional Structure of Human Cervical Mucus. Acta Obstet

Gynecol Scand [Internet]. 1968 Jan [cited 2018 Jul 31];47(s1):57–79. Available from: http://doi.wiley.com/10.3109/00016346809156845

53. Zuckerman H, Kahana A, Carmel S. Antibacterial Activity of Human Cervical Mucus. Gynecol Obstet Invest [Internet]. 1975 [cited 2018 Jul 31];6(5):265–71. Available from: https://www.karger.com/Article/FullText/301522

54. Leppert PC. Cervical Softening, Effacement, and Dilatation. J Matern Neonatal Med [Internet]. 1992 Jan [cited 2018 Jul 31];1(4):213–23. Available from: http://www.tandfonline.com/doi/full/10.3109/14767059209161921

55. Hendricks CH, Brenner WE, Kraus G. Normal cervical dilatation pattern in late pregnancy and labor. Am J Obstet Gynecol [Internet]. 1970 Apr 1 [cited 2018 Jul 31];106(7):1065–82. Available from: http://linkinghub.elsevier.com/retrieve/pii/S0002937816340923

56. Romero R, Espinoza J, Kusanovic JP, Gotsch F, Hassan S, Erez O, et al. The preterm parturition syndrome. BJOG An Int J Obstet Gynaecol. 2006;113(SUPPL. 3):17–42.

57. Mercer BM, Goldenberg RL, Moawad AH, Meis PJ, Iams JD, Das AF, et al. The Preterm Prediction Study: Effect of gestational age and cause of preterm birth on subsequent obstetric outcome. Am J Obstet Gynecol [Internet]. 1999 Nov 1 [cited 2018 Jun 7];181(5):1216–21. Available from: https://www.sciencedirect.com/science/article/pii/S0002937899701110

58. Adams MM, Elam-Evans LD, Wilson HG, Gilbertz DA. Rates of and Factors Associated With Recurrence of Preterm Delivery. JAMA [Internet]. 2000 Mar 22 [cited 2018 Jun 7];283(12):1591. Available from: http://jama.jamanetwork.com/article.aspx?doi=10.1001/jama.283.12.1591

59. Bloom SL, Yost NP, McIntire DD, Leveno KJ. Recurrence of preterm birth in singleton and twin pregnancies. Obstet Gynecol [Internet]. 2001 Sep 1 [cited 2018 Jun 7];98(3):379–85. Available from: https://www.sciencedirect.com/science/article/pii/S0029784401014661?via%3Dihub

60. Svensson AC, Sandin S, Cnattingius S, Reilly M, Pawitan Y, Hultman CM, et al. Maternal Effects for Preterm Birth: A Genetic Epidemiologic Study of 630,000 Families. Am J Epidemiol [Internet]. 2009 Dec 1 [cited 2018 Jul 31];170(11):1365–72. Available from: https://academic.oup.com/aje/article-lookup/doi/10.1093/aje/kwp328

61. Guo S-W. Familial Aggregation of Environmental Risk Factors and Familial Aggregation of Disease. Am J Epidemiol [Internet]. 2000 Jun 1 [cited 2018 Jul 31];151(11):1121–31. Available from: https://academic.oup.com/aje/article-lookup/doi/10.1093/oxfordjournals.aje.a010156

62.   Plunkett J, Borecki I, Morgan T, Stamilio D, Muglia LJ. Population-based estimate of sibling risk for preterm birth, preterm premature rupture of membranes, placental abruption and pre-eclampsia. BMC Genet [Internet]. 2008 Jul 8 [cited 2018 Jul 31];9(1):44. Available from: http://bmcgenet.biomedcentral.com/articles/10.1186/1471-2156-9-44

63.   Kistka ZA-F, Palomar L, Lee KA, Boslaugh SE, Wangler MF, Cole FS, et al. Racial disparity in the frequency of recurrence of preterm birth. Am J Obstet Gynecol [Internet]. 2007 Feb 1 [cited 2018 Jun 7];196(2):131.e1-131.e6. Available from: https://www.sciencedirect.com/science/article/pii/S0002937806011501?via%3Dihub

64.   Shiono PH, Klebanoff MA, Graubard BI, Berendes HW, Rhoads GG. Birth Weight Among Women of Different Ethnic Groups. JAMA J Am Med Assoc [Internet]. 1986 Jan 3 [cited 2018 Jun 6];255(1):48. Available from: http://jama.jamanetwork.com/article.aspx?doi=10.1001/jama.1986.03370010054024

65.   Goldenberg RL, Cliver SP, Mulvihill FX, Hickey CA, Hoffman HJ, Klerman L V., et al. Medical, psychosocial, and behavioral risk factors do not explain the increased risk for low birth weight among black women. Am J Obstet Gynecol [Internet]. 1996 Nov 1 [cited 2018 Jun 6];175(5):1317–24. Available from: https://www.sciencedirect.com/science/article/pii/S0002937896700480

66.   Smith LK, Draper ES, Manktelow BN, Dorling JS, Field DJ. Socioeconomic inequalities in very preterm birth rates. Arch Dis Child Fetal Neonatal Ed [Internet]. 2007 Jan 1 [cited 2018 Jun 6];92(1):F11-4. Available from: http://www.ncbi.nlm.nih.gov/pubmed/16595590

67.   Saurel-Cubizolles MJ, Zeitlin J, Lelong N, Papiernik E, Di Renzo GC, Bréart G, et al. Employment, working conditions, and preterm birth: results from the Europop case-control survey. J Epidemiol Community Health [Internet]. 2004 May 1 [cited 2018 Jun 6];58(5):395–401. Available from: http://www.ncbi.nlm.nih.gov/pubmed/15082738

68.   Brett KM, Strogatz DS, Savitz DA. Employment, job strain, and preterm delivery among women in North Carolina. Am J Public Health [Internet]. 1997 Feb 7 [cited 2018 Jun 6];87(2):199–204. Available from: http://www.ncbi.nlm.nih.gov/pubmed/9103097

69.   Copper RL, Goldenberg RL, Das A, Elder N, Swain M, Norman G, et al. The preterm prediction study: Maternal stress is associated with spontaneous preterm birth at less than thirty-five weeks' gestation. Am J Obstet Gynecol [Internet]. 1996 Nov 1 [cited 2018 Jun 7];175(5):1286–92. Available from: https://www.sciencedirect.com/science/article/pii/S000293789670042X

70.   Orr ST, Miller CA. Maternal Depressive Symptoms and the Risk of Poor Pregnancy Outcome Review of the Literature and Preliminary Findings.

Epidemiol Rev [Internet]. 1996 [cited 2018 Jun 7];17(1). Available from:
https://watermark.silverchair.com/17-1-
165.pdf?token=AQECAHi208BE49Ooan9kkhW_Ercy7Dm3ZL_9Cf3qfKAc4
85ysgAAAdIwggHOBgkqhkiG9w0BBwagggG_MIIBuwIBADCCAbQGCSq
GSIb3DQEHATAeBglghkgBZQMEAS4wEQQMhbYKxk17K6JhQdYOAgE
QgIIBhfAL0HftmV2xnvlGt09VQajFlOBOOXTwCs5B16mF9OP0_h

71. Simpson WJ. A preliminary report on cigarette smoking and the incidence of
    prematurity. Am J Obstet Gynecol [Internet]. 1957 Apr 1 [cited 2018 Jun
    7];73(4):808–15. Available from:
    http://linkinghub.elsevier.com/retrieve/pii/0002937857903915

72. Shiono PH, Klebanoff MA, Rhoads GG. Smoking and Drinking During
    Pregnancy. JAMA [Internet]. 1986 Jan 3 [cited 2018 Jun 7];255(1):82.
    Available from:
    http://jama.jamanetwork.com/article.aspx?doi=10.1001/jama.1986.033700100
    88030

73. Meis PJ, Michielutte R, Peters TJ, Wells HB, Sands RE, Coles EC, et al.
    Factors associated with preterm birth in Cardiff, Wales: I. Univariable and
    multivariable analysis. Am J Obstet Gynecol [Internet]. 1995 Aug 1 [cited
    2018 Jun 7];173(2):590–6. Available from:
    https://www.sciencedirect.com/science/article/pii/0002937895902872?via%3
    Dihub

74. Kyrklund-Blomberg NB, Cnattingius S. Preterm birth and maternal smoking:
    Risks related to gestational age and onset of delivery. Am J Obstet Gynecol
    [Internet]. 1998 Oct 1 [cited 2018 Jun 7];179(4):1051–5. Available from:
    https://www.sciencedirect.com/science/article/pii/S0002937898702145?via%3
    Dihub

75. Ludmir J, Samuels P, Brooks S, Mennuti MT. Pregnancy outcome of patients
    with uncorrected uterine anomalies managed in a high-risk obstetric setting.
    Obstet Gynecol [Internet]. 1990 Jun [cited 2018 Jun 6];75(6):906–10.
    Available from: http://www.ncbi.nlm.nih.gov/pubmed/2342734

76. Hill LM, Breckle R, Thomas ML, Fries JK. Polyhydramnios: ultrasonically
    detected prevalence and neonatal outcome. Obstet Gynecol [Internet]. 1987
    Jan [cited 2018 Jun 6];69(1):21–5. Available from:
    http://www.ncbi.nlm.nih.gov/pubmed/3540761

77. Phelan JP, Park YW, Ahn MO, Rutherford SE. Polyhydramnios and perinatal
    outcome. J Perinatol [Internet]. 1990 Dec [cited 2018 Jun 6];10(4):347–50.
    Available from: http://www.ncbi.nlm.nih.gov/pubmed/2277279

78. Tucker J, Mcguire W. ABC of preterm birth Epidemiology of preterm birth
    Gestational age versus birth weight. BMJ [Internet]. 2004 [cited 2018 Jun
    6];329:675–8. Available from:
    https://www.ncbi.nlm.nih.gov/pmc/articles/PMC517653/pdf/bmj32900675.pdf

79.   Laudański T, Rocki W. The effects on stretching and prostaglandin F2alpha on the contractile and bioelectric activity of the uterus in rat. Acta Physiol Pol [Internet]. 1975 [cited 2018 Jun 6];26(4):385–93. Available from: http://www.ncbi.nlm.nih.gov/pubmed/1199746

80.   Kloeck FK, Jung H. In vitro release of prostaglandins from the human myometrium under the influence of stretching. Am J Obstet Gynecol [Internet]. 1973 Apr 15 [cited 2018 Jun 6];115(8):1066–9. Available from: https://www.sciencedirect.com/science/article/pii/0002937873905553

81.   Ou C-W, Orsino A, Lye SJ. Expression of Connexin-43 and Connexin-26 in the Rat Myometrium during Pregnancy and Labor Is Differentially Regulated by Mechanical and Hormonal Signals*. Endocrinology [Internet]. 1997 [cited 2018 Jun 6];138(12):5398–407. Available from: https://watermark.silverchair.com/endo5398.pdf?token=AQECAHi208BE49O oan9kkhW_Ercy7Dm3ZL_9Cf3qfKAc485ysgAAAccwggHDBgkqhkiG9w0B BwagggG0MIIBsAIBADCCAakGCSqGSIb3DQEHATAeBglghkgBZQMEA S4wEQQMDhQOaplLifiHVSFhAgEQgIIBegye5ZgaNQuqmzGFeKGsIGJW H5oylG4wPg13rRbMyVFb6Z

82.   Ou C-W, Chen Z-Q, Qi S, Lye SJ, Health F. Increased Expression of the Rat Myometrial Oxytocin Receptor Messenger Ribonucleic Acid during Labor Requires Both Mechanical and Hormonal Signals Program in Development and. Biol Reprod [Internet]. 1998 [cited 2018 Jun 6];59:1055–61. Available from: https://watermark.silverchair.com/biolreprod1055.pdf?token=AQECAHi208B E49Ooan9kkhW_Ercy7Dm3ZL_9Cf3qfKAc485ysgAAAdgwggHUBgkqhkiG 9w0BBwagggHFMIIBwQIBADCCAboGCSqGSIb3DQEHATAeBglghkgBZ QMEAS4wEQQMV51SW43VVbSwSZ42AgEQgIIBiwVoWkxOBfjTlj47r2y MB-lm80Pc1R8gOGejHjbe

83.   Nemeth E, Tashima LS, Yu Z, Bryant-Greenwood GD. Fetal membrane distention. Am J Obstet Gynecol [Internet]. 2000 Jan 1 [cited 2018 Jun 6];182(1):50–9. Available from: http://linkinghub.elsevier.com/retrieve/pii/S000293780070490X

84.   Nemeth E, Millar LK, Bryant-Greenwood G. Fetal membrane distention. Am J Obstet Gynecol [Internet]. 2000 Jan 1 [cited 2018 Jun 6];182(1):60–7. Available from: http://linkinghub.elsevier.com/retrieve/pii/S0002937800704911

85.   Ananth C V., Berkowitz GS, Savitz DA, Lapinski RH. Placental abruption and adverse perinatal outcomes. JAMA [Internet]. 1999;282(17):1646–51. Available from: http://jama.ama-assn.org/cgi/doi/10.1001/jama.282.17.1646%5Cnhttp://www.ncbi.nlm.nih.gov /pubmed/10553791%5Cnhttp://jama.jamanetwork.com/article.aspx?doi=10.10 01/jama.282.17.1646

86.   Elovitz MA, Saunders T, Ascher-Landsberg J, Phillippe M. Effects of

thrombin on myometrial contractions in vitro and in vivo. Am J Obstet Gynecol. 2000;183(4):799–804.

87.   Bauer ST, Bonanno C. Abnormal Placentation. Semin Perinatol [Internet]. 2009 Apr 1 [cited 2018 Jul 31];33(2):88–96. Available from: https://www.sciencedirect.com/science/article/pii/S0146000508001481

88.   Kim YM, Bujold E, Chaiworapongsa T, Gomez R, Yoon BH, Thaler HT, et al. Failure of physiologic transformation of the spiral arteries in patients with preterm labor and intact membranes. Am J Obstet Gynecol. 2003;189(4):1063–9.

89.   Chaiworapongsa T, Romero R, Tarca A, Pedro Kusanovic J, Mittal P, Kwon Kim S, et al. A subset of patients destined to develop spontaneous preterm labor has an abnormal angiogenic/anti-angiogenic profile in maternal plasma: Evidence in support of pathophysiologic heterogeneity of preterm labor derived from a longitudinal study. J Matern Neonatal Med. 2009;22(12):1122–39.

90.   Rowe JH, Ertelt JM, Xin L, Way SS. Pregnancy imprints regulatory memory that sustains anergy to fetal antigen. Nature [Internet]. 2012;490(7418):102–6. Available from: http://dx.doi.org/10.1038/nature11462

91.   Mold JE, Michaëlsson J, Burt TD, Muench MO, Beckerman KP, Busch MP, et al. Maternal Alloantigens Promote the Development of Tolerogenic Fetal Regulatory T Cells in Utero. Science (80-). 2009;1562(2008):1562–6.

92.   Kim CJ, Romero R, Kusanovic JP, Yoo W, Dong Z, Topping V, et al. The frequency, clinical significance, and pathological features of chronic chorioamnionitis: A lesion associated with spontaneous preterm birth. Mod Pathol [Internet]. 2010;23(7):1000–11. Available from: http://dx.doi.org/10.1038/modpathol.2010.73

93.   Harrison MR, Keller RL, Hawgood SB, Kitterman J a, Sandberg PL, Farmer DL, et al. A randomized trial of fetal endoscopic tracheal occlusion for severe fetal congenital diaphragmatic hernia. N Engl J Med. 2003;349(20):1916–24.

94.   Scott Adzick N, Thom EA, Spong CY, Brock JW, Burrows PK, Johnson MP, et al. A Randomized Trial of Prenatal versus Postnatal Repair of Myelomeningocele. N Engl J Med. 2011;364(11):993.

95.   Wegorzewska M, Nijagal A, Wong CM, Le T, Lescano N, Tang Q, et al. Fetal Intervention Increases Maternal T Cell Awareness of the Foreign Conceptus and Can Lead to Immune-Mediated Fetal Demise. J Immunol [Internet]. 2014;192(4):1938–45. Available from: http://www.jimmunol.org/cgi/doi/10.4049/jimmunol.1302403

96.   Iams JD, Goldenberg RL, Meis PJ, Mercer BM, Moawad A, Das A, et al. The Length of the Cervix and the Risk of Spontaneous Premature Delivery. N Engl

J Med [Internet]. 1996 Feb 29 [cited 2018 Jun 17];334(9):567–73. Available from: http://www.nejm.org/doi/abs/10.1056/NEJM199602293340904

97.   Ludmir J, Jackson GM, Samuels P. Transvaginal cerclage under ultrasound guidance in cases of severe cervical hypoplasia. Obstet Gynecol [Internet]. 1991 Dec [cited 2018 Jun 17];78(6):1067–72. Available from: http://www.ncbi.nlm.nih.gov/pubmed/1945209

98.   Goldstein DP. Incompetent cervix in offspring exposed to diethylstilbestrol in utero. Obstet Gynecol [Internet]. 1978 Jul [cited 2018 Jun 17];52(1 Suppl):73S–75S. Available from: http://www.ncbi.nlm.nih.gov/pubmed/683647

99.   Harger JH. Cerclage and cervical insufficiency: An evidence-based analysis. Obstet Gynecol [Internet]. 2002 Dec 1 [cited 2018 Jun 17];100(6):1313–27. Available from: https://www.sciencedirect.com/science/article/pii/S0029784402023657

100. Warren JE, Silver RM. Genetics of the Cervix in Relation to Preterm Birth. Semin Perinatol [Internet]. 2009 Oct 1 [cited 2018 Jun 17];33(5):308–11. Available from: https://www.sciencedirect.com/science/article/pii/S0146000509000433?via%3Dihub

101. Warren JE, Silver RM, Dalton J, Nelson LT, Branch DW, Porter TF. Collagen 1A1 and Transforming Growth Factor-β Polymorphisms in Women With Cervical Insufficiency. Obstet Gynecol [Internet]. 2007 Sep [cited 2018 Jun 17];110(3):619–24. Available from: http://content.wkhealth.com/linkback/openurl?sid=WKPTLP:landingpage&an=00006250-200709000-00014

102. Mann V, Hobson EE, Li B, Stewart TL, Grant SF, Robins SP, et al. A COL1A1 Sp1 binding site polymorphism predisposes to osteoporotic fracture by affecting bone density and quality. J Clin Invest [Internet]. 2001 Apr 1 [cited 2018 Jun 17];107(7):899–907. Available from: http://www.ncbi.nlm.nih.gov/pubmed/11285309

103. Blobe GC, Schiemann WP, Lodish HF. Role of Transforming Growth Factor β in Human Disease. Epstein FH, editor. N Engl J Med [Internet]. 2000 May 4 [cited 2018 Jun 17];342(18):1350–8. Available from: http://www.nejm.org/doi/10.1056/NEJM200005043421807

104. Lee K-Y, Jun H-A, Kim H-B, Kang S-W. Interleukin-6, but not relaxin, predicts outcome of rescue cerclage in women with cervical incompetence. Am J Obstet Gynecol [Internet]. 2004 Sep 1 [cited 2018 Jun 17];191(3):784–9. Available from: https://www.sciencedirect.com/science/article/pii/S0002937804004144

105. Warren JE, Nelson LM, Stoddard GJ, Esplin MS, Varner MW, Silver RM.

Polymorphisms in the promoter region of the interleukin-10 (IL-10) gene in women with cervical insufficiency. Am J Obstet Gynecol [Internet]. 2009 [cited 2018 Jun 17];201(4):372.e1-372.e5. Available from: https://www.ajog.org/article/S0002-9378(09)00530-4/pdf

106. Knox IC, Hoerner JK. The role of infection in premature rupture of the membranes. Am J Obstet Gynecol [Internet]. 1950 Jan 1 [cited 2018 Jun 7];59(1):190–4. Available from: https://www.sciencedirect.com/science/article/pii/000293785090370X?via%3Dihub

107. Gilles HM, Lawson JB, Sibelas M, Voller A, Allan N. Malaria, anaemia and pregnancy. Ann Trop Med Parasitol [Internet]. 1969 Jun 15 [cited 2018 Jun 7];63(2):245–63. Available from: http://www.tandfonline.com/doi/full/10.1080/00034983.1969.11686625

108. Patrick MJ. Influence of maternal renal infection on the foetus and infant. Arch Dis Child [Internet]. 1967 Apr 1 [cited 2018 Jun 7];42(222):208–13. Available from: http://www.ncbi.nlm.nih.gov/pubmed/6024471

109. Benedetti TJ, Valle R, Ledger WJ. Antepartum pneumonia in pregnancy. Am J Obstet Gynecol [Internet]. 1982 Oct 15 [cited 2018 Jun 7];144(4):413–7. Available from: https://www.sciencedirect.com/science/article/pii/0002937882902460?via%3Dihub

110. Romero R, Oyarzun E, Mazor M, Sirtori M, Hobbins JC, Bracken M. Meta-analysis of the relationship between asymptomatic bacteriuria and preterm delivery/low birth weight. Obstet Gynecol [Internet]. 1989 Apr [cited 2018 Jun 7];73(4):576–82. Available from: http://www.ncbi.nlm.nih.gov/pubmed/2927852

111. Xiong X, Buekens P, Fraser W, Beck J, Offenbacher S. Periodontal disease and adverse pregnancy outcomes: a systematic review. BJOG An Int J Obstet Gynaecol [Internet]. 2006 Feb [cited 2018 Jun 7];113(2):135–43. Available from: http://doi.wiley.com/10.1111/j.1471-0528.2005.00827.x

112. Romero R, Salafia CM, Athanassiadis AP, Hanaoka S, Mazor M, Sepulveda W, et al. The relationship between acute inflammatory lesions of the preterm placenta and amniotic fluid microbiology. Am J Obstet Gynecol [Internet]. 1992 May 1 [cited 2018 Jun 7];166(5):1382–8. Available from: https://www.sciencedirect.com/science/article/pii/000293789291609E?via%3Dihub

113. Goldenberg RL, Hauth JC, Andrews WW. Intrauterine Infection and Preterm Delivery. N Engl J Med. 2000;342(20):1500–7.

114. Yoon BH, Romero R, Park JS, Kim M, Oh S-Y, Kim CJ, et al. The relationship among inflammatory lesions of the umbilical cord (funisitis),

umbilical cord plasma interleukin 6 concentration, amniotic fluid infection, and neonatal sepsis. Am J Obstet Gynecol [Internet]. 2000 Nov 1 [cited 2018 Jun 9];183(5):1124–9. Available from: https://www.sciencedirect.com/science/article/pii/S0002937800530610?via%3 Dihub

115.   Mueller-Heubach E, Rubinstein DN, Schwarz SS. Histologic chorioamnionitis and preterm delivery in different patient populations. Obstet Gynecol [Internet]. 1990 Apr [cited 2018 Jun 9];75(4):622–6. Available from: http://www.ncbi.nlm.nih.gov/pubmed/2314782

116.   Romero R, Mazor M, Tarkakovsky B. Systemic administration of interleukin-1 induces preterm parturition in mice. Am J Obstet Gynecol. 1991;165(4):969–71.

117.   McDuffie R, Sherman MP, Gibbs RS. Amniotic fluid tumor necrosis factor-α and interleukin-1 in a rabbit model of bacterially induced preterm pregnancy loss. Am J Obstet Gynecol [Internet]. 1992 Dec 1 [cited 2018 Jun 9];167(6):1583–8. Available from: https://www.sciencedirect.com/science/article/pii/000293789291745V?via%3 Dihub

118.   Gravett MG, Witkin SS, Haluska GJ, Edwards JL, Cook MJ, Novy MJ. An experimental model for intraamniotic infection and preterm labor in rhesus monkeys. Am J Obstet Gynecol [Internet]. 1994 Dec 1 [cited 2018 Jun 9];171(6):1660–7. Available from: https://www.sciencedirect.com/science/article/pii/0002937894904189?via%3 Dihub

119.   Fidel P, Ghezzi F, Romero R, Chaiworapongsa T, Espinoza J, Cutright J, et al. The effect of antibiotic therapy on intrauterine infection-induced preterm parturition in rabbits. J Matern Neonatal Med [Internet]. 2003 Jan 7 [cited 2018 Jun 9];14(1):57–64. Available from: http://www.tandfonline.com/doi/full/10.1080/jmf.14.1.57.64

120.   Smaill F. Antibiotics for asymptomatic bacteriuria in pregnancy. In: Smaill F, editor. The Cochrane Database of Systematic Reviews [Internet]. Chichester, UK: John Wiley & Sons, Ltd; 2001 [cited 2018 Jun 9]. Available from: http://doi.wiley.com/10.1002/14651858.CD000490

121.   Kenyon S, Taylor D, Tarnow-Mordi W. Broad-spectrum antibiotics for spontaneous preterm labour: the ORACLE II randomised trial. Lancet [Internet]. 2001 Mar 31 [cited 2018 Jun 9];357(9261):989–94. Available from: https://www.sciencedirect.com/science/article/pii/S0140673600042343?via%3 Dihub

122.   Wenstrom KD, Andrews WW, Hauth JC, Goldenberg RL, DuBard MB, Cliver SP. Elevated second-trimester amniotic fluid interleukin-6 levels predict preterm delivery. Am J Obstet Gynecol [Internet]. 1998 Mar 1 [cited 2018 Jun

9];178(3):546–50. Available from:
https://www.sciencedirect.com/science/article/pii/S0002937898704363?via%3
Dihub

123. Yoon BH, Oh S-Y, Romero R, Shim S-S, Han S-Y, Park JS, et al. An elevated
amniotic fluid matrix metalloproteinase-8 level at the time of mid-trimester
genetic amniocentesis is a risk factor for spontaneous preterm delivery. Am J
Obstet Gynecol [Internet]. 2001 Nov 1 [cited 2018 Jun 9];185(5):1162–7.
Available from:
https://www.sciencedirect.com/science/article/pii/S0002937801609050?via%3
Dihub

124. Romero R, Munoz H, Gomez R, Sherer DM, Ghezzi F, Ghidini A, et al. Two
thirds of spontaneous abortion/fetal deaths after genetic midtrimester
amniocentesis are the result of a pre-existing subclinical inflammatory process
of the amniotic cavity. Am J Obstet Gynecol [Internet]. 1995 Jan 1 [cited 2018
Jun 9];172(1):261. Available from:
http://linkinghub.elsevier.com/retrieve/pii/0002937895907157

125. Hargreaves DC, Medzhitov R. Innate Sensors of Microbial Infection. J Clin
Immunol [Internet]. 2005 [cited 2018 Jun 9];25(6):503–10. Available from:
https://link.springer.com/content/pdf/10.1007%2Fs10875-005-8065-4.pdf

126. Fazeli A, Bruce C, Anumba DO. Characterization of Toll-like receptors in the
female reproductive tract in humans. Hum Reprod [Internet]. 2005 May 1
[cited 2018 Jun 9];20(5):1372–8. Available from:
http://academic.oup.com/humrep/article/20/5/1372/2356767/Characterization-
of-Tolllike-receptors-in-the

127. Pioli PA, Amiel E, Schaefer TM, Connolly JE, Wira CR, Guyre PM.
Differential expression of Toll-like receptors 2 and 4 in tissues of the human
female reproductive tract. Infect Immun [Internet]. 2004 Oct 1 [cited 2018 Jun
9];72(10):5799–806. Available from:
http://www.ncbi.nlm.nih.gov/pubmed/15385480

128. Krikun G, Lockwood CJ, Abrahams VM, Mor G, Paidas M, Guller S.
Expression of toll-like receptors in the human decidua. Histol Histopathol
[Internet]. 2007 [cited 2018 Jun 9];22(8):847–54. Available from:
http://www.hh.um.es/pdf/Vol_22/22_8/Krikun-22-847-854-2007.pdf

129. Youssef RE, Ledingham MA, Bollapragada SS, O 'gorman N, Jordan F,
Young A, et al. The Role of Toll-Like Receptors (TLR-2 and -4) and
Triggering Receptor Expressed on Myeloid Cells 1 (TREM-1) in Human
Term and Preterm Labor. Reprod Sci [Internet]. 2009 [cited 2018 Jun
9];16(9):843–56. Available from:
http://journals.sagepub.com/doi/pdf/10.1177/1933719109336621

130. Kim YM, Romero R, Chaiworapongsa T, Kim GJ, Kim MR, Kuivaniemi H, et
al. Toll-like receptor-2 and -4 in the chorioamniotic membranes in

spontaneous labor at term and in preterm parturition that are associated with chorioamnionitis. Am J Obstet Gynecol [Internet]. 2004 Oct 1 [cited 2018 Jun 9];191(4):1346–55. Available from: https://www.sciencedirect.com/science/article/pii/S0002937804007598?via%3Dihub

131.   Li L, Kang J, Lei W. Role of Toll-like receptor 4 in inflammation-induced preterm delivery. Mol Hum Reprod [Internet]. 2010 Apr 1 [cited 2018 Jun 10];16(4):267–72. Available from: https://academic.oup.com/molehr/article-lookup/doi/10.1093/molehr/gap106

132.   Chin PY, Dorian CL, Hutchinson MR, Olson DM, Rice KC, Moldenhauer LM, et al. Novel Toll-like receptor-4 antagonist (+)-naloxone protects mice from inflammation-induced preterm birth. Sci Rep [Internet]. 2016 Dec 7 [cited 2018 Jun 10];6(1):36112. Available from: http://www.nature.com/articles/srep36112

133.   Wang H, Hirsch E. Bacterially-Induced Preterm Labor and Regulation of Prostaglandin-Metabolizing Enzyme Expression in Mice: The Role of Toll-Like Receptor 41. Biol Reprod [Internet]. 2003 Dec 1 [cited 2018 Jun 10];69(6):1957–63. Available from: https://academic.oup.com/biolreprod/article-lookup/doi/10.1095/biolreprod.103.019620

134.   Robertson SA, Wahid HH, Chin PY, Hutchinson MR, Moldenhauer LM, Keelan JA. Toll-like Receptor-4: A New Target for Preterm Labour Pharmacotherapies? Curr Pharm Des [Internet]. 2018 May 18 [cited 2018 Jun 10];24(9):960–73. Available from: http://www.ncbi.nlm.nih.gov/pubmed/29384054

135.   Moço NP, Martin LF, Pereira AC, Polettini J, Peraçoli JC, Coelho KIR, et al. Gene expression and protein localization of TLR-1, -2, -4 and -6 in amniochorion membranes of pregnancies complicated by histologic chorioamnionitis. Eur J Obstet Gynecol Reprod Biol [Internet]. 2013 Nov 1 [cited 2018 Jun 14];171(1):12–7. Available from: https://www.sciencedirect.com/science/article/pii/S0301211513003436?via%3Dihub

136.   Waring GJ, Robson SC, Bulmer JN, Tyson-Capper AJ. Inflammatory Signalling in Fetal Membranes: Increased Expression Levels of TLR 1 in the Presence of Preterm Histological Chorioamnionitis. Gay N, editor. PLoS One [Internet]. 2015 May 12 [cited 2018 Jun 14];10(5):e0124298. Available from: http://dx.plos.org/10.1371/journal.pone.0124298

137.   Muzio M, Ni J, Feng P, Dixit VM. IRAK (Pelle) Family Member IRAK-2 and MyD88 as Proximal Mediators of IL-1 Signaling. Science (80-) [Internet]. 1997 Nov 28 [cited 2019 Feb 6];278(5343):1612–5. Available from: http://science.sciencemag.org/content/278/5343/1612

138. Fitzgerald KA, Palsson-McDermott EM, Bowie AG, Jefferies CA, Mansell AS, Brady G, et al. Mal (MyD88-adapter-like) is required for Toll-like receptor-4 signal transduction. Nature [Internet]. 2001 Sep 6 [cited 2019 Feb 6];413(6851):78–83. Available from: http://www.nature.com/doifinder/10.1038/35092578

139. Yamamoto M, Sato S, Mori K, Hoshino K, Takeuchi O, Takeda K, et al. Cutting edge: a novel Toll/IL-1 receptor domain-containing adapter that preferentially activates the IFN-beta promoter in the Toll-like receptor signaling. J Immunol [Internet]. 2002 Dec 15 [cited 2019 Feb 6];169(12):6668–72. Available from: http://www.ncbi.nlm.nih.gov/pubmed/12471095

140. Oshiumi H, Matsumoto M, Funami K, Akazawa T, Seya T. TICAM-1, an adaptor molecule that participates in Toll-like receptor 3–mediated interferon-β induction. Nat Immunol [Internet]. 2003 Feb 21 [cited 2019 Feb 6];4(2):161–7. Available from: http://www.nature.com/articles/ni886

141. Picard C, Puel A, Bonnet M, Ku C-L, Bustamante J, Yang K, et al. Pyogenic bacterial infections in humans with IRAK-4 deficiency. Science [Internet]. 2003 Mar 28 [cited 2019 Feb 6];299(5615):2076–9. Available from: http://www.ncbi.nlm.nih.gov/pubmed/12637671

142. Suzuki N, Chen N-J, Millar DG, Suzuki S, Horacek T, Hara H, et al. The Journal of Immunology. J Immunol [Internet]. 2003 Apr 15 [cited 2019 Feb 6];163(2):978–84. Available from: http://www.jimmunol.org/content/170/8/4031

143. Li S, Strelow A, Fontana EJ, Wesche H. IRAK-4: a novel member of the IRAK family with the properties of an IRAK-kinase. Proc Natl Acad Sci U S A [Internet]. 2002 Apr 16 [cited 2019 Feb 6];99(8):5567–72. Available from: http://www.ncbi.nlm.nih.gov/pubmed/11960013

144. Wang C, Deng L, Hong M, Akkaraju GR, Inoue J, Chen ZJ. TAK1 is a ubiquitin-dependent kinase of MKK and IKK. Nature [Internet]. 2001 Jul 19 [cited 2019 Feb 6];412(6844):346–51. Available from: http://www.nature.com/articles/35085597

145. Akira S, Takeda K. Toll-like receptor signalling. Nat Rev Immunol. 2004;4(July):499–511.

146. Romero R, Brody DT, Oyarzun E, Mazor M, King Wu Y, Hobbins JC, et al. Infection and labor: III. Interleukin-1: A signal for the onset of parturition. Am J Obstet Gynecol [Internet]. 1989 May 1 [cited 2018 Jun 12];160(5):1117–23. Available from: https://www.sciencedirect.com/science/article/pii/0002937889901725?via%3Dihub

147. Romero R, Durum S, Dinarello CA, Oyarzun E, Hobbins JC, Mitchell MD.

Interleukin-1 stimulates prostaglandin biosynthesis by human amnion. Prostaglandins [Internet]. 1989 Jan 1 [cited 2018 Jun 12];37(1):13–22. Available from: https://www.sciencedirect.com/science/article/pii/0090698089900282?via%3Dihub

148.   Romero R, Wu YK, Brody DT, Oyarzun E, Duff GW, Durum SK. Human decidua: a source of interleukin-1. Obstet Gynecol [Internet]. 1989 Jan [cited 2018 Jun 12];73(1):31–4. Available from: http://www.ncbi.nlm.nih.gov/pubmed/2642326

149.   Sadowsky DW, Novy MJ, Witkin SS, Gravett MG. Dexamethasone or interleukin-10 blocks interleukin-1β-induced uterine contractions in pregnant rhesus monkeys. Am J Obstet Gynecol [Internet]. 2003 Jan 1 [cited 2018 Jun 12];188(1):252–63. Available from: https://www.sciencedirect.com/science/article/pii/S0002937802714002?via%3Dihub

150.   Romero R, Mazor M, Tartakovsky B. Systemic administration of interleukin-1 induces preterm parturition in mice. Am J Obstet Gynecol [Internet]. 1991;165(4):969–71. Available from: http://dx.doi.org/10.1016/j.ajog.2009.06.027

151.   Romero R, Tartakovsky B. The natural interleukin-1 receptor antagonist prevents interleukin-l-induced preterm delivery in mice. Am J Obstet Gynecol [Internet]. 1992 Oct 1 [cited 2018 Jun 12];167(4):1041–5. Available from: https://www.sciencedirect.com/science/article/pii/S0002937812800354?via%3Dihub

152.   Sims JE, Smith DE. The IL-1 family: regulators of immunity. Nat Rev Immunol [Internet]. 2010 Feb 18 [cited 2019 Feb 6];10(2):89–102. Available from: http://www.nature.com/articles/nri2691

153.   Marucha PT, Zeff RA, Kreutzer DL. Cytokine regulation of IL-1 beta gene expression in the human polymorphonuclear leukocyte. J Immunol [Internet]. 1990 Nov 1 [cited 2019 Feb 19];145(9):2932–7. Available from: http://www.ncbi.nlm.nih.gov/pubmed/2212667

154.   Li P, Allen H, Banerjee S, Franklin S, Herzog L, Johnston C, et al. Mice deficient in IL-1β-converting enzyme are defective in production of mature IL-1β and resistant to endotoxic shock. Cell [Internet]. 1995 Feb 10 [cited 2019 Feb 19];80(3):401–11. Available from: https://www.sciencedirect.com/science/article/pii/0092867495904905?via%3Dihub

155.   Martinon F, Burns K, Tschopp J. The Inflammasome: A Molecular Platform Triggering Activation of Inflammatory Caspases and Processing of proIL-β. Mol Cell [Internet]. 2002 Aug 1 [cited 2019 Feb 19];10(2):417–26. Available from:

https://www.sciencedirect.com/science/article/pii/S1097276502005993?via%3
Dihub

156. Franchi L, Eigenbrod T, Muñoz-Planillo R, Nuñez G. The inflammasome: a caspase-1-activation platform that regulates immune responses and disease pathogenesis. Nat Immunol [Internet]. 2009 Mar 1 [cited 2019 Feb 19];10(3):241–7. Available from: http://www.nature.com/articles/ni.1703

157. O'Connor W, Harton JA, Zhu X, Linhoff MW, Ting JP-Y. Cutting edge: CIAS1/cryopyrin/PYPAF1/NALP3/CATERPILLER 1.1 is an inducible inflammatory mediator with NF-kappa B suppressive properties. J Immunol [Internet]. 2003 Dec 15 [cited 2019 Feb 19];171(12):6329–33. Available from: http://www.ncbi.nlm.nih.gov/pubmed/14662828

158. Romero R, Avila C, Santhanam U, Sehgal PB. Amniotic fluid interleukin 6 in preterm labor. Association with infection. J Clin Invest [Internet]. 1990 May 1 [cited 2018 Jun 12];85(5):1392–400. Available from: http://www.ncbi.nlm.nih.gov/pubmed/2332497

159. Gomez R, Romero R, Galasso M, Behnke E, Insunza A, Cotton DB. The Value of Amniotic Fluid Interleukin-6, White Blood Cell Count, and Gram Stain in the Diagnosis of Microbial Invasion of the Amniotic Cavity in Patients at Term. Am J Reprod Immunol [Internet]. 1994 Oct [cited 2018 Jun 12];32(3):200–10. Available from: http://doi.wiley.com/10.1111/j.1600-0897.1994.tb01115.x

160. Andrews WW, Hauth JC, Goldenberg RL, Gomez R, Romero R, Cassell GH. Amniotic fluid interleukin-6: Correlation with upper genital tract microbial colonization and gestational age in women delivered after spontaneous labor versus indicated delivery. Am J Obstet Gynecol [Internet]. 1995 Aug 1 [cited 2018 Jun 12];173(2):606–12. Available from: https://www.sciencedirect.com/science/article/pii/0002937895902902?via%3
Dihub

161. Ghezzi F, Gomez R, Romero R, Yoon BH, Edwin SS, David C, et al. Elevated interleukin-8 concentrations in amniotic fluid of mothers whose neonates subsequently develop bronchopulmonary dysplasia. Eur J Obstet Gynecol Reprod Biol [Internet]. 1998 May 1 [cited 2018 Jun 12];78(1):5–10. Available from:
https://www.sciencedirect.com/science/article/pii/S0301211597002364?via%3
Dihub

162. Romero R, Ceska M, Avila C, Mazor M, Behnke E, Lindley I. Neutrophil attractant/activating peptide-1 / interleukin-8 in term and preterm parturition. Am J Obstet Gynecol [Internet]. 1991 Oct 1 [cited 2018 Jun 12];165(4):813–20. Available from:
https://www.sciencedirect.com/science/article/pii/000293789190422N?via%3
Dihub

163.   Romero R, Manogue KR, Mitchell MD, Wu YK, Oyarzun E, Hobbins JC, et al. Infection and labor: IV. Cachectin—tumor necrosis factor in the amniotic fluid of women with intraamniotic infection and preterm labor. Am J Obstet Gynecol [Internet]. 1989 Aug 1 [cited 2018 Jun 12];161(2):336–41. Available from: https://www.sciencedirect.com/science/article/pii/0002937889905152?via%3Dihub

164.   Casey ML, Cox SM, Beutler B, Milewich L, MacDonald PC. Cachectin/tumor necrosis factor-alpha formation in human decidua. Potential role of cytokines in infection-induced preterm labor. J Clin Invest [Internet]. 1989 Feb 1 [cited 2018 Jun 12];83(2):430–6. Available from: http://www.ncbi.nlm.nih.gov/pubmed/2913048

165.   Romero R, Mazor M, Manogue K, Oyarzun E, Cerami A. Human decidua: a source of cachectin-tumor necrosis factor. Eur J Obstet Gynecol Reprod Biol [Internet]. 1991 Sep 13 [cited 2018 Jun 12];41(2):123–7. Available from: https://www.sciencedirect.com/science/article/pii/0028224391900894?via%3Dihub

166.   Saito S, Kasahara T, Kato Y, Ishihara Y, Ichijo M. Elevation of amniotic fluid interleukin 6 (IL-6), IL-8 and granulocyte colony stimulating factor (G-CSF) in term and preterm parturition. Cytokine [Internet]. 1993 Jan 1 [cited 2018 Jun 12];5(1):81–8. Available from: https://www.sciencedirect.com/science/article/pii/1043466693900273?via%3Dihub

167.   Hillier S, Witkin S, Krohn M, … DW-O and, 1993 undefined. The relationship of amniotic fluid cytokines and preterm delivery, amniotic fluid infection, histologic chorioamnionitis, and chorioamnion infection. europepmc.org [Internet]. [cited 2018 Jun 12]; Available from: http://europepmc.org/abstract/med/8497360

168.   Messer J, Eyer D, Donato L, Gallati H, Matis J, Simeoni U. Evaluation of interleukin-6 and soluble receptors of tumor necrosis factor for early diagnosis of neonatal infection. J Pediatr [Internet]. 1996 Oct 1 [cited 2018 Jun 12];129(4):574–80. Available from: https://www.sciencedirect.com/science/article/pii/S0022347696701233?via%3Dihub

169.   Hirsch E, Filipovich Y, Mahendroo M. Signaling via the type I IL-1 and TNF receptors is necessary for bacterially induced preterm labor in a murine model. Am J Obstet Gynecol [Internet]. 2006 May 1 [cited 2018 Jun 12];194(5):1334–40. Available from: https://www.sciencedirect.com/science/article/pii/S000293780502449X?via%3Dihub

170.   Rinaldi SF, Makieva S, Frew L, Wade J, Thomson AJW, Moran CM, et al. Ultrasound-Guided Intrauterine Injection of Lipopolysaccharide as a Novel

Model of Preterm Birth in the Mouse. Am J Pathol [Internet].
2015;185(5):1201–6. Available from:
http://linkinghub.elsevier.com/retrieve/pii/S0002944015000772

171. Kajikawa S, Kaga N, Futamura Y, Kakinuma C, Shibutani Y. Lipoteichoic
acid induces preterm delivery in mice. J Pharmacol Toxicol Methods
[Internet]. 1998 Apr 1 [cited 2018 Jun 12];39(3):147–54. Available from:
https://www.sciencedirect.com/science/article/pii/S105687199800015X?via%
3Dihub

172. Olson DM. The role of prostaglandins in the initiation of parturition. Best
Pract Res Clin Obstet Gynaecol [Internet]. 2003 Oct 1 [cited 2018 Jun
13];17(5):717–30. Available from:
https://www.sciencedirect.com/science/article/pii/S1521693403000695?via%3
Dihub

173. Geng J, Huang C, Jiang S. Roles and Regulation of the Matrix
Metalloproteinase System in Parturition Any significant imbalance of the
MMPs or their inhibitors during pregnancy can result in pathologies. Mol
Reprod Dev Mol Reprod Dev [Internet]. 2016 [cited 2018 Jun
13];83(83):276–86. Available from:
https://onlinelibrary.wiley.com/doi/pdf/10.1002/mrd.22626

174. Rauk PN, Chiao J-P. Interleukin-1 Stimulates Human Uterine Prostaglandin
Production Through Induction of Cyclooxygenase-2 Expression. Am J Reprod
Immunol [Internet]. 2000 Mar [cited 2018 Jun 13];43(3):152–9. Available
from: http://doi.wiley.com/10.1111/j.8755-8920.2000.430304.x

175. Hertelendy F, Romero R, Molnár M, Todd H, Baldassare JJ. Cytokine-
initiated signal transduction in human myometrial cells. Am J Reprod
Immunol [Internet]. 1993 [cited 2018 Jun 13];30(2–3):49–57. Available from:
http://www.ncbi.nlm.nih.gov/pubmed/8311930

176. Mitchell MD, Edwin SS, Silver RM, Romero RJ. Potential agonist action of
the interleukin-1 receptor antagonist protein: implications for treatment of
women. J Clin Endocrinol Metab [Internet]. 1993 May 13 [cited 2018 Jun
13];76(5):1386–8. Available from:
http://www.ncbi.nlm.nih.gov/pubmed/8496334

177. Lundin-Schiller S, Mitchell MD. Prostaglandin production by human chorion
laeve cells in response to inflammatory mediators. Placenta [Internet]. 1991
Jul 1 [cited 2018 Jun 13];12(4):353–63. Available from:
https://www.sciencedirect.com/science/article/pii/014340049190343E

178. Bry K, Hallman M. Transforming growth factor-β opposes the stimulatory
effects of interleukin-1 and tumor necrosis factor on amnion cell prostaglandin
E2 production: Implication for preterm labor. Am J Obstet Gynecol [Internet].
1992 Jul 1 [cited 2018 Jun 13];167(1):222–6. Available from:
https://www.sciencedirect.com/science/article/pii/S0002937811916627

179. Mitchell MD, Dudley DJ, Edwin SS, Schiller SL. Interleukin-6 stimulates prostaglandin production by human amnion and decidual cells. Eur J Pharmacol [Internet]. 1991 Jan 3 [cited 2018 Jun 13];192(1):189–91. Available from: https://www.sciencedirect.com/science/article/pii/001429999190090D

180. Dudley DJ, Edwin SS, Mitchell MD. Macrophage inflammatory protein-I alpha regulates prostaglandin E2 and interleukin-6 production by human gestational tissues in vitro. J Soc Gynecol Investig [Internet]. [cited 2018 Jun 13];3(1):12–6. Available from: http://www.ncbi.nlm.nih.gov/pubmed/8796800

181. Mohler KM, Torrance DS, Smith CA, Goodwin RG, Stremler KE, Fung VP, et al. Soluble tumor necrosis factor (TNF) receptors are effective therapeutic agents in lethal endotoxemia and function simultaneously as both TNF carriers and TNF antagonists. J Immunol [Internet]. 1993 Aug 1 [cited 2018 Jun 13];151(3):1548–61. Available from: http://www.ncbi.nlm.nih.gov/pubmed/8393046

182. Allport VC, Pieber D, Slater DM, Newton R, White JO, Bennett PR. Human labour is associated with nuclear factor- κ B activity which mediates cyclo-oxygenase-2 expression and is involved with the ' functional progesterone withdrawal .' Mol Hum Reprod. 2001;7(6):581–6.

183. Mitchell MD, Goodwin V, Mesnage S, Keelan JA. Cytokine-induced coordinate expression of enzymes of prostaglandin biosynthesis and metabolism: 15-hydroxyprostaglandin dehydrogenase. Prostaglandins, Leukot Essent Fat Acids [Internet]. 2000 Jan 1 [cited 2018 Jun 13];62(1):1–5. Available from: https://www.sciencedirect.com/science/article/pii/S0952327899901175

184. Brown NL, Alvi SA, Elder MG, Bennett PR, Sullivan MHF. Interleukin-1β and bacterial endotoxin change the metabolism of prostaglandins E2 and F2α in intact term fetal membranes. Placenta [Internet]. 1998 Nov 1 [cited 2018 Jun 13];19(8):625–30. Available from: https://www.sciencedirect.com/science/article/pii/S0143400498900248

185. Pomini F, Patel FA, Mancuso S, Challis JRG. Activity and expression of 15-hydroxyprostaglandin dehydrogenase in cultured chorionic trophoblast and villous trophoblast cells and in chorionic explants at term with and without spontaneous labor. Am J Obstet Gynecol [Internet]. 2000 Jan 1 [cited 2018 Jun 13];182(1):221–6. Available from: https://www.sciencedirect.com/science/article/pii/S0002937800705163

186. Meisser A, Chardonnens D, Campana A, Bischof P. Effects of tumour necrosis factor-alpha, interleukin-1 alpha, macrophage colony stimulating factor and transforming growth factor on trophoblastic matrix metalloproteinases. Mol Hum Reprod [Internet]. 1999 Mar 1 [cited 2018 Jun 13];5(3):252–60. Available from: https://academic.oup.com/molehr/article-lookup/doi/10.1093/molehr/5.3.252

187. Katsura M, Ito A, Hirakawa S, Mori Y. Human recombinant interleukin- 1α increases biosynthesis of collagenase and hyaluronic acid in cultured human chorionic cells. FEBS Lett [Internet]. 1989 Feb 27 [cited 2018 Jun 13];244(2):315–8. Available from: https://www.sciencedirect.com/science/article/pii/0014579389805538

188. Vadillo-Ortega F, Sadowsky DW, Haluska GJ, Hernandez-Guerrero C, Guevara-Silva R, Gravett MG, et al. Identification of matrix metalloproteinase-9 in amniotic fluid and amniochorion in spontaneous labor and after experimental intrauterine infection or interleukin-1β infusion in pregnant rhesus monkeys. Am J Obstet Gynecol [Internet]. 2002 Jan 1 [cited 2018 Jun 13];186(1):128–38. Available from: https://www.sciencedirect.com/science/article/pii/S0002937802606283

189. Ulug U, Goldman S, Ben-Shlomo I, Shalev E. Matrix metalloproteinase (MMP)-2 and MMP-9 and their inhibitor, TIMP-1, in human term decidua and fetal membranes: the effect of prostaglandin F2alpha and indomethacin. Mol Hum Reprod [Internet]. 2001 Dec 1 [cited 2018 Jun 13];7(12):1187–93. Available from: https://academic.oup.com/molehr/article-lookup/doi/10.1093/molehr/7.12.1187

190. Fortunato SJ, Menon R, Lombardi SJ, LaFleur B. Interleukin-10 inhibition of gelatinases in fetal membranes: therapeutic implications in preterm premature rupture of membranes. Obstet Gynecol [Internet]. 2001 Aug 1 [cited 2018 Jun 13];98(2):284–8. Available from: https://www.sciencedirect.com/science/article/pii/S0029784401014417

191. Watari M, Watari H, DiSanto ME, Chacko S, Shi G-P, Strauss JF. Pro-Inflammatory Cytokines Induce Expression of Matrix-Metabolizing Enzymes in Human Cervical Smooth Muscle Cells. Am J Pathol [Internet]. 1999 Jun 1 [cited 2018 Jun 12];154(6):1755–62. Available from: https://www.sciencedirect.com/science/article/pii/S0002944010654314?via%3Dihub

192. Osmers RGW, Adelmann-Grill BC, Rath W, Stuhlsatz HW, Tschesche H, Kuhn W. Biochemical Events in Cervical Ripening Dilatation during Pregnancy and Parturition. J Obstet Gynaecol (Lahore) [Internet]. 1995 Apr [cited 2018 Jun 13];21(2):185–94. Available from: http://doi.wiley.com/10.1111/j.1447-0756.1995.tb01092.x

193. Winkler M, Fischer D-C, Ruck P, Marx T, Kaiserling E, Oberpichler A, et al. Parturition at term: parallel increases in interleukin-8 and proteinase concentrations and neutrophil count in the lower uterine segment. Hum Reprod [Internet]. 1999 Apr 1 [cited 2018 Jun 13];14(4):1096–100. Available from: https://academic.oup.com/humrep/article-lookup/doi/10.1093/humrep/14.4.1096

194. Osmers RGW, Blaser J, Kuhn W, Tschesche H. Interleukin-8 synthesis and the onset of labor. Obstet Gynecol [Internet]. 1995 Aug 1 [cited 2018 Jun

13];86(2):223–9. Available from:
https://www.sciencedirect.com/science/article/pii/0029784495937044

195. Ito A, Sato T, Iga T, Mori Y. Tumor necrosis factor bifunctionally regulates matrix metalloproteinases and tissue inhibitor of metalloproteinases (TIMP) production by human fibroblasts. FEBS Lett [Internet]. 1990 Aug 20 [cited 2018 Jun 13];269(1):93–5. Available from:
https://www.sciencedirect.com/science/article/pii/001457939081127A

196. Goldenberg RL, Culhane JF, Iams JD, Romero R. Epidemiology and causes of preterm birth. Lancet. 2008;371(9606):75–84.

197. Romero R, Sirtori M, Oyarzun E, Avila C, Mazor M, Callahan R, et al. Infection and labor V. Prevalence, microbiology, and clinical significance of intraamniotic infection in women with preterm labor and intact membranes. Am J Obstet Gynecol [Internet]. 1989 Sep 1 [cited 2018 Jun 13];161(3):817–24. Available from:
https://www.sciencedirect.com/science/article/pii/0002937889904092

198. Hillier SL, Martius J, Krohn M, Kiviat N, Holmes KK, Eschenbach DA. A Case–Control Study of Chorioamnionic Infection and Histologic Chorioamnionitis in Prematurity. N Engl J Med [Internet]. 1988 Oct 13 [cited 2018 Jun 13];319(15):972–8. Available from:
http://www.nejm.org/doi/abs/10.1056/NEJM198810133191503

199. Krohn MA, Hillier SL, Nugent RP, Cotch MF, Carey JC, Gibbs RS, et al. The Genital Flora of Women with Intraamniotic Infection. J Infect Dis [Internet]. 1995 Jun 1 [cited 2018 Jun 13];171(6):1475–80. Available from:
https://academic.oup.com/jid/article-lookup/doi/10.1093/infdis/171.6.1475

200. Ernest JM, Wasilauskas B. Capnocytophaga in the amniotic fluid of a woman in preterm labor with intact membranes. Am J Obstet Gynecol [Internet]. 1985 Nov [cited 2018 Jun 14];153(6):648–9. Available from:
http://linkinghub.elsevier.com/retrieve/pii/S0002937885802519

201. Kim MJ, Romero R, Gervasi MT, Kim J-S, Yoo W, Lee D-C, et al. Widespread microbial invasion of the chorioamniotic membranes is a consequence and not a cause of intra-amniotic infection. Lab Investig [Internet]. 2009 Aug 8 [cited 2018 Jun 14];89(8):924–36. Available from:
http://www.nature.com/articles/labinvest200949

202. Gerber S, Vial Y, Hohlfeld P, Witkin SS. Detection of *Ureaplasma urealyticum* in Second-Trimester Amniotic Fluid by Polymerase Chain Reaction Correlates with Subsequent Preterm Labor and Delivery. J Infect Dis [Internet]. 2003 Feb 1 [cited 2018 Jun 14];187(3):518–21. Available from:
https://academic.oup.com/jid/article-lookup/doi/10.1086/368205

203. Namba F, Hasegawa T, Nakayama M, Hamanaka T, Yamashita T, Nakahira K, et al. Placental Features of Chorioamnionitis Colonized With Ureaplasma

Species in Preterm Delivery. Pediatr Res [Internet]. 2010 Feb 1 [cited 2018 Jun 14];67(2):166–72. Available from: http://www.nature.com/doifinder/10.1203/PDR.0b013e3181c6e58e

204. Cox C, Saxena N, Watt AP, Gannon C, McKenna JP, Fairley DJ, et al. The common vaginal commensal bacterium *Ureaplasma parvum* is associated with chorioamnionitis in extreme preterm labor. J Matern Neonatal Med [Internet]. 2016 Nov 16 [cited 2018 Jun 14];29(22):3646–51. Available from: https://www.tandfonline.com/doi/full/10.3109/14767058.2016.1140734

205. Shepard MC. The recovery of pleuropneumonia-like organisms from Negro men with and without nongonococcal urethritis. Am J Syph Gonorrhea Vener Dis [Internet]. 1954 Mar [cited 2018 Jun 14];38(2):113–24. Available from: http://www.ncbi.nlm.nih.gov/pubmed/13138817

206. Robertson JA. Effect of Gaseous Conditions on Isolation and Growth of Ureaplasma urealyticum on Agar. J Clin Microbiol [Internet]. 1982 [cited 2018 Jun 14];15(2):200–3. Available from: http://jcm.asm.org/content/15/2/200.full.pdf

207. Smith DG, Russell WC, Ingledew WJ, Thirkell D. Hydrolysis of urea by Ureaplasma urealyticum generates a transmembrane potential with resultant ATP synthesis. J Bacteriol [Internet]. 1993 Jun 1 [cited 2018 Jun 14];175(11):3253–8. Available from: http://www.ncbi.nlm.nih.gov/pubmed/8501029

208. Ford DK, Harasawa R, Kong F, Thirkell D, Robertson JA, Stemke GW, et al. Proposal of Ureaplasma parvum sp. nov. and emended description of Ureaplasma urealyticum (Shepard et al. 1974) Robertson et al. 2001. Int J Syst Evol Microbiol [Internet]. 2002 Mar 1 [cited 2018 Jun 14];52(2):587–97. Available from: http://ijs.microbiologyresearch.org/content/journal/ijsem/10.1099/00207713-52-2-587

209. Paralanov V, Lu J, Duffy LB, Crabb DM, Shrivastava S, Methé BA, et al. Comparative genome analysis of 19 Ureaplasma urealyticum and Ureaplasma parvum strains. BMC Microbiol [Internet]. 2012 May 30 [cited 2018 Jun 14];12(1):88. Available from: http://bmcmicrobiol.biomedcentral.com/articles/10.1186/1471-2180-12-88

210. Fanrong K, James G, Zhenfang M, Gordon S, Wang B, Gilbert GL. Phylogenetic analysis of Ureaplasma urealyticum - support for the establishment of a new species, Ureaplasma parvum. Int J Syst Bacteriol [Internet]. 1999 Oct 1 [cited 2018 Jun 14];49(4):1879–89. Available from: http://ijs.microbiologyresearch.org/content/journal/ijsem/10.1099/00207713-49-4-1879

211. Teng LJ, Zheng X, Glass JI, Watson HL, Tsai J, Cassell GH. Ureaplasma urealyticum biovar specificity and diversity are encoded in multiple-banded

antigen gene. J Clin Microbiol [Internet]. 1994 Jun 1 [cited 2018 Jun 14];32(6):1464–9. Available from: http://www.ncbi.nlm.nih.gov/pubmed/8077390

212. Knox CL, Giffard P, Timms P. The phylogeny of Ureaplasma urealyticum based on the mba gene fragment. Int J Syst Bacteriol [Internet]. 1998 Oct 1 [cited 2018 Jun 14];48(4):1323–31. Available from: http://ijs.microbiologyresearch.org/content/journal/ijsem/10.1099/00207713-48-4-1323

213. Saada A-B, Terespolski Y, Adoni A, Kahane' I. Adherence of Ureaplasma urealyticum to Human Erythrocytes [Internet]. Vol. 59, INFECTION AND IMMUNITY. 1991 [cited 2019 Feb 5]. Available from: https://www.ncbi.nlm.nih.gov/pmc/articles/PMC257768/pdf/iai00037-0487.pdf

214. Smith DGE, Russell WC, Thirkell D. Adherence of Ureaplasma urealyticum to human epithelial cells [Internet]. Vol. 140, Microbiology. 1994 [cited 2019 Feb 5]. Available from: www.microbiologyresearch.org

215. Padmini E, Uthra V. Role of Ureaplasma urealyticum in altering the endothelial metal concentration during preeclampsia. Placenta [Internet]. 2012 Apr 1 [cited 2019 Feb 5];33(4):304–11. Available from: https://www.sciencedirect.com/science/article/pii/S0143400412000379?via%3Dihub

216. Nishimura H, Emoto M, Kimura K, Yoshikai Y. Hsp70 protects macrophages infected with Salmonella choleraesuis against TNF-alpha-induced cell death. Cell Stress Chaperones [Internet]. 1997 Mar [cited 2019 Feb 5];2(1):50–9. Available from: http://www.ncbi.nlm.nih.gov/pubmed/9250395

217. Konturek J, Fischer H, … PK-J of P, 2001 U. Heat shock protein 70 (HSP70) in gastric adaptation to aspirin in Helicobacter pylori infection. J Physiol Pharmacol [Internet]. 2001 [cited 2019 Feb 5];52(1):153–64. Available from: http://agro.icm.edu.pl/agro/element/bwmeta1.element.agro-article-6db2d138-7c1b-4b18-89d0-c7f940a33a30/c/153_03_01_article.pdf

218. Li Y-H, Chen M, Brauner A, Zheng C, Skov Jensen J, Tullus K. Ureaplasma urealyticum Induces Apoptosis in Human Lung Epithelial Cells and Macrophages. Neonatology [Internet]. 2002 [cited 2019 Feb 5];82(3):166–73. Available from: http://www.ncbi.nlm.nih.gov/pubmed/12373067

219. Xiao L, Crabb DM, Dai Y, Chen Y, Waites KB, Atkinson TP. Suppression of antimicrobial peptide expression by ureaplasma species. Infect Immun [Internet]. 2014 Apr 1 [cited 2019 Feb 5];82(4):1657–65. Available from: http://www.ncbi.nlm.nih.gov/pubmed/24491573

220. Watson HL, Blalock DK, Cassell GH. Variable antigens of Ureaplasma urealyticum containing both serovar-specific and serovar-cross-reactive

epitopes. Infect Immun [Internet]. 1990 Nov 1 [cited 2019 Feb 5];58(11):3679–88. Available from: http://www.ncbi.nlm.nih.gov/pubmed/1699897

221. Glass JI, Lefkowitz EJ, Glass JS, Heiner CR, Chen EY, Cassell GH. The complete sequence of the mucosal pathogen Ureaplasma urealyticum. Nature [Internet]. 2000 Oct 12 [cited 2019 Feb 5];407(6805):757–62. Available from: http://www.nature.com/articles/35037619

222. von Chamier M, Allam A, Brown MB, Reinhard MK, Reyes L. Host Genetic Background Impacts Disease Outcome During Intrauterine Infection with Ureaplasma parvum. PLoS One. 2012;7(8):1–10.

223. Shimizu T, Kida Y, Kuwano K. Ureaplasma parvum lipoproteins, including MB antigen, activate NF-kB through TLR1, TLR2 and TLR6. Microbiology. 2008;154(5):1318–25.

224. Triantafilou M, De Glanville B, Aboklaish AF, Spiller OB, Kotecha S, Triantafilou K. Synergic Activation of Toll-Like Receptor (TLR) 2/6 and 9 in Response to Ureaplasma parvum & urealyticum in Human Amniotic Epithelial Cells. PLoS One. 2013;8(4).

225. Uchida K, Nakahira K, Mimura K, Shimizu T, De Seta F, Wakimoto T, et al. Effects of Ureaplasma parvum lipoprotein multiple-banded antigen on pregnancy outcome in mice. J Reprod Immunol [Internet]. 2013;100(2):118–27. Available from: http://dx.doi.org/10.1016/j.jri.2013.10.001

226. De Silva NS, Quinn PA. Endogenous activity of phospholipases A and C in Ureaplasma urealyticum. J Clin Microbiol [Internet]. 1986 Feb 1 [cited 2019 Feb 5];23(2):354–9. Available from: http://www.ncbi.nlm.nih.gov/pubmed/3700618

227. De Silva NS, Quinn PA. Localization of endogenous activity of phospholipases A and C in Ureaplasma urealyticum. J Clin Microbiol [Internet]. 1991 Jul 1 [cited 2019 Feb 5];29(7):1498–503. Available from: http://www.ncbi.nlm.nih.gov/pubmed/1885745

228. De Silva NS, Quinn PA. Characterization of phospholipase A1, A2, C activity in Ureaplasma urealyticum membranes. Mol Cell Biochem [Internet]. 1999 [cited 2019 Feb 5];201(1/2):159–67. Available from: http://link.springer.com/10.1023/A:1007082507407

229. Lin JS, Radnay K, Kendrick MI, Rosner B, Kass EH. Serologic studies of human genital mycoplasmas: distribution of titers of mycoplasmacidal antibody to Ureaplasma urealyticum and Mycoplasma hominis in pregnant women. J Infect Dis [Internet]. 1978 Mar [cited 2018 Jun 14];137(3):266–73. Available from: http://www.ncbi.nlm.nih.gov/pubmed/632625

230. Quinn PA, Shewchuk AB, Shuber J, Lie KI, Ryan E, Sheu M, et al. Serologic

evidence of ureaplasma urealyticum infection in women with spontaneous pregnancy loss. Am J Obstet Gynecol [Internet]. 1983 Jan 15 [cited 2018 Jun 14];145(2):245–50. Available from: http://www.ncbi.nlm.nih.gov/pubmed/6849359

231. Kong F, Ma Z, James G, Gordon S, Gilbert GL. Species identification and subtyping of Ureaplasma parvum and Ureaplasma urealyticum using PCR-based assays. J Clin Microbiol [Internet]. 2000 Mar 1 [cited 2018 Jun 14];38(3):1175–9. Available from: http://www.ncbi.nlm.nih.gov/pubmed/10699016

232. Francesco MA, Negrini R, Pinsi G, Peroni L, Manca N. Detection of Ureaplasma biovars and polymerase chain reaction-based subtyping of Ureaplasma parvum in women with or without symptoms of genital infections. Eur J Clin Microbiol Infect Dis [Internet]. 2009 Jun 8 [cited 2018 Jun 14];28(6):641–6. Available from: http://link.springer.com/10.1007/s10096-008-0687-z

233. Liu L, Cao G, Zhao Z, Zhao F, Huang Y. High bacterial loads of Ureaplasma may be associated with non-specific cervicitis. Scand J Infect Dis [Internet]. 2014 Sep 14 [cited 2018 Jun 14];46(9):637–41. Available from: http://www.tandfonline.com/doi/full/10.3109/00365548.2014.922696

234. Plummer DC, Garland SM, Gilbert GL. Bacteraemia and pelvic infection in women due to Ureaplasma urealyticum and Mycoplasma hominis. Med J Aust [Internet]. 1987 Feb 2 [cited 2018 Jun 14];146(3):135–7. Available from: http://www.ncbi.nlm.nih.gov/pubmed/3574192

235. Latthe PM, Toozs-Hobson P, Gray J. Mycoplasma and ureaplasma colonisation in women with lower urinary tract symptoms. J Obstet Gynaecol (Lahore) [Internet]. 2008 Jan 2 [cited 2018 Jun 14];28(5):519–21. Available from: http://www.tandfonline.com/doi/full/10.1080/01443610802097690

236. Povlsen K, Thorsen P, Lind I. Relationship of Ureaplasma urealyticum biovars to the presence or absence of bacterial vaginosis in pregnant women and to the time of delivery. Eur J Clin Microbiol Infect Dis [Internet]. 2001 Jan [cited 2018 Jun 14];20(1):65–7. Available from: http://www.ncbi.nlm.nih.gov/pubmed/11245329

237. Kataoka S, Yamada T, Chou K, Nishida R, Morikawa M, Minami M, et al. Association between preterm birth and vaginal colonization by mycoplasmas in early pregnancy. J Clin Microbiol [Internet]. 2006 Jan 1 [cited 2018 Jun 15];44(1):51–5. Available from: http://www.ncbi.nlm.nih.gov/pubmed/16390947

238. Kafetzis DA, Skevaki CL, Skouteri V, Gavrili S, Peppa K, Kostalos C, et al. Maternal Genital Colonization with Ureaplasma urealyticum Promotes Preterm Delivery: Association of the Respiratory Colonization of Premature Infants with Chronic Lung Disease and Increased Mortality. Clin Infect Dis

[Internet]. 2004 Oct 15 [cited 2018 Jun 15];39(8):1113–22. Available from: https://academic.oup.com/cid/article-lookup/doi/10.1086/424505

239. González Bosquet E, Gené A, Ferrer I, Borrás M, Lailla JM. Value of endocervical ureaplasma species colonization as a marker of preterm delivery. Gynecol Obstet Invest [Internet]. 2006 [cited 2018 Jun 15];61(3):119–23. Available from: http://www.ncbi.nlm.nih.gov/pubmed/16272816

240. Abele-Horn M, Scholz M, Wolff C, Kolben M. High-density vaginal Ureaplasma urealyticum colonization as a risk factor for chorioamnionitis and preterm delivery. Acta Obstet Gynecol Scand [Internet]. 2000 Nov [cited 2018 Jun 15];79(11):973–8. Available from: http://doi.wiley.com/10.1034/j.1600-0412.2000.079011973.x

241. Kwak D-W, Cho H-Y, Kwon J-Y, Park Y-W, Kim Y-H. Usefulness of maternal serum C-reactive protein with vaginal Ureaplasma urealyticum as a marker for prediction of imminent preterm delivery and chorioamnionitis in patients with preterm labor or preterm premature rupture of membranes. J Perinat Med [Internet]. 2015 Jan 1 [cited 2018 Jun 15];43(4):409–15. Available from: https://www.degruyter.com/view/j/jpme.2015.43.issue-4/jpm-2014-0142/jpm-2014-0142.xml

242. Vogel I, Thorsen P, Hogan VK, Schieve LA, Jacobsson B, Ferre CD. The joint effect of vaginal *Ureaplasma urealyticum* and bacterial vaginosis on adverse pregnancy outcomes. Acta Obstet Gynecol Scand [Internet]. 2006 Jan [cited 2018 Jun 15];85(7):778–85. Available from: http://doi.wiley.com/10.1080/00016340500442423

243. Cassell GH, Younger JB, Brown MB, Blackwell RE, Davis JK, Marriott P, et al. Microbiologic Study of Infertile Women at the Time of Diagnostic Laparoscopy. N Engl J Med [Internet]. 1983 Mar 3 [cited 2018 Jun 15];308(9):502–5. Available from: http://www.ncbi.nlm.nih.gov/pubmed/6218407

244. Taylor-Robinson D, Jensen JS, Svenstrup H, Stacey CM. Difficulties experienced in defining the microbial cause of pelvic inflammatory disease. Int J STD AIDS [Internet]. 2012 Jan 1 [cited 2018 Jun 15];23(1):18–24. Available from: http://journals.sagepub.com/doi/10.1258/ijsa.2011.011066

245. Urszula K, Joanna E, Marek E, Beata M, Magdalena SB. Colonization of the lower urogenital tract with Ureaplasma parvum can cause asymptomatic infection of the upper reproductive system in women: a preliminary study. Arch Gynecol Obstet [Internet]. 2014 May 7 [cited 2018 Jun 15];289(5):1129–34. Available from: http://link.springer.com/10.1007/s00404-013-3102-7

246. Tita ATN, Andrews WW. Diagnosis and Management of Clinical Chorioamnionitis. Clin Perinatol [Internet]. 2010 [cited 2018 Jun 15];37(2):339–54. Available from: https://www.clinicalkey.com/service/content/pdf/watermarked/1-s2.0-

S0095551081000217.pdf?locale=en_US

247.   Shurin PA, Alpert S, Rosner B, Driscoll SG, Lee Y-H, McCormack WM, et al. Chorioamnionitis and Colonization of the Newborn Infant with Genital Mycoplasmas. N Engl J Med [Internet]. 1975 Jul 3 [cited 2018 Jun 15];293(1):5–8. Available from: http://www.nejm.org/doi/abs/10.1056/NEJM197507032930102

248.   Viscardi RM, Hashmi N, Gross GW, Sun C-C, Rodriguez A, Fairchild KD. Incidence of invasive Ureaplasma in VLBW infants: relationship to severe intraventricular hemorrhage. J Perinatol [Internet]. 2008 Nov 3 [cited 2018 Jun 15];28(11):759–65. Available from: http://www.nature.com/articles/jp200898

249.   Hassanein SMA, El-Farrash RA, Hafez HM, Hassanin OM, Abd El Rahman NAE. Cord blood interleukin-6 and neonatal morbidities among preterm infants with PCR-positive *ureaplasma urealyticum*. J Matern Neonatal Med [Internet]. 2012 Oct 3 [cited 2018 Jun 15];25(10):2106–10. Available from: http://www.tandfonline.com/doi/full/10.3109/14767058.2012.678435

250.   Musilova I, Kutová R, Pliskova L, Stepan M, Menon R, Jacobsson B, et al. Intraamniotic Inflammation in Women with Preterm Prelabor Rupture of Membranes. Kanellopoulos-Langevin C, editor. PLoS One [Internet]. 2015 Jul 24 [cited 2018 Jun 15];10(7):e0133929. Available from: http://dx.plos.org/10.1371/journal.pone.0133929

251.   Stepan M, Cobo T, Musilova I, Hornychova H, Jacobsson B, Kacerovsky M. Maternal Serum C-Reactive Protein in Women with Preterm Prelabor Rupture of Membranes. Kanellopoulos-Langevin C, editor. PLoS One [Internet]. 2016 Mar 4 [cited 2018 Jun 15];11(3):e0150217. Available from: http://dx.plos.org/10.1371/journal.pone.0150217

252.   Kundsin RB, Driscoll SG, Monson RR, Yeh C, Biano SA, Cochran WD. Association of *Ureaplasma urealyticum* in the Placenta with Perinatal Morbidity and Mortality. N Engl J Med [Internet]. 1984 Apr 12 [cited 2018 Jun 15];310(15):941–5. Available from: http://www.nejm.org/doi/abs/10.1056/NEJM198404123101502

253.   Sweeney EL, Kallapur SG, Gisslen T, Lambers DS, Chougnet CA, Stephenson S-A, et al. Placental Infection With *Ureaplasma* species Is Associated With Histologic Chorioamnionitis and Adverse Outcomes in Moderately Preterm and Late-Preterm Infants. J Infect Dis [Internet]. 2016 Apr 15 [cited 2018 Jun 15];213(8):1340–7. Available from: https://academic.oup.com/jid/article-lookup/doi/10.1093/infdis/jiv587

254.   Olomu IN, Hecht JL, Onderdonk AO, Allred EN, Leviton A. Perinatal Correlates of Ureaplasma urealyticum in Placenta Parenchyma of Singleton Pregnancies That End Before 28 Weeks of Gestation for the Extremely Low Gestational Age Newborn Study Investigators. Pediatrics [Internet]. 2009

[cited 2018 Jun 15];123(5):1329–36. Available from: http://pediatrics.aappublications.org/content/pediatrics/123/5/1329.full.pdf

255. Van Marter LJ, Dammann O, Allred EN, Leviton A, Pagano M, Moore M, et al. Chorioamnionitis, mechanical ventilation, and postnatal sepsis as modulators of chronic lung disease in preterm infants. J Pediatr [Internet]. 2002 Feb 1 [cited 2018 Jun 15];140(2):171–6. Available from: https://www.sciencedirect.com/science/article/pii/S0022347602667083?via%3Dihub

256. Allam AB, von Chamier M, Brown MB, Reyes L. Immune profiling of BALB/C and C57BL/6 mice reveals a correlation between ureaplasma parvum-induced fetal inflammatory response syndrome-like pathology and increased placental expression of TLR2 and CD14. Am J Reprod Immunol. 2014;71(3):241–51.

257. Espinoza J, Chaiworapongsa T, Romero R, Gomez R, Kim JC, Yoshimatsu J, et al. Evidence of participation of soluble CD14 in the host response to microbial invasion of the amniotic cavity and intra-amniotic inflammation in term and preterm gestations. J Matern Neonatal Med [Internet]. 2002 Jan 7 [cited 2018 Jun 15];12(5):304–12. Available from: http://www.tandfonline.com/doi/full/10.1080/jmf.12.5.304.312

258. Dando SJ, Nitsos I, Kallapur SG, Newnham JP, Polglase GR, Pillow JJ, et al. The Role of the Multiple Banded Antigen of Ureaplasma parvum in Intra-Amniotic Infection: Major Virulence Factor or Decoy? Ratner AJ, editor. PLoS One [Internet]. 2012 Jan 12 [cited 2018 Jun 15];7(1):e29856. Available from: http://dx.plos.org/10.1371/journal.pone.0029856

259. Moss TJM, Knox CL, Kallapur SG, Nitsos I, Theodoropoulos C, Newnham JP, et al. Experimental amniotic fluid infection in sheep: Effects of Ureaplasma parvum serovars 3 and 6 on preterm or term fetal sheep. Am J Obstet Gynecol [Internet]. 2008 Jan 1 [cited 2018 Jun 15];198(1):122.e1-122.e8. Available from: https://www.sciencedirect.com/science/article/pii/S0002937807008411?via%3Dihub

260. Yoder BA, Coalson JJ, Winter VT, Siler-Khodr T, Duffy LB, Cassell GH. Effects of Antenatal Colonization with Ureaplasma urealyticum on Pulmonary Disease in the Immature Baboon. Pediatr Res [Internet]. 2003 Dec 1 [cited 2018 Jun 15];54(6):797–807. Available from: http://www.nature.com/doifinder/10.1203/01.PDR.0000091284.84322.16

261. Senthamaraikannan P, Presicce P, Rueda CM, Maneenil G, Schmidt AF, Miller LA, et al. Intra-amniotic *Ureaplasma parvum* –Induced Maternal and Fetal Inflammation and Immune Responses in Rhesus Macaques. J Infect Dis [Internet]. 2016 Nov 15 [cited 2018 Jun 15];214(10):1597–604. Available from: https://academic.oup.com/jid/article-lookup/doi/10.1093/infdis/jiw408

262. Novy MJ, Duffy L, Axthelm MK, Sadowsky DW, Witkin SS, Gravett MG, et al. Ureaplasma parvum or Mycoplasma hominis as sole pathogens cause chorioamnionitis, preterm delivery, and fetal pneumonia in rhesus macaques. Reprod Sci. 2009;16(1):56–70.

263. Read CP, Word RA, Ruscheinsky MA, Timmons BC, Mahendroo MS. Cervical remodeling during pregnancy and parturition: molecular characterization of the softening phase in mice. Reproduction [Internet]. 2007 Aug 1 [cited 2018 Jun 16];134(2):327–40. Available from: http://www.ncbi.nlm.nih.gov/pubmed/17660242

264. Akins ML, Luby-Phelps K, Bank RA, Mahendroo M. Cervical Softening During Pregnancy: Regulated Changes in Collagen Cross-Linking and Composition of Matricellular Proteins in the Mouse. Biol Reprod [Internet]. 2011 May 1 [cited 2018 Jun 16];84(5):1053–62. Available from: https://academic.oup.com/biolreprod/article-lookup/doi/10.1095/biolreprod.110.089599

265. Akins ML, Luby-Phelps K, Mahendroo M. Errata: Second harmonic generation imaging as a potential tool for staging pregnancy and predicting preterm birth. J Biomed Opt [Internet]. 2010 [cited 2018 Jun 16];15(3):039802. Available from: http://biomedicaloptics.spiedigitallibrary.org/article.aspx?doi=10.1117/1.3459021

266. Bornstein P, Sage EH. Matricellular proteins: extracellular modulators of cell function. Curr Opin Cell Biol [Internet]. 2002 Oct 1 [cited 2018 Jun 16];14(5):608–16. Available from: https://www.sciencedirect.com/science/article/pii/S0955067402003617?via%3Dihub

267. Timmons B, Akins M, Mahendroo M. Cervical remodeling during pregnancy and parturition. Trends Endocrinol Metab [Internet]. 2010 Jun 1 [cited 2018 Jun 16];21(6):353–61. Available from: https://www.sciencedirect.com/science/article/pii/S1043276010000251?via%3Dihub

268. Blaskewicz CD, Pudney J, Anderson DJ. Structure and Function of Intercellular Junctions in Human Cervical and Vaginal Mucosal Epithelia1. Biol Reprod [Internet]. 2011;85(1):97–104. Available from: https://academic.oup.com/biolreprod/article-lookup/doi/10.1095/biolreprod.110.090423

269. Timmons BC, Mitchell SM, Gilpin C, Mahendroo MS. Dynamic changes in the cervical epithelial tight junction complex and differentiation occur during cervical ripening and parturition. Endocrinology. 2007;148(3):1278–87.

270. Furuse M, Furuse K, Sasaki H, Tsukita S. Conversion of zonulae occludentes from tight to leaky strand type by introducing claudin-2 into Madin-Darby

canine kidney I cells. J Cell Biol [Internet]. 2001 Apr 16 [cited 2018 Jun 16];153(2):263–72. Available from: http://www.ncbi.nlm.nih.gov/pubmed/11309408

271. Furuse M, Hata M, Furuse K, Yoshida Y, Haratake A, Sugitani Y, et al. Claudin-based tight junctions are crucial for the mammalian epidermal barrier. J Cell Biol [Internet]. 2002 Mar 18 [cited 2018 Jun 16];156(6):1099–111. Available from: http://www.ncbi.nlm.nih.gov/pubmed/11889141

272. Zeng R, Li X, Gorodeski GI. Estrogen Abrogates Transcervical Tight Junctional Resistance by Acceleration of Occludin Modulation. J Clin Endocrinol Metab [Internet]. 2004 Oct 1 [cited 2018 Jun 16];89(10):5145–55. Available from: https://academic.oup.com/jcem/article-lookup/doi/10.1210/jc.2004-0823

273. Zhu L, Li X, Zeng R, Gorodeski GI. Changes in Tight Junctional Resistance of the Cervical Epithelium Are Associated with Modulation of Content and Phosphorylation of Occludin 65-Kilodalton and 50-Kilodalton Forms. Endocrinology [Internet]. 2006 Feb 1 [cited 2018 Jun 16];147(2):977–89. Available from: https://academic.oup.com/endo/article-lookup/doi/10.1210/en.2005-0916

274. Mendoza-Rodriguez CA, Gonzalez-Mariscal L, Cerbon M. Changes in the distribution of ZO-1, occludin, and claudins in the rat uterine epithelium during the estrous cycle. Cell Tissue Res [Internet]. 2005 Feb 19 [cited 2018 Jun 16];319(2):315–30. Available from: http://link.springer.com/10.1007/s00441-004-1010-7

275. Parris JJ, Cooke VG, Skarnes WC, Duncan MK, Naik UP. JAM-A expression during embryonic development. Dev Dyn [Internet]. 2005 Aug [cited 2018 Jun 16];233(4):1517–24. Available from: http://www.ncbi.nlm.nih.gov/pubmed/15977176

276. Hassan SS, Romero R, Pineles B, Tarca AL, Montenegro D, Erez O, et al. MicroRNA expression profiling of the human uterine cervix after term labor and delivery. Am J Obstet Gynecol [Internet]. 2010 Jan 1 [cited 2018 Jun 16];202(1):80.e1-80.e8. Available from: https://www.sciencedirect.com/science/article/pii/S0002937809009417?via%3Dihub

277. Sanders AP, Burris HH, Just AC, Motta V, Svensson K, Mercado-Garcia A, et al. microRNA expression in the cervix during pregnancy is associated with length of gestation. Epigenetics [Internet]. 2015 Mar 4 [cited 2018 Jun 16];10(3):221–8. Available from: http://www.tandfonline.com/doi/full/10.1080/15592294.2015.1006498

278. Elovitz MA, Brown AG, Anton L, Gilstrop M, Heiser L, Bastek J. Distinct cervical microRNA profiles are present in women destined to have a preterm birth. Am J Obstet Gynecol [Internet]. 2014 Mar 1 [cited 2018 Jun

16];210(3):221.e1-221.e11. Available from:
https://www.sciencedirect.com/science/article/pii/S0002937813022886?via%3
Dihub

279. Anton L, DeVine A, Sierra L-J, Brown AG, Elovitz MA. miR-143 and miR-145 disrupt the cervical epithelial barrier through dysregulation of cell adhesion, apoptosis and proliferation. Sci Rep [Internet]. 2017 Dec 8 [cited 2018 Jun 16];7(1):3020. Available from: http://www.nature.com/articles/s41598-017-03217-7

280. Akgul Y, Word RA, Ensign LM, Yamaguchi Y, Lydon J, Hanes J, et al. Hyaluronan in cervical epithelia protects against infection-mediated preterm birth. J Clin Invest. 2014;124(12):5481–9.

281. Lashkari BS, Shahana S, Anumba DO. Toll-like receptor 2 and 4 expression in the pregnant and non-pregnant human uterine cervix. J Reprod Immunol [Internet]. 2015;107:43–51. Available from: http://dx.doi.org/10.1016/j.jri.2014.10.001

282. Nallasamy S, Mahendroo M. Distinct Roles of Cervical Epithelia and Stroma in Pregnancy and Parturition. Semin Reprod Med. 2017;35(2):190–9.

283. Itaoka N, Nagamatsu T, Schust DJ, Ichikawa M, Sayama S, Iwasawa-Kawai Y, et al. Cervical expression of elafin and SLPI in pregnancy and their association with preterm labor. Am J Reprod Immunol. 2015;73(6):536–44.

284. Stock SJ, Duthie L, Tremaine T, Calder A a, Kelly RW, Riley SC. Elafin (SKALP/Trappin-2/proteinase inhibitor-3) is produced by the cervix in pregnancy and cervicovaginal levels are diminished in bacterial vaginosis. Reprod Sci. 2009;16(12):1125–34.

285. Frew L, Makieva S, McKinlay ATM, McHugh BJ, Doust A, Norman JE, et al. Human cathelicidin production by the cervix. PLoS One. 2014;9(8):1–10.

286. Racicot K, Cardenas I, Wünsche V, Aldo P, Guller S, Means RE, et al. Viral infection of the pregnant cervix predisposes to ascending bacterial infection. J Immunol [Internet]. 2013;191(2):934–41. Available from: http://www.ncbi.nlm.nih.gov/pubmed/23752614

287. Hein M, Valore E V., Helmig RB, Uldbjerg N, Ganz T. Antimicrobial factors in the cervical mucus plug. Am J Obstet Gynecol. 2002;187(1):137–44.

288. Helmig R, Uldbjerg N, Ohlsson K. Secretory leukocyte protease inhibitor in the cervical mucus and in the fetal membranes. Eur J Obstet Gynecol Reprod Biol. 1995;59(1):95–101.

289. Rizzo G, Capponi A, Rinaldo D, Tedeschi D, Arduini D, Romanini C. Interleukin-6 concentrations in cervical secretions identify microbial invasion of the amniotic cavity in patients with preterm labor and intact membranes. Am J Obstet Gynecol [Internet]. 1996 Oct 1 [cited 2018 Jun 17];175(4):812–7.

Available from:
https://www.sciencedirect.com/science/article/pii/S0002937896800044?via%3
Dihub

290. Jacobsson B, Mattsby-Baltzer I, Hagberg H. Interleukin-6 and interleukin-8 in cervical and amniotic fluid: relationship to microbial invasion of the chorioamniotic membranes. BJOG An Int J Obstet Gynaecol [Internet]. 2005 Jun [cited 2018 Jun 17];112(6):719–24. Available from: http://doi.wiley.com/10.1111/j.1471-0528.2005.00536.x

291. Jacobsson B, Holst R-M, Mattsby-Baltzer I, Nikolaitchouk N, Wennerholm U-B, Hagberg H. Interleukin-18 in cervical mucus and amniotic fluid: relationship to microbial invasion of the amniotic fluid, intra-amniotic inflammation and preterm delivery. BJOG An Int J Obstet Gynaecol [Internet]. 2003 Jun [cited 2018 Jun 17];110(6):598–603. Available from: http://doi.wiley.com/10.1046/j.1471-0528.2003.02445.x

292. Rizzo G, Capponi A, Vlachopoulou A, Angelini E, Grassi C, Romanini C. Interleukin-6 concentrations in cervical secretions in the prediction of intrauterine infection in preterm premature rupture of the membranes. Gynecol Obstet Invest [Internet]. 1998 Aug [cited 2018 Jun 17];46(2):91–5. Available from: http://www.ncbi.nlm.nih.gov/pubmed/9701687

293. Lockwood CJ, Ghidini lessandro, Wein R, Lapinski R, Casal D, Berkowitz RL. Increased interleukin-6 concentrations in cervical secretions are associated with preterm delivery. Am J Obstet Gynecol [Internet]. 1994 Oct 1 [cited 2018 Jun 17];171(4):1097–102. Available from: https://www.sciencedirect.com/science/article/pii/0002937894900434?via%3
Dihub

294. Lange M, Chen FK, Wessel J, Buscher U, Dudenhausen JW. Elevation of interleukin-6 levels in cervical secretions as a predictor of preterm delivery. Acta Obstet Gynecol Scand [Internet]. 2003 Apr [cited 2018 Jun 17];82(4):326–9. Available from: http://doi.wiley.com/10.1034/j.1600-0412.2003.00149.x

295. Holst R-M, Mattsby-Baltzer I, Wennerholm U-B, Hagberg H, Jacobsson B. Interleukin-6 and interleukin-8 in cervical fluid in a population of Swedish women in preterm labor: relationship to microbial invasion of the amniotic fluid, intra-amniotic inflammation, and preterm delivery. Acta Obstet Gynecol Scand [Internet]. 2005 Jun [cited 2018 Jun 17];84(6):551–7. Available from: http://doi.wiley.com/10.1111/j.0001-6349.2005.00708.x

296. Hein M, Petersen AC, Helmig RB, Uldbjerg N, Reinholdt J. Immunoglobulin levels and phagocytes in the cervical mucus plug at term of pregnancy. Acta Obstet Gynecol Scand [Internet]. 2005 Aug [cited 2018 Jun 17];84(8):734–42. Available from: http://www.blackwell-synergy.com/doi/abs/10.1111/j.0001-6349.2005.00525.x

297. Saha K, Bhatia G, Mukherjee S, Mitra A, Luthra U. Fluctuation of immunoglobulin levels in cervical mucus during the various phases of female reproductive life and its alteration in uterine disorders. 1981 [cited 2018 Jun 17]; Available from: https://scholar.google.com/scholar_lookup?hl=en&volume=74&publication_year=1981&pages=696-704&journal=Indian+J+Med+Res.&author=K+Sahaauthor=G+Bhatiaauthor=S+Mukherjeeauthor=AB+Mitraauthor=UK+Luthra&title=Fluctuation+of+immunoglobulin+levels+in+cervical+mucus+during+the+various+phases+of+female+reproductive+life+and+its+alteration+in+uterine+disorders

298. Hein M, Helmig RB, Schønheyder HC, Ganz T, Uldbjerg N. An in vitro study of antibacterial properties of the cervical mucus plug in pregnancy. Am J Obstet Gynecol [Internet]. 2001 Sep 1 [cited 2018 Jun 17];185(3):586–92. Available from: https://www.sciencedirect.com/science/article/pii/S0002937801510728?via%3Dihub

299. Prendiville W, Cullimore J, Norman S. Large loop excision of the transformation zone (LLETZ). A new method of management for women with cervical intraepithelial neoplasia. BJOG An Int J Obstet Gynaecol [Internet]. 1989 Sep [cited 2018 Jun 17];96(9):1054–60. Available from: http://doi.wiley.com/10.1111/j.1471-0528.1989.tb03380.x

300. Sadler L, Saftlas A, Wang W, Exeter M, Whittaker J, McCowan L. Treatment for Cervical Intraepithelial Neoplasia and Risk of Preterm Delivery. JAMA [Internet]. 2004 May 5 [cited 2018 Jun 17];291(17):2100. Available from: http://jama.jamanetwork.com/article.aspx?doi=10.1001/jama.291.17.2100

301. Albrechtsen S, Rasmussen S, Thoresen S, Irgens LM, Iversen OE. Pregnancy outcome in women before and after cervical conisation: population based cohort study. BMJ [Internet]. 2008 Sep 18 [cited 2018 Jun 17];337:a1343. Available from: http://www.ncbi.nlm.nih.gov/pubmed/18801869

302. Noehr B, Jensen A, Frederiksen K, Tabor A, Kjaer SK. Loop electrosurgical excision of the cervix and subsequent risk for spontaneous preterm delivery: a population-based study of singleton deliveries during a 9-year period. Am J Obstet Gynecol [Internet]. 2009 Jul 1 [cited 2018 Jun 17];201(1):33.e1-33.e6. Available from: https://www.sciencedirect.com/science/article/pii/S0002937809001896?via%3Dihub

303. Poon L, Savvas M, Zamblera D, Skyfta E, Nicolaides K. Large loop excision of transformation zone and cervical length in the prediction of spontaneous preterm delivery. BJOG An Int J Obstet Gynaecol [Internet]. 2012 May [cited 2018 Jun 17];119(6):692–8. Available from: http://doi.wiley.com/10.1111/j.1471-0528.2011.03203.x

304. Kyrgiou M, Koliopoulos G, Martin-Hirsch P, Arbyn M, Prendiville W,

Paraskevaidis E. Obstetric outcomes after conservative treatment for intraepithelial or early invasive cervical lesions: Systematic review and meta-analysis. Lancet. 2006;367(9509):489–98.

305. Bruinsma F, Quinn M. The risk of preterm birth following treatment for precancerous changes in the cervix: a systematic review and meta-analysis. BJOG An Int J Obstet Gynaecol [Internet]. 2011 Aug [cited 2018 Jun 17];118(9):1031–41. Available from: http://doi.wiley.com/10.1111/j.1471-0528.2011.02944.x

306. Mitchell BF, Taggart MJ. Are animal models relevant to key aspects of human parturition? Am J Physiol Integr Comp Physiol [Internet]. 2009 Sep [cited 2018 Jun 19];297(3):R525–45. Available from: http://www.physiology.org/doi/10.1152/ajpregu.00153.2009

307. Barry JS, Anthony RV. The pregnant sheep as a model for human pregnancy. Theriogenology [Internet]. 2008 Jan 1 [cited 2018 Jul 31];69(1):55–67. Available from: https://www.sciencedirect.com/science/article/pii/S0093691X07005717

308. Kemp MW, Saito M, Newnham JP, Nitsos I, Okamura K, Kallapur SG. Preterm Birth, Infection, and Inflammation Advances From the Study of Animal Models. Reprod Sci [Internet]. 2010 [cited 2018 Jun 19];17(7):619–28. Available from: http://journals.sagepub.com/doi/pdf/10.1177/1933719110373148

309. Liggins GC. Premature parturition after infusion of corticotrophin or cortisol into foetal lambs. J Endocrinol [Internet]. 1968 Oct 1 [cited 2018 Jun 20];42(2):323–9. Available from: http://www.ncbi.nlm.nih.gov/pubmed/4307649

310. Liggins GC. Premature delivery of foetal lambs infused with glucocorticoids. J Endocrinol [Internet]. 1969 Dec 1 [cited 2018 Jun 20];45(4):515–23. Available from: http://www.ncbi.nlm.nih.gov/pubmed/5366112

311. Cahill L, Knee B, And RL-J of reproduction, 1976 U. Proceedings: Induction of parturition in sheep with a single dose of oestradiol benzoate. J Reprod Fertil [Internet]. 1976 [cited 2018 Jun 20];46(2):528–9. Available from: http://europepmc.org/abstract/med/1255624

312. Liggins GC, Grieves S. Possible Role for Prostaglandin F2α in Parturition in Sheep. Nature [Internet]. 1971 Aug 27 [cited 2018 Jun 20];232(5313):629–31. Available from: http://www.nature.com/doifinder/10.1038/232629a0

313. Harman EL, Slyter AL. Induction of Parturition in the Ewe. J Anim Sci [Internet]. 1980 Mar 1 [cited 2018 Jun 20];50(3):391–3. Available from: https://academic.oup.com/jas/article/50/3/391-393/4744240

314. Taylor MJ, Webb R, Mitchell MD, Robinson JS. Effect of progesterone

withdrawal in sheep during late pregnancy. J Endocrinol [Internet]. 1982 Jan 1 [cited 2018 Jun 20];92(1):85–93. Available from: http://www.ncbi.nlm.nih.gov/pubmed/7057124

315.	Young IR, Deayton JM, Hollingworth SA, Thorburn GD. Continuous intrafetal infusion of prostaglandin E2 prematurely activates the hypothalamo-pituitary-adrenal axis and induces parturition in sheep. Endocrinology [Internet]. 1996 Jun 1 [cited 2018 Jun 20];137(6):2424–31. Available from: https://academic.oup.com/endo/article-lookup/doi/10.1210/endo.137.6.8641195

316.	Smith R. Parturition. N Engl J Med. 2007;356(3):271–83.

317.	Schlafer DH, Yuh B, Foley GL, Elssaser TH, Sadowsky D, Nathanielsz PW. Effect of Salmonella Endotoxin Administered to the Pregnant Sheep at 133–142 Days Gestation on Fetal Oxygenation, Maternal and Fetal Adrenocorticotropic Hormone and Cortisol, and Maternal Plasma Tufnor Necrosis Factor α Concentrations1. Biol Reprod [Internet]. 1994 Jun 1 [cited 2018 Jun 20];50(6):1297–302. Available from: https://academic.oup.com/biolreprod/article-lookup/doi/10.1095/biolreprod50.6.1297

318.	Masaoka N, Watanabe M, Nakajima Y. The effects of sivelestat sodium hydrate on uterine contraction and the concentration of maternal and fetal blood cytokines in a sheep model of intra-amniotic infection induced by lipopolysaccharide. J Matern Neonatal Med [Internet]. 2011 Aug 24 [cited 2018 Jun 20];24(8):1013–8. Available from: http://www.tandfonline.com/doi/full/10.3109/14767058.2010.545904

319.	Grigsby PL, Hirst JJ, Scheerlinck J-P, Phillips DJ, Jenkin G. Fetal Responses to Maternal and Intra-Amniotic Lipopolysaccharide Administration in Sheep1. Biol Reprod [Internet]. 2003 May 1 [cited 2018 Jun 20];68(5):1695–702. Available from: https://academic.oup.com/biolreprod/article-lookup/doi/10.1095/biolreprod.102.009688

320.	Kallapur SG, Willet KE, Jobe AH, Ikegami M, Bachurski CJ. Intra-amniotic endotoxin: chorioamnionitis precedes lung maturation in preterm lambs. Am J Physiol Cell Mol Physiol [Internet]. 2001 Mar [cited 2018 Jun 20];280(3):L527–36. Available from: http://www.physiology.org/doi/10.1152/ajplung.2001.280.3.L527

321.	Moss TJ., Nitsos I, Newnham JP, Ikegami M, Jobe AH. Chorioamnionitis induced by subchorionic endotoxin infusion in sheep. Am J Obstet Gynecol [Internet]. 2003 Dec 1 [cited 2018 Jun 20];189(6):1771–6. Available from: https://www.sciencedirect.com/science/article/pii/S000293780300810X

322.	Moss TJM, Nitsos I, Ikegami M, Jobe AH, Newnham JP. Experimental intrauterine Ureaplasma infection in sheep. Am J Obstet Gynecol [Internet]. 2005 Apr 1 [cited 2018 Jun 20];192(4):1179–86. Available from:

https://www.sciencedirect.com/science/article/pii/S0002937804020769?via%3
Dihub

323. Elovitz M a., Mrinalini C. Animal models of preterm birth. Trends Endocrinol
Metab. 2004;15(10):479–87.

324. Adams Waldorf K, Rubens C, Gravett M. Use of nonhuman primate models to
investigate mechanisms of infection-associated preterm birth. BJOG An Int J
Obstet Gynaecol [Internet]. 2011 Jan [cited 2018 Jun 19];118(2):136–44.
Available from: http://doi.wiley.com/10.1111/j.1471-0528.2010.02728.x

325. Bryant JM. Vest and tethering system to accommodate catheters and a
temperature monitor for nonhuman primates. Lab Anim Sci [Internet]. 1980
Aug [cited 2018 Jul 31];30(4 Pt 1):706–8. Available from:
http://www.ncbi.nlm.nih.gov/pubmed/6775135

326. Novy M, Walsh S, … MC in fetal, 1980 U. Chronic implantation of catheters
and electrodes in pregnant nonhuman primates. Elsevier/north-holl Biomed …
[Internet]. 1980 [cited 2018 Jul 31]; Available from:
https://scholar.google.co.uk/scholar?hl=en&as_sdt=0%2C5&q=Chronic+Impl
antation+of+Catheters+and+Electrodes+in+Pregnant+Nonhuman+Primates&b
tnG=

327. Germain G, Cabrol D, Visser A, Sureati C. Electrical activity of the pregnant
uterus in the cynomolgus monkey. Am J Obstet Gynecol [Internet]. 1982 Mar
1 [cited 2018 Jun 20];142(5):513–9. Available from:
https://www.sciencedirect.com/science/article/pii/0002937882907530

328. Reinheimer TM. Barusiban suppresses oxytocin-induced preterm labour in
non-human primates. BMC Pregnancy Child Birth [Internet]. 2007 [cited 2018
Jun 20];7(Supp l1):S15. Available from:
https://www.ncbi.nlm.nih.gov/pmc/articles/PMC1892056/pdf/1471-2393-7-
S1-S15.pdf

329. Reinheimer TM, Chellman GJ, Resendez JC, Meyer JK, Bee WH. Barusiban,
An Effective Long-Term Treatment of Oxytocin-Induced Preterm Labor in
Nonhuman Primates1. Biol Reprod [Internet]. 2006 Nov 1 [cited 2018 Jun
20];75(5):809–14. Available from:
https://academic.oup.com/biolreprod/article-
lookup/doi/10.1095/biolreprod.106.053637

330. Gravett MG, Witkin SS, Haluska GJ, Edwards JL, Cook MJ, Novy MJ. An
experimental model for intraamniotic infection and preterm labor in rhesus
monkeys. Am J Obstet Gynecol [Internet]. 1994 Dec 1 [cited 2018 Jun
20];171(6):1660–7. Available from:
https://www.sciencedirect.com/science/article/pii/0002937894904189?via%3
Dihub

331. Grigsby PL, Novy MJ, Waldorf KMA, Sadowsky DW, Gravett MG.

Choriodecidual Inflammation: A Harbinger of the Preterm Labor Syndrome. Reprod Sci [Internet]. 2010 [cited 2018 Jun 20];17(1):85–94. Available from: http://journals.sagepub.com/doi/pdf/10.1177/1933719109348025

332. Gravett MG, Adams KM, Sadowsky DW, Grosvenor AR, Witkin SS, Axthelm MK, et al. Immunomodulators plus antibiotics delay preterm delivery after experimental intraamniotic infection in a nonhuman primate model. Am J Obstet Gynecol [Internet]. 2007 Nov 1 [cited 2018 Jun 20];197(5):518.e1-518.e8. Available from: https://www.sciencedirect.com/science/article/pii/S0002937807004309?via%3Dihub

333. Baggia S, Gravett MG, Witkin SS, Haluska GJ, Novy MJ. Interleukin-Iβ Intra-Amniotic Infusion Induces TUmor Necrosis Factor-α, Prostaglandin Production, and Preterm COntractions in Pregnant Rhesus Monkeys. J Soc Gynecol Investig [Internet]. 1996 May 5 [cited 2018 Jun 20];3(3):121–6. Available from: http://www.ncbi.nlm.nih.gov/pubmed/8796819

334. Sadowsky DW, Adams KM, Gravett MG, Witkin SS, Novy MJ. Preterm labor is induced by intraamniotic infusions of interleukin-1β and tumor necrosis factor-α but not by interleukin-6 or interleukin-8 in a nonhuman primate model. Am J Obstet Gynecol [Internet]. 2006 Dec 1 [cited 2018 Jun 20];195(6):1578–89. Available from: https://www.sciencedirect.com/science/article/pii/S0002937806008313

335. Sadowsky DW, Haluska GJ, Gravett MG, Witkin SS, Novy MJ. Indomethacin blocks interleukin 1β–induced myometrial contractions in pregnant rhesus monkeys. Am J Obstet Gynecol [Internet]. 2000 Jul 1 [cited 2018 Jun 20];183(1):173–80. Available from: https://www.sciencedirect.com/science/article/pii/S0002937800339746

336. Adams Waldorf KM, Persing D, Novy MJ, Sadowsky DW, Gravett MG. Pretreatment with toll-like receptor 4 antagonist inhibits lipopolysaccharide-induced preterm uterine contractility, cytokines, and prostaglandins in rhesus monkeys. Reprod Sci [Internet]. 2008 Feb [cited 2018 Jun 20];15(2):121–7. Available from: http://www.ncbi.nlm.nih.gov/pubmed/18187405

337. Rendi MH, Muehlenbachs A, Garcia RL, Boyd KL. Female Reproductive System [Internet]. First Edit. Comparative Anatomy and Histology. Elsevier Inc.; 2012. 253-284 p. Available from: http://dx.doi.org/10.1016/B978-0-12-381361-9.00017-2

338. Pang SC, Janzen-Pang J, Tse MY, Croy BA, Lima PDA. The Cycling and Pregnant Mouse [Internet]. The Guide to Investigation of Mouse Pregnancy. Elsevier; 2014. 3-19 p. Available from: http://linkinghub.elsevier.com/retrieve/pii/B9780123944450000011

339. Hilliard J. Corpus Luteum Function in Guinea Pigs, Hamsters, Rats, Mice and Rabbits1. Biol Reprod [Internet]. 1973 Mar 1 [cited 2018 Jul 31];8(2):203–21.

Available from: https://academic.oup.com/biolreprod/article-lookup/doi/10.1093/biolreprod/8.2.203

340. Tuckey RC. Progesterone synthesis by the human placenta. Placenta [Internet]. 2005 Apr 1 [cited 2018 Jul 31];26(4):273–81. Available from: https://www.sciencedirect.com/science/article/pii/S0143400404001705

341. Lefebvre D, Giaid A, Bennett H, Lariviere R, Zingg H, Nishimura T, et al. Oxytocin gene expression in rat uterus. Science (80-) [Internet]. 1992 Jun 12 [cited 2018 Jul 31];256(5063):1553–5. Available from: http://www.ncbi.nlm.nih.gov/pubmed/1598587

342. Mitchell BF, Wong S. Changes in 17β,20α-hydroxysteroid dehydrogenase activity supporting an increase in the estrogen/progesterone ratio of human fetal membranes at parturition. Am J Obstet Gynecol [Internet]. 1993 May 1 [cited 2018 Jul 31];168(5):1377–85. Available from: http://linkinghub.elsevier.com/retrieve/pii/S0002937811907686

343. Chaim W, Mazor M. The relationship between hormones and human parturition. Arch Gynecol Obstet [Internet]. 1998 Nov 2 [cited 2018 Jul 31];262(1–2):43–51. Available from: http://link.springer.com/10.1007/s004040050226

344. Hirsch E, Muhle R. Intrauterine Bacterial Inoculation Induces Labor in the Mouse by Mechanisms Other than Progesterone Withdrawal1. Biol Reprod [Internet]. 2002 Oct 1 [cited 2018 Jun 20];67(4):1337–41. Available from: https://academic.oup.com/biolreprod/article-lookup/doi/10.1095/biolreprod67.4.1337

345. Elovitz M, Wang Z. Medroxyprogesterone acetate, but not progesterone, protects against inflammation-induced parturition and intrauterine fetal demise. Am J Obstet Gynecol [Internet]. 2004 Mar [cited 2018 Jun 20];190(3):693–701. Available from: http://linkinghub.elsevier.com/retrieve/pii/S0002937803019501

346. Strauss JF, Sokoloski J, Capole P, Duffy P, Mintz G, Stambaugh RL. On the Role of Prostaglandins in Parturition in the Rat. Endocrinology [Internet]. 1975 Apr 1 [cited 2018 Jun 21];96(4):1040–3. Available from: https://academic.oup.com/endo/article-lookup/doi/10.1210/endo-96-4-1040

347. Celik H, Ayar A. Effects of erythromycin on pregnancy duration and birth weight in lipopolysaccharide-induced preterm labor in pregnant rats. Eur J Obstet Gynecol Reprod Biol [Internet]. 2002 Jun [cited 2018 Jun 21];103(1):22–5. Available from: http://linkinghub.elsevier.com/retrieve/pii/S0301211502000180

348. Bennett WA, Terrone DA, Rinehart BK, Kassab S, Martin JN, Granger JP. Intrauterine endotoxin infusion in rat pregnancy induces preterm delivery and increases placental prostaglandin F2α metabolite levels. Am J Obstet Gynecol

[Internet]. 2000 Jun [cited 2018 Jun 21];182(6):1496–501. Available from: http://linkinghub.elsevier.com/retrieve/pii/S0002937800576285

349. Terrone DA, Rinehart BK, Granger JP, Barrilleaux PS, Martin JN, Bennett WA. Interleukin-10 administration and bacterial endotoxin-induced preterm birth in a rat model. Obstet Gynecol [Internet]. 2001 Sep 1 [cited 2018 Jun 21];98(3):476–80. Available from: https://www.sciencedirect.com/science/article/pii/S0029784401014247?via%3Dihub

350. Fang X, Wong S, Mitchell BF. Effects of LPS and IL-6 on Oxytocin Receptor in Non-Pregnant and Pregnant Rat Uterus. Am J Reprod Immunol [Internet]. 2000 Aug [cited 2018 Jun 21];44(2):65–72. Available from: http://doi.wiley.com/10.1111/j.8755-8920.2000.440201.x

351. Hirsch E, Filipovich Y, Romero R. Failure of E. coli bacteria to induce preterm delivery in the rat. J Negat Results Biomed [Internet]. 2009 Dec 4 [cited 2018 Jun 21];8(1):1. Available from: http://jnrbm.biomedcentral.com/articles/10.1186/1477-5751-8-1

352. Sugimoto Y, Yamasaki A, Segi E, Tsuboi K, Aze Y, Nishimura T, et al. Failure of Parturition in Mice Lacking the Prostaglandin F Receptor. Science (80-) [Internet]. 1997 Jun 12 [cited 2018 Jun 22];277(5326):681–3. Available from: http://www.ncbi.nlm.nih.gov/pubmed/1598587

353. Gross GA, Imamura T, Luedke C, Vogt SK, Olson LM, Nelson DM, et al. Opposing actions of prostaglandins and oxytocin determine the onset of murine labor. Proc Natl Acad Sci U S A [Internet]. 1998 Sep 29 [cited 2018 Jun 22];95(20):11875–9. Available from: http://www.ncbi.nlm.nih.gov/pubmed/9751758

354. Zhao B, Koon D, Curtis AL, Soper J, Bethin KE. Identification of 9 uterine genes that are regulated during mouse pregnancy and exhibit abnormal levels in the cyclooxygenase-1 knockout mouse. Reprod Biol Endocrinol [Internet]. 2007 Jul 6 [cited 2018 Jun 22];5(1):28. Available from: http://rbej.biomedcentral.com/articles/10.1186/1477-7827-5-28

355. Wang H, Xie H, Dey SK. Loss of Cannabinoid Receptor CB1 Induces Preterm Birth. Fisher SJ, editor. PLoS One [Internet]. 2008 Oct 3 [cited 2018 Jun 22];3(10):e3320. Available from: http://dx.plos.org/10.1371/journal.pone.0003320

356. Brown A, Cornwell T, Korniyenko I, Solodushko V, Bond CT, Adelman JP, et al. Myometrial expression of small conductance Ca $^{2+}$ -activated K $^{+}$ channels depresses phasic uterine contraction. Am J Physiol Physiol [Internet]. 2007 Feb [cited 2018 Jun 22];292(2):C832–40. Available from: http://www.physiology.org/doi/10.1152/ajpcell.00268.2006

357. Pierce SL, Kresowik JDK, Lamping KG, England SK. Overexpression of SK3

Channels Dampens Uterine Contractility to Prevent Preterm Labor in Mice1. Biol Reprod [Internet]. 2008 Jun 1 [cited 2018 Jun 22];78(6):1058–63. Available from: https://academic.oup.com/biolreprod/article-lookup/doi/10.1095/biolreprod.107.066423

358. Döring B, Shynlova O, Tsui P, Eckardt D, Janssen-Bienhold U, Hofmann F, et al. Ablation of connexin43 in uterine smooth muscle cells of the mouse causes delayed parturition. J Cell Sci [Internet]. 2006 May 1 [cited 2018 Jun 22];119(Pt 9):1715–22. Available from: http://www.ncbi.nlm.nih.gov/pubmed/16595547

359. Filipovich Y, Lu S-J, Akira S, Hirsch E. The adaptor protein MyD88 is essential for E coli–induced preterm delivery in mice. Am J Obstet Gynecol [Internet]. 2009 Jan 1 [cited 2018 Jun 22];200(1):93.e1-93.e8. Available from: https://www.sciencedirect.com/science/article/pii/S0002937808009678

360. Hirsch E, Muhle RA, Mussalli GM, Blanchard R. Bacterially induced preterm labor in the mouse does not require maternal interleukin-1 signaling. Am J Obstet Gynecol [Internet]. 2002 Mar 1 [cited 2018 Jun 22];186(3):523–30. Available from: https://www.sciencedirect.com/science/article/pii/S000293780216515X?via%3Dihub

361. Schmitz T, Souil E, Hervé R, Nicco C, Batteux F, Germain G, et al. PDE4 inhibition prevents preterm delivery induced by an intrauterine inflammation. J Immunol [Internet]. 2007 Jan 15 [cited 2018 Jun 22];178(2):1115–21. Available from: http://www.ncbi.nlm.nih.gov/pubmed/17202375

362. Tahara M, Kawagishi R, Sawada K, Morishige K, Sakata M, Tasaka K, et al. Tocolytic effect of a Rho-kinase inhibitor in a mouse model of lipopolysaccharide-induced preterm delivery. Am J Obstet Gynecol [Internet]. 2005 Mar 1 [cited 2018 Jun 22];192(3):903–8. Available from: https://www.sciencedirect.com/science/article/pii/S0002937804010348

363. Fidel PL, Romero R, Wolf N, Cutright J, Ramirez M, Araneda H, et al. Systemic and local cytokine profiles in endotoxin-induced preterm parturition in mice. Am J Obstet Gynecol [Internet]. 1994 May 1 [cited 2018 Jun 22];170(5):1467–75. Available from: https://www.sciencedirect.com/science/article/pii/S0002937813904890?via%3Dihub

364. Elovitz M a., Wang Z, Chien EK, Rychlik DF, Phillippe M. A New Model for Inflammation-Induced Preterm Birth. Am J Pathol [Internet]. 2003;163(5):2103–11. Available from: http://dx.doi.org/10.1016/S0002-9440(10)63567-5

365. Gonzalez JM, Franzke CW, Yang F, Romero R, Girardi G. Complement activation triggers metalloproteinases release inducing cervical remodeling and preterm birth in mice. Am J Pathol [Internet]. 2011;179(2):838–49.

Available from: http://dx.doi.org/10.1016/j.ajpath.2011.04.024

366. Kajikawa S, Kaga N, Futamura Y, Kakinuma C, Shibutani Y. Lipoteichoic acid induces preterm delivery in mice. J Pharmacol Toxicol Methods [Internet]. 1998 Apr 1 [cited 2018 Jun 22];39(3):147–54. Available from: https://www.sciencedirect.com/science/article/pii/S105687199800015X?via%3Dihub

367. Ilievski V, Hirsch E. Synergy Between Viral and Bacterial Toll-Like Receptors Leads to Amplification of Inflammatory Responses and Preterm Labor in the Mouse1. Biol Reprod [Internet]. 2010 Nov 1 [cited 2018 Jun 22];83(5):767–73. Available from: https://academic.oup.com/biolreprod/article-lookup/doi/10.1095/biolreprod.110.085464

368. Cardenas I, Mulla MJ, Myrtolli K, Sfakianaki AK, Norwitz ER, Tadesse S, et al. Nod1 activation by bacterial iE-DAP induces maternal-fetal inflammation and preterm labor. J Immunol [Internet]. 2011 Jul 15 [cited 2018 Jun 22];187(2):980–6. Available from: http://www.ncbi.nlm.nih.gov/pubmed/21677137

369. Pal S, Peterson EM, De La Maza LM. A murine model for the study of Chlamydia trachomatis genital infections during pregnancy. Infect Immun [Internet]. 1999 May 1 [cited 2018 Jun 23];67(5):2607–10. Available from: http://www.ncbi.nlm.nih.gov/pubmed/10225927

370. Han YW, Redline RW, Li M, Yin L, Hill GB, McCormick TS. Fusobacterium nucleatum induces premature and term stillbirths in pregnant mice: implication of oral bacteria in preterm birth. Infect Immun [Internet]. 2004 Apr 1 [cited 2018 Jun 23];72(4):2272–9. Available from: http://www.ncbi.nlm.nih.gov/pubmed/15039352

371. Chaim W, Mazor M. Intraamniotic infection with fusobacteria. Arch Gynecol Obstet [Internet]. 1992 [cited 2018 Jun 23];251(1):1–7. Available from: http://www.ncbi.nlm.nih.gov/pubmed/1550388

372. Dudley DJ, Branch DW, Edwin SS, Mitchell MD. Induction of Preterm Birth in Mice by RU486. Biol Reprod [Internet]. 1996 Nov 1 [cited 2018 Jun 23];55(5):992–5. Available from: https://academic.oup.com/biolreprod/article/2760615/Induction

373. Cook JL, Randall CL. Early onset of parturition induced by acute alcohol exposure in C57BL/6J mice: role of uterine PGE and PGF2a. Reprod Fertil Dev [Internet]. 1997 [cited 2018 Jun 23];9(8):815. Available from: http://www.publish.csiro.au/?paper=R97083

374. Kurtzman JT, Spinnato JA, Goldsmith LJ, Zimmerman MJ, Klem M, Lei ZM, et al. Human chorionic gonadotropin exhibits potent inhibition of preterm delivery in a small animal model. Am J Obstet Gynecol [Internet]. 1999 Oct 1

[cited 2018 Jun 23];181(4):853–7. Available from:
http://linkinghub.elsevier.com/retrieve/pii/S0002937899703133

375. Tiboni GM, Giampietro F. Inhibition of nitric oxide synthesis causes preterm delivery in the mouse. Hum Reprod [Internet]. 2000 Aug 1 [cited 2018 Jun 23];15(8):1838–42. Available from: https://academic.oup.com/humrep/article-lookup/doi/10.1093/humrep/15.8.1838

376. Zhang W-S, Xie Q-S, Wu X-H, Liang Q-H. Neuromedin B and Its Receptor Induce Labor Onset and Are Associated with the RELA (NFKB P65)/IL6 Pathway in Pregnant Mice1. Biol Reprod [Internet]. 2011 Jan 1 [cited 2018 Jun 23];84(1):113–7. Available from: https://academic.oup.com/biolreprod/article-lookup/doi/10.1095/biolreprod.110.085746

377. Mendelson CR, Condon JC. New insights into the molecular endocrinology of parturition. J Steroid Biochem Mol Biol [Internet]. 2005 Feb 1 [cited 2018 Jun 23];93(2–5):113–9. Available from: https://www.sciencedirect.com/science/article/pii/S0960076004004273?via%3Dihub

378. Mogami H, Kishore AH, Shi H, Keller PW, Akgul Y, Word RA. Fetal fibronectin signaling induces matrix metalloproteases and cyclooxygenase-2 (COX-2) in amnion cells and preterm birth in mice. J Biol Chem [Internet]. 2013 Jan 18 [cited 2018 Jun 23];288(3):1953–66. Available from: http://www.ncbi.nlm.nih.gov/pubmed/23184961

379. Gomez-Lopez N, Romero R, Plazyo O, Panaitescu B, Furcron AE, Miller D, et al. Intra-Amniotic Administration of HMGB1 Induces Spontaneous Preterm Labor and Birth. Am J Reprod Immunol [Internet]. 2016 Jan [cited 2018 Jun 23];75(1):3–7. Available from: http://doi.wiley.com/10.1111/aji.12443

380. Schill W-B, Wolff HH. Ultrastructure of Human Spermatozoa in the Presence of the Spermicide Nonoxinol-9 and a Vaginal Contraceptive Containing Nonoxinol-9. Andrologia [Internet]. 2009 Apr 24 [cited 2018 Jun 24];13(1):42–9. Available from: http://doi.wiley.com/10.1111/j.1439-0272.1981.tb00006.x

381. Wilborn WH, Hahn DW, McGuire JJ. Scanning electron microscopy of human spermatozoa after incubation with the spermicide nonoxynol-9. Fertil Steril [Internet]. 1983 May 1 [cited 2018 Jun 24];39(5):717–9. Available from: https://www.sciencedirect.com/science/article/pii/S0015028216470743?via%3Dihub

382. Zavos P., Correa J., Kaskar K, Zarmakoupis-Zavos P. Time dependent pattern of activity of the spermicide nonoxynol-9 on sperm qualitative characteristics. Fertil Steril [Internet]. 2001 Sep 1 [cited 2018 Jun 24];76(3):S263. Available from:

https://www.sciencedirect.com/science/article/pii/S0015028201027881?via%3
Dihub

383. Sexually transmitted diseases treatment guidelines 2002. Centers for Disease Control and Prevention. MMWR Recomm reports Morb Mortal Wkly report Recomm reports [Internet]. 2002 May 10 [cited 2018 Jun 24];51(RR-6):1–78. Available from: http://www.ncbi.nlm.nih.gov/pubmed/12184549

384. Eckstein P, Jackson MC, Millman N, Sobrero AJ. Comparison of vaginal tolerance tests of spermicidal preparations in rabbits and monkeys. J Reprod Fertil [Internet]. 1969 Oct [cited 2018 Jun 24];20(1):85–93. Available from: http://www.ncbi.nlm.nih.gov/pubmed/4982533

385. D'Cruz OJ, Zhu Z, Yiv SH, Chen C-L, Waurzyniak B, Uckun FM. WHI-05, a novel bromo-methoxy substituted phenyl phosphate derivative of zidovudine, is a dual-action spermicide with potent anti-HIV activity. Contraception [Internet]. 1999 May 1 [cited 2018 Jun 24];59(5):319–31. Available from: https://www.sciencedirect.com/science/article/pii/S0010782499000414

386. Tryphonas L, Buttar HS. Morphologic evidence for vaginal toxicity of Delfen contraceptive cream in the rat. Toxicol Lett [Internet]. 1984 Mar 1 [cited 2018 Jun 24];20(3):289–95. Available from: https://www.sciencedirect.com/science/article/pii/0378427484901620?via%3
Dihub

387. Levin RJ. Bioelectric Activity as a Quantifiable Index of Acute Spermicide (Nonoxynol-9) Actions on Rat Vaginal Epithelial Function during the Oestrous Cycle. Pharmacol Toxicol [Internet]. 1987 Mar [cited 2018 Jun 24];60(3):175–8. Available from: http://doi.wiley.com/10.1111/j.1600-0773.1987.tb01728.x

388. Patton DL, Kidder GG, Sweeney YC, Rabe LK, Clark AM, Hillier SL. Effects of nonoxynol-9 on vaginal microflora and chlamydial infection in a monkey model. Sex Transm Dis [Internet]. 1996 [cited 2018 Jun 24];23(6):461–4. Available from: http://www.ncbi.nlm.nih.gov/pubmed/8946629

389. Milligan GN, Dudley KL, Bourne N, Reece A, Stanberry LR. Entry of inflammatory cells into the mouse vagina following application of candidate microbicides: comparison of detergent-based and sulfated polymer-based agents. Sex Transm Dis [Internet]. 2002 Oct [cited 2018 Jun 24];29(10):597–605. Available from: http://www.ncbi.nlm.nih.gov/pubmed/12370527

390. Patton DL, Kiddera GG, Sweeney YC, Rabeb LK, Hillier SL. Effects of multiple applications of benzalkonium chloride and nonoxynol 9 on the vaginal epithelium in the pigtailed macaque (Macaca nemestrina). Am J Obstet Gynecol [Internet]. 1999 May 1 [cited 2018 Jun 24];180(5):1080–7. Available from: https://www.sciencedirect.com/science/article/pii/S0002937899705983?via%3
Dihub

391. Catalone BJ, Kish-Catalone TM, Budgeon LR, Neely EB, Ferguson M, Krebs FC, et al. Mouse model of cervicovaginal toxicity and inflammation for preclinical evaluation of topical vaginal microbicides. Antimicrob Agents Chemother. 2004;48(5):1837–47.

392. Lozenski K, Ownbey R, Wigdahl B, Kish-Catalone T, Krebs FC. Decreased cervical epithelial sensitivity to nonoxynol-9 (N-9) after four daily applications in a murine model of topical vaginal microbicide safety. BMC Pharmacol Toxicol [Internet]. 2012;13(1):9. Available from: http://www.pubmedcentral.nih.gov/articlerender.fcgi?artid=3519674&tool=pmcentrez&rendertype=abstract

393. Fichorova RN, Rheinwald JG, Anderson DJ. Generation of Papillomavirus-lmmortalized Cell Lines from Normal Human Ectocervical , Endocervical , and Vaginal Epithelium That Maintain Expression of Tissue-Specific Differentiation Proteins '. Biol Reprod. 1997;855(57):847–55.

394. Halbert CL, Demers GW, Galloway DA. The E7 gene of human papillomavirus type 16 is sufficient for immortalization of human epithelial cells. J Virol [Internet]. 1991 Jan 1 [cited 2019 Jan 8];65(1):473–8. Available from: http://www.ncbi.nlm.nih.gov/pubmed/1845902

395. Perez-Reyes N, Halbert CL, Smith PP, Benditt EP, McDougall JK. Immortalization of primary human smooth muscle cells. Proc Natl Acad Sci U S A [Internet]. 1992 Feb 15 [cited 2019 Jan 8];89(4):1224–8. Available from: http://www.ncbi.nlm.nih.gov/pubmed/1311088

396. Tsao S-W, Mok SC, Fey EG, Fletcher JA, Wan TSK, Chew E-C, et al. Characterization of Human Ovarian Surface Epithelial Cells Immortalized by Human Papilloma Viral Oncogenes (HPV-E6E7 ORFs). Exp Cell Res [Internet]. 1995 Jun 1 [cited 2019 Jan 8];218(2):499–507. Available from: https://www.sciencedirect.com/science/article/pii/S0014482785711846?via%3Dihub

397. Scherer WF, Syverton JC, Gey GO. Studies on the propagation in vitro of poliomyelitis viruses. IV. Viral multiplication in a stable strain of human malignant epithelial cells (strain Hela) derived from an epidermoid carcinoma of the cervix. J Exp Med [Internet]. 1953;97(5):695–710. Available from: http://www.jem.org/cgi/doi/10.1084/jem.97.5.695

398. Krikun G, Mor G, Alvero A, Guller S, Schatz F, Sapi E, et al. A novel immortalized human endometrial stromal cell line with normal progestational response. Endocrinology. 2004;145(5):2291–6.

399. Straszewski-Chavez SL, Abrahams VM, Alvero AB, Aldo PB, Ma Y, Guller S, et al. The Isolation and Characterization of a Novel Telomerase Immortalized First Trimester Trophoblast Cell Line, Swan 71. Placenta [Internet]. 2009;30(11):939–48. Available from: http://dx.doi.org/10.1016/j.placenta.2009.08.007

400. Hall MP, Unch J, Binkowski BF, Valley MP, Butler BL, Wood MG, et al. Engineered luciferase reporter from a deep sea shrimp utilizing a novel imidazopyrazinone substrate. ACS Chem Biol. 2012;7(11):1848–57.

401. Anderl J, Ma J, Armstrong L. Improved Assays for Quantification of In Vitro Vascular Permeability. Nat Methods [Internet]. 2012 [cited 2018 Jul 10];10(38):10–4. Available from: https://www.nature.com/app_notes/nmeth/2012/121007/pdf/an8623.pdf

402. Beeton ML, Chalker VJ, Maxwell NC, Kotecha S, Spiller OB. Concurrent titration and determination of antibiotic resistance in Ureaplasma species with identification of novel point mutations in genes associated with resistance. Antimicrob Agents Chemother. 2009;53(5):2020–7.

403. Migale R, Herbert BR, Lee YS, Sykes L, Waddington SN, Peebles D, et al. Specific Lipopolysaccharide Serotypes Induce Differential Maternal and Neonatal Inflammatory Responses in a Murine Model of Preterm Labor. Am J Pathol [Internet]. 2015 Sep 1 [cited 2018 Jul 9];185(9):2390–401. Available from: https://www.sciencedirect.com/science/article/pii/S0002944015003624?via%3Dihub

404. Helenius A, Simons K. Solubilization of membranes by detergents. Biochim Biophys Acta - Rev Biomembr [Internet]. 1975 Mar 25 [cited 2018 Jun 24];415(1):29–79. Available from: https://www.sciencedirect.com/science/article/pii/0304415775900167?via%3Dihub

405. Yu K, Bagdon RE, Chien YW, Yurkow EJ. Spermicidal Activity of nonoxynol-9 and Analogs: Quantitative Assessments by Flow Cytometry. Drug Dev Ind Pharm [Internet]. 1995 Jan 20 [cited 2018 Jun 24];21(2):243–56. Available from: http://www.tandfonline.com/doi/full/10.3109/03639049509048107

406. Hillier SL, Moench T, Shattock R, Black R, Reichelderfer P, Veronese F. In Vitro and In Vivo: The story of Nonoxynol-9. JAIDS J Acquir Immune Defic Syndr [Internet]. 2005;39(1):1–8. Available from: http://content.wkhealth.com/linkback/openurl?sid=WKPTLP:landingpage&an=00126334-200505010-00001

407. Tryphonas L, Buttar HS. Genital tract toxicity of nonoxynol-9 in female rats: temporal development, reversibility and sequelae of the induced lesions. Fundam Appl Toxicol. 1982;2(5):211–9.

408. Patton DL, Kidder GG, Sweeney YC, Rabe LK, Hillier SL. Effects of multiple applications of benzalkonium chloride and nonoxynol 9 on the vaginal epithelium in the pigtailed macaque (Macaca nemestrina). Am J Obstet Gynecol. 1999;180(5):1080–7.

409. Acatürk F, Robinson JR. Effect of the Spermicide, Nonoxynol 9, on Vaginal Permeability in Normal and Ovariectomized Rabbits. Pharm Res [Internet]. 1996 [cited 2018 Jun 24];13(6):950–1. Available from: http://link.springer.com/10.1023/A:1016077801253

410. DiGiulio DB. Diversity of microbes in amniotic fluid. Semin Fetal Neonatal Med. 2012;17(1):2–11.

411. Normann E, Lacaze-Masmonteil T, Eaton F, Schwendimann L, Gressens P, Thébaud B. A novel mouse model of Ureaplasma-induced perinatal inflammation: Effects on lung and brain injury. Pediatr Res. 2009;65(4):430–6.

412. D'Cruz OJ, Shih M-J, Yiv SH, Chen C-L, Uckun FM. Synthesis, characterization and preclinical formulation of a dual-action phenyl phosphate derivative of bromo-methoxy zidovudine (compound WHI-07) with potent anti-HIV and spermicidal activities. Mol Hum Reprod [Internet]. 1999 May 1 [cited 2018 Jul 10];5(5):421–32. Available from: https://academic.oup.com/molehr/article-lookup/doi/10.1093/molehr/5.5.421

413. Fichorova RN, Tucker LD, Anderson DJ. The molecular basis of nonoxynol-9-induced vaginal inflammation and its possible relevance to human immunodeficiency virus type 1 transmission. J Infect Dis. 2001;184(4):418–28.

414. Fuchs EJ, Schwartz JL, Friend DR, Coleman JS, Hendrix CW. A Pilot Study Measuring the Distribution and Permeability of a Vaginal HIV Microbicide Gel Vehicle Using Magnetic Resonance Imaging, Single Photon Emission Computed Tomography/Computed Tomography, and a Radiolabeled Small Molecule. AIDS Res Hum Retroviruses [Internet]. 2015 Nov 6 [cited 2018 Jul 10];31(11):1109–15. Available from: http://online.liebertpub.com/doi/10.1089/aid.2015.0054

415. Fuchs EJ, Grohskopf LA, Lee LA, Bakshi RP, Hendrix CW. Quantitative assessment of altered rectal mucosal permeability due to rectally applied nonoxynol-9, biopsy, and simulated intercourse. J Infect Dis [Internet]. 2013;207(9):1389–96. Available from: http://www.ncbi.nlm.nih.gov/entrez/query.fcgi?cmd=Retrieve&db=PubMed&dopt=Citation&list_uids=23325915

416. Sweeney EL, Dando SJ, Kallapur SG, Knox L. The Human Ureaplasma Species as Causative Agents of Chorioamnionitis. Clin Microbiol Rev. 2017;30(1):349–79.

417. Eming SA, Martin P, Tomic-Canic M. Wound repair and regeneration: Mechanisms, signaling, and translation. Sci Transl Med [Internet]. 2014 [cited 2018 Jul 7];6(265):1–16. Available from: www.ScienceTranslationalMedicine.org

418.   Van Damme L, Ramjee G, Alary M, Vuylsteke B, Chandeying V, Rees H, et al. Effectiveness of COL-1492, a nonoxynol-9 vaginal gel, on HIV-1 transmission in female sex workers: A randomised controlled trial. Lancet. 2002;360(9338):971–7.

419.   Kaminsky M, Szivos MM, Brown KR, Willigan DA. Comparison of the sensitivity of the vaginal mucous membranes of the albino rabbit and laboratory rat to nonoxynoxynol-9. Food Chem Toxicol [Internet]. 1985 Jul 1 [cited 2018 Jun 29];23(7):705–8. Available from: https://www.sciencedirect.com/science/article/pii/0278691585901619?via%3Dihub

420.   Chvapil M, Droegemueller W, Owen JA, Eskelson CD, Betts K. Studies of nonoxynol-9. I. The effect on the vaginas of rabbits and rats. Fertil Steril [Internet]. 1980 [cited 2018 Jun 29];33(4):445–50. Available from: http://www.fertstert.org/article/S0015-0282(16)44665-0/abstract

421.   Niruthisard S, Roddy RE, Chutivongse S. The Effects of Frequent Nonoxynol-9 Use on the Vaginal and Cervical Mucosa. Sex Transm Dis [Internet]. 1991 [cited 2018 Jun 29];18(3):176–9. Available from: https://insights.ovid.com/crossref?an=00007435-199107000-00010

422.   Poindexter AN, Levine H, Sangi-Haghpeykar H, Frank ML, Grear A, Reeves KO. Comparison of spermicides on vulvar, vaginal, and cervical mucosa. Contraception [Internet]. 1996 Mar 1 [cited 2018 Jun 29];53(3):147–53. Available from: https://www.sciencedirect.com/science/article/pii/0010782496000029?via%3Dihub

423.   Stafford MK, Ward H, Flanagan A, Rosenstein IJ, Taylor-Robinson D, Smith JR, et al. Safety study of nonoxynol-9 as a vaginal microbicide: evidence of adverse effects. J Acquir Immune Defic Syndr Hum Retrovirol [Internet]. 1998 Apr 1 [cited 2018 Jun 29];17(4):327–31. Available from: http://www.ncbi.nlm.nih.gov/pubmed/9525433

424.   Roddy RE, Cordero M, Cordero C, Fortney JA. A Dosing Study of Nonoxynol-9 and Genital Irritation. Int J STD AIDS [Internet]. 1993 May 25 [cited 2018 Jun 29];4(3):165–70. Available from: http://journals.sagepub.com/doi/10.1177/095646249300400308

425.   Gagné N, Cormier H, Omar, Rabeea F. Désormeaux A, Gourde P, Tremblay MJ, Juhász J, et al. Protective Effect of a Thermoreversible Gel Against the Toxicity of Nonoxynol-9. Sex Transm Dis. 1999;26(3):177–1.

426.   Phillips DM, Zacharopoulos VR. Nonoxynol-9 enhances rectal infection by herpes simplex virus in mice. Contraception [Internet]. 1998 May 1 [cited 2018 Jul 8];57(5):341–8. Available from: https://www.sciencedirect.com/science/article/pii/S0010782498000407?via%3Dihub

427.   Milligan GN, Dudley KL, Bourne N, Reece A, Stanberry LR. Application of
        Candidate Microbicides Comparison of Detergent-Based and Sulfated
        Polymer – Based Agents. Sex Transm Dis. 2002;29(10):597–605.

428.   Phillips DM, Taylor CL, Zacharopoulos VR, Maguire RA. Nonoxynol-9
        causes rapid exfoliation of sheets of rectal epithelium. Contraception
        [Internet]. 2000 Sep 1 [cited 2018 Jul 8];62(3):149–54. Available from:
        https://www.sciencedirect.com/science/article/pii/S0010782400001566?via%3
        Dihub

429.   Barberini F, De Santis F, Correr S, Motta PM. The mucosa of the rabbit
        vagina: a proposed experimental model for correlated morphofunctional
        studies in humans. Eur J Obstet Gynecol Reprod Biol [Internet]. 1992 [cited
        2018 Jul 8];44:221–7. Available from: https://ac.els-
        cdn.com/0028224392901036/1-s2.0-0028224392901036-
        main.pdf?_tid=8dc29055-56c3-479a-8244-
        21a52a729bcd&acdnat=1531056600_8708c0ec785f2a1a59d8a7ffae12d09a

430.   Croy BA, Yamada AT, DeMayo FJ, Adamson SL. The Guide of Investigation
        of Mouse Pregnancy. 2014.

431.   Holt R, Timmons BC, Akgul Y, Akins ML, Mahendroo M. The molecular
        mechanisms of cervical ripening differ between term and preterm birth.
        Endocrinology [Internet]. 2011;152(3):1036–46. Available from:
        http://www.pubmedcentral.nih.gov/articlerender.fcgi?artid=3040055&tool=p
        mcentrez&rendertype=abstract

432.   Traurig HH. Epithelial Cell Proliferation in the Mouse Vagina during the
        Estrous Cycle, Pregnancy and Lactation: A Radioautographic Study. Anat Rec
        [Internet]. 1971 [cited 2019 Mar 17];170(4):457–70. Available from:
        https://onlinelibrary.wiley.com/doi/pdf/10.1002/ar.1091700407

433.   Li S, Herrera GG, Tam KK, Lizarraga JS, Beedle M-T, Winuthayanon W.
        Estrogen Action in the Epithelial Cells of the Mouse Vagina Regulates
        Neutrophil Infiltration and Vaginal Tissue Integrity. Sci Rep [Internet]. 2018
        Dec 26 [cited 2019 Mar 17];8(1):11247. Available from:
        http://www.nature.com/articles/s41598-018-29423-5

434.   Yao L, Agoulnik AI, Cooke PS, Meling DD, David Sherwood O, Y Acad Sci
        Author manuscript AN. Relative Roles of the Epithelial and Stromal Tissue
        Compartment(s) in Mediating the Actions of Relaxin and Estrogen on Cell
        Proliferation and Apoptosis in the Mouse Lower Reproductive. Ann N Y Acad
        Sci [Internet]. 2009 [cited 2019 Mar 17];1160:121–9. Available from:
        https://www.ncbi.nlm.nih.gov/pmc/articles/PMC2743517/pdf/nihms122671.p
        df

435.   Timmons BC, Mahendroo MS. Timing of Neutrophil Activation and
        Expression of Proinflammatory Markers Do Not Support a Role for
        Neutrophils in Cervical Ripening in the Mouse. Biol Reprod [Internet].

2006;74(2):236–45. Available from:
http://www.biolreprod.org/cgi/doi/10.1095/biolreprod.105.044891

436. Gonzalez JM, Xu H, Chai J, Ofori E, Elovitz M a. Preterm and term cervical ripening in CD1 Mice (Mus musculus): similar or divergent molecular mechanisms? Biol Reprod [Internet]. 2009;81(6):1226–32. Available from: http://www.ncbi.nlm.nih.gov/pubmed/19684330

437. Lettieri L, Vintzileos AM, Rodis JF, Albini SM, Salafia CM. Does "idiopathic" preterm labor resulting in preterm birth exist? Am J Obstet Gynecol. 1993;168(5):1480–5.

438. Witt A, Berger A, Gruber CJ, Petricevic L, Apfalter P, Worda C, et al. Increased intrauterine frequency of Ureaplasma urealyticum in women with preterm labor and preterm premature rupture of the membranes and subsequent cesarean delivery. Am J Obstet Gynecol [Internet]. 2005 Nov 1 [cited 2018 Jul 3];193(5):1663–9. Available from: https://www.sciencedirect.com/science/article/pii/S0002937805005053?via%3Dihub

439. Hannaford K, Todd DA, Jeffery H, John E, Blyth K, Gilbert GL. Role of ureaplasma urealyticum in lung disease of prematurity. Arch Dis Child Fetal Neonatal Ed [Internet]. 1999 Nov [cited 2018 Jul 3];81(3):F162-7. Available from: http://www.ncbi.nlm.nih.gov/pubmed/10525015

440. Kafetzis DA, Skevaki CL, Skouteri V, Gavrili S, Peppa K, Kostalos C, et al. Maternal Genital Colonization with Ureaplasma urealyticum Promotes Preterm Delivery: Association of the Respiratory Colonization of Premature Infants with Chronic Lung Disease and Increased Mortality. Clin Infect Dis [Internet]. 2004 Oct 15 [cited 2018 Jul 3];39(8):1113–22. Available from: https://academic.oup.com/cid/article-lookup/doi/10.1086/424505

441. Singh B, Cutler JC, Utidjian HM. Studies on the development of a vaginal preparation providing both prophylaxis against venereal disease and other genital infections and contraception. II. Effect in vitro of vaginal contraceptive and non-contraceptive preparations on Treponema pallidum and Neisseria gonorrhoeae. Br J Vener Dis [Internet]. 1972 Feb [cited 2018 Jul 30];48(1):57–64. Available from: http://www.ncbi.nlm.nih.gov/pubmed/4622671

442. Singh B, Cutler JC, Utidjian HMD. Studies on development of a vaginal preparation providing both prophylaxis against venereal disease, other genital infections and contraception: III. In vitro effect of vaginal contraceptive and selected vaginal preparations of Candida albicans and Trichomonas vaginalis. Contraception [Internet]. 1972 May 1 [cited 2018 Jul 30];5(5):401–11. Available from: https://www.sciencedirect.com/science/article/pii/0010782472900327?via%3Dihub

443. Jones BM, Willcox LM. The susceptibility of organisms associated with bacterial vaginosis to spermicidal compounds, in vitro. Genitourin Med [Internet]. 1991 Dec [cited 2018 Jul 30];67(6):475–7. Available from: http://www.ncbi.nlm.nih.gov/pubmed/1774052

444. Patton DL, Wang SK, Kuo CC. In vitro activity of nonoxynol 9 on HeLa 229 cells and primary monkey cervical epithelial cells infected with Chlamydia trachomatis. Antimicrob Agents Chemother [Internet]. 1992 Jul [cited 2018 Jul 30];36(7):1478–82. Available from: http://www.ncbi.nlm.nih.gov/pubmed/1324646

445. Krebs FC, Miller SR, Malamud D, Howett MK, Wigdahl B. Inactivation of human immunodeficiency virus type 1 by nonoxynol-9, C31G, or an alkyl sulfate, sodium dodecyl sulfate. Antiviral Res [Internet]. 1999 Oct 1 [cited 2018 Jul 9];43(3):157–73. Available from: https://www.sciencedirect.com/science/article/pii/S0166354299000443

446. Harrison C, Chantler E. The effect of nonoxynol-9 and chlorhexidine on HIV and sperm in vitro. Int J STD AIDS [Internet]. 1998 Feb 25 [cited 2018 Jul 9];9(2):92–7. Available from: http://journals.sagepub.com/doi/10.1258/0956462981921747

447. Chvapil M, Eskelson CD, Stiffel V, Owen JA, Droegemueller W. Studies on nonoxynol-9. II. Intravaginal absorption, distribution, metabolism and excretion in rats and rabbits. Contraception [Internet]. 1980 Sep 1 [cited 2018 Jul 9];22(3):325–39. Available from: https://www.sciencedirect.com/science/article/pii/S0010782480800102?via%3Dihub

448. Roberts JN, Buck CB, Thompson CD, Kines R, Bernardo M, Choyke PL, et al. Genital transmission of HPV in a mouse model is potentiated by nonoxynol-9 and inhibited by carrageenan. Nat Med. 2007;13(7):857–61.

449. Mcgee D, Smith A, Poncil S, Patterson A, Bernstein AI, Racicot K. Cervical HSV-2 infection causes cervical remodeling and increases risk for ascending infection and preterm birth. PLoS One. 2017;12(11):1–15.

450. Barnhart KT, Stolpen A, Pretorius ES, Malamud D. Distribution of a spermicide containing Nonoxynol-9 in the vaginal canal and the upper female reproductive tract. Hum Reprod [Internet]. 2001 Jun [cited 2018 Jun 24];16(6):1151–4. Available from: http://www.ncbi.nlm.nih.gov/pubmed/11387285

451. Fux CA, Stoodley P, Hall-Stoodley L, Costerton JW. Bacterial biofilms: a diagnostic and therapeutic challenge. Expert Rev Anti Infect Ther [Internet]. 2003 Dec 10 [cited 2018 Jul 17];1(4):667–83. Available from: http://www.tandfonline.com/doi/full/10.1586/14787210.1.4.667

452. Hall-Stoodley L, Keevil CW, Lappin-Scott HM. Mycobacterium fortuitum

and Mycobacterium chelonae biofilm formation under high and low nutrient conditions. J Appl Microbiol [Internet]. 1998 Dec [cited 2018 Jul 17];85(S1):60S–69S. Available from: http://doi.wiley.com/10.1111/j.1365-2672.1998.tb05284.x

453. Domann E, Wehland J, Rohde M, Pistor S. A novel bacterial virulence gene in Listeria monocytogenes required for host cell microfilament interaction with homology to the proline-rich region of vinculin. EMBO J [Internet]. 1992 [cited 2018 Jul 17];11(5):1981–90. Available from: https://onlinelibrary.wiley.com/doi/abs/10.1002/j.1460-2075.1992.tb05252.x

454. Kim J-H, Park J-Y, Kim D-Y, Kim Y-M, Kim Y-T, Nam J-H. Fertility-sparing laparoscopic radical trachelectomy for young women with early stage cervical cancer. BJOG An Int J Obstet Gynaecol [Internet]. 2010 Feb 1 [cited 2019 Feb 5];117(3):340–7. Available from: http://doi.wiley.com/10.1111/j.1471-0528.2009.02446.x

455. Bernardini M, Barrett J, Seaward G, Covens A. Pregnancy outcomes in patients after radical trachelectomy. Am J Obstet Gynecol [Internet]. 2003 Nov 1 [cited 2019 Feb 5];189(5):1378–82. Available from: https://www.sciencedirect.com/science/article/pii/S0002937803007762?via%3Dihub

456. Shepherd JH, Crawford RAF, Oram DH. Radical trachelectomy: a way to preserve fertility in the treatment of early cervical cancer. BJOG An Int J Obstet Gynaecol [Internet]. 1998 Aug 1 [cited 2019 Feb 5];105(8):912–6. Available from: http://doi.wiley.com/10.1111/j.1471-0528.1998.tb10238.x

457. Castanon A, Landy R, Brocklehurst P, Evans H, Peebles D, Singh N, et al. Risk of preterm delivery with increasing depth of excision for cervical intraepithelial neoplasia in England: nested case-control study. BMJ [Internet]. 2014 Nov 5 [cited 2019 Feb 5];349:g6223. Available from: http://www.ncbi.nlm.nih.gov/pubmed/25378384

458. Khalid S, Dimitriou E, Conroy R, Paraskevaidis E, Kyrgiou M, Harrity C, et al. The thickness and volume of LLETZ specimens can predict the relative risk of pregnancy-related morbidity. BJOG An Int J Obstet Gynaecol [Internet]. 2012 May 1 [cited 2019 Feb 5];119(6):685–91. Available from: http://doi.wiley.com/10.1111/j.1471-0528.2011.03252.x

459. Heinonen A, Gissler M, Riska A, Paavonen J, Tapper A-M, Jakobsson M, et al. Loop Electrosurgical Excision Procedure and the Risk for Preterm Delivery. Obs Gynecol [Internet]. 2013 [cited 2019 Feb 5];121(5):1063–71. Available from: www.stat.fi/meta/luokitukset/

460. Miyako J, Iwanari O, Kitao M. Immunohistochemical studies of the uterine cervix after CO2 laser conization. Int J Gynecol Obstet [Internet]. 1993 Jul 1 [cited 2019 Feb 5];42(1):9–13. Available from: http://doi.wiley.com/10.1016/0020-7292%2893%2990438-3

461. Leitich H, Kiss H. Asymptomatic bacterial vaginosis and intermediate flora as risk factors for adverse pregnancy outcome. Best Pract Res Clin Obstet Gynaecol [Internet]. 2007 Jun 1 [cited 2018 Jul 17];21(3):375–90. Available from: https://www.sciencedirect.com/science/article/pii/S1521693406001635?via%3Dihub

462. Hillier SL, Nugent RP, Eschenbach DA, Krohn MA, Gibbs RS, Martin DH, et al. Association between Bacterial Vaginosis and Preterm Delivery of a Low-Birth-Weight Infant. N Engl J Med [Internet]. 1995 Dec 28 [cited 2018 Jul 17];333(26):1737–42. Available from: http://www.nejm.org/doi/abs/10.1056/NEJM199512283332604

463. Ghartey J, Bastek JA, Brown AG, Anglim L, Elovitz MA. Women with preterm birth have a distinct cervicovaginal metabolome. Am J Obstet Gynecol [Internet]. 2015 Jun 1 [cited 2018 Jul 17];212(6):776.e1-776.e12. Available from: https://www.sciencedirect.com/science/article/pii/S0002937815003336?via%3Dihub

464. Critchfield AS, Yao G, Jaishankar A, Friedlander RS, Lieleg O, Doyle PS, et al. Cervical Mucus Properties Stratify Risk for Preterm Birth. Zakar T, editor. PLoS One [Internet]. 2013 Aug 1 [cited 2018 Jul 17];8(8):e69528. Available from: http://dx.plos.org/10.1371/journal.pone.0069528

465. Blanc WA. Pathways of fetal and early neonatal infection: Viral placentitis, bacterial and fungal chorioamnionitis. J Pediatr [Internet]. 1961 Oct 1 [cited 2018 Jul 18];59(4):473–96. Available from: https://www.sciencedirect.com/science/article/pii/S0022347661802321

466. Aaltonen R, Heikkinen J, Vahlberg T, Jensen J, Alanen A. Local inflammatory response in choriodecidua induced by Ureaplasma urealyticum. BJOG An Int J Obstet Gynaecol [Internet]. 2007 Oct 17 [cited 2018 Jul 29];114(11):1432–5. Available from: http://doi.wiley.com/10.1111/j.1471-0528.2007.01410.x

467. Glaser K, Silwedel C, Fehrholz M, Henrich B, Waaga-Gasser AM, Claus H, et al. Ureaplasma isolates stimulate pro-inflammatory CC chemokines and matrix metalloproteinase-9 in neonatal and adult monocytes. Balish MF, editor. PLoS One [Internet]. 2018 Mar 20 [cited 2018 Jul 27];13(3):e0194514. Available from: http://dx.plos.org/10.1371/journal.pone.0194514

468. Beall MH, Wang S, Yang B, Chaudhri N, Amidi F, Ross MG. Placental and Membrane Aquaporin Water Channels: Correlation with Amniotic Fluid Volume and Composition. Placenta [Internet]. 2007 May 1 [cited 2018 Jul 17];28(5–6):421–8. Available from: https://www.sciencedirect.com/science/article/pii/S0143400406001597

469. Glass JI, Lefkowitz EJ, Glass JS, Heiner CR, Chen EY, Cassell GH. The

complete sequence of the mucosal pathogen Ureaplasma urealyticum. Nature [Internet]. 2000 Oct 12 [cited 2018 Jul 17];407(6805):757–62. Available from: http://www.nature.com/articles/35037619

470. Johnson DR. Genes and genotypes affecting embryonic fluid relations in the mouse. Genet Res [Internet]. 1971 [cited 2018 Jul 16];18(1):71–9. Available from: https://doi.org/10.1017/S0016672300012428

471. Glaser K, Silwedel C, Fehrholz M, Waaga-Gasser AM, Henrich B, Claus H, et al. Ureaplasma Species Differentially Modulate Pro- and Anti-Inflammatory Cytokine Responses in Newborn and Adult Human Monocytes Pushing the State Toward Pro-Inflammation. Front Cell Infect Microbiol [Internet]. 2017 Nov 28 [cited 2018 Jul 27];7:484. Available from: http://journal.frontiersin.org/article/10.3389/fcimb.2017.00484/full

472. Peltier MR, Freeman AJ, Mu HH, Cole BC. Characterization of the Macrophage-Stimulating Activity from Ureaplasma urealyticum. Am J Reprod Immunol [Internet]. 2007 Mar [cited 2018 Jul 17];57(3):186–92. Available from: http://doi.wiley.com/10.1111/j.1600-0897.2006.00460.x

473. Lindström TM, Bennett PR. The role of nuclear factor kappa B in human labour. Reproduction [Internet]. 2005 Nov [cited 2015 Jan 12];130(5):569–81. Available from: http://www.ncbi.nlm.nih.gov/pubmed/16264088

474. MacIntyre D a., Lee YS, Migale R, Herbert BR, Waddington SN, Peebles D, et al. Activator protein 1 is a key terminal mediator of inflammation-induced preterm labor in mice. FASEB J. 2014;28:2358–68.

475. Ip YT, Davis RJ. Signal transduction by the c-Jun N-terminal kinase (JNK) — from inflammation to development. Curr Opin Cell Biol [Internet]. 1998 Apr 1 [cited 2018 Jul 18];10(2):205–19. Available from: https://www.sciencedirect.com/science/article/pii/S0955067498801439?via%3Dihub

476. Schmidt D, Wilson MD, Spyrou C, Brown GD, Odom DT. ChIP-seq : using high-throughput sequencing to discover protein-DNA interactions. Methods. 2014;48(3):240–8.

477. Ligon J V, Kenny GE. Virulence of ureaplasmal urease for mice. Infect Immun [Internet]. 1991 Mar 1 [cited 2018 Jul 18];59(3):1170–1. Available from: http://www.ncbi.nlm.nih.gov/pubmed/1997418

478. Takebe S, Numata A, Kobashi K. Stone formation by Ureaplasma urealyticum in human urine and its prevention by urease inhibitors. J Clin Microbiol [Internet]. 1984 Nov 1 [cited 2018 Jul 18];20(5):869–73. Available from: http://www.ncbi.nlm.nih.gov/pubmed/6549013

479. Robinson JW, Dando SJ, Nitsos I, Newnham J, Polglase GR, Kallapur SG, et al. Ureaplasma parvum Serovar 3 Multiple Banded Antigen Size Variation

after Chronic Intra-Amniotic Infection/Colonization. Frasch MG, editor. PLoS One [Internet]. 2013 Apr 26 [cited 2018 Jul 18];8(4):e62746. Available from: http://dx.plos.org/10.1371/journal.pone.0062746

480. Istivan TS, Coloe PJ. Phospholipase A in Gram-negative bacteria and its role in pathogenesis. Microbiology [Internet]. 2006 May 1 [cited 2018 Jul 18];152(5):1263–74. Available from: http://mic.microbiologyresearch.org/content/journal/micro/10.1099/mic.0.286 09-0

481. Robertson JA, Stemler ME, Stemke GW. Immunoglobulin A protease activity of Ureaplasma urealyticum. J Clin Microbiol [Internet]. 1984 Feb 1 [cited 2018 Jul 18];19(2):255–8. Available from: http://www.ncbi.nlm.nih.gov/pubmed/6365962

482. Kilian M, Sciences EF-I journal of medical, 1984 U. Exclusive occurrence of an extracellular protease capable of cleaving the hinge region of human immunoglobulin A1 in strains of Ureaplasma urealyticum. Isr J Med Sci [Internet]. 1984 [cited 2018 Jul 18];20(10):938–41. Available from: https://europepmc.org/abstract/med/6392177

483. Kilian M, Brown M, Brown T, Freundt E, Cassell G. Immunoglobulin A1 protease activity in strain of Ureaplasma urealyticum. Acta Pathol Microbiol Scand [Internet]. 2009 Aug 15 [cited 2018 Jul 18];92B(1–6):61–4. Available from: http://doi.wiley.com/10.1111/j.1699-0463.1984.tb02794.x